Final Report

FIRE ALERT SYSTEMS FOR METAL AND NON-METAL MINES

Contract No. S0144131

by

John P. Wagner, Abraham Fookson, Allan Harper,
Mary May, Roger Welker

Gillette Research Institute

Final Report

FIRE ALERT SYSTEMS FOR METAL AND NON-METAL MINES

Contract No. SO144131

by

John P. Wagner, Abraham Fookson, Allan Harper,
Mary May, Roger Welker

for

U. S. Department of the Interior
Bureau of Mines
Pittsburgh Mining and Safety Research Center
4800 Forbes Avenue
Pittsburgh, Pennsylvania 15213

August 22, 1975

Gillette Research Institute
1413 Research Boulevard
Rockville, Maryland 20850

FOREWARD

This report was prepared by the Gillette Research Institute, Rockville, Maryland, under USBM Contract No. SO144131. The Contract was initiated under the Metal and Non-Metal Mine Health and Safety Research Program. It was administered under the technical direction of the Pittsburgh Mining and Safety Research Center with Dr. Martin Hertzberg acting as the Technical Project Officer. Mr. Albert G. Young was the Contract Administrator for the Bureau of Mines.

This report is a summary of the work recently completed as part of this Contract during the period June 14, 1974 to June 14, 1975. This report was submitted by the authors on July 22, 1975.

ABSTRACT

The details of a three-phase study (total time period of 12 months) entitled "Fire Alert Systems for Metal and Non-Metal Mines," are presented. Phase 1 consists of a state of the art survey on fire detection devices and gas sensing techniques. Phases 2 and 3 include laboratory screening and systems concepts testing on various detectors classified as products of combustion, optical view-field and contact (or thermal) types under incipient and flaming combustion conditions. Recommendations for a mine fire detection system to protect shaft, sealed off or mined out (from spontaneous combustion of sulfide containing ores and cellulosic materials), and fuel storage areas are also included.

The principal problem area noted during Phase 1 study is the high expected occurrence of false alarming of products of combustion detectors (POC's) subjected to normal mining operations—diesel vehicles and equipment and shot firing or blasting operations. Simultaneous gas sensing of either the ratio of CO/NO_x or CO_2/NO_x with detection of one or more fire signatures (smoke, radiant energy, or heat sensing) is the recommended approach to discriminate against these operations.

A brief accounting of the more pertinent Phases 2 and 3 Conclusions (summarized beginning on page 69) is as follows:

1. POC's

a. Ionization Detectors - PYR-A-LARM DI-2S, Honeywell TC100A, Fire Alert CPD1212, and Becon MKII are unsuitable for detection of pyrolytic combustion products from plastics—polyvinylchloride (three different formulations), polyethylene (from high amperage power cable), and flexible polyurethane foam. Smoke levels at alarm (apparent alarm for TC100A since its output was analogue in nature) ranged from about 10 to 40%/ft smoke obscuration. This is 2.5 to 10 times the national standard for smoke detectors which requires alarm at 4%/ft or lower.

b. Photoelectric Detectors - Pyrotector SK700 (a near IR LED device), ESL's 724 (a beacon lamp), and 724L (visible LED) on an overall basis performed well in contrast to the aforementioned ionization detectors. Pyrotector SK700, because of excellent response to pyrolitic combustion products, above average response to flaming combustion tests, insensitivity to water mists, ease of cleaning (external to the detector components), and relatively low cost (approximately 1/2 to 1/5 lower than the aforementioned ionization detectors), is the recommended smoke detector.

c. Semiconductor Devices - "Taguchi" gas sensor (TGS) #109 performed well at two different heater voltages—V_h = 0.8 and 1.2 volts for several different fuels in pyrolytic or smoldering (with much glowing) combustion modes. It exhibited some, perhaps serious, shortcomings in selected flaming combustion tests.

2. Optical View-Field (UV and IR Detectors) and Contact (Thermal) Type Detectors

a. Pyrotector UV 30-2021 exhibited satisfactory test performance to flaming combustion tests of selected liquid fuels, and was unaffected by the presence of water sprays. Periodic cleaning of the UV tube is required since this unit became inoperative upon coating with a fine layer of #9 diesel oil.

b. Pyrotector IR 30-2025 was judged to be unsatisfactory for mine applications. It did not respond to bluish methanol and yellowish ethanol flames. Its performance was furthermore affected significantly by the presence of both smoke and water mists.

c. Rate compensated detectors, Fenwal Detectafire (vertical #27121-1 and horizontal #27020-0 oriented types) and Thermotech No. 302AW (vertical orientation) were subjected to rather large temperature increases—18-47°F/min as based on air temperature from pan burnings of liquid hydrocarbons. These tests indicated Fenwal vertical superior to Fenwal horizontal as the former was also to Thermotech vertical. However, close to a factor of three higher in cost for Fenwal vertical versus Thermotech vertical required us to recommend the Thermotech unit.

3. Pneumatic Gas-Sampling System Behavior

Analytical calculations based on a mean flow velocity, an isothermal form of the Bernoulli equation, and Poiseuille's equation for laminar flow for the residence time to convey a "slug" of gas through 1,000 to 5,000 ft of 3/8" I.D. tubing are compared with experiment for three different pressure ratios. The best overall agreement was obtained with the Bernoulli equation, whereas, the poorest was based on Pouiseuille's equation.

The effects of dilution of a volumetric input concentration of a carrier gas by air contained in the tubing were observed to be fairly strong for input concentrations of 0.13 and 2.25% of CO_2.

The opinions expressed herein are those of the authors and should not be interpreted as necessarily representing the official policies of the Interior Department's Bureau of Mines or of the U. S. Government. Commercial trade names and selection of fire detection devices for Phase 2 and Phase 3 Study do not necessarily constitute Bureau endorsement of these devices.

TABLE OF CONTENTS

TABLE OF CONTENTS (cont'd)

Tables

TABLE OF CONTENTS (cont'd)

Page

Tables (cont'd)

Figures

Page

Figures (cont'd)

Page

Figures (cont'd)

Page

Figures (cont'd)

I. INTRODUCTION

This final report is the result of a one-year project titled, "Fire Alert Systems for Metal and Non-Metal Mines." The program was divided into three distinct, although interrelated, phases covering the total time period of 12 months. The principal objectives of the program are summarized below by paraphrasing the contract work statement as follows:

Phase 1 - Consultation, Data Acquisition and Analyses

Collect, analyze and evaluate the available domestic and foreign published or recorded data on metal and non-metal mine fires; their causes, their rates of growth, the extent of contamination of exit passageways and the use and effectiveness of fire detection and alarm systems. Consult with Bureau of Mines personnel currently preparing "Fire Protection Standards for Metal and Non-Metal Mines," bureau contractors, mining companies, fire suppression or detector manufacturers, independent testing laboratories, insurance companies, and make a thorough survey of the existing state of the art. Analyze data and opinions thus obtained, and select sensors whose method of detection indicates that they are most likely to function reliably, to be of reasonable cost and to be compatible with proposed Bureau regulations and requirements concerning escape plans, alarm systems, ventilation requirements and fire suppression methods (Phase 1 completed October 1, 1974).

Phase 2 - Design, Development and Fabrication

Based upon Phase 1 and related efforts determine the extent to which existing systems can provide effective solutions to the problem of reliable detection of real fire hazards in metal and non-metal mines. If such a reliable system is already available, proceed to design, fabricate, test and assemble such a system.

Alternatively, if the analysis indicates the available systems are not sufficiently specific, sensitive or reliable, then proceed to develop new detection systems.

This phase could include laboratory screening of the performance of detectors in the presence of both incipient and actual fires. Screening should facilitate selection of detectors that are specific to mine combustibles and that discriminate against ambient sources from normal mining operations (Phase 2 completed February 28, 1975).

Phase 3 - Laboratory

This phase will consist of a laboratory test program to evaluate the reliability of the proposed detection system.

The experimental data obtained during screening, testing and approval of various fire detector types will provide important practical inputs into a possible system installation in a metal or non-metal mine should this be compatible with Bureau of Mines ultimate objectives and mining companies or mining unions safety requirements. It is to be emphasized that an actual system installation is outside the scope of work of the present contracted effort.

This final report brings together the subject matter which was presented earlier in our interim Phases 1 and 2 technical reports. It also includes the results of the laboratory work which comprised Phase 3.

The Phase 1 effort includes information obtained from detailed literature searches, on-site and telephone consultations with various knowledgeable personnel, mine visits and mine fire interactions with our subcontractor, H. A. Spalding, Inc., a mining consulting engineering firm, and subsequent data analyses. Primary consideration was given toward a detailed study of the operational characteristics of fire detectors (conventional and non-conventional) and gas sensors; potentially promising detector hybrids were also given appropriate consideration. Likely problem areas such as, for example, those dealing with mine detector spacing and positioning, were examined.

In Phase 2, laboratory screening of the performance of detectors in the presence of incipient and flaming combustion sources is documented. This approach follows the results of our Phase 1 study which led us to conclude that an off-the-shelf reliable (low frequency of false alarms) system for detection of real fire hazards in the extreme metal and non-metal mine environments may not be available. Alternatively, since for many generic types of detectors test data were lacking upon which one could form a firm conclusion concerning the merits of the given detector in the mine environ- we were not justified in proceeding to develop new detection systems. That is, screening of the detector's performance characteristics prior to new detector development was the adopted approach. Furthermore, it was emphasized in our Technical Proposal that new detector designs will be limited to hybrid units, i.e., systems comprised of state-of-the-art detectors operating on different detection principles and other off-shelf items that may surface during the course of the proposed study. The timing for the various phases is such that only existing detectors under current development or used in other areas not familiar to us could be screened, evaluated for reliability, etc., within a one-year time period.

The Phase 3 effort includes testing of various fire detectors under flaming and smoldering combustion conditions, and simulated mine ambient contaminants—water mist, and rock dust clouds.

II. BACKGROUND AND DISCUSSION

The need for reliable and timely detection of the onset of fires in metal and non-metal mines cannot be underscored too greatly in light of the recent major disaster from fire and smoke contamination at the Sunshine Mine in which 91 men died (the worst fire tragedy in the U. S. in 1971) (1, 2). Although it may be argued that this represents a statistical deviation from the general fire behavior in such mines, the occurrent of fires of various origins throughout the years where documentation is available (2-25)* illustrates the importance of incipient fire detection. That is, detection at the incipient stage of a fire, followed by warning and subsequent evacuation of personnel, minimizes exposure to buildup of toxic gases and smoke likely to obscure vision and prolong egress. The release rates of products of combustion and thermal energy cover a very wide range of problems between two limiting cases: 1) ignited or open fire (slow to rapid temperature versus time histories) due to ignition of NFPA class A-C fuels in production or transport areas and 2) spontaneous combustion in larger unattended regions (weeks to several months or even longer). Rapid release rates due to fuel/air ignitions or explosions in gassy or combustible ore mines, such as in sulfide orebodies, are excluded from the present study since they are receiving considerable long range attention in related areas involving expanding flames via methane-air ignitions and coal dust-air explosions (26).

Properly used and reliable fire sensors, categorized as direct contact, optical view field and products of combustion, are highly desirable from a life safety viewpoint in metal and non-metal mines. Since it is well-known that fire damage in such mines generally involves only property and downtime, minimization of such losses through use of fire detection devices also readily follows. Questions arise concerning proper use and reliability of state-of-the-art sensors, which were developed for normal industrial or residential use, military or commercial aviation fire protection, in mines. Proper use includes not only the selection of the appropriate sensor(s) for the area to be protected, but critical questions concerning minimum detector spacing and positioning. Detailed protection methodology based on National Fire Protection Association (NFPA) standards for the various sensors in industrial and residential use is inapplicable from simple cost considerations, i.e., a typical large mine may have around 300 miles of tunnels. Protection of high risk areas such as rubber conveyor belts for haulage (27), large diesel powered trucks (28, 29), and the working face (drill-vein interface) in coal mines from methane ignitions (30) are illustrative examples of proper protection.

---

*Reports provided by John Nagy of MESA, Pittsburgh, Penna. Only those reports judged most relevant to the present study and from which legible duplicates could be obtained were examined herein.

The reliability aspects of the more sensitive optical view field and products of combustion detectors must be subjected to even more critical evaluation in mines since these sensors are prone to false alarming in industrial/residential use (31). Thus, mine environmental extremes:

a) temperatures—sub zero °F depending on mine location and tunnel elevation, to 100°F or even higher;

b) from dry air to 100% relative humidity resembling a dense fog or mist;

c) high air velocities—up to around 40 miles/hr in ventilation air intakes; and

d) pressure drops up to around 12" H_2O across pressure doors

upon which diesel exhaust fumes, shot-firing gases, and normal mine gases can be superimposed, pose formidable obstacles on state-of-the art sensors. Simultaneously sensing CO, CO_2, NO_x* and O_2 gaseous species affords possible techniques to circumvent these complexities. Carbon monoxide sensing, in particular, is viewed as a reliable method for detecting cellulosic and hydrocarbon fires. For spontaneous combustion at least in coal mines, the ratio of carbon monoxide concentration to oxygen deficiency may be a reliable fire detection criterion. Under certain conditions air ventilation networks can enhance detector sensitivity and effectiveness. Sampling tube networks or remote in situ detectors also appear useful for monitoring of several locations individually.

In spite of the aforementioned complexities certain detectors appear applicable in protecting specific mine combustibles or regions while meeting the aforementioned ambient fluctuations and aerosol or particulate contaminant insensitivity. For example, direct contact detectors based on heat detection principles—fixed temperature, rate of rise, rate compensated devices—would appear to provide adequate protection of NFPA Class B fuel storage areas. Alternatively, these devices would not respond to smoldering fires having low heat release rates. The successful demonstration of an infrared/heat sensor system for large diesel trucks (28, 29) appears directly applicable to NFPA Class B fuel storage areas.

The important aspects pertaining to mine fire detection discussed briefly in the preceding paragraphs will be considered in greater detail in the following subsections because of its importance to the detection problem.

---

*Pertains to total oxides of nitrogen, primarily NO and NO_2. At flame temperatures NO_x is essentially entirely NO.

2.1 Metal and Non-Metal Mine Fire Data

Detailed fire statistics similar to that compiled for coal mines (for the past 20 years an average of roughly 50 major fires resulting in an average fatality rate of 4 per year in the U. S. A. coal mines (32, 33)) are apparently not available for domestic or foreign metal and non-metal mines (34). Nevertheless, the comprehensive report by Harrington in 1933 (4) and Bureau of Mines reports Refs. 2-25 and recent detailed contractor reports in Refs. 35 and 36 provide adequate information for assessing fire types, potential causes and fire detection effectiveness in these widely varying situations.

Harrington's report not only presents detailed fire statistics but also various important mine operating and fire control procedures many of which are applicable to this day. Although it is reported that in 90% of metal mine fires there was no loss to life, heavy losses occurred in property. The statistical data contained therein are summarized in tabular form in Table I. It is interesting to note the roughly 10-fold increase in electrically caused fires with increased use in place of open flame lighting devices. Other important aspects of this report may be paraphrased as follows:

1) Timbered stopes back filled with waste-rock material containing considerable percentages of finely divided copper or iron sulfides, once ignited, constitute a most difficult fire.

2) Careless practices in leaving chips or shavings of timbers, excelsior, sawdust, oily waste, old clothing and other combustible refuse in abandoned workings have resulted in starting or aiding destructive fire growths.

3) A large proportion of fires in metal mines originate at or near shafts. Intake-air shafts are generally dry and if timbered constitute a fire hazard. Downcast shafts should be concrete and if not feasible, timbered shafts and shaft stations should be fireproofed. Since many fires in timbered shafts are started by electrical wires, it is desirable, where feasible to transmit electric power underground through drill holes.

4) Have available water lines at least 2" in diameter with suitable surface storage and valve control on important levels, not only in shafts and shaft stations, to combat fire hazards.

5) There should be at least two openings through either of which one may escape without danger or difficulty; if the mine is deep (say, 500 feet or over) and employs a considerable number of men (say 25 or more underground on one shift), two shafts should be available, each with hoisting equipment capable of removing the men from the lowest levels with minimum delay.

6) Use of a properly controlled and maintained ventilation system with a) air-tight doors so placed as to be able to isolate shafts from mine levels; b) air splits held absolutely separate from each other—hence,

able to confine smoke to but a small part of the mine; and c) the main man way downcast or on the intake—hence, allowing escape in fresh air unless the fire is in the main travel way, is probably the best and most effective method of life and property protection in the event of a fire.

7) Fans should have reversing features if main shafts or travelways are upcast.

8) Properly supplied refuge chambers with air-tight doors are suggested for mines with bad fire hazards, or should be required for mines with only one opening to the surface.

Observation of these recommendations of Harrington would appear to have been sufficient for preventing the major Sunshine disaster. That is, Riley (37) points out that air from the main fans fed the fire in a worked-out and abandoned area of the mine and forced toxic gases and smoke through abandoned raises to two major haulage levels contaminating the main intake airstreams. Smoke then followed the normal air path into the work areas then back up through the active stopes to the exhaust airway, forming in effect a closed circuit.

A summary of probably fire origins or causes of fires in Refs. 2 and 4-25, is given in Table II. This tabulation is far from complete. Since September 16, 1966, the effective date of the Metal and Non-metallic Mine Safety Act, 33 recorded fires resulted in a total of 114 deaths (37). These fires involved nearly every type of fuel and circumstance. Actually, at the Sunshine Mine alone, prior to their major disaster, several fires occurred—involving a conveyor belt, cable reel machine, battery powered locomotive, and two involving transformers; fortunately no fatalities occurred.

The Table II data are informative since they show a fairly high percentage of fires of electrical origin. Thus, it seems important to examine detection of such types of fires in the laboratory screening of Phase 2 of our study. Likewise, solid fuels such as wood, selected plastics such as fire retarded polyurethane foam, various sulfide ores in conjunction with cellulosic combustibles, selected liquid fuels such as lubricating oils and brake fluids also merit attention.

The compendium of Greuer (35) having 147 references contains a detailed accounting of the influence of mine fires on the ventilation of underground mines; thus important fire detection information such as rates of fire growth, extent of contamination of ducts, etc., are contained therein. Some of the important highlights are, therefore, given in abbreviated version in the following paragraphs.

The greatest hazards of mine fires are caused by:

1) Toxic and sometimes explosive products of combustion carried by the ventilation system through the mine.

2) Unexpected airflow reversals carrying toxic fumes to intake air ventilation areas, such as, fire escape routes, hoist areas, i.e., areas generally considered safe in event of a fire.

Mine fires may be of two distinctly different types—oxygen rich or overventilated or fuel rich or underventilated. Parameters that influence these types are chemical nature of the fuel, fuel loading, ignition source, airflow rate or in other words, the fuel to air ratio, in "classical" combustion terminology. Some highlights for selected mine combustibles are given in Table III. For timber fires, the fuel rich fire type represents an extreme toxicity hazard due to very low O_2 concentrations (16% O_2 is minimum required to sustain life over short time periods) and high CO and CO_2 concentrations. In comparison with fuel lean conditions, the amount of smoke given off for fuel rich conditions is also greater; thus egress times are prolonged due to obscured vision and toxic species exposure correspondingly increases. Polyurethane foam seems to represent an extreme hazard not only since its mass rate of fuel evolution per area is roughly triple that of timber, but also since its products of combustion are more toxic* (LTV of HCN and CO are 10 ppm and 50 ppm, respectively) and emit denser smoke (38, 39). It is important, therefore to detect these hazardous fire types at the earliest possible stage.

The analytical prediction of airflow reversal in a mine even with idealized geometry is an extremely difficult task. Greuer (35) expends considerable effort examining various aspects involved in reversing ventilation airflows. For the three types of airways, horizontal, ascentionally and descensionally ventilated airways, the following important qualitative predictions warrant mention:

1) Horizontal airways: open fires with only negligible temperature changes in following non-horizontal airways produce a throttling effect which produces an airflow decrease in the airway and all airways in series with it. Airflow reversal cannot occur in the airway and the series airways.

It is possible to reverse airflow in diagonal airways which are connections between parallel airways.

2) Ascentionally ventilated airways: natural convection will generally be stronger than throttling effect and increase airflow for at least moderate temperature differences and elevations and not too large air flows. The increased airflow is accompanied by a decrease in parallel airways. For small ventilation pressures in these airways airflow standstills and reversals can occur with known dangerous effects.

3) Descensionally ventilated airways: natural convection for a sufficient driving force decreases, or, can even reverse the original ventilation

*Flame retarded polyurethane will burn at a slower rate and produce denser smoke than the non-retarded variety; additional toxic species result from the degradation of the flame retardants.

flow even though they are opposed in direction. Violent fluctuations in air flow is expected during fire.

For an actual mine under operating conditions, it appears inconceivable for one to predict the occurrences and paths of air flow reversal(s) within the time scales necessary for rapid mine evacuation. The need for reliable fire sensors is once again evident.

2.2 Metal and Non-Metal Mine Environments

Typical mine environmental extremes in temperature, humidity, air velocity, in addition to background aerosol signatures due to diesel exhaust fumes and shot-firing gases, etc. were mentioned on page 4. Discrimination against these normal mine ambient parameters appears important in the design of reliable fire detection systems. The analysis of noncoal mine atmospheres by Mine Safety Appliances (MSA) Research Corporation under a Bureau of Mines contract (40) provides CO, CO_2, condensation nuclei, NO_x (also NO breakdown), and SO_2 concentration data for shot firing and diesel operations for selected mines and sampling sites. A brief tabulation of the highlights of their study is given in Table IV. The high particulate concentrations expressed in terms of condensation nuclei, are indicative of an actual fire situation. Photoelectric products of combustion detectors sensitive to visible particulates would seem to be less sensitive to these operations. However, it must be emphasized that the visible particle fraction was not determined, and since shot firing and diesel operations are known to give off visible smokes, it is probable that photoelectric sensors will false alarm during these operations.

The measurement and control of diesel emissions is a subject of much concern to Bureau of Mines personnel (41, 42). Figure 1 shows the principal diesel pollutants. Under typical combustion conditions, one pound of fuel produces approximately 200 ft^3 of exhaust gas which is comprised roughly of 20 ft^3 CO_2, 1/3 ft^3 CO, 1/3 ft^3 NO_x, with remainder N_2 and H_2O vapor. Methods for control of a) diesel smoke, b) CO, total hydrocarbons, and odor and c) NO_x are presently available and either have been, or are being incorporated into today's diesel equipment. CO_2, however, cannot be controlled. It is directly and linearly dependent upon the amount of fuel burned, and since it is produced in large quantities Bureau emphasis is upon CO_2 monitoring as the indicator of residual exhaust contamination. It is interesting to examine Figure 2 in the low concentration range for which the ratio of CO/CO_2 is constant. For typical operations the ratio CO/CO_2 is approximately 1/50 to 1/125. The value 1/50 is surprisingly close to the mean of the CO/CO_2 values obtained by MSA given in Table IV. One reason for not approaching the 1/125 ratio is apparently due to more complete combustion conditions in the testing of Refs. 41 and 42 while in the actual mine environment more complete combustion would seem difficult to attain. Although discrimation against diesel exhaust and shot firing operations based on differences in the ratio of CO/CO_2 initially appeared promising, more recent in-mine sampling data (Table XII) show only slight differences in the CO/CO_2 values for these operations versus actual fires. The concept of gas sensing the ratio of two species nevertheless remains valid for CO/NO_x and CO_2/NO_x as shown in this Table. This will be considered in some detail in later sections.

In order to obtain actual fire detector performance information in a mine, battery powered ionization detectors were taken below ground by Gillette Research Institute (43, 44). Performance behavior may be summarized as follows:

1) Statitrol-Smokeguard I was unsatisfactory on an overall basic in the Bunker Hill Mine, Kellogg, Idaho, primarily in areas contaminated with high concentrations of aerosols and in regions of high ventilation air flows. Satisfactory performance was obtained in regions supplied by low-velocity intake air.

2) BRK Electronics Model SS74R (a dual gate type ionization detector) performed reliably in Central Rock Company (CRC), Lexington, Kentucky. It should not be inferred that the BRK detector is superior to the Statitrol unit since the Bunker Hill mine presented far greater environmental extremes than the CRC mine. Since the Bunker Hill data was short term in nature, i.e., poor performance obtained after just a few hours in the mine, it appears unlikely that any ionization detector can perform satisfactorily in active mine areas for periods of even a few months.

III. DETECTOR ENVIRONMENTAL CONSIDERATIONS

A survey of the current state-of-the-art of fire detection devices (conventional and non-conventional types) and gas sensors is presented. In certain cases there is overlap between the classification schemes, since certain types of fire detection devices are gas sensors and gas sensors such as, CO, CO_2, NO_x may be loosely interpreted as non-conventional products of combustion type fire detectors. In various aspects this review reflects the earlier studies of Refs. 45 and 46; however, recent pertinent information obtained from literature searches and fire detection study programs updates these earlier works. The fire and normal mine environment detailed in Section II preceding is again considered here emphasizing fire detection concepts.

The objectives of this review section are to examine the operational characteristics of fire and gas detection devices under different test conditions and to outline potential areas of mine applicability and likely problem areas. Furthermore, promising detector hybrids and modifications to existing devices which could minimize some of the mine environmental extremes and thereby extend the useful life of sensitive detectors in a mine are also considered. This is done within the framework of detector reliability, reasonable cost, compatibility with Bureau regulations and requirements and fire suppression methods.

3.1 Fire Detector Reliability

The present status of the reliability of fire detectors obtained in industrial/residential embodiments up to 1970 is illustrated by the Joint Fire Research Organization (JFRO) data in Tables V and VI which show very high false alarm ratios—average being 11:1.

In the extreme environment of aircraft engine nacelles of USAF aircraft, 83% of all reported alarms are false (47). This covered the time period from 1965-1970 and 1250 total alarm cases with 1036 false alarms. It was also found that in roughly 50% of the engine nacelle fires, where detection system performance could be determined, the system did not alarm at all. The detection systems were primarily direct contact thermal sensors involving continuous overheat line and thermocouple sensors of several different commercial vendor types. By utilizing an integrated systems approach involving four pairs of fire sensors in each nacelle, with UV and IR sensor in each pair and a dual-loop overheat sensor coupled with computer control for signal processing and crew warning false alarms are expected to be eliminated (48). The important detection criterion here, requires that two sensors with the same optical field of view must indicate the existence of a fire before a fire warning is signalled to crew readout. Actual tests results are not yet available. Such an approach is certainly applicable in a mine in areas where fuels that undergo flaming combustion are stored.

If we take a closer look at existing fire detectors—Table VII, one observes that those detectors having rapid response times also have high false alarm ratios. The numbers 1 through 5 indicate the fastest to slowest response times, respectively. It should be pointed out that this behavior applies specifically to residential and certain industrial types of ambient environments. For example, returning to the engine nacelle fire, fixed temperature heat sensors would almost certainly receive a 1-2 classification because of very rapid heat release rates for jet fuels coupled with the confined nacelle environment and close proximity of the sensor. A 6 to 8 second response time for overheat sensors is generally required (47).

A generalization of Table II performance data to the metal and non-metal mine environment is not possible at present because of lack of adequate experimental data. However, one might expect higher false alarming ratios in the mine environment because of far greater adverse ambient conditions, as well as mechanical, electrical, and communication difficulties therein. This has already been observed for the ionization detector (page 9). Utilization of an integrated or hybrid system concept does not follow as readily as for the engine nacelle fire since mine fires cover spontaneous combustion to flash fire types. For example, we wish to protect an area from a potentially slowly developing fire expected to give off large quantities of smoke, coupling say an ionization or photoelectric detector with a fixed temperature/rate of rise thermal sensor by requiring alarm for both sensors. This could possibly not lead to alarm or alarm at a very late stage when the fire is already out of control because of the delayed response of the thermal sensor. This hypothetical example seems realistic, especially if the heated combustion products are diluted with cool inlet ventilation air. The integrated concept appears applicable only when one couples different detectors of similar time responses.

Detector companies state that improper maintenance is an important factor contributing to the 46% mechanical and electrical failure rate (50) in Table II. However, recommended cleaning procedures, such as dust or adsorbed

combustion products removal from electrode plates of ionization detectors via disassembling the detector head or inserting a new detector followed by cleaning of the used detector above ground, appear to pose a heavy burden on effective maintenance in environmentally extreme regions of the mine. Other problem areas come to mind which will be discussed under the behavior of the various detector types.

Since it is recognized that there is no universally applicable fire detector, i.e., one which responds accurately and uniformly to all types of fires, the various detector types will each have certain advantages and disadvantages (see Table VII for sensitivity versus frequency of false alarming). Tradeoffs in detector characteristics are also common, e.g., increased sensitivity to a lower threshold level of combustion product versus an increase in the integrated time for detection.

It is interesting to note that there is no published long-term information (say around a year or so) on detector sensitivity under conceivable extremes of ambient conditions, such as high relative humidity, vibration, concentration fluctuations from diesel exhausts, shot-firing gases, high concentration of dusts, oily or corrosive vapors, etc. Such information is vital to the detection problem in mines.

One way of summarizing our feelings about mine fire detector installation(s) is that, unreliable fire detectors should not be installed in mines. This follows from numerous verbal disclosures pertaining to industrial fire detection where frequent false alarming led to turning the detection system off while not notifying the proper personnel followed by the fire scenario. Documentation is available for aircraft where fire detection systems were partially or totally removed to reduce or eliminate false alarming (47). Applying this form of thinking to the mine problem, it is concluded that considerable harm or damage to life and property could result if a miner is operating under a false sense of security. An actual fire not followed by alarm even though smoke is detected by the senses could be ignored since it was conjectured to be due to normal mine blasting or diesel operations.

3.2 Fire Environment/Detector System Design

In order to design an effective fire detection system, one needs to assess available information on at least the following factors:

a) Fire Itself - Need to know the relationship between the fuel (NFPA classes A-C*) and surroundings. The type, the amount, the arrangement, heat release rate, as well as the nature, size, and ventilation patterns of the enclosure enter into the picture.

---

*Class A: Fires involving ordinary combustible materials (wood linings, timber supports, ventilation supports, packaging materials, conveyor belts, polyurethane, polyvinylchloride, etc., and, in a loose sense, combustible ores, shales, and explosives.
Class B: Fires involving flammable or combustible liquids, gases, and greases; for example, petroleum fuels, lubricating oils, hydraulic brake fluids, and combustible mine gases.
Class C: Fires involving electrical equipment; for example, overheating of polyethylene insulated (neoprene coated) power line cord.

b) Mine Environment - Specified previously.

c) Damageability of Area and Life Hazard - Areas in the mine which represent high risks to personnel and property would require increased numbers of detectors per given area versus low risk area. High risk areas would seem to include fuel storage depots, regions at or near shafts and abandoned or worked-out areas containing combustibles capable of undergoing spontaneous combustion.

d) Response Time of the Agent that Puts the Fire Out and Application Mode - Halon 1301; AFFF, high expansion foams, chemical foams alone/or with dry powder; manual, automatically actuated system, or crash truck system. Temperature-time histories for Class A-C fuels encompass very slow conditions (spontaneous combustion-orders or weeks or months or even longer) to very rapid (essentially instantaneous, i.e., order milliseconds such as ignition of methane-air or dust-air mixtures) (26).

Major problem areas besides the effects of fire on ventilation or vice versa and mine environment on detector integrity would also appear to include system installation ease, portability—thus ruggedness and adaptability to another location differing in size, geometry, ventilation patterns and ambient environment. As active areas of the mine are worked out, combustibles necessary to sustain normal operations are often moved closer to the new active area in order to operate efficiently. These problems imposed by system portability are of course not inherent to fixed installations.

3.3 Aerosol and Gaseous Fire Signatures

Characteristics common to mine fires of primary concern are the generation of aerosols and release of gaseous combustion products, notably CO and CO_2. Aerosols cover a particle size range of from 5×10^{-3} microns (values down to 1×10^{-3} are doubtful) up to 50 microns—Table VIII (51). Heating materials first produce submicron particulates around 1×10^{-3} microns with particle sizes ranging from 0.01-1 microns around ignition temperatures. A particle size of 0.3 microns is the dividing point between invisible and visible particles, i.e., particles less than 0.3 microns do not scatter light very well and are thus classified as invisible, whereas, particles greater than 0.3 microns do scatter light and are classified as visible. The size range of 0.01-1 microns covers smokes; an upper range of 5 microns is given in Ref. 52 for smokes. Smokes are defined here as low vapor pressure particulates which settle slowly under gravity. In the upper aerosol size range, mists are also given off during the combustion process. Mists are liquid droplets which can be formed by condensation of vapor following cooling of heated fire gases, e.g., via turbulent heat and mass transfer exchange with cold ambient air.

The generation of smoke or its dependence on specific physio-chemical parameters has not been rigorously determined for fire related problems. The problem of particle aging as pertains to fire detector response also

comes to mind. Nevertheless, fundamental information derived from air pollution studies contained in a number of monographs, such as Refs. 52, 53, and 54; and current literature, such as Refs. 55, 56, 57, and 58, is applicable in limited regions.

One of the main characteristics of particulate clouds is their instability. Particles may grow by coagulation or by vapor condensation on smaller nuclei. They may disappear by evaporation, sedimentation or diffusion to confining walls of enclosures. If a certain fraction of the heterogeneous mixture is charged unipolarily then increased stability almost comparable to hydrosols can be obtained. Another complication can arise from aerosol formation by mixing of vapor-laden gas streams at difference temperatures, e.g., a clean burning fuel giving rise to a free convective turbulent plume that entrains cold atmospheric air. The phenomenon of thermally induced stratification of smoke can adversely influence particle movement. For example, a thermal gradient beneath a ceiling can prevent smoke from penetrating the ceiling's thermal boundary layer. In Ref. 59, a vertical temperature gradient of only approximately 5°C in 100 feet was required to stratify cold smoke at the 75 foot level. There is every indication that this phenomenon can occur at much smaller heights since thermal stratification was actually an early technique used in aerosol studies for particle sizing (60).

Another important characteristic of particulate clouds is their ability to scatter, reflect, and absorb radiation to a degree depending on their size, color, shape, and wave length of incident radiation. Mie theory describes the scattering of radiation by optically isotropic spheres, i.e., non-absorbing substances. The commonly used Lambert-Beer law, also frequently referred to as Bouguer's law, is used to describe the absorption of radiation as a function of absorbency index, concentration, and path length.

Considerable practical information on smoke produced from burning of various materials exists in Refs. 39 and 61. The important findings on over 100 different materials under a 2.5 W/cm^2 radiant heat flux exposure (39) may be paraphrased as follows:

1) Woods, including solid woods, plywood and other cellulosics show specific optical density versus exposure time variations similar to those for red oak in flaming and non-flaming exposures, both with and without ventilation. Fire retardant treatments produced denser smokes under flaming conditions.

2) Plastics may be divided into two broad categories: A) produce no visible smoke under either flaming or non-flaming exposure—few in number; B) smoke producers—vast majority—subdivided further as: a) behave similarly to wood, slowly building up to a high density; b) build up fairly rapidly but to about the same density.

3) In presence of heat and flame two separate phenomena were observed: a) plastics which tend to burn cleanly are similar to wood under similar conditions; b) those which do not burn cleanly, i.e., are fire retarded, rapidly evolve dense to very dense smokes. These are not readily cleared away by ventilating.

In mines, likely sources of dense smokes include at least the following: synthetics or plastic materials, such as polyurethane and various packaging materials, clothing items, flame-retarded conveyor belts, electrical insulation, lubricating oils and greases, petroleum fuels (increased smoke density with an increase in aromatics and higher molecular weight straight chain hydrocarbons), hydraulic brake fluids, and shales. Cellulosic fuels such as wood linings, timber supports, cardboard boxes, mine gases such as CH_4 would seem to comprise the more important fuels of lower density smokes. Wood age and moisture content would be important variables in this classification scheme. In addition, mine dust, its color and concentration, would also appear to be of importance.

The release of gaseous species depends strongly on the chemical composition of the material and its mode of heating. For wood, four distinct temperature zones are given for thermal decomposition as follows (45):

Zone A: below 200°C. Appearance of non-combustible gases, primarily H_2O vapor, traces of CO_2, formic and acetic acids, and glyoxal. Dehydration of sorbed water is complete.

Zone B: 200°C to 280°C. Some gases as in Zone A are produced along with greatly reduced quantities of water vapor and CO. Reactions are endothermic and products are almost entirely non-flammable.

Zone C: 280°C to 500°C. Active pyrolysis takes place under exothermic conditions leading to secondary reactions among the products. Largely combustible products, CO, CH_4, etc., and flammable tars in form of smoke particles.

Zone D: above 500°C. Residue consists primarily of charcoal, which provides an extremely active site for secondary reactions.

The early combustion stages are similar to the pyrolysis stages, modified slightly by oxidation. These stages are categorized as follows:

Zone A - Similar to Zone A above but slightly affected by some exothermic oxidation processes.

Zone B - Primarily exothermic reaction takes place without ignition.

Zone C - Combustible gases that are ignitable are produced after secondary pyrolysis. Flaming combustion can occur in the gas phase if the gases are ignited. If ignition is not induced, flaming may not occur until near the end of pyrolysis when the evolved gases cannot insulate the charcoal layer from O_2. Spontaneous ignition of charcoal takes place at a temperature lower than any of the products evolved.

Zone D - Greater than 500°C the charcoal glows and is consumed; greater than 1000°C non-luminous flames are supported by the combustion of H_2 and CO.

These zones illustrate in an elementary way the complexity of cellulosic combustion processes. In a mine environment an agglomeration of solid and liquid aerosols and gaseous species will be present in various degrees.

For combustion of various other mine materials other gaseous species besides CO and CO_2 may include, at least, lower molecular weight hydrocarbons, NO_x, NH_3, HCl, HCN, HF, aand H_2S (38, 62). With the exception of certain plastics known to yield high concentrations of these gases, e.g., PVC which yields roughly 50% by weight of HCl upon heating to temperatures in excess of 300°C (63), designing fuel specific detectors offers limited applicability. For example, PVC pyrolysis and/or combustion produces copious quantities of smoke and, thus, this signature can be detected by conventional means.

The gases of importance appear to be CO, CO_2, O_2 deficiency, and NO_x. The ratio of CO/O_2 deficiency appears to be a reliable parameter to follow the onset of spontaneous combustion in coal mines. O_2 deficiency is also the result of fuel rich burning—Table III. CO and CO_2 need no further amplification here. NO_x is important only because it is a product of high temperature combustion, such as, in a deflagration wave in diesel engines and controlled mine blasting or explosion operations. Most naturally occurring and synthetic materials, excluding those containing high nitrogen contents, such as the acrylonitriles (64) and possibly polyurethane, under fire conditions will not produce the temperatures for high NO concentrations. Thus, sensing NO_x appears to afford a means for discriminating against ambient diesel and blasting signatures which have all the characteristics of an actual fire. This point will be discussed further, in connection with multipoint gas sampling systems.

Sensing CO, CO_2, or the ratio of CO/CO_2 as an indicator of a fire requies comment. Presently, it appears that sensing CO or CO_2 separately is limited to a hybrid system, i.e., one used in conjunction with other existing detectors, whereas, sensing CO/CO_2 may prove reliable for the following reasons:

1) The lower threshold value (LTV) based on an eight-hour exposure to CO is 50 ppm; thus, certain types of fires may go undetected if the CO detector is of a low sensitivity type. The lower limit of CO will be determined by the type of sensor and its environment*.

2) Employing a CO detector that responds at say 1/2 the LTV value or 25 ppm would seem to be prone to false alarming. Nearness to a source of

---

*At the Sunshine Mine, Kellogg, Idaho, CO levels (using a hopcalite catalyst (see Ref. 43) as a sensor) for closing fire doors had to be set at roughly 300-400 ppm to avoid false alarming.

discrimination portion responds to approximately 4000 to 5500A°. The two elements function as a spectral voltage divider to detect flame and discriminate against ambient light such as from sunlight, incandescent and fluorescent lighting. Its quoted sensitivity is 20 ft to 1 ft^2 of hydrocarbon fire at 10 ft candle ambient light level (higher ambient light levels decrease its sensitivity); its cone of vision is 120 degrees. It is recommended for use in low ambient light regions (such as in a mine) because of desensitization by high ambient light.

Infrared detectors are also classified broadly according to their response to heat and a photon flux:

1) Thermal Detectors - energy absorbed by a temperature sensitive material or absorbing film in contact with the temperature sensitive material. Here one placed thermocouples, metals or semiconducting layers with resistance a function of temperature (bolometer), pyroelectric detectors whose polarization is temperature dependent, and gases with pressure (in a pneumatic cell) being temperature dependent.

2) Quantum Detectors - Photon flux incident on sensing element excites electrons in a bound state to a free or conducting state.

Another classification is to subdivide the IR spectrum into three divisions according to the different detector types required for each area (85).

1) Near-infrared - conventional Si and Ge detectors

2) Intermediate - special IR detectors

3) Far infrared (20 μm) - Thermal detectors such as thermistors or thermocouples are required (see contact detectors).

PbS is one of the most versatile photoconductors which responds to the IR from approximately 1 to 4 μm. Intrinsic, i.e., undoped, Si and Ge detectors have limited near IR response. However, doping with Hg and Cu extends the Ge operation up to 8 to 14 μm. Far infrared detectors are generally of the bolometer (IR heat detector for special applications) or thermocouple types.

Although there are numerous detectors presently available, most require cooling. Generally, detectors with response up to around 3 μm and 180° field of view looking into ambient background (25°C) require little if any cooling (86). Spectral response, speed of response, and the reciprocal of the noise equivalent power or detectivity, D*, provide further detector characterization. Here D* is the detectivity of a detector of a 1 cm^2 area whose noise is reduced to that obtained with an amplifier of 1 Hz bandwith

$$D^* = \frac{S/N}{P_D} \left(\frac{\Delta f}{A} \right)^{1/2} \qquad (1)$$

where S and N - signal and noise, respectively
P_D - power density received by detector
A - detector area
Δf - amplifier bandwith

Sensitive areas vary from 0.01 mm^2 to 1 cm^2, with time constants shorter than 1 nanosec. PbS, one of the earliest IR photon detectors, responds well to low wave lengths; InSb, however, is more useful since it covers the CO, CO_2 bands (66). An IR detector using selectively the 4.4 μm CO_2 band in a Wheatstone bridge circuit is described in Ref. 87.

The newer pyroelectric type detectors consist of a slice of ferroelectric material (typically triglycine sulfate, tourmaline, Rochelle Salt, barium titanate) and more recently polyvinylfluoride (86, 88, 89). Electrically, the material behaves similar to a capacitor with a strong temperature dependent polarization of the magnetic domains. Small temperature increases caused by IR radiation through a transparent electrode produce a polarization charge on the pyroelectric material and a corresponding voltage change across the two electrodes of the sensing cell. Because of its high impedance a field effect transitor (FET) is utilized to lower the output impedance. Ref. 88 deals with use of polyvinylfluoride sensing material in a scanning thermal setup for fire detection. Commercially available pyroelectric IR detectors of triglycine fluoroberyllate and triglycine sulfate require no cyrogenic cooling and operate at ambient temperature ranges from -10°C to 60°C, and -10°C to 40°C, respectively (90). With a standard window (model type KRS-5) the spectral response is from 1 to 45 μm with a total sensitivity up to 500 μm. Because of its higher operating temperature, the fluoroberyllate would appear more useful than the sulfate for mine applicability.

The number of semiconductor ultraviolet detectors (UV) (wave lengths less than roughly 4000A°) is very small compared to the IR region (86). This is due to basic problems encountered in UV detection.

1) Conventional glass windows cut off below around 3000A° and even quartz and UV-grade sapphire become opaque below 1800A°.

2) Below around 1000A° suitable UV windows are lacking. Detection in the intermediate or vacuum ultraviolet is generally accomplished by multiplier phototubes with photocathodes that are blind to wave lengths greater than 3000A°.

The Honeywell basic UV detector Model No. C7037A now acquired by Detector Electronics Corporation (Det Tronics Corp.) (91) designed to operate in the 1850-2450A° region is insensitive to both sunlight and artificial light. Its cone of vision is 90°. The quoted sensitivity is a 1 square foot flame from 15 feet. The sensing element is a gas filled, UV sensitive tube operating on the Geiger-Muller principle.

When an energetic photon in the UV spectral range strikes an appropriate cathode (tungsten is used in this device because it is not sensitive to the sun's radiation, etc.) and exceeds the work function of the cathode, an electron is emitted and is accelerated toward the anode (positive) plate. In passage through an ionizable gas toward the anode, the electron strikes gas molecules causing further electron emission. The total electron flow

is typically several million times that of the single electron emitted from the cathode. This leads to an increase in current flow which may readily be measured. The detector is operated in a pulsed mode by allowing current to flow for a very short period of time before the voltage is reduced to stop current flow. Amplification is, thus, required with this device.

Fenwal's UV detector (92) responds to UV radiation in the range 1900A° to 2500A°. It operates on the ionization principle similar to the Honeywell model. It has a 120° cone of vision. The response time given is 15 millisec for a propane/air flame 1.75 inches high at a distance of 8 inches from the flame source.

Other suppliers include McGraw-Edison Company (range 2000-2750A°) (93) and Pyrotector (1700-2900A°, maximum response at approximately 2100A°) which also operate on the Geiger-Muller principle. The latter device is particularly interesting not only from its outward compact design appearance but more importantly it contains a solid state AC-DC converter section to provide the necessary voltage for the detection tube and a signal integrator delay circuit (3 sec. delay) to minimize false alarms from aparks, lightning, etc. (84). Its quoted head-on sensitivity is 6 ft to flame from a 3/4" diameter candle.

Besides the normal problems associated with the inverse square law of radiant energy transmission which include view factors, temperature differences, etc., as well as additional difficulties cited earlier, added factors due to moisture laden environment resembling a fog or a mist would have to be assessed. This follows from the example that radiant energy propagation through a coal dust (a strong absorber of radiant energy) cloud could adversely affect fire detector response (30). Also, contamination of the viewing window with oily film deposits would require attention. Because of the extreme mine environment, we have omitted a discussion of light sensitive laboratory devices such as optical spectrometers or spectrophotometers, since they would not be expected to demonstrate reliability without continuous maintenance.

The likely area of applicability for IR and UV detection is in protecting fuel storage areas since these sensors are known to respond rapidly to flash fires.

4.3 Products of Combustion

Products of combustion in fires include solid particulates and liquid mists (including invisible and visible particle sizes), ionized species, gases, and radiant energy. Combustion product detectors sense one or more of these constituents excluding heat or flame.

Zone D - Greater than 500°C the charcoal glows and is consumed; greater than 1000°C non-luminous flames are supported by the combustion of H_2 and CO.

These zones illustrate in an elementary way the complexity of cellulosic combustion processes. In a mine environment an agglomeration of solid and liquid aerosols and gaseous species will be present in various degrees.

For combustion of various other mine materials other gaseous species besides CO and CO_2 may include, at least, lower molecular weight hydrocarbons, NO_x, NH_3, HCl, HCN, HF,aand H_2S (38, 62). With the exception of certain plastics known to yield high concentrations of these gases, e.g., PVC which yields roughly 50% by weight of HCl upon heating to temperatures in excess of 300°C (63), designing fuel specific detectors offers limited applicability. For example, PVC pyrolysis and/or combustion produces copious quantities of smoke and, thus, this signature can be detected by conventional means.

The gases of importance appear to be CO, CO_2, O_2 deficiency, and NO_x. The ratio of CO/O_2 deficiency appears to be a reliable parameter to follow the onset of spontaneous combustion in coal mines. O_2 deficiency is also the result of fuel rich burning—Table III. CO and CO_2 need no further amplification here. NO_x is important only because it is a product of high temperature combustion, such as, in a deflagration wave in diesel engines and controlled mine blasting or explosion operations. Most naturally occurring and synthetic materials, excluding those containing high nitrogen contents, such as the acrylonitriles (64) and possibly polyurethane, under fire conditions will not produce the temperatures for high NO concentrations. Thus, sensing NO_x appears to afford a means for discriminating against ambient diesel and blasting signatures which have all the characteristics of an actual fire. This point will be discussed further, in connection with multipoint gas sampling systems.

Sensing CO, CO_2, or the ratio of CO/CO_2 as an indicator of a fire requies comment. Presently, it appears that sensing CO or CO_2 separately is limited to a hybrid system, i.e., one used in conjunction with other existing detectors, whereas, sensing CO/CO_2 may prove reliable for the following reasons:

1) The lower threshold value (LTV) based on an eight-hour exposure to CO is 50 ppm; thus, certain types of fires may go undetected if the CO detector is of a low sensitivity type. The lower limit of CO will be determined by the type of sensor and its environment*.

2) Employing a CO detector that responds at say 1/2 the LTV value or 25 ppm would seem to be prone to false alarming. Nearness to a source of

---

*At the Sunshine Mine, Kellogg, Idaho, CO levels (using a hopcalite catalyst (see Ref. 43) as a sensor) for closing fire doors had to be set at roughly 300-400 ppm to avoid false alarming.

products of combustion such as diesel exhaust, shot-firing gases would seem to promote unwanted false alarms. Alternatively, formulation of a detection principle based on alarm only after continuous sensing of a predetermined CO level for orders of tens of seconds would seem dangerous since rapidly developing fires might get out of control.

3) CO_2 is a product of complete combustion and human exhalation and, thus, could be unduly high in certain areas indicative of fire conditions.

4) The ratio of CO/CO_2 for idealized burning of various fuels is well known to be in the ratio 1:2. However, combustion processes in mines are rarely ideal. More recent MSA sampling data (see Table XII) for CO/CO_2 ratios which differ by only factors of 1.25 to 5 for diesel and actual mine fires obviate use of this approach.

Table XII data for CO/NO_x and CO_2/NO_x nevertheless show that values for these ratios may be used to discriminate blasting and diesel operations from mine fires. If CO or CO_2 sensing were to be used for fire sensing because of the high cost of NO_x monitors and the availability of various sensitive CO and CO_2 monitors (65, 66), then false alarming will have to be an accepted consequence. Because of the complexity of sensitive NO_x, CO, and CO_2 monitors which require highly-skilled maintenance, such hardware is recommended only for use in a multipoint gas analysis system.

IV. OPERATIONAL CHARACTERISTICS OF CONVENTIONAL AND NON-CONVENTIONAL FIRE DETECTORS AND GAS SENSORS

The categorization of the various sensors into three classes—direct contact, optical view field and products of combustion requires clarification since, even conventional fire detector devices have back-up features and respond to more than one parameter. For example, ionization type products of combustion (POC) detectors are sometimes equipped with back-up heat detectors; similar features are also available with photoelectric type detectors of visible smoke. For these hybrid types, classification will be according to the primary intended use. For non-conventional fire detectors, many of which have applicability in gas analysis or are outgrowths of gas chromatography, and gas sensors, classification is not that direct as previously pointed out. A few examples are offered for clarification purposes. Thermal conductivity detectors which are classified as filament type detectors in conventional gas sensor terminology will here come under POC detectors since the fire application is to employ differences in thermal conductivity between fire and ambient background as a criterion of the presence of a fire. Non-dispersive infrared analyzers for important fire gases CO and CO_2 usually come under optical methods would here come under products of combustion type sensors. Classification in such a manner is required, although not necessarily the best classification scheme, since it maintains self-consistency and minimizes the numerous possible classified schemes. The detector types may be further divided into the point source, spot or local type depending on preferred terminology (i.e., one actuated by a combustion product or heat brought to the detector by free or forced convective heat and mass transfer mechanisms) or the extended area type.

Information on the different types of fire detectors is now available in comprehensive survey articles (45, 46, 67, 68), NFPA reference books (69, 70), recently proposed standards (71), and corporate sales brochures. Excellent detailed information on gas sensors exists in the monograph of Verdin (66) and recent translations of Russian texts and articles (72-74). Ref. 68 besides including much of the technical information in Refs. 45, 46, 67, 69, and 70, and then some, also contains important discussions of U. S. and foreign performance standards and acceptance criteria for detection devices.

The specific operating characteristics discussed in the sections to follow are based primarily on the updating of Refs. 45 and 46 from information derived from computer searches of the technical literature conducted through National Technical Information Service (NTIS), Smithsonian Data Bank, Chemical Abstracts (using the Knowledge Availability Systems Center, University of Pittsburgh), surveys of open literature, and existing detector programs.

4.1 Direct Contact

Direct contact detectors, or heat sensors, are of two general types; those employing the fixed temperature principle and those employing the rate of rise principle (69). In the fixed temperature approach, an ideal temperature level is first selected, say 131°F ± 5°F. When the active element is completely heated to its operating temperature, the heat sensitive material will bend, expand rapidly, fuse or produce a current which can be used to actuate an alarm. Commercial devices include ampoules, bi-metallic elements, eutectic solders or salts, snap discs, thermocouples, thermistors, continuous wire types—thermistor, eutectic salt or twisted cable (under tension)/ fusible plastic types and certain photoconductors. Major disadvantages, excluding rapid response thermocouples, include slow response times because of built-in thermal inertia and inability to detect certain slow smoldering fires. Response times for commercial fire detector thermocouples are around a few tenths of a second. Primary advantages are low cost, reliability, freedom from maintenance, insensitivity to vibration and dust laden atmosphere.

Suppliers of continuous line heat sensors are Fenwal, Walter Kidde, and Protectowire Company. The sensing element in the Fenwal system is an Inconel tube packed with a thermally sensitive eutectic salt and a nickel wire center conductor (78). When a fire situation occurs at any point along the entire element length, the resistance of the salt drops sharply, thus causing increased current flow. This current flow is sensed by a control unit which produces an output signal to actuate an alarm. The Kidde sensing element contains a ceramic-like thermistor material in which are embedded electrical conductors also housed within an Inconel sheath. Electrically the element behaves as an infinite number of unit thermistors connected in parallel along its entire length (79). The response to fire is to the sum of resistances (in parallel) which reflects a non-arithmetic average. Both units reset themselves upon removal of the fire condition and are rugged enough to withstand severe vibration and shock. A disadvantage is the lowest temperature sensing salt presently available is around 250°F.

The Protectowire line detector is comprised of two twisted high tensile spring steel wires individually encased in a thermoplastic or heat-sensitive material (80). This is spirally wrapped with a protective tape and provided with an outer covering. Upon heating any point along its length to alarm temperature the plastic yields under its applied tension causing the actuators to move into contact with each other. The electrical connections consist of a series connection of a power source, a supervisory relay and a resistor connected to the end of the wire actuators, so that a small current continuously flows through the system. A break in an actuator or loss of power triggers the supervisory relay and it produces a trouble signal from a second power source. Other system arrangements are possible. Following a fire the heated part of the line will look swollen and must be cut out and a new piece spliced in using splicing sleeves. The lowest operating temperature is 155°F and thus appears ideal for mine use. However, while Protectowire is resistant to moisture, chemical fumes, and other deteriorants, the standard type is not intended for use in the presence of extreme moisture, or other deleterious service conditions. However, a waterproofed version is presently available and should prove adequate in the generally moist metal and non-metal mine atmospheres.

A heat-sensing transmission line has been proposed as a possible method of protecting automatic warehouses from fire (81). It operates on the principle that an electrical pulse traveling down the line must sense a discontinuity in the characteristic impedance of the line due to the fire. The line requires characteristics which change rapidly with temperature in order to minimize response time. Experimental results are needed on the parameters associated with fire-damaged transmission lines before this device can be put into operation.

Rate-of-rise detectors are designed to respond to changes in temperature at a rate of around 15°F/min. They are fairly reliable and will not alarm for slow increases in ambient temperature. They are not suitable for smoldering type fires and also where rapid temperature changes are natural occurrences such as near mine ventilation doors connecting tunnels or passageways of widely varying temperatures. Two fairly common rate-of-rise detectors are the pneumatic tube detector which affords extended area protection and an orifice type detector. In the former device, a pressure buildup in a detector diaphragm chamber is used to close a set of contact points at some predetermined value of pressure (67, 69). The latter device relies upon pressure increases resulting from differences in flow rates of an expanding gas passing through an orifice (75). Here sensitivity is directly related to orifice size.

A rate-compensated device of Fenwal and Notifier Corporation combines the fixed temperature principle with the rate of rise (76, 77). The key requirements are materials of different coefficients of expansion. For very low rates of rise, both materials line up evenly and the device operates as a fixed temperature device. For rapid rates of rise the materials no longer expand evenly, which leads to an alarm even though the fixed temperature is not reached. This device also does not have the capability to detect slow smoldering fires.

Our assessment of contact detector applicability in mines is that: applicability is limited to regions where slow smoldering fires are unlikely and the preceding ambient criteria are satisfied; also in regions where products of combustion such as from diesel exhausts, etc., could lead to high false alarm ratios for sensitive combustion product detectors. The distance from the diesel combustion source to detector is important since mixing of heated exhaust products with cooler ambient air is necessary in order that the temperature of the air parcel reaching the sensor not exceed its alarm temperature. Alternatively diluting heated fire gases with cooler ventilation air should not be too great so as to prevent alarm from small flaming combustion sources. Proper detector spacing is viewed as one way to design against this unwanted behavior (see page 36).

4.2 Optical View-Field

Fire detection devices under this category respond to radiant energy in the ultraviolet (UV) and infrared (IR) portions of the electromagnetic spectrum generated during flaming combustion of materials. Many problem areas exist for these devices as illustrated by their high frequency of false alarming—Tables V, VII—and their rather high cost. Principle sensing elements include solid state detectors, tubes—vacuum or gas filled, and thermocouples or thermistors for specialized applications. A summary of the operational principles of photodetectors—photoemissive, photovoltive, photoconductive junction type, and photoconductive bulk effects is given in Table IX (82). Of particular interest in the fire detector field are the photovoltaic devices, which presently often require some degree of amplification. One might expect future devices to respond to fires in a similar way to the RCA light sensitive monolithic IC on page 21 of Ref. 82.

For the infrared detector, background radiation at ambient temperatures from walls (25°C) and people is entirely in the infrared region (wave lengths greater than roughly 8000A°). Discrimination against background is frequently handled by chopping the incident radiant flux so that the detector receives only a fixed radiant frequency, typically 4-30 Hz. One version of an IR fire detector employs a system of optical and electronic filters which limits detection to a narrow signal wave length of range 1-2.75 μm and frequency 4-15 Hz (83). The Infrascan detector described in this reference has a scanning reflector which rotates at 6 rpm. When infrared radiation of the proper characteristic is reflected from it onto a sensitive cell for an uninterrupted period of 15 seconds, an alarm will sound. The radius of scan is up to 400 feet through 360° horizontally. Infrastat, a variation of Infrascan, does not employ a scanner. It is similar to a camera. A photocell is mounted inside a collimating tube protected by a quartz shield. By adjusting this tube, one can vary the angle of the cone of detection from 15° to 160°. Fires outside of this cone of detection will go undetected.

Pyrotector's near IR flame detector (discriminating) responds in the spectral range 6500 to 8500A°. The detection cell is a dual element photoresistive solid state device with appropriate optical filters (84). The

discrimination portion responds to approximately 4000 to 5500A°. The two elements function as a spectral voltage divider to detect flame and discriminate against ambient light such as from sunlight, incandescent and fluorescent lighting. Its quoted sensitivity is 20 ft to 1 ft^2 of hydrocarbon fire at 10 ft candle ambient light level (higher ambient light levels decrease its sensitivity); its cone of vision is 120 degrees. It is recommended for use in low ambient light regions (such as in a mine) because of desensitization by high ambient light.

Infrared detectors are also classified broadly according to their response to heat and a photon flux:

1) Thermal Detectors - energy absorbed by a temperature sensitive material or absorbing film in contact with the temperature sensitive material. Here one placed thermocouples, metals or semiconducting layers with resistance a function of temperature (bolometer), pyroelectric detectors whose polarization is temperature dependent, and gases with pressure (in a pneumatic cell) being temperature dependent.

2) Quantum Detectors - Photon flux incident on sensing element excites electrons in a bound state to a free or conducting state.

Another classification is to subdivide the IR spectrum into three divisions according to the different detector types required for each area (85).

1) Near-infrared - conventional Si and Ge detectors

2) Intermediate - special IR detectors

3) Far infrared (20 μm) - Thermal detectors such as thermistors or thermocouples are required (see contact detectors).

PbS is one of the most versatile photoconductors which responds to the IR from approximately 1 to 4 μm. Intrinsic, i.e., undoped, Si and Ge detectors have limited near IR response. However, doping with Hg and Cu extends the Ge operation up to 8 to 14 μm. Far infrared detectors are generally of the bolometer (IR heat detector for special applications) or thermocouple types.

Although there are numerous detectors presently available, most require cooling. Generally, detectors with response up to around 3 μm and 180° field of view looking into ambient background (25°C) require little if any cooling (86). Spectral response, speed of response, and the reciprocal of the noise equivalent power or detectivity, D*, provide further detector characterization. Here D* is the detectivity of a detector of a 1 cm^2 area whose noise is reduced to that obtained with an amplifier of 1 Hz bandwith

$$D^* = \frac{S/N}{P_D} \left(\frac{\Delta f}{A}\right)^{1/2} \qquad (1)$$

where S and N - signal and noise, respectively
P_D - power density received by detector
A - detector area
Δf - amplifier bandwith

Sensitive areas vary from 0.01 mm^2 to 1 cm^2, with time constants shorter than 1 nanosec. PbS, one of the earliest IR photon detectors, responds well to low wave lengths; InSb, however, is more useful since it covers the CO, CO_2 bands (66). An IR detector using selectively the 4.4 μm CO_2 band in a Wheatstone bridge circuit is described in Ref. 87.

The newer pyroelectric type detectors consist of a slice of ferroelectric material (typically triglycine sulfate, tourmaline, Rochelle Salt, barium titanate) and more recently polyvinylfluoride (86, 88, 89). Electrically, the material behaves similar to a capacitor with a strong temperature dependent polarization of the magnetic domains. Small temperature increases caused by IR radiation through a transparent electrode produce a polarization charge on the pyroelectric material and a corresponding voltage change across the two electrodes of the sensing cell. Because of its high impedance a field effect transitor (FET) is utilized to lower the output impedance. Ref. 88 deals with use of polyvinylfluoride sensing material in a scanning thermal setup for fire detection. Commercially available pyroelectric IR detectors of triglycine fluoroberyllate and triglycine sulfate require no cyrogenic cooling and operate at ambient temperature ranges from -10°C to 60°C, and -10°C to 40°C, respectively (90). With a standard window (model type KRS-5) the spectral response is from 1 to 45 μm with a total sensitivity up to 500 μm. Because of its higher operating temperature, the fluoroberyllate would appear more useful than the sulfate for mine applicability.

The number of semiconductor ultraviolet detectors (UV) (wave lengths less than roughly 4000A°) is very small compared to the IR region (86). This is due to basic problems encountered in UV detection.

1) Conventional glass windows cut off below around 3000A° and even quartz and UV-grade sapphire become opaque below 1800A°.

2) Below around 1000A° suitable UV windows are lacking. Detection in the intermediate or vacuum ultraviolet is generally accomplished by multiplier phototubes with photocathodes that are blind to wave lengths greater than 3000A°.

The Honeywell basic UV detector Model No. C7037A now acquired by Detector Electronics Corporation (Det Tronics Corp.) (91) designed to operate in the 1850-2450A° region is insensitive to both sunlight and artificial light. Its cone of vision is 90°. The quoted sensitivity is a 1 square foot flame from 15 feet. The sensing element is a gas filled, UV sensitive tube operating on the Geiger-Muller principle.

When an energetic photon in the UV spectral range strikes an appropriate cathode (tungsten is used in this device because it is not sensitive to the sun's radiation, etc.) and exceeds the work function of the cathode, an electron is emitted and is accelerated toward the anode (positive) plate. In passage through an ionizable gas toward the anode, the electron strikes gas molecules causing further electron emission. The total electron flow

is typically several million times that of the single electron emitted from the cathode. This leads to an increase in current flow which may readily be measured. The detector is operated in a pulsed mode by allowing current to flow for a very short period of time before the voltage is reduced to stop current flow. Amplification is, thus, required with this device.

Fenwal's UV detector (92) responds to UV radiation in the range 1900A° to 2500A°. It operates on the ionization principle similar to the Honeywell model. It has a 120° cone of vision. The response time given is 15 millisec for a propane/air flame 1.75 inches high at a distance of 8 inches from the flame source.

Other suppliers include McGraw-Edison Company (range 2000-2750A°) (93) and Pyrotector (1700-2900A°, maximum response at approximately 2100A°) which also operate on the Geiger-Muller principle. The latter device is particularly interesting not only from its outward compact design appearance but more importantly it contains a solid state AC-DC converter section to provide the necessary voltage for the detection tube and a signal integrator delay circuit (3 sec. delay) to minimize false alarms from aparks, lightning, etc. (84). Its quoted head-on sensitivity is 6 ft to flame from a 3/4" diameter candle.

Besides the normal problems associated with the inverse square law of radiant energy transmission which include view factors, temperature differences, etc., as well as additional difficulties cited earlier, added factors due to moisture laden environment resembling a fog or a mist would have to be assessed. This follows from the example that radiant energy propagation through a coal dust (a strong absorber of radiant energy) cloud could adversely affect fire detector response (30). Also, contamination of the viewing window with oily film deposits would require attention. Because of the extreme mine environment, we have omitted a discussion of light sensitive laboratory devices such as optical spectrometers or spectrophotometers, since they would not be expected to demonstrate reliability without continuous maintenance.

The likely area of applicability for IR and UV detection is in protecting fuel storage areas since these sensors are known to respond rapidly to flash fires.

4.3 Products of Combustion

Products of combustion in fires include solid particulates and liquid mists (including invisible and visible particle sizes), ionized species, gases, and radiant energy. Combustion product detectors sense one or more of these constituents excluding heat or flame.

1) α-Ray Ionization

This type of a detector employs a radioactive α emitter* (e.g., $Ra_2^{226}SO_4$, Am^{241}, etc.) to ionize air in a chamber between two electronic plates. Current in the picoamp range results from production and transport of positive and negative ions to opposite poles of the plates. A decrease in the current, relative to air, is obtained when combustion products enter the chamber because of their lower effective ionic mobility and increased absorption and scattering of the α particles by the aerosol fraction of the gas. This decrease is monitored electronically, leading to the triggering of an alarm.

At high sensitivity settings, aerosols such as cigarette smoke, room deodorant sprays, and dust particles will trigger false alarms. Heat sensing thermocouples are recommended for use in conjunction with an ionization detector in order to circumvent this problem (94). The ionization detector will also not function properly in regions where there is a high radiation background (95). Alarm dependence on air flow velocity, particularly in ventilation duct works, is also reasonably well-known. Questions concerning the ability to detect slow smoldering polyvinyl chloride (PVC) line cord degradation products at an early stage have also appeared (this has now been confirmed by us—See Experimental Results). Table X contains a listing of chemicals that can react with ammonia to produce air-borne particulates also sufficient to produce alarm. Possible explanation for the PVC behavior based on charge transport mechanisms in the ionization chamber is provided in Ref. 46.

With the need for periodic cleaning of the detector plates cited previously, our performance evaluation in mines (page 9), as well as the factors mentioned here, we see limited applicability for the ionization detector in the mine environment.

2) Argon Ionization Detector** - Operates on the principle of ionization of foreign molecules by collision with high energy Ar atoms leading to high concentrations of metastable Ar* of long half-life (10^{-4} sec.) (97).

---

*β-Ray Ionization detectors are also available, but not in common use. Differences result from the β-ray source (e.g., Sr^{90}) used to ionize the gas since an α particle produces around 10^3 times more ions than a β particle over the range of ionization chamber voltages. A β-ray detector would have to be operated as a proportional type counter at a much higher voltage, around 550 volts, to produce equal ion currents. This high voltage is undesirable. Alternatively, a β-ray detector could achieve the same result by incorporating a larger amount of β emitter.

**Devices or techniques used in other fields that upon suitable modification or use in a hybrid mode offer some possibility for future mine detection devices.

$$Ar + \beta \xrightarrow{-15.7ev} Ar^+ + e$$

$$Ar^+ + e \xrightarrow{11.6ev} Ar^*$$

$$Ar^* + \text{Impurities} \longrightarrow Ar + M^+ + e$$

$$Ar^* + \text{Combustion Gas} \longrightarrow Ar + M^+ + e + \text{Signal}$$

Either β or α radiation in the 10 to 50 millicurie range placed in an electronic chamber will provide background currents around (10^{-9} - 10^{-8}) amps.

Most organic compounds will be detected because their ionization potentials are in the range 9 to 11 ev; however, two important flame gases CO and CO_2 which have ionization potentials of 14.1 and 14.4 ev, respectively, will not be detected. The argon detector is best suited for very small concentrations of gases. It is relatively insensitive to changes in detector body temperature.

This device could possibly be used to detect combustible organic vapors. It would complement the ionization detector because of the latter's inability to detect organic vapors (67). Used jointly, the ionization detector could be set at high sensitivity and its output signal would be an input to the Ar detector to sample the gas. If the argon detector responded according to some predetermined level, one would have a double check on the presence of a fire. The occurrence of false alarms could be minimized with this hybrid setup.

3) Flame Ionization* - A hydrogen - O_2 (or air) flame which makes up one of the electrodes, is used to induce electron emission in various types of organic and inorganic molecules having low work functions. Electrodes under imposed voltages are used to collect the resulting ions. High sensitivity, reasonable stability, moderate flow insensitivity, and linearity over a wide range are the highlights of this device (97).

Use of this technique for a fire detection device is again limited to a hybrid system in a similar manner to the Ar detector.

4) Kryptonate Type Sensors* - A laboratory study for detecting automobile pollutants based on $PdCl_2$ Kryptonate for CO, hydroquinone clathrate for NO_x and PtO_2 Kryptonate for hydrocarbons is described in Ref. 98. The detection principle involves radiochemical exchange via Kryptonates, which are solid sources containing the radioisotope Kr^{85}. The solid Kryptonates release activity upon subjection to gaseous constituents at a rate proportional to the concentration of the reacting gas. A Geiger-Muller tube is used to count the released radiation.

---

*Devices or techniques used in other fields that upon suitable modification or use in a hybrid mode offer some possibility for future mine detection devices.

Selection of $PdCl_2$ for a CO sensor follows readily since $PdCl_2$ dispersed on silica gel is an indicator for CO. The lower limit of detection for the Kryptonate $PdCl_2$ sensor was 125 PPM.

A sensitized hydroquinone-Kr^{85} clathrate, responding similarly as a Kryptonate, i.e., rupture of the sensitized clathrate cage by oxidizing agents causes immediate release of Kr^{85}, was found to be highly sensitive to NO_2 (down to 2 ppm). However, since it gave no response to NO, the latter gas had to be oxidized to NO_2. The sensitized clathrate was subject to interferences at R.H. > 90%.

The PtO_2 Kryptonate sensor responded to various hydrocarbons (down to 13 ppm C_3H_8) and also to H_2.

Since this technique requires consumption of the sensing material for detection of the various species, it would be limited to discreet sensing in a hybrid setup for a fire detector based on CO and NO_x discrimination in a mine. However, the major drawback is with the NO determination since essentially all NO_x is NO at flame temperatures, thus requiring an oxidation step to obtain NO_2. This is viewed as undesirable.

5) Laser Beam

Research at the Boreham Wood Fire Research Station in England has led to the development of a laser beam fire detection system for extended area coverage (99). It operates on the principle of deflection of the laser beam due to differences in the index of refraction of the combustion gases versus air. Ambient fluctuations in temperature are discriminated against by tuning an amplifier to receive a frequency of 40-70 Hz. The corner-cube mirror used with a checkered mask prevents slight changes in the reflected beam due to small movements in the mirror mounting and the laser itself, respectively, from triggering false alarms. Although the laser device offers tremendous potential for large area coverage its sensitivity to these movements, and expected ease of damage from vibrations obviates its use in a mine.

6) Photoelectric

The basic requirements for Photoelectric fire detectors are two: a light source (such as beacon lamp, light emitting diode, pulsed laser, etc.) and a detector (photocell, phototube, or solid state device) to measure the radiant power of the light. Four different modes of operation presently used are based on the amount of light:

a) transmitted or absorbed by the medium*

b) reflected

c) scattered

d) refracted

*Not commonly used as a fire detector.

In the light transmission or absorption case, a light source and detector are arranged in line at opposite extremes of the test area giving extended area coverage. When smoke crosses the beam path, the radiant power reaching the detector is reduced which leads to a current reduction. This reduction can be monitored to sound an alarm at a predetermined value of light transmittance, absorbance, or specific optical density corresponding to a given smoke concentration (2% smoke obscuration/ft is commonly used).

Extended area coverage is also provided with the reflection technique although in a slightly different manner. Both the light source and the detector are integrated into a single unit. A mirror (possibly a suitable arrangement of mirrors) located at some pre-determined position, not necessarily on the light source axis, is used to reflect light back to the receiver. Here the increase in radiant energy is used in appropriate circuitry to produce alarm.

Photoelectric scattering devices contain the source and detector within a single unit but unlike the beam devices they are open to the atmosphere. Smoke particles must be present in the sensing chamber in order to scatter the light beam so that it strikes the photocell. Extended area coverage is not provided with the scattering detector since the smoke contained in the sampling chamber represents a local property. Its response time is usually slower than the other two types of photoelectric detectors since it is a point source detector. Auxiliary or back-up heat detection is often provided with these detectors. This will minimize the effects of thermally induced smoke stratification mentioned earlier.

Refraction devices also contain the source and detector in a single unit. Locating a target disc in line with light source and receiver causes light to be bent by refraction, when smoke particles enter the sensing chamber, around the disc onto the receiver.

The primary light sources in current use are beacom lamps (i.e., miniature incandescent lamps—output spectrum resembles familiar blackbody radiation curves) and light emitting diodes (LED's). Detector stability is affected by lamp aging, film build-up on lens surface, or fluctuations in lamp supply voltage. Lamp life is a question of much concern; under normal use around two years is expected. Field experience indicates that shock and vibration can reduce life, particularly during power failure. Also lamp filaments are more fragile when old and cold. In order to overcome some of these difficulties balanced, ratio-bridge arrangements are used. One photocell senses smoke scattered from a primary beam while the other views only the primary beam (100).

The recent dramatic growth in the field of optoelectronics has led to the introduction of LED photoelectric detectors. Under excitation provided by an electrostatic field a junction diode can emit light or exhibit electroluminescence. GaAs is one of the best materials for infrared LED's while GaP and GaAsP are used to produce the visible spectrum. The main advantages for these devices functioning as fire detectors are the following:

1) Long life compared to lamps

2) Low cost

3) Output power linearity with input current over a wide range.

Their disadvantages include:

1) Ease of damageability by over-voltage and -currents

2) Radiant power output is temperature dependent.

Because of the requirement for a rugged fire detector LED's are clearly preferred over beacon lamps. We likewise require the detector to be a solid state device. Primary sensors include cadmium sulfide or cadmium-sulfo-selenide photoconductors. Extended area devices using mirrors also do not appear applicable to the mine environment for similar reasons as well as others cited earlier. Thus, we are left with the point source detectors based on light scattering and refraction, and light transmission or absorption detectors.

In dusty mine environments the frequency of false alarming for the latter two detectors might limit further their applicability. However, scattering detectors are known to be rather insensitive to black smokes, e.g., 2% obscuration/ft for greyish white smoke corresponds roughly to 10% obscuration/ft for black smoke, and thus, at least for certain types of mines reliable detection might be expected. Periodic removal of accumulated dust particles surrounding porous protective shrouds would be required. This can be accomplished by external means, whereas detector head disassembly is required for cleaning of electrode plates in ionization devices.

For wet mines containing water in aerosol form of fogs or mists, light transmission or absorption detectors, suitably calibrated for light intensity in the mine, seem to afford potentially reliable fire detection capabilities. That is, both the light source and receiver can be hermetically sealed and positioned in line (by means of a metal bar to prevent movement) for ceiling mounting.

7) Filament Sensors*

a) Thermal Conductivity - A set of heated matched metal filaments (generally nickel, platinum or tunsten at filament temperatures of around 200°C) or thermistors are used to follow changes in thermal conductivity. A pure carrier gas is passed over a reference junction while the carrier gas plus a mixture eluted from a suitable column passes through the detector element. In the differential type setup, the resistance of the detector element changes relative to the fixed junction, and is a measure of the

*Devices or techniques used in other fields that upon suitable modification or use in a hybrid mode offer some possibility for future mine detection devices.

concentration of the component in the gas stream.

It appears that with some modifications of this technique the device could function as a fire detector (45). With air in a thin-walled, sealed reference compartment (of high thermal conductivity metal) and with the detector element open to the atmosphere, differences in composition and temperature will lead to bridge imbalance. One could also fabricate the two compartments out of different pore size electromesh screens. Variations in the mass throughput leading to thermal conductivity imbalances and/or in temperature in the two compartments will lead to bridge imbalance.

If the proposed device operates there are many unanswered questions pertaining to response time, the need of a separation column, etc. The latter does not appear to be necessary since we are not interested in resolving the various combustion products. Actually, some degree of separation will probably be obtained if fine electromesh screens are used. Study in this area appears warranted because this device could respond simultaneously to composition and temperature changes.

b) Catalytic Elements - Platinum wire, alloys, and activated platinum wound into a coil containing dual chambers (one chamber is inactive or sealed, the other open to atmosphere) in a Wheatstone bridge circuit is the usual sensing device (66). Instruments are of two main types: remote head or sampling devices. Gases to be sampled reach the filaments through a sintered metal disc or protective gauze which acts as a flame arrestor for prevention of flame propagation into a combustible mixture (as present in many gassy mines). Another set-up has the complete bridge and possibly an amplifier located in the head such that its response is essentially independent of the location of the control unit.

Studies at the Safety in Mines Research Establishment (SMRE), U. K. have led to development of pellistors or pelements for CH_4 sensing (101, 66). The ceramic catalyst consists of a mixture of thorium and palladium salts which are decomposed by heating and then aged in a methane/air stream. The change in temperature of the element is followed by using the platinum coil as a resistance thermometer.

Selectivity toward a particular gas may be obtained by measuring the net signal from two catalytically active elements. Further selectivity may be obtained through use of molecular sieves which allow only certain molecular diameters to reach the active element and by measuring signal differences between molecular sieves of different molecular pore sizes. Modifications of this basic technique also allow measurement of oxygen and certain inhibiting gases.

Besides the applications cited above, combustible gas sensor, specific gases depending on molecular sieve diameters, etc., these pellistor elements appear similar, at least on a overall basis, to "Taguchi" type POC sensors and, thus, might be expected to have fire detection applicability.

8) Solid State Devices

a) "Taguchi" Gas Sensor (TGS) - The Taguchi Gas Sensor (TGS) composed of bulk N-type metal oxides such as SnO_2, ZnO, and ferric sesquioxide, decreases its electrical resistance upon absorption of deoxidizing or combustible gases such as CO, alcohol, volatile oil, carbon-dust containing air or smoke, etc. Its ease of alarming in areas containing engine combustion products necessitates some judgement for it to be used in mines. However, its low cost is a definite plus, and assuming one can modify the sensor appropriately, it could receive widespread acceptance in the detection field. For mine applicability it may be limited to sampling applications in a hybrid setup.

b) Polymeric Film Sensors - The use of organic semiconductors with p-n junction devices for gas detection is detailed in Ref. 102; recent studies using this approach are concerned with the development of a polymeric film fire detector (103). The approach is based on the reversible and specific adsorption of gas on thin films of organic solids and the consequent change in density of electronic charge carriers. Two different devices based on: 1) variation of charge carrier density as a source of current change under an applied voltage; 2) charge density—capacity change followed by variation of capacity.

Since direct capacitance or current measurements for low dielectric constant, low conductivity films are difficult, amplification of the resulting charge is required. Two possibilities are as follows:

(1) Combination of organic film and p-n junction of a silicon diode reverse biased. Electrically, the high resistance reverse current path of the diode is paralleled by the relatively conductive organic film.

(2) Film used in conjunction with metal oxide silicon field effect transistor. Here the separate capacitive variations in the film are amplified. Materials of interest include poly (phenylacetylene), poly (p-nitrophenlacetylene), poly (p-formamidophonylacetylene), poly (p-aminophenylacetylene) and various related or substituted compounds.

Ref. 104 contains an interesting study involving the use of stable lipid membranes with multiple resistance states as sensors for air-borne organic vapors based upon membrane interface relations. Significant sensitivities to a number of organic compounds were obtained. Film resistivity studies have shown non-linear characteristics cast upon glass or aqueous surfaces. Films prepared from ethyl cellulose, polycarbonate or polyamide (1-3 micrometers thick) or combinations thereof and with lipids may have significant non-linear resistances including partial rectification characteristics.

Ref. 105 examines impregnation of fluorocarbon polymers with electrically conducting oxides of rhenium and molybdenum. It appears to us that the intent here is to eventually develop a polymeric film sensor having properties similar to or better than "Taguchi" devices.

Presently, these studies are in the research stage and it appears that considerably more effort is required before a commercial prototype will become available. Although it may be premature to speculate on the fire detection capabilities on any devices based on polymeric film sensor techniques, it appears that sensitivity to various gases might preclude its acceptance as a fire detector similarly to the present stand concerning "Taguchi" devices. In the mine environment false alarming seems to present a potentially serious problem. Low cost gas sensing capability is a possibility; however, selectivity or specific species sensitivity must be demonstrated.

4.4 Gas Sensors

This section will be limited to a review of pertinent techniques for sensing the important fire gases CO-CO_2, NO_x from a discrimination viewpoint (see pages 4, 12, 60) and O_2 deficiency (the ratio of CO/O_2 deficiency being an indicator of spontaneous combustion—pages 4,and 27). An excellent breakdown of the principal methods used in gas sensing, the range and region of applicability is given in Table XI (73). Many of the more compact sensors are outgrowths of innovations in the field of gas chromatography.

Detectors besides the specific classification of Table XI are broadly classified as integral and differential types (66). Integral types record the properties followed in a number of steps while differential detectors respond essentially instantaneously to gas properties. The latter have high sensitivity, precision and other desirable properties while the former integral types have low sensitivity, narrow range of applicability, high inertia, etc. Most detection systems are, therefore, of the differential type. The input-output signal response relationship for nearly all differential detectors is given by solution to the simple linear differential equation

$$\tau \frac{dy}{dt} + y = kx$$

where x - input

y - output, such as, electrical, or pneumatic signal

τ - time constant of detector

k - amplification factor related to detector sensitivity

t - time

We will not utilize this type of classification here, and have included it mainly for the sake of completeness. Furthermore, complex devices requiring specialized maintenance such as mass-spectrometers, UV and IR spectrophotometers are also excluded here for reasons previously covered. In addition, only the highlights of the more interesting sensors as pertains to the present fire detection applications are considered, since gas sensors are treated in considerable detail elsewhere. We are excluding, therefore, length of stain indicator tubes, cumbersome wet chemical techniques, and other non-continuous operations that do not have readily replaceable sensing elements.

Refs. 66, 72, 73, and 74, previously cited as well as Refs. 106, 107, and 108, contain much useful descriptive information dealing with CO, CO_2, NO_x, and O_2 sensors. Ref. 107 examines the accuracy and precision of several portable gas detectors and makes comparisons of portable detector response to CO, CO_2 with sensitive long path infrared analyzers.

CO, CO_2, NO_x, O_2 Sensing Techniques

1) CO Sensing Techniques

Ref. 65 presents a detailed review of CO monitoring techniques. The classification method is according to mode of operation, i.e., colorimetric change, catalytic, etc.

The sensor in Unico Corporation CO alarm is high impact polystyrene which changes color from yellow to brownish-black in presence of CO. The change of color is followed in a photoelectric system. Maintenance is a major problem since the detection sensor must be replaced after exposure to CO. In a similar way light reflection from a $PdCl_2$ disc, which darkens when CO is present, is used for CO detection.

Mine Safety Appliances CO detector (MSA Model C portable CO sensor) consists of beds of active and inactive hopcalite catalyst surrounding two thermistors in a Wheatstone bridge circuit (109). An exothermic reaction of CO to CO_2 leads to bridge imbalance and causes a proportional "upscale" meter reading thereby giving the CO concentration. This device can be hooked up to an alarm system. Catalyst life limits its use to a toxic gas detector since ambient CO levels in a mine are fairly high during certain periods (see page 15). High humidity will shorten life, and tobacco smoke will seriously impair the accuracy of this instrument.

Electrochemical techniques for CO sensing are commercially available in Energetics Science, Inc. CO Ecolyzer (110). The sensor consists of a three-electrode system—a sensing electrode, a counter electrode, a reference electrode in a housing containing sulfuric acid solution and two face plates. The reaction scheme is

a) $CO + H_2O \longrightarrow CO_2 + 2H^+ + 2e$

between working and counter electrodes,

b) $O_2 + 4H^+ + 4e \longrightarrow H_2O$

at counter electrode, giving the overall cell reaction

c) $2CO + O_2 \longrightarrow 2CO_2$

Besides the known interference from ethylene (1 ppm ethylene corresponds to 3 ppm CO) (110), MSA has observed that 50 ppm NO gives 40 ppm CO on the Ecolyzer (40). MSA found that 20% acidic solution of $K_2Cr_2O_7$ on silica gel completely removed the NO interference.

A polarographic sensor for detection of CO is described in Ref. 111. In the SMRE device a metallized membrane (anode) in conjunction with a membrane of polytetrafluoroethylene (PTFE - 6 μM thick) or silicone rubber coated with a thin layer of gold and similar layer of silver by vacuum evaporation (which serves as the cathode in the cell) and then with anodic catalyst metals is under laboratory study for use as a portable CO sensor. This device operating similarly to the filament sensor described on page 28 in a remote head/amplifier set-up, offers considerable potential for monitoring CO buildup in worked out or abandoned mine regions. Coupled with a similar sensor for O_2 (page 34) the ratio CO/O_2 deficiency could be monitored at a central station with instantaneous signalling since live current is involved in contrast to the long time delays obtained during pneumatic conveying of gases through tubes (page 35).

An earlier proposed fuel cell sensor for CO is given in Ref. 45. Here fuel cell operation may be analogized to an electrochemical cell in that conventional fuels react at the anode while O_2 or air reacts at the cathode. The electrodes, which are usually sintered porous metals, serve as reaction sites where electrons are transferred to an external circuit. The electrodes, are considered inert since they do not undergo the mass transfer exchange accompanying oxidation and reduction as in a typical electrochemical cell. The fuels most often used are hydrogen, hydrocarbons, and hydrazine.

Carbon monoxide fuel cells are unimportant in the fuel cell field. They appear to be of potential use in the fire detection area. For example, mixed electrocatalysts (e.g., $Pt\text{-}WO_2$) consume appreciable amounts of CO along with H_2, and alloy electrocatalysts promote selective anodic oxidation of hydrogen. An application of this principle would seem to offer promise for combustion gases. With a liquid electrolyte 5 N H_2SO_4 and special CO sensitive electrodes appreciable voltage changes occur for small variations of % CO (112). From a best estimate of the graphical results, an increase in CO concentration from just 1% to 3% leads to a voltage increase from 13.75 mv up to 23.8 mv. Changes of this magnitude could easily be monitored and circuitry designed to trigger an alarm.

Sensitive optical methods for detection of CO (and also CO_2) applicable to the single station sampling on page 35 (80) use non-dispersive infrared analyzers (NDIR) taking advantage of the strong adsorption band of CO at 4.65 μm (CO_2 band referred to is often the 4.4 μm band). The system consists of a radiation source (e.g., nichrome wires, lasers) usually chopped mechanically, a cell through which the sample gas flows and radiation is absorbed by the CO molecule, a detector for the radiant signal and appropriate filters depending on desired discrimination. The detector is usually set to measure the amount of radiation transmitted, i.e., the energy which would reach the detector if there were no absorption in the gas, less the amount absorbed (66). The sample and reference cells are metallic parallel tubes, gold plated to insure maximum radiation at the sensor. Cell lengths vary from 0.1 - 25 cm with length being a compromise between sufficient length for a strong signal and short enough to have a reasonably linear full-scale output. The solid state detectors of interest have been reviewed previously on pages 19 to 21. Interference to the CO band from CO_2 is generally negligible except for the case of low CO in a high CO_2 concentration. Here filters are required to cut off the lower absorption spectrum of CO_2.

An interesting trigas development study for CO, CH_4, and NO_2 using both infrared (for CO and CH_4) and visible (NO_2 channels) is currently under development by Andros, Inc. for the Bureau of Mines (113). The analyzer is a portable (hand-held) battery powered device for in-mine monitoring applications. Present test results for noise, sensitivity and stability on both infrared and visible channels showed peak-to-peak drifts of 7 ppm NO_2 and 2 ppm CO. Extended life tests are currently in progress.

2) CO_2 Sensing Techniques

The NDIR analyzers are similar in behavior to the CO analyzers with differences in the solid state sensors, filters, etc.

An interesting solid state semiconductor sensor for CO_2 (also H_2, CH_4) from Thunder Scientific operates in the range 0-100% CO_2 in air with a 0-1% resolution at temperatures from 60°F-90°F (114). No requirements for chemical or catalytic conversion are necessary prior to sensing. Response times are not cited. In Ref. 115 the operating behavior of this solid-state sensor is discussed for a humidity sensor (gas sensor behavior is considered proprietary to Thunder Scientific). Since the humidity sensor behavior is described as a bulk effect semiconductor device which changes resistivity as water molecules drift through a precise array of crystals, similar behavior for CO_2 might be expected. Response times as a humidity sensor are given as 300 milliseconds or less for 63% of the reading.

A novel carbon dioxide sensor based on monitoring changes in electrical resistance of an anion-exchange resin proportional to the ambient partial pressure of CO_2 is given in Ref. 116. Change in resistance is due to increased ionization of a weekly ionized base in the presence of a slightly acid gas. The optimum material consisted of a condensation polymer of resorcinol, formaldehyde and triethylenetetramine. A dual chamber device containing two sensing elements (one being a reference) was used to minimize humidity and temperature effects. Interesting features of the sensor are its size—around 50 in^3, weight of less than 6 ounces and a power requirement of less than 0.5 watts.

Another interesting electrochemical sensor is detailed in Ref. 117. The sensor utilized a pH electrode and a Ag-AgCl reference electrode with a tris (hydroxymethyl) aminomethane buffer containing an enzyme carbonic anhydrase as a catalyst. A FET incorporated into the probe assembly increased electrical stability as well as simplified the electronics. Response times of less than 2 seconds for 98% step change of 14 to 35 mm Hg P_{CO_2} were obtained.

A recent device based on pressure/density differences for CO_2 (also O_2 sensing) analysis is described as an analog fluidic gas concentration sensor (118, 119). The sensor is a passive resistor bridge that consists of two identical flow channels each of which consists of a linear resistor and a non-linear orifice resistor. A reference gas and a similar gas mixture (identical to the reference except for the presence of one other gas component) flow through the individual channels. When the sample gas is the

same as the reference, the differential output pressure is zero; when different, the differential pressure is a measure of the concentration of the foreign gas. This technique is limited to clean regions since orifice clogging is possible in dusty or contaminated atmospheres.

3) NO_x Sensing Techniques

Detailed reviews of NO_x instrumental techniques are given in Ref. 108. The recently accepted approach for NO_x analysis involves chemiluminescence, which is, the emission of light directly from a chemical reaction. For NO_x the reactions are

$$NO + O_3 \longrightarrow NO_2^* + O_2$$

$$NO_2^* \longrightarrow NO_2 + h\nu$$

Ozone is generated at low pressures from high voltage discharge in O_2 or air. For NO_2 measurement the sample is passed through a converter in which NO_2 is converted to NO. If NO and NO_2 are both present NO_x is measured. NO_2 may be obtained by difference from the NO_x and NO concentrations. A number of commercial instruments are described in the monograph of Ref. 66. An application of chemiluminescent techniques for measurement of NO_x from pyrolysis/combustion of nitrogen containing plastics is described in Ref. 64.

4) O_2 Sensing Techniques

Paramagnetic O_2 analyzers because of their inherent stability and require less maintenance than electrochemical analyzers are used for nearly all continuous analysis in the percentage range (66). They are recommended, therefore, for the pneumatic sampling approach (page 35). At lower concentrations (see Table XI) or when portability or remote sampling is required electrochemical techniques come to mind.

The polarographic sensor of SMRE (111) described on page 32 was developed originally for sensing oxygen deficiency. It is essentially identical to the CO sensor with the principal difference being omission of the anodic catalyst metals. This device is not affected by shock, vibration, wind speed, and orientation. The device is temperature sensitive since O_2 permeability of the PTFE membrane was found to be exponentially dependent on temperature. Since resistance of commercial thermistors varies similarly with temperature, the two functions can be matched over several decades of temperature and thus compensated. SMRE over the range 5 to 35°C has obtained an overall accuracy of ±2% of the reading. An application of a polaragraphic O_2 membrane sensor in CO sampling for evaluation of fire fighter exposures is given in Ref. 120. General design considerations for membrane-covered polarographic gas detectors is contained in Ref. 121.

An application of the fluoric oscillator technique for O_2 sensing (also H_2 detection) is similar to the approach for CO_2 described on page 33.

4.5 Single Station Detection Using Sampling Tube Networks

Continuous monitoring of CO, CO_2, NO_x, and O_2 deficiency using sensitive NDIR analyzers for CO and CO_2, and chemiluminescent and paramagnetic analyzers for NO_x and O_2, respectively at a single station* from several spatial locations appears appropriate for detecting spontaneous combustion and other slow burning phenomena. A gas sampling system would require probes/tubing, traps and filters, remotely actuated solenoid valves, and a high capacity pump to produce a pressure gradient (auxiliary pumping on the analyzers is also required) (123, 124, 125). Computer processing of the data is often desirable (124).

Time lags in concentration sampling resulting from fluid dynamical factors in the tubing, filters, and traps, as well as instrumental delays in the various analyzer types, are not of primary concern since they are small (for reasonable tube lengths and a properly designed system) relative to the time scales for spontaneous combustion. However, in order to design an optimum system, which might also apply to more rapidly occurring combustion modes, i.e., one which allows frequent sampling from the individual locations at a minimum cost, a knowledge of the important parameters controlling response time is important. Work carried out at GRI in investigating the suitability of this optimized system approach both in the laboratory and through analytical calculations will be discussed later in this report.

V. DETECTOR EXPERIMENTS

Detector experiments upon which parts of Table VII are based on, are covered in Ref. 45. Recently, additional detector performance data appears to be limited to Refs. 71 and 126. The performance data from Ref. 71 illustrate the ease of entrance effect at lower flow velocities. That is, detectors that have improperly or restricted flow entry designs show a pronounced dependence of sensitivity, as expressed in terms of smoke obscuration, on flow velocity. Smoke is prevented from getting into the sensing chamber. While this poses no problem in most mine areas, it does cause one to reflect on the overall merits of this type of commercial supplier as pertains to their in-house testing prior to marketing.

Ref. 126 contains much useful information relevant to the applicability of fire detection in apartments located in high rise buildings. Of interest here is the following:

---

*At ground level or at selected horizontal levels close to likely sources of spontaneous combustion. Rooms at these levels are assumed to be dust free; instruments are also shock and vibration protected through appropriate mountings.

1) Ionization detectors generally respond adequately to flaming fire starts and inadequately to smoldering fire starts. The reverse is true for photoelectric smoke detectors.

2) Fixed temperature and rate-of-rise heat detectors were found to be uniformly inadequate.

3) The selected photoelectric smoke detector exhibited a strong sensitivity dependence to orientation (roughly a four-fold variation with smoke concentration expressed in terms of optical density per foot) with respect to the smoke front vector in a flat ceiling impinging jet type setup. The ionization detector was insensitive to orientation. This strong smoke detector orientation detector dependence was not observed in testing using nationally approved smoke boxes such as those at Underwriters Laboratories and Factory Mutual (127). Thus far, there is no cogent explanation for such behavior.

VI. DETECTOR SPACING AND POSITIONING CRITERIA

As implied earlier on pages 3 and 4, there is no national code similar to the NFPA codes dealing with detector positioning and arrangement within residential and commercial embodiments for mines. Whether such a code is feasible or desirable is subject to conjecture since mines vary so widely in distribution of combustibles, ventilation patterns, timbered supports as in the deep-vein mines of Northern Idaho contrasted to the absence of timber as in certain cavernous trackless mining operations, etc. Nevertheless, some rules of thumb, would be desirable. For example, Ref. 128 shows for a smooth ceiling housing fire detectors subjected to a radially expanding ceiling jet and other restructions, notably drafts induced by room ventilation and non temperature stratifications at the ceiling, that:

1) Fire detectors should be located a vertical distance below the ceiling of no more than 6% of the ceiling height.

2) For optimum response time, fire detectors should be spaced at intervals of ¼ of the ceiling height. Spacings smaller than this value will yield no significant improvement in detector response time. While calculations such as this might have some applicability in a mine, such as in intake or exhaust shafts, the complicated ventilation patterns as well as random ceiling obstructions and tunnel shapes obviates general applicability.

We, therefore, recommend examining the positioning of detectors based on continuous release of a suitable aerosol and location of the selected detector at the point of maximum response. This should permit in-mine sensitivity positionings to be made.

VII. SUMMARY REMARKS ON THE STATE-OF-THE-ART SURVEY

An examination of the state of the art of fire detection devices and gas sensing techniques as pertains to applicability in metal and non-metal mines reveals numerous problem areas. A summary of the more important factors is as follows:

1) High frequency of false alarming for sensitive products of combustion (ionization and photoelectric types) and optical view field detectors (infrared and ultraviolet types), in industrial and residential embodiments, pose serious problems concerning reliable use of these devices in metal and non-metal mines. Less sensitive direct contact or thermal detectors appear capable of operating reliably in various mine environmental extremes; however, their inability to detect slow smoldering fires precludes widespread applicability.

2) Insensitivity of conventional products of combustion fire detectors to normal mine operations involving emission of aerosol contaminants from diesel equipment and blasting is, at best, tenuous. It appears that development of a hybrid or integrated systems approach involving simultaneous sampling of gaseous species in the ratios CO/NO_x and CO_2/NO_x (to discriminate against diesel and blasting operations), with detection of one or more fire signatures (smoke, radiant energy, or heat sensing) is required for reliable fire detection in mines.

3) Neither ionization nor photoelectric (scattering or refraction types) detectors, which are open to the mine atmosphere, appear to offer long term reliability in active mine areas. Maintenance problems are judged to be more critical for the ionization detector. Furthermore, a strong dependence on flow velocity precludes use of the ionization detector in regions close to ventilation fans and/or in ventilation duct works.

Operating a sealed photoelectric detection system based on light obscuration or transmittance appears to afford some promise for reliable detection.

4) Use of sampling tubes to monitor combustion products at a central station appears promising for detection of slowly developing phenomena, such as, spontaneous combustion and slow smoldering fires.

5) Not much is known about optimum detector positioning and spacing in mines. Protection methodology based on accepted NFPA installation standards for industrial or residential environments is not applicable to the mine problem.

VIII. APPARATUS AND EXPERIMENTAL PROCEDURE

The important test apparatus, which consisted of two smoke boxes for detector performance evaluations under incipient and flaming combustion sources, a multipoint gas sampling system, specialized laboratory equipment, and the experimental procedures employed therewith, are detailed in the subsections to follow.

8.1 The FM-GRI Modified Smoke Box

The basic smoke box constructed from 5/8" thick plywood used in screening of products of combustion (POC) type detectors is illustrated schematically in Figure 3. Its dimensions (18" H x 13¼" W x 5'6" L), basic internals—tungsten filament No. 4515 sealed beam 6 v. spot lamp for the light source and barrier layer type selenium photovoltaic cell (Weston Photronic Cell, Model 594) enclosed in a hermetically sealed case and air circulation patterns are similar to that of the Factory Mutual (FM) smoke box. A regulated DC power supply (Harrison 6439B, made by Hewlett-Packard) was used to power the 6v. spot lamp at 3 v., or half its rated voltage. A circuit based on an op. amp. type 741C was used to measure the current output of the photocell (see Figure 4A). Here the input impedance, given by

$$Z_{in} = R_1/Av$$

where Av = open loop gain (typically, 2×10^5 for the 741C) was kept less than 100Ω. This op. amp. circuitry was used in place of a low impedance microammeter, such as, Weston Model 622.

Other modifications include provisions for testing over an increased flow velocity range—25 ft/min to 225 ft/min* (by addition of a recirculating fan rated at 265 cfm free air capacity), removal of smoke samples for particle size analysis (see Section 10.3), and provisions for pyrolytic heating. The heater was an automotive type cigarette lighter ($R_{25°C} \simeq 1\,\Omega$) operated at 12 volts AC from a Variac to provide a range of smoke obscuration curves for the various fuels examined. The heater required only occasional replacement under the heaviest periods of testing.

With this basic setup, products of combustion (POC) type detectors were screened for their response to selected mine fuels. The alarm condition or a characteristic voltage output (for those POC's that were analogue in nature) was related to smoke concentration expressed in terms of percent obscuration per foot, Ou. Ou is given by

$$Ou = \left[1 - \left(\frac{I_s}{I_o}\right)^{1/\ell}\right] 100 \qquad (1)$$

*Flow velocity was measured with a calibrated hot wire anemometer - Disa 55 D01.

where: I_s - smoke density meter reading with smoke

I_o - smoke density meter reading with clean air

ℓ - distance from light source to receiver

or by

$$Ou_{\ell} = \left[1 - \frac{I_s}{I_o}\right] 100 \qquad (2)$$

where: Ou_{ℓ} is the percent obscuration of light for the full length of the beam at any distance, ℓ.

In our test setup ℓ = 5 ft. Both I_o and I_s are directly proportional to the output voltage*, V_o and V_s, from the op. amp. setup. V_o was adjusted by varying the op. amp. feed-back resistor to read 10 volts at zero obscuration. A series of charts was then constructed to relate I_s directly to Ou to allow rapid determination of Ou in all subsequent tests.

Hot wire anemometry surveys showed that the velocity profile was uniform in the cross-sectional plane of the smoke box and also at various axial positions along the 5 ft. light path. Furthermore, smoke properties are also essentially independent of axial position since similar POC detector performance was obtained at various positions. Thus, it may be concluded that the detectors screened in the Figure 3 smoke box were subjected to a homogeneous smoke front.

Because of smoke box design, its contents, and wood construction, this basic unit is unsuitable for testing of flaming combustion sources. Construction of a suitable box was subsequently undertaken. It is described in the following subsection.

8.2 Test Box for Flaming and/or Smoldering Combustion Sources

A test setup (L = W = 4', H = 8') to evaluate detector performance primarily to flaming combustion sources is illustrated schematically in Figure 5. Testing in this chamber allows:

1) Convenient and reproducible testing of a wide variety of fuels in both flaming, smoldering, and pyrolytic modes of combustion. Point source and distributed fire sources can also be examined.

2) Examination of smoke aging.

*A Fluke digital voltmeter Model No. 8000A was used.

3) Convenient comparisons between detector types (four in each test) under identical combustion conditions.

4) Monitoring of smoke obscuration versus fuel weight loss on a precision load cell.

5) Convenient introduction of mine dusts, water mists, and aerosol contaminants.

6) Examination of possible detector dependences on angular orientation to the fire source.

7) Effect of distance from fire source to detector.

Liquid fuels and selected plastics, all ignited by an electrically heated coil, were examined herein. The coil was made of No. 24 gauge Chromel-A wire; a 20-cm length, with a measured resistance of 1.2 ohms and was wound on a rod to give a tight coil 4 mm in diameter with 50 mm leads. A pair of "crocodile" clips was fastened about 15 mm apart to a strip of Transite board with C-clamps. The coil was clipped by its leads to the "crocodile" clips, and a source of electrical energy was also attached to these clips. This source was a DC power supply, from which the coil drew 7.5 amp at 9 v., or about 68 watts, when operating; with this particular power supply, it required an open-circuit voltage of approximately 20 v. to provide these operating conditions. The coil took about 3-5 seconds to reach its steady-state temperature after being switched on; the coil glowed bright orange-yellow at this temperature. With this ignition set-up, the liquid fuels were ignited in three seconds or less after the coil reached its maximum temperature. Solid combustibles, such as polystyrene pellets or wood chips (see Table XV), were ignited by embedding the coil in the charge of combustble in a porcelain evaporating dish, then energizing the coil. In general, it took about 5-10 seconds, depending upon the material, after the coil reached maximum temperature for self-sustaining combustion to be achieved. Detectors were ceiling mounted (on hinged doors for easy access and changeability) and arranged in a three-foot circular ring. The optical setup for monitoring smoke obscuration—light source and photocell and accessory op. amp. circuitry—was identical to that used in the GRI box described previously (Figure 4). Here the beam length exposed to smoke was 4 ft. and the lamp voltage was 6 v. The addition of a load cell—Statham Universal Transducing Cell, Model UC3—would allow monitoring the weight loss of burning materials. Its intended use was for weight loss determinations on solid polymeric materials of complicated geometries. No weight loss data were examined in this study.

A fine water fog (mean particle size 14 μm) was injected at various times (before, during, and after fuel ignition) using a Fogmaster Tri-Jet fogger #6208 manufactured by the Afa Corporation.

Variable height provisions are important not only to assess performance of optical view-field and thermal devices but also for POC detector types, though no such work has been carried out on this project. This requires investigation since long times for smoke ascent, e.g., such as under slow smoldering conditions, will concentrate the smoke such that the initial front reaching the detector head might be of order Ou = 10%/ft. Thus, sensitive combustion product detectors would be expected to respond immediately; however, no indication whether they responded at a quoted lower value (as determined in a standard smoke box) would be obtained. By judiciously varying heating rate, fuel size and geometry, and height, it is expected that an orderly increase in Ou can be achieved. This will allow comparisons of detector performance to be made between both boxes. It should be emphasized that a highly non-homogeneous smoke flow at the detector is achieved with the present setup. Recall that smoke properties and flow velocity are uniform in the Figure 3 box. The transport of heat and mass (i.e., smoke and reaction products) is achieved through a free convective jet impinging on the center of the ceiling and then spreading radially outward to the detectors. Because of these differences, the Ou values at alarm are expected to vary between the two boxes. It is conceivable that placing a fine mesh screen in a cross-sectional plane of the box at a suitable height might minimize these inhomogeneities.

In addition to the important features outlined here, the box contained a removable door for personnel access, a small viewing port for observing ignition of the fuel source, and a 4" diameter exhaust port with flow damper connected by household clothes dryer exhaust tubing to an exhaust fan for smoke removal.

8.3 Multipoint Gas Sampling System

The use of sampling tube networks for continuous monitoring of mine environments from several locations at a single station* using the tube and bundle technique is detailed in Refs. 123 and 124. The gases most commonly sensed are CO and O_2. In coal mines the ratio of CO to O_2 depletion actually appears to be a reliable indicator of the presence of spontaneous combustion (129). For metal and non-metal mines the use of diesel equipment and trucks introduces large amounts of CO_2 and much smaller though roughly equivalent amounts of CO and NO_x as background contaminants (41, 42). Simultaneous sampling of two or more of these gases in a suitable ratio, such as CO/CO_2 (130) and more recently CO_2/NO_x and/or CO/NO_x appears necessary to reliably detect slowly developing fires while discriminating against diesel exhausts in metal and non-metal mines. The latter recommendation follows from some recent Mine Safety Appliances (MSA) Research Corporation gas sampling data tabulated in Table XII (131).

*At ground level or at selected horizontal levels close to likely sources of spontaneous combustion. Rooms at these levels are assumed to be dust-free; instruments are also shock and vibration protected through appropriate mountings.

Besides the known capabilities of mine sampling tube networks for air monitoring and spontaneous combustion, this approach might be applicable toward indicating the onset of flow reversals during actual mine fires. This is an area in which future work should be directed. For example, two probes oriented 180° with respect to each other at the same location would normally record essentially similar species concentrations; however, during flow reversal the probe facing an oncoming smoke front would record higher (CO/CO_2, etc.) concentrations than the probe whose opening is in line with the smoke vector. These questions were not studied in this work. However, in order to address the flow reversal problem as well as detection of more rapidly developing fires, an investigation pertaining to design of an optimized system was undertaken.

A gas sampling system would require probes/tubing, traps and filters, remotely actuated solenoid valves, and a high capacity pump to produce a pressure gradient (auxilliary pumping on the analyzers is also assumed). Time lags in concentration sampling resulting from fluid dynamic factors in the tubing, filters, and traps, as well as instrumental delays in the various gas analyzers are of little concern for spontaneous combustion, since the sum total of all delays is small relative to the time scales for occurrence of this phenomenon. However, for more rapidly occurring combustion modes, these parameters are important since frequent sampling from the individual tube locations is required.

In Ref. 125 it was demonstrated for small lengths of tubing, i.e., up to a few hundred feet, that the principal requirements to decrease the response time for pneumatic gas conveying were:

1) Increased mass flow rate (by increased pumping rate) and decreased frictional resistance in the tubing (by increasing the tube diameter up to a certain maximum diameter).

2) Minimized internal volume of the system, i.e., traps and manifold volume primarily.

Selection of the proper pumping capability is based on determining the required pump horsepower (hp) to produce acceptable pressure ratios for selected tubing lengths. Too large a pump-free volume rating, exceeding the maximum permissible flow throughput for the sampling system determined by the laws of fluid mechanics, does not produce increased response. Actually, to produce the maximum flow velocity or sonic flow in long tubes requires a pump of unrealistically high hp rating. Cost trade-offs for pumping capability versus actual performance also have to be considered.

To build a multipoint system incorporating these considerations, the one illustrated in Figure 6 was developed. Analytical calculations based on the equations formulated in Appendix A led to calculated transient response times/pump horsepower requirements for two pressure ratios and laminar flow shown in Figure 7. Based on this data, it was concluded that a 3/8" I.D. tube represents a reasonable compromise between minimum response

time and moderate horsepower requirement. The ¼" and 1/8" tubes have significantly longer response times, whereas the ½" tube has only a slightly better response time than the 3/8" tube, but significantly higher horsepower requirement.

The basic parts of the system from left to right are as follows:

1) Sintered metal filters - 200 micron sintered stainless steel filters from Pall Corporation.

2) Sample tubes - 3/8" I.D. soft-wall polyvinylchloride (PVC) tubing* from Fisher Scientific.

3) Sampling manifold - fashioned from 3/8" copper tubing and tees soldered together, thus representing a negligible internal volume - a few hundred cm^3.

4) Solenoid valves - two-way (normally closed settings) electronically actuated solenoid valves from ASCO Corporation Model No. 8030B13.

5) Programmer - (twelve step switch programmer) sixteen positions per switch from GW Eagle Signal Industries Model No. MT-12A61602.

6) Pumps - The exhaust pump for the sampling system is a rotary vane vacuum and positive pressure pump from Gast Corporation - Model No. 7055-03.

7) Fine filter and H_2O traps - a 5 micron Millipore or Gelman replaceable filter contained in an appropriate filter holder. An ice/salt water bath for removal of H_2O or other suitable technique is preferred. Desiccants which would remove H_2O/CO_2 mixtures as carbonic acid are not recommended.

8) Gas analyzers - Infrared Industries non-dispersive infrared analyzers (NDIR) Model Nos. 703-021/146 and 703-022/148 were used for CO and CO_2, respectively. The concentration ranges selected were 20 ppm-1,000 ppm and 250 ppm-25,000 ppm for CO and CO_2, respectively. Thus far an NO_x analyzer has not been added to the sampling train primarily because of high cost - $2,000-$5,000, depending on choice of operating principle (electrochemical versus chemiluminescent). The oxygen analyzer is a Beckman Instruments Model OM-11 polarographic sensor - sensitivity range 0-100% O_2.

The CO, CO_2 and O_2 analyzers were calibrated according to factory recommended procedures, which required the introduction of known gas concentrations. A description of the preparation of a 2.25% CO_2 mixture in N_2 follows:

A 2.25% CO_2 mixture in N_2 was prepared from 100% CO_2 by diluting a known amount of this CO_2 concentration with N_2 according to the ideal laws of partial pressures for gas mixtures. A precision pressure tranducer manufactured

---

*Soft-wall tubing was selected over hard-wall PVC because of a factor of three lower cost. It is <u>not</u> recommended for in-mine sampling. It is useful for laboratory testing at pressures not lower than around 500 mm Hg, where it deforms.

by Computer Instruments Corporation was used in all pressure measurements; its output voltage was monitored on a Fluke digital voltmeter. The tank used in the mixing process was an expended high pressure Freon tank of about 23 liters volume. The mixing of nitrogen and pure carbon dioxide is as follows:

1) Flush the 23 liter tank three times with pure N_2 to assure that no CO_2 is present in the tank from a preceding determination.

2) Pressurize the tank with pure N_2 to 100 psig.

3) Add 3.375 psig of pure CO_2.

4) Fill the tank with pure N_2 to 150 psig.

Following preparation of the calibration mixture and instrument warming, pure N_2 was purged through the analyzer at a flow rate of 2-4 cfh, and the ZERO level was adjusted. The N_2 flow was turned off and 2-4 cfh of span gas was introduced to adjust the SPAN control until the meter pointer coincided with the certified value for the span gas. A similar method was used for the calibrated mixture gas prepared according to the procedure previously described.

Transient time responses were measured for various tubing lengths as a function of pressure using an input gas mixture of 2.25% CO_2. The manifold pressure was adjusted by varying the valve opening on the large rotary pump to produce pressures ranging from 500 mm to 685 mm Hg. As stated previously, lower pressures were possible; however, collapsing of the soft-wall PVC tubing at 500 mm Hg limited the lower range to this value. Next a "slug" of 2.25% CO_2 gas (usually approx. 1 liter) was introduced at the suction end of the tube and a timer was simultaneously started. The time for arrival of the peak concentration reading on the CO_2 analyzer was taken as the transient response time.

8.4 Particle Size Measurements

1) Pulsing Laser Photomicrography Analysis

The Pulsing Laser Photomicrograph, or PLP, a technique utilized extensively by GRI to photograph aerosol particles in flight, is a prototype instrument purchased from Laser Holography Laboratories. It was employed to evaluate gross dissimilarities in particle size distributions of smokes from various fuel sources. Also, since the cascade impactor (see Section 8.4-2) is generally considered inappropriate for evaluation of particle distributions containing significant fractions of large (diameter > 16 μm) particles, the PLP can be used as a screening tool for later impactor analysis.

Pulsing Laser Photomicrography is a technique for determining particle sizes of aerosol droplets in flight. The particles are stroboscopically illuminated by a 337.1 nm pulsed ultraviolet laser. Shadow images of the

particles are magnified using simple convex-convex quartz lenses and the magnified images are focused on the vidicon sensor of a conventional television camera; together the quartz lenses and camera are considered analogous to the objective and eyepiece of an ordinary light microscope. The signal from the TV camera is recorded on video tape which can be played back and observed on the TV monitor, stop action, for particle size analysis (Figure 8).

The technique of using PLP may be summarized as follows: A calibration reticle is used to establish the magnification of an object placed at the object (focal) point of the lens system. The reticle is removed and the aerosol spray is photographed at 60 fields of view per second. Particle shadow images are recorded on video tape which may then be played back one field of view at a time and observed on the monitor. Each field, consisting of 262 television lines, may then be analyzed to ascertain if it contains particle images. Some of the images seen on the monitor are those of focused particles and some are those of non-focused particles. It is the decision of the observer which particles to accept as focused and which to reject as non-focused. When observing particles whose images span many lines on the monitor, sharp, focused particle images can be easily distinguished from fuzzy, non-focused particle images. On the other hand, a focused particle image which occupies only one line can never be distinguished from a non-focused particle image which also spans one line. Thus, somewhere between these two extremes the ability of the observer to distinguish focused from non-focused particle images becomes limited by the number of lines the image spans. When the observed particle image approaches this limit, our confidence in the observation is reduced. With the presently available optics, PLP is capable of resolving images down to 5 μm in diameter. The presence of particles between 1 and 5 μm diameter may be noted; but since the images may not be confidently differentiated as focused or non-focused, no size may be reported.

2) Cascade Impactor Analysis - Operation and Data Presentation

The Tech Ecology Model 253 Ambient Cascade Impactor was also used for particle analysis of smokes. The impactor, which utilizes Sierra Instruments radial slot design, consists of five collection stages and a sixth filter stage measures the aerodynamic particle size of an aerosol. Sampling was according to ASTM standards which recommend isokinetic conditions; i.e., the sampling velocity was always within 10% of the flow velocity as measured with the calibrated hot wire anemometer.

Tech Ecology describes the operation of the impactor as follows:

"The particle laden flow stream sampled by the radial slot impactor accelerated through four radial slots in the first impactor stage, and large particles impact on the first slotted glass fiber collection paper. The flow stream continues accelerating through smaller slots in the second impactor stage, and particles greater than the cut-off size of the second impact stage adheres to the second collection filter . . . This process is repeated at every stage. The size of the radial slots is constant for each

stage and smaller for each succeeding stage. Thus, the jet velocity is higher for each succeeding stage, and smaller particles acquire sufficient momentum to adhere to one of the collection filters. After the last impactor stage, the remaining fine particles are collected in a built-in, high efficiency glass fiber filter. The collection and filter papers are weighed on a standard microbalance before and after the test to determine the particle mass distribution. Since all particles are collected, the impactor head yields total particle mass concentration, as well as the particle size distribution." The glass filters also provide a suitable inert medium for later possible chemical analysis.

The collection efficiency for the impactor has been determined and calibrated at the factory. The particle size cut-offs may be summarized as shown in Table XIII.

A smoke sample containing particles of various shapes and densities is fractionated and collected according to its aerodynamic characteristics. The mass collected on each stage is thus equivalent to the mass of spherical particles of density 1 g/cm^3 which has the same terminal settling velocity as the sampled particle. The data obtained by impactor analysis must therefore be expressed in these terms. Some of the phenomena observed in the performance of various smoke detectors, such as entry problems, will be aerodynamic in nature. Conversely, many other phenomena, such as light scattering, are more directly size and shape related phenomena, so that variability in density of smoke particles for different fuel sources may need evaluation. To this end the collection papers may be omitted and the particles collected directly on the surface of the stainless steel impactor stages. The surface can be coated with a thin layer of silicone grease before collection to minimize particle reentrainment. After collection the impactor may be disassembled and the stages may then be microscopically examined for collected particles. Particle size distributions are normally plotted cumulatively on log-probability graph paper. In this format, the total mass W_i on all stages, including the back-up filter, is added up and the percent less than the 50% cut-off size $D_{p,50}$ for each stage plotted against D_p. In the particle size distribution field, the size typically is plotted in terms of "Equivalent Aerodynamic Diameter": the size of a spherical particle of density 1 g/cc which has the same terminal settling velocity as the sampled particle. On log-probability paper the particle size distribution of emissions sources often is close to a straight line. Once the cumulative particle size distribution is plotted, the two major parameters of particle size distributions can be determined: (1) the "Mass Median Diameter" $D_{p,50\%}$, the particle size at 50%—which is an overall measure of the size of the particles, whether large or small and (2) the "Geometric Standard Deviation" σ_g, the ratio $D_{p,84\%}/D_{p,50\%}$--which is a measure of the "spread" in the particle size distribution (if $\sigma_g = 1$, the aerosol is monodisperse; typically $\sigma_g > 1$). Alternatively, the particle size distribution can be presented as the percentage of particles in the size range captured by each stage:

$$\frac{W_i}{W_{tot}} \times 100 \text{ (in percent)}$$

where: W_{tot} = sum of particles collected on all stages, including the filter stage.

This can be presented as a bar chart where W_i is taken as the mass of particles in size range $(D_{p,50})_i$ to $(D_{p,50})_{i-1}$.

IX. DETECTOR SELECTION AND FUEL SOURCES

9.1 Selection of Sensors for Laboratory Screening and Possible Modifications Thereof

Based on efforts conducted during Phase 1 (130), the detectors recommended for screening and testing on the Phase 2 effort are listed in Table XIV. Note that not all items were purchased and/or tested. Our purchasing and testing philosophy requires comment. For example, for UV detectors which operate on a similar principle, such as the Pyrotector 30-2021 ($95.00 each) versus Fenwal's 102 unit ($289 each), we would purchase and test the cheaper unit. Only if some basic operation problems became evident with the Pyrotector device would we then consider the more expensive unit. Similar reasoning applies to the α versus β ray ionization detectors. In other cases where basic differences in either smoke entry inlet design or circuitry are evident, we would purchase similar detector types, e.g., ESL 724 versus Pyrotector near-IR and Pyrotronics DI-2S versus Honeywell TC-100A.

It should be emphasized that no modifications have been made to these detectors. Furthermore, within the time scope of the Phase 2 and Phase 3 (future) efforts, modifications would be limited to off-the-shelf attachments, e.g., addition of known pore size filters to remove dusts from ionization type detector chambers.

9.2 Fuel Selection

Fire statistics on metal and non-metal mine fires show that a large percentage of fires are of electrical origin and welding/cutting operations (130, 132). The recent statistics compiled by Stevens and Blake of FMC (132) show that 27 and 52 percent of these fire types, respectively, are mine shaft fires. Selection of fuels for fire detector testing are based primarily on their frequency of having caused fires and their potential fire hazards as derived from known burning rate and toxic species evolution data as outlined in Refs. 38 and 133. A greater emphasis was placed on detection of fires in the incipient stage in contrast to flaming combustion tests. Thus, a larger percentage of tests was conducted in the small smoke box described earlier in Section 8.1.

The fuel selection and the test chambers employed are given in Table XV. Punk smoke was selected as the standard solid fuel because of its known reproducible burning behavior. Three different types of PVC materials were tested to examine the effects of non-uniformities in the chemical and physical nature of the fuel source. Close examination of PVC formulations reveals considerable composition variability among different manufacturers' products. A typical additive breakdown for PVC is (by weight) 50% Cl, 30% plasticizer, 5% organo-metallic stabilizer, with the remainder split between filler, pigments and other additives. Wide variations in plasticizers are also common. The polyethylene examined was the outer insulation (black in color and containing an antioxidant) of a 65 amp. coaxial cable (inner insulation was polyethylene - white color) used by Collins Radio in their mine communications systems installation. The polyurethane foam was a non-flame retarded flexible type* (cell structure was reticulated or open-cell type). Pine of two moisture levels and diesel fuel or hydraulic brake fluid represent the remaining realistic mine solid and liquid fuels. Slivered (approximately ½" long) pieces of pine were dried in an oven overnight at 100°C and kept in a desiccator containing Drierite until used. The remaining wood was wrapped in water-soaked paper towels. Approximately 0.5 gm of wood was heated in the crucible to produce smoke. No flaming was observed, but the wood did produce glowing embers.

Several solid combustibles were tested in the large box, under conditions of flaming combustion. These included the wood and the polyurethane foam described above; also included were corrugated cardboard and polystyrene pellets (type 303 injection molding grade resin, Shell Chemical Company). Foamed polystyrene packaging material was also tried. However, a stable burning situation could not be achieved since the material burned locally to completion in the vicinity of the igniter coil, without igniting additional surrounding fuel.

Source liquid fuels were based on their flame colors and their smoke emission characteristics in order to assess the performance of optical view field devices. Methanol, ethanol and isopropanol were selected giving a blue, yellowish, and yellow (with much smoke) flame, respectively.

The amounts of fuels used in testing varied considerably from the small to the larger box. In the small box the weight of plastics and wood varied from about 0.2 to 0.8 gm, while from one to four punks sticks were used, depending on the time rate of Ou desired. For the liquid fuels tested in the large box, 140 ml of fuel in a 14 cm diameter Pyrex petri dish (pan height 21 mm; fuel height = 9 mm max.) was used; 30 ml of fuel in a 10 cm dish and 20 ml of fuel in a 6 cm dish.

---

*Originally, we intended to test various flame-retarded rigid polyurethane foams. However, a CPSC note disclosed that certain types of phosphorus-based flame retardants in combination with polyurethanes made with trimethylolpropane forms a highly toxic 4-alkyl bicyclic phosphorus ester which necessitated caution. Details are given in Ref. 134.

X. EXPERIMENTAL RESULTS

The experimental results obtained for the detectors listed as tested in Table III, subjected to a variety of Table IV fuels and combustion conditions are presented in the following subsections. In addition experimental results and analytical calculations for our multipoint gas analysis systems are also included.

10.1 Products of Combustion (POC) Detector Test Results - FM/GRI Modified Smoke Box

1) Photoelectric Smoke Detectors

The units selected for testing - Electro Signal Lab Model 724 and Pyrotector SK 700 operate on a light scattering principle. Both units contain the light source and detector within the unit and both must sample the local atmosphere. Both are factory calibrated to alarm at 1%/ft at approximately 40 ft/min flow velocity. The ESL unit uses a beacon lamp for the light source and right angle light scattering. The primary sensing device is either a cadmium sulfide or cadmium-sulfo-selenide photoconductive cell.

The Pyrotector unit utilizes a pulsed (1 pulse every 2 seconds) LED near IR light source (single LED) in a 135° forward scattering mode and a high speed silicon detector. Alarm condition requires continuous sensing of 2 to 3 successive pulses. The unit we tested was an experimental model which did not contain the manufacturer's intended power source - 6 V Pb/acid gel cell. We were provided with a Ni - Cd rechargeable battery pack rated at 6 V which presented minor problems in prolonged recharging times and one dead battery.

Data for ESL No. 724 are given in Figures 9-12. In Figure 9, the orientation of 0° means that a convenient reference point on the detector housing (the outer smoke labyrinth in our case) was directly facing the flow field; thus, 90°, 180°, and 270° are orientations in the quadrants of a circle. The data in Figure 9 not only show a dependence of the smoke concentration, expressed in terms of obscuration per foot at alarm, on the chemical nature of the fuel but also a fairly strong dependence of this parameter on the rate of change of percent obscuration per foot. The latter observation is somewhat surprising since one would expect the opposite behavior or no dependence at all. That is, the more rapidly smoke is being generated the more readily it can be detected. An offsetting or possibly dominant factor could be a change in particle size distribution with increased smoke generation rate such that increased Ou values are required for alarm. Furthermore, since the ESL 724 detector is based on light scattering principles, we would expect polyvinylchloride (PVC) smoke (a white aerosol under slow smoldering conditions) to alarm earlier than punk smoke (a greyish-white aerosol) since increased scattering is observed for white over black smokes. It has been shown (135) that cascade impactors for sampling atmospheric aerosol collect particles efficiently with no

adhesive coating on the plates provided that the R.H. exceeds 75%. At low humidities the composition of the sample may change due to the preferential deposition of water-soluble material. Roughly 50% by weight of PVC ends up as HCl, in the presence of H_2O, following thermal decomposition of the solid material. Since this material is water-soluble, the detector in its labyrinthine housing may "see" a smoke of appreciably different composition than that seen by the light-and-photocell assembly in the smoke box. Some evidence of an orientation dependence on flow direction for the detector positioned on the inner support floor of the smoke box is also observed.

In Figure 10 the effect of increased flow velocity was examined. By normalizing the rate of change of percent obscuration per foot with the mean linear flow velocity (determined with a calibrated hot wire anemometer) the data for $\bar{v}$ = 64 ft/min were reduced to a single curve. As already shown in Figure 9, the Ou* data for $\bar{v}$ = 23 ft/min show a dependence on the nature of the fuel.

We are not certain of the exact reasons for the behavior of the data in Figures 9 and 10. We do know that the smoke is essentially independent of position along the entire path length of 5 ft since similar fire detector performance was obtained for various spatial positions. The velocity profile is also uniform in the cross-sectional plane of the smoke box. It is possible that physiochemical differences in the nature of the smokes as well as/or a flow entry problem associated with detector design could be responsible for such behavior.

In order to examine the effects of more realistic detector mounting (side wall and ceiling mounting) on orientation for a range of flow velocities the data in Figure 11 and 12 were obtained. The data in Figures 11 and 12 show a fairly strong orientation dependence with the flow vector for both ceiling and side wall mounting positions; performance differences between these mountings are also noted. These data are in contrast to Figures 9 and 10 data for the detector positioned on the inner support floor of the smoke box, which showed only some evidence of an orientation sensitivity. It is important to point out that some nationally recognized fire detector laboratories test detectors in the latter position; thus, such data as shown in Figures 11 and 12 would go unnoticed. Alternatively, one may argue that this orientation sensitivity is of limited importance since the detector alarmed before the national code limit of 4% obscuration/ft. However, in contrast to other detectors which show essentially no orientation dependence, it is of some consequence.

In Figure 13 the performance data for punk, dry and moist wood, and plastic smokes are given for Pyrotector SK 700 LED smoke detector. The data clearly show outstanding performance for all fuels tested. For polyethylene, polyurethane, dry and moist wood pyrolysis products, Ou* values at alarm ranged from around 1/2 to 3/4%/ft, while for punk Ou* was around 2%/ft; velocity independence was found for all fuels tested. Flow orientation tests were not conducted because the sensing parts of this unit are entirely open to the environment.

2) Ionization Detectors

Three α ray source ionization detectors - Fire Alert CPD 1212, Honeywell TC100A, Pyrotronics DI-2S, each utilizing the dual chamber design concept* and a β ray unit containing a single ionization chamber of South African origin - Anglo American Electronics Corporation - Becon MKII were screened.

The Fire Alert CPD 1212 detector is designed to operate from 22-28 V D.C. unfiltered; at 24 V D.C. its current drain is 30 ma. It is factory pre-set to detect a nominal value of 6 milligrams of combustion products per cubic meter. The contact rating at alarm is 3 A at 24 V D.C. Only 1.5 μC of Ra^{226} is used for the radioactive α emitter. In all tests this unit was operated at 24 V D.C. The unit was ceiling mounted in all tests.

The data obtained for punk smoke, three different PVC samples, and polyurethane over a range of flow velocities and smoke generation rates expressed by Δ Ou/Δ t are given in Figures 14 to 17. The data in Figure 14 show essentially no orientation dependence. Since smoke entry is through a symmetrical entry region in the Fire Alert unit, an orientation dependence was not expected; thus only a 0° and 90° orientation were used to test our hypothesis. All subsequent testing was consequently conducted at the arbitrarily assigned o° orientation. It is interesting to note that after repeated testing (data in Figures 15 and 16 were obtained) there is, at most, only a slight difference in detector sensitivity to punk smoke shown in Figure 14.

The data in Figures 15-17 were obtained for the three different PVC materials, and a single polyurethane foam for a range of flow velocities (25-225 ft/min), ambient relative humidities (23-58% R.H.), and smoke generation rates (expressed as an average rate of change of percent obscuration per foot, Δ Ou/Δ t (%/ft-min), from 1 to 15%/ft-min).

The data in Figure 15 show a number of important and interesting results:

a) The response to pyrolytic PVC degradation products is such that Ou* at alarm for Fire Alert 1212 ranges from two to ten times greater than the national standard (for approval of smoke detectors Ou* must not exceed 4% obscuration/ft).

b) Fire Alert 1212 showed a roughly twofold increase in sensitivity following repeated PVC exposure (data illustrated by the solid and open diamonds were obtained after the solid triangles, solid squares and open circles were obtained). However, immediately following this observed behavior, testing with the standard punk smoke as shown in Figure 14 shows essentially no change in sensitivity. Thus, the PVC results are not artifactual.

---

*One chamber detects the presence of combustion products, the other serves as a reference for sensitivity stabilization to environmental changes in temperature, humidity and pressure.

c) There is essentially no difference in ionization detector response to PVC flexible tubing and PVC line cord; however, PVC No. 1120 rigid pipe is easier to detect (i.e., alarms at lower Ou*).

d) There is some indication of a humidity dependence as illustrated by the PVC tubing data at 26% R.H. (solid triangles) versus that at 52% (solid square).

The data in Figures 16 and 17 also show a number of interesting though confusing results:

a) Ou* is a function of Δ Ou/Δ t for both PVC and polyurethane (note that the best straight lines were drawn through these data for comparative purposes; the polyurethane data more correctly follow curves).

b) The polyurethane data in Figure 17 show a complex dependence on flow velocity. However, at a controlled Δ Ou/Δ t, varying only from 2-4%/ft-min, the parameter Ou* is essentially independent of flow velocity (Figure 16).

c) For polyurethane Ou* is roughly triple the standard Ou* for smoke detectors.

Performance data for Honeywell TC100A, which operates at 24 VDC and utilizes 12.2 μC Am^{241}, are given in Figures 18-21 for punk, plastic and wood (moist and dry conditions) smokes. In Figure 18, a comparison of the performance behavior for Honeywell TC100A is made for punk versus plastic smokes for various flow velocities. Note that the ordinate is Ou not Ou*, since this detector has an analogue output and, thus, is not equipped with a relay or horn to signal a pre-set alarm condition. Also note a roughly 6% change in output voltage versus flow velocity for clean air, i.e., Ou = 0, and a fairly strong though orderly dependence on flow velocity in the presence of smoke. It is our belief that a 20-30% change in output voltage or 2 to 3 volts above baseline (roughly 14 to 15 volt range on the abscissa) represents a reasonable compromise between adequate detection capabilities (at least for punk smoke) and unwanted false alarms. This condition is readily met for punk smoke corresponding to conditions of Ou = 4%/ft and under. However, for plastic smokes the data in Figure 19 show that the 14-15 voltage output corresponds to Ou ranging from 10 to 30%/ft. For moist wood smoke the data in Figure 20 show an orderly trend in variation of output voltage with increased flow velocity up to around 100 ft/min. Completely different behavior is observed for the 170 ft/min and 225 ft/min runs. For dry wood (Figure 21) behavior opposite to moist wood was obtained for 35 ft/min and 100 ft/min flow tests. Note that larger changes in output voltage are obtained for correspondingly lower Ou levels for $\bar{v}$ = 35 ft/min than for the other flow velocities tested. As far as ease of detection is concerned, wood smokes fall in between punk and plastic smokes.

Data in Figure 22 for Pyrotronics PYR-A-LARM DI-2S ionization detector which operates at 22 V D.C. and contains a small amount of radioactive material (type and amount not indicated on label) show, on an overall basis, behavior

similar to the Honeywell and Fire Alert ionization detectors for punk and plastic smokes. That is, adequate response to punk (Ou* less than around 4%/ft except for the data point at 170 ft/min) and poor response to plastic smokes (2.5 to 8 times the accepted standard of 4%/ft or in terms of Ou* values of 10-35%/ft). Furthermore, a strong velocity dependence is noted for plastic smokes (i.e., essentially resembling a parabola) while overall velocity insensitivity is apparent for punk smoke.

The operational details of Becon MKII may be obtained from Ref. 136. For operation it requires 15 V D.C. at approximately 2.5 ma. It has an analogue output and alarm is indicated by a sharp rise in the power supply current from its quiescent value of 2.5 ma to 16 ma every 3 seconds, accompanied by the flashing of an LED. This unit was designed to overcome the stringent environmental conditions encountered in the S.A. gold mines which include:

a) Corrosive atmospheres - unit contains conductive plastics in place of metals for grids, guard rings, etc., and the connection box is made of fiberglass.

b) Temperatures up to 40°C (104°F).

c) Air velocities up to 6 m/sec (1180 ft/min) - by means of baffles.

d) R.H.'s so high that condensation may occur.

e) Dust - uses β radioactive source since it is more penetrating than the α sources.

f) Changes in atmospheric pressure - sensitivity or trigger level adjusted in situ.

The unit uses a fairly high radioactive β source - 5 mC Kr 85 (note that this radioactive source is 400 to 3,330 times the α sources used in Honeywell TC100A and Fire Alert CPD 1212) to minimize the effects of dust and create similar ionization currents to the α detectors. It is not clear why the single chamber design is used since the dual chamber was designed specifically to minimize erratic behavior from environmental changes (see footnote, page 51). Perhaps radiotoxicity and/or labelling factors were involved. For example, Ref. 137 lists Kr^{85} as a slight hazard from a radiotoxicity classification, with 1-10 mC being of intermediate activity limit, while above 10 mC it is of high activity. Thus, a dual chamber device requiring 10 mC, based on the same 5 mC Kr^{85} per chamber, or possibly even slightly greater amounts depending on system design and desired performance is on the lower limit of the high activity classification.

The time period for cleaning of Becon MKII detectors based on actual use is presently unknown. It is also pointed out that condensed moisture on certain parts eventually causes detector malfunction.

Test data were obtained for several different fuels in the small GRI smoke box* for three different trigger level adjustments:

a) Adjusting the unit's sensitivity potentiometer such that it exhibited its maximum response to punk smoke under actual flow conditions - Figure 23 data were then obtained.

b) Readjusting the pot to alarm at a 2-3%/ft level to punk - Table XVI.

c) Adjusting with a bar magnet as specified in the corporate literature - Table V.

In Figure 23 the following trends are noted:

a) Exceptionally good response to punk - values as low as 0.1%/ft for velocities exceeding around 100 ft/min.

b) Good response to moist wood, polyurethane and polyethylene - around 2 to 6%/ft for velocities exceeding 100 ft/min.

c) Somewhat poorer response to PVC - around 4 to 6%/ft for the same velocities.

d) Rapidly increasing Ou* values for velocities less than around 80 ft/min for all fuels. Note that Ou* levels were 18%/ft and 40%/ft for PVC and polyethylene, respectively, at $\bar{v}$ = 35 ft/min - the lowest flow velocity examined.

Table XVI compares data obtained at a 2-3% punk setting at 100 ft/min with the manufacturer's setting using the bar magnet. With the exception of punk ($\bar{v} \gtrsim$ 100 ft/min) and moist wood, considerably higher values of Ou* were obtained for polyurethane, PVC, and polyethylene than for a 2-3% punk calibration and the most sensitive punk calibration which produced the Figure 23 data. The Ou* levels for polyurethane, PVC and polyethylene obtained with the manufacturer's settings are similar to the levels presented earlier for the α ray detectors.

This latter data raises a number of important questions for which we can only speculate on at this time. Was our initial sensitivity setting much too sensitive, so as, in actuality it would promote unwanted false alarms? The manufacturer's bar magnet trigger level adjustment corresponds to a 30% reduction in ionization current or a voltage decrease from 13 to 12 volts. They state that it seems possible to set the detectors more sensitively, i.e., to trigger at 12.5 volts or a 15% reduction in ionization current. If we compare the Figure 23 data with the Table XVII data, it must be concluded that our initial setting is below that required for a 30% ionization current reduction. How far below is not presently known.

---

*The Becon MKII was mounted in the side wall of the GRI smoke box.

Since this detector will undoubtedly be adjusted in situ using the manufacturer's method, we must conclude that this unit does not respond favorably to plastic smokes—polyurethane, PVC, and polyethylene.

Based on known problem areas for ionization detectors, such as need for periodic cleaning in dusty environment, alarm to various non-fire produced aerosols in two different metal mines for exposure times of a few hours for battery powered ionization detectors BRK Electronics SS74R and Statitrol's Smokeguard No. 1 (Ref. 138), etc. (see Ref. 130), and poor response to wood and plastic smokes, it must be concluded that ionization detectors with perhaps the exception being Becon MKII are unsuitable in metal and non-metal mine environments. A closer examination of some of the problems discussed above are required for the Becon MKII detector.

Thus, the ionization detectors tested—Fire Alert CPD 1212, Honeywell TC100A, PYR-A-LARM DI-2S, Becon MKII—show on an overall basis a decreasing sensitivity (as based on increased Ou levels) in order with punk - polyurethane - polyethylene - PVC. Or to generalize, the sensitivity of ionization detectors decreases with increasing particle size (see Section 10.4 Particle Size Analysis).

The important conclusions may be summarized as follows:

a) Ionization detector sensitivity to punk and plastic smokes show a decrease with increasing particle size.

b) Increased R.H.'s for similar smoke levels, i.e., Ou and Δ Ou/Δ t's, lead to increased particle sizes.

c) Low smoke generation rates lead to increased particle sizes at fixed R.H.'s

d) Rate of smoke generation and R.H. also affect ultimate grain loading and particle statistics.

e) Plastic degradation products produce larger sized particles than the standard calibration fuel - punk.

f) Sampling should be taken in at least triplicate.

g) There is a need for additional efforts to obtain a better understanding of how aged smokes and other parameters such as Δ Ou/Δ t, R.H., etc., affect POC detector performance.

3) "Taguchi" Gas Sensor (TGS) #109

The Taguchi gas sensor is a semi-conductor device whose resistance is an inverse function of the amount of certain material, such as CO or hydrocarbons, it adsorbs from the ambient air. To be effective, the adsorbing surface must be maintained at an elevated temperature by a heater which is energized by voltage V_h.

The performance of this device is assessed by measuring its resistance. The circuit employed is shown in Figure 4B. It is similar to that of Figure 4A, except that in Figure 4B the feedback resistor R_1 is fixed rather than variable, and, also, the output terminals are paralleled by resistor R_3, whose value is 10K. With this circuit, the resistance of the TGS device, R_o is given by $R_o = V_h/V_o\ R_1$. In these experiments, R_1 was a nominal 10K resistor, whose actual value was 10.57K.

Since V_h and R_1 are selected, hence known circuit parameters, and V_o is measured, the value of R_o can be calculated. In the following discussion this calculation was not made; instead, the discussion is in terms of V_o. It can be seen from the equation above that increasing V_o implies decreasing R_o, which is the condition resulting from increasing response by the device to adsorbable combustion gases. Thus, the performance of the TGS can be studied quite adequately by examining V_o.

Performance data for Taguchi gas sensor (TGS) No. 109* are given in Figures 24-29 and Table XVII for a heater voltage of $V_h = 0.8$ volts and in Figures 30-36 and Table XVIII for $V_h = 1.2$ volts. At the lower heater voltage $V_h = 0.8$ volts, TGS sensors are known to exhibit increased sensitivity to CO while simultaneously decreasing sensitivity to hydrocarbons. While at $V_h = 1.2$ increased sensitivity to both CO and hydrocarbons is expected. Thus, at $V_h = 1.2$ volts an increased frequency of false alarming from ambient contaminants would be expected. Testing at the higher voltage was conducted since the results obtained at $V_h = 0.8$ volts showed some unsatisfactory features—primarily reduced sensitivity for selected tests to PVC and polyurethane and long decay times to return to normal operating voltage following exposure to PVC degradation products. The same sensor was used for both test series; around three months separated the tests during which the sensor was left in an energized state (i.e., heater voltage, V_h, on).

In Figure 24 a maximum change in the voltage output of 50% from the baseline is noted to occur at around 1/2 min. over the range of velocities tested. At around 5 min. the voltage transients decay to baseline. Some form of baffling, such as, for example a sintered stainless steel filter, would appear appropriate if: a) the ambient flow velocity first exceeds 100 ft/min and b) cannot be maintained reasonably constant. Operating at $V_h = 1.2$ volts (Figure 30) minimizes considerably the initial baseline voltage deviation; however, after around three minutes the voltage levels off and never returns to its zero value.

TGS No. 109 performance to punk, PVC, and polyurethane are given in Figures 25-29 and Figures 31-33 for the low and high heater voltages, respectively. The response to punk smoke in Figure 25 shows increased sensitivity with increase in flow velocity ($\Delta Ou/\Delta t$ essentially constant). It is noted that the 170 ft/min run does not follow the expected performance pattern. Inspection of our data revealed that this run was carried out

---

*Positioned on inner support floor of smoke box.

after the PVC tests in Figure 26 were conducted. It is possible that the HCl aerosol fraction (roughly 50% by weight of the virgin PVC) poisoned the surface of the No. 109 sensor (a sintered n-type semiconductor composed mainly of SnO_2). We are inclined to believe that this so-called poisoning is reversible, i.e., required a longer burn-off time than for punk and polyurethane (see Figure 29) and was not due to formation of a new compound such as $SnCl_4$ through chemical reaction) since the polyurethane data (selected highlights given in Figures 27-28, decay curves in Figure 30) which were obtained shortly after the PVC data show orderly behavior. Similar orderly behavior was also obtained for punk in Figure 31 (increased in sensitivity over the Figure 25 data) and the various other fuels in Figures 31-36 after a three-month time difference.

The data in Figure 26 show a greatly reduced sensitivity to PVC degradation products in contrast to punk as evidenced by the much higher Ou levels required for similar voltage outputs. The voltage output is also noted to be dependent on Δ Ou/Δ t and $\bar{v}$. However, at the higher heater voltage (Figure 32) the sensitivity is greatly increased—comparable almost to the punk response in Figures 25 and 31.

In Figures 27 and 28 selected TGS 109 behavior at V_h = 0.8 volts for polyurethane smoke and flaming combustion conditions are plotted along with their Ou curves. In both Figures 27 and 28 the TGS output voltage curves (dashed lines) for smoldering conditions trace similarly shaped curves to the Ou data (solid lines). These data are somewhat surprising since the national fire codes in the U.S.A., Europe, and Japan (where the Taguchi sensors originated) classify Taguchi type sensors strictly as gas sensors. Based on this information, we would not have expected the close similarity between the TGS output voltage curves and the Ou curve; however, the data for the onset of flaming combustion (when the Ou curves reach a maximum and then level off or decay while the output voltage increase) would be expected. That is, partially oxidized gases primarily CO and hydrocarbons are generated during flaming combustion. At this time, based on the limited data we have, we can say only that for the slow rates of smoke generation examined (Δ Ou/Δ t $\leq$ 1%/ft-min) Taguchi sensors appear to have smoke detection capabilities. Whether it is smoke in a strict aerosol definition of smoke, or adsorbed condensates, or gases present in proportion to the smoke concentration or a combination thereof that the TGS 109 responds to is a moot question. In Figure 33 a similar response to polyurethane smoke is noted. In comparison with the other fuels tested at V_h = 1.2 V, polyurethane gave the poorest response.

Additional tests at V_h = 1.2 volts were conducted with polyethylene, and moist and dry pine smokes. The data in Figures 33-35 show good sensitivity to all fuels with minor differences noted between moist and dry wood.

Selected decay curves for PVC, punk, and polyurethane are given in Figure 29 at V_h = 0.8 V and in Figure 36 for V_h = 1.2 V, respectively (time t = 0 corresponds to the maximum voltage output). These represent, essentially, recovery of the sensor from alarm conditions. For the Figure 29

data it is seen that the TGS 109 decays most rapidly on a percentage basis for punk smoke while all smokes permit a voltage decay to 75% of their maximum in under 5 minutes. However, in order to decay to the 90-100% level PVC required roughly 1 hour (data not plotted) whereas punk and polyurethane required around ten minutes. For the V_h = 1.2 V data punk again decays the most rapidly. Now polyurethane takes slightly longer to decay than does PVC. With the exception of the 50% decay time for the PVC run, the V_h = 1.2 V curves decay more rapidly than the corresponding lower voltage curves.

The data tabulated in Tables XVII and XVIII illustrate the highlights of the results given previously (symbols used correspond to data in Figures 24-36; two runs for polyurethane - Table XVII were not plotted and thus are not denoted by symbols). It is important to note the large to very large increases in the TGS 109 output voltage corresponding to the 4%/ft or the 2%/ft Ou level for all fuels and test conditions. Furthermore, it is to be emphasized that these runs were not conducted under favorable or idealized conditions. For example, we deliberately avoided allowing the output voltage to reach its baseline value—generally 0.17 volts for our circuitry, and used values as high as 0.4 volts; nevertheless, the large to very large output voltage increases already noted were obtained in the presence of smoke and flame. Thus, contrary to our earlier opinion expressed in our tehhnical proposal to BuMines and Phase Report No. 1 (131) which was based on the NFPA opinion concerning TGS devices, we conclude that TGS devices might afford low cost fire protection in the metal and non-metal mine environments. However, because of the known strong response of TGS devices to hydrocarbons some form of gas sensing in addition to the TGS capabilities for gas detection appears necessary to discriminate against diesel exhaust and shot firing. Our opinion on this matter remains as expressed in our Phase Report No. 1.

10.2 Optical View-Field and Contact (Thermal) Type Detector Behavior

The test chamber for evaluating detector performance to flaming combustion sources was described previously in Section 8.2. A circuit schematic for simultaneous screening of heat detectors - Fenwal Detectafire* (vertical #27121-1 and horizontal #27020-0 oriented types) and optical view-field detectors - Pyrotector 30-2021 (UV) and Pyrotector 30-2025 (IR) illustrating their downward positions is given in Figure 37. Also tested was Thermotech* Model No. 302AW135 (vertical orientation) which was substituted for Fenwal's horizontally oriented heat sensor. This permitted comparative testing of different vendor devices of similar operational principals and geometry but of widely different costs (Fenwal unit: $29; Thermotech: $11).

---

*These thermal sensors are classified as "rate compensated" devices. The ratings for the Fenwal units are the same - 140°F set point at +5°F and -10°F, while the Thermotech is rated simply as a 135°F rate anticipation heat detector. Their operational behavior is discussed in Section 4.1, page 18.

The test conditions included the following:

1) Fuel type - methanol, ethanol, and isopropanol were ignited by a glowing filament in a shallow (pan height = 21 mm; fuel height = 9 mm max.) 14 cm diameter Pyrex petri dish.

2) Distance from fire source to detector - nominally 3, 5, and 7 feet.

3) Injection of aerosol contaminants - A fine water fog (mean particle size 14 μm) was injected at various times (before, during, and after fuel ignition) using a Fogmaster Tri-Jet fogger #6208 manufactured by the Afa Corporation.

4) Surface contaminant coatings - A thin layer of No. 9 diesel oil was used to coat the sensing tube of the UV sensor, in one test.

The parameters monitored during a run were: time to alarm or detector response time, air and detector temperature (by fixing a #24 iron-constantan thermocouple directly to the thermal sensor) as functions of time (thus the rate of temperature rise in °F/minute), and smoke obscuration.

The test highlights may be summarized as follows:

Pyrotector UV 30-2021 - Responded in 5 seconds or less* (for closer distances to the burning fuels) for the three test fuels and was completely independent of the operation of the Fogmaster. The coating of the UV tube with #9 diesel oil rendered the sensor inoperative and extensive cleaning with trichloroethylene and ethanol was required to return the detector to its normal operating condition.

Pyrotector IR 30-2025 - Responded in 7 seconds or less (1 second for the 5 and 3 ft. distances from the burning fuel) for the yellow isopropanol flame. No response was obtained for the bluish CH_3OH or C_2H_5OH flames. This device returned to a non-alarm condition when the smoke generated during the isopropyl alcohol burn became sufficiently dense** (usually after around 4-5 minutes). In other cases it alternated between the alarm and non-alarm state for periods of up to 5 minutes. The fog cloud generated by the Fogmaster was found to cause a behavior similar to the alarm/non-alarm oscillations for the dense isopropanol smokes.

---

*This is to be interpreted essentially as instaneous response since a 3-second delay circuit is built-in to prevent unwanted false alarms from sparks and other short duration UV sources.

**A meaningful value of O_D* for the 4 ft. light beam cannot be quoted. That is, the smoke coated the photocell, and its subsequent voltage output was diminished appreciably; the photocell had to be cleaned to return to a base line operating condition.

Heat Detectors - Response times ranged from around ½ minute (most favorable conditions) to several minutes or even no alarm in certain cases (see Table VIII, also Figure 38). Alarm times and detector temperatures at alarm were consistently lower for the Fenwal unit (always below its set point 140°F-10°F) than for the Thermotech device (always above its 135°F rating excepting one case where alarm was obtained at 127°F). Note that these units were subjected to rather large temperature rate increases - 18-47°F/minute as based on air temperature.

The data in Figure 38 show that the Fenwal vertical oriented detector responds faster than the horizontal. Also, it responded at a consistently lower temperature than the horizontal detector* - Figure 39.

Based on these screening tests, it is concluded that:

1) The IR sensor - Pyrotector 30-2025 is unsatisfactory for mine applications.

2) The UV sensor appears acceptable; thus, further systems testing is warranted.

3) Thermotech (vertical) is preferred to Fenwal (vertical) in a systems installation because of its cost; i.e., $11 versus $29 for the Fenwal detector. Although Fenwal's performance was superior, we believe that three Thermotech units suitably positioned in a given enclosure would out-perform a single Fenwal unit. Exceptions of course would include the case where a fire occurs under the Fenwal and Thermotech units. However, this has a low probability of occurrence.

The sensitivity of Becon MKII, tested earlier in the smoke box (see Sec. 10.1-1), was examined in two tests under flaming combustion of isopropanol in the large test box. The sensitivity or trigger level setting of the detector was at its maximum with regard to punk smoke; it produced Ou* values as low as 0.1%/ft for flow velocities exceeding around 100 ft/min).

For test #1, a 5.7 cm petri dish was filled with isopropanol; alarm was at Ou* = 0.4%/ft. Following extinguishment of the fire and exhausting of the test box, the detector remained in alarm. However, following exhausting of the small smoke box with the detector's sensitivity set according to the manufacturer's procedure, the detector returned to its non-alarm state.

In test #2, Becon MKII in its most sensitive setting was subjected to a 14 μm water mist from a tri-jet fogger until it was dripping wet. The detector did not go into alarm. Now subjecting it to an isopropanol flame - here a 9.6 mm petri dish was used - alarm was at Ou* = 1%/ft. Once again, following flame extinguishment and exhausting the smoke box, the detector remained in its alarm state. These two tests imply that although the detector will not false alarm to a fine water mist, its setting is still too sensitive for an actual field installation. Frequent false alarming would more than likely be encountered in various mine areas at this sensitivity setting.

---

*An explanation for such behavior would have to be based on a modelling study of a turbulent ceiling jet which is outside the scope of the present study.

10.3 Flaming Combustion Tests Using Solid Combustibles

A number of tests were carried out in the large flaming combustion test chamber using solid combustibles. The detectors included two which had been previously tested in the smoke box, Pyrotector SK700 and TGS 109, one which had been tested with liquid combustibles previously, Thermotech 302AW135, and one which had not been tested before, ESL 724L.* Since three of these units had never been tested under flaming conditions at all, several runs in this series were made with our smoke-generating liquid combustible—isopropanol. The other test conditions included combustibles—polystyrene (type 303 injection molding grade resin in pellet form from Shell Chemical Company), corrugated cardboard, flexible polyurethane foam, wood, and ambient contaminants—water mist and rock dust. Foamed polystyrene packaging material was also examined; however, a stable burning situation could not be effected since the material burned locally to completion without igniting additional surrounding fuel.

The highlights of the test series are given in Table XX. Here ESL 724L responded at consistently lower values of Ou* at earlier response times than Pyrotector SK 700. In spite of this excellent performance, it, however, exhibited a few serious shortcomings:

1) Response to burning wood slivers at Ou* = 0.35%/ft (the maximum value of Δ Ou/Δ t was Δ Ou/Δ t $\simeq$ 0.3%/ft-min) well below its pre-set alarm level of Ou* = 1%/ft. This behavior would seem to promote unwanted false alarms. Figure 9 shows a fairly strong dependence of Ou* on Δ Ou/Δ t which exhibits increased sensitivity with decreasing rates of smoke generation+. That is, the more slowly smoke is being generated, say Δ Ou/Δ t $\lesssim$ 0.2%/ft-min, the more readily alarm can occur below the factory setting of Ou* = 1%/ft.

2) Responded to a 14 μm water mist** after an exposure time of 4.3 minutes in contrast to Pyrotector SK700 which showed no response.

3) Required much longer periods to recover from an alarm condition to normal operation than Pyrotector SK700.

4) Alarmed after approximately 10 seconds upon exposure to a rock dust cloud obtained from a 5-second blast from an air jet (35 psig setting).

SK700 also alarmed within several seconds in the rock dust cloud.

---

*ESL 724L utilizes a LED for its light source that emits in the visible rebion of the spectrum. It was provided free of charge by the manufacturer. This detector was new and thus not subjected to the repeated tests from various smokes that Pyrotector SK700 and TGS 109 were. Strictly speaking, this test series would, therefore, be biased toward the ESL unit.

**All detectors were dripping wet at the end of the 10-minute test period.

+Note Figure 9 data is strictly valid for ESL 724. Since 724L, excluding the light source and related circuitry, is similar to 724, it is reasonable to assume a similar smoke generation dependence.

Pyrotector SK700 performed quite well in this test series, although not quite as spectacularly as obtained earlier in the FM/GRI modified smoke box testing with pyrolytic combustion products. Ou* values ranged from 1.8 to 5.6%/ft for the various Table XX fuels; it was insensitive to water mist and did not alarm to a wood fire for Ou_{max} = 0.67%/ft. The latter may be viewed two different ways:

1) Positively (as in the preceding sentence) - Since the alarm setting was Ou* = 1%/ft, alarm was not anticipated. Thus, this observation shows good stability characteristics around the alarm point for this flaming combustion test.

2) Negatively - Earlier (see Figure 13) Ou* values as low as 0.5%/ft were obtained for moist wood and polyurethane degradation products. Thus, alarm at a closely similar level for flaming combustion of wood (for which Ou $\sim$ 0.6 for approximately 40 seconds) might also be expected. Alarm to a rock dust cloud in ten seconds or under was unsatisfactory. It should be pointed out that after being subjected to ten minutes of the water mist detector indicated trouble. Since the back side of the detector had completely exposed electronic circuitry, it was not surprising to obtain this result. Normal operation was restored after drying with warm air. Proper packaging is, therefore, warranted for any mine systems installation.

In contrast to the earlier response tests to pyrolytic combustion products, the Taguchi 109 showed some unexpected flaming combustion results:

1) No response to polyurethane foam, i.e., no change in output voltage, $\Delta V = 0$.

2) No response to the initial (one minute or greater) flaming starts (without much smoke) for polystyrene and corrugated cardboard. Also, essentially no response to wood, i.e., $\Delta V = 0.12$ volts for the first 1.1 minutes of the test. Only after the flames went out with the cardboard and the wood slivers and smoldering with much glowing took place did the Taguchi 109 respond adequately.

Total insensitivity to the water mist and rock dust testing were very encouraging TGS results.

The performance of the rate compensated Thermotech 302AW135 detector was pretty much as expected. Adequate response to fairly large amounts of NFPA Class B type fuels (liquid hydrocarbons generally having high heats of combustion) and no or poor response to small fires of Class A solid fuels. No response to a rock dust cloud or to water mists, as anticipated.

In brief, it may be concluded that use of Pyrotector SK700 in conjunction with TGS 109 in a hybrid or integrated systems approach will provide low cost fire protection for a wide range of mine fuels while affording insensitivity to two important contaminants—water mists and rock dust. It has already been pointed out that we feel the diesel and shot firing discrimination problem may be best handled by gas sensing of the ratios of

of CO/NO_x or CO_2/NO_x. Low values for these ratios indicate diesel exhaust and shot firing, whereas high values indicate an actual fire. The cutoff point between low and high values of these ratios is presently unknown.

10.4 Particle Size Analysis

1) Pulsing Laser Photomicrography (PLP) Analysis

The smoke box described in Section 8.1 was used to generate smoke obscuration levels of Ou = 4%/ft for smoldering punk and 4% and 10%/ft for pyrolysis of polyurethane. When the appropriate Ou was achieved the smoke source was removed and the smoke box atmosphere exhausted through the optical path of the laser (aerosol spray position in Figure 8). The recorded smokes were then analyzed as previously described in Section 8.4-1.

An analysis of particle size determination using the PLP systems showed that:

a) For punk smoke at Ou = 4%/ft - no particles were observed > 5 μm. Few particles observed 1 to 5 μm.

b) For polyurethane smoke Ou = 4%/ft - no particles > 5 μm were observed. A fairly large number of particles was observed between 1-5 μm.

c) For polyurethane smoke Ou = 10%/ft - same behavior as for polyurethane at Ou = 4%/ft.

d) Particle size distributions for punk and polyurethane differed considerably.

e) Analysis using cascade impactors will be appropriate as little of the aerosol is of a large particle size.

2) Cascade Impactor Analysis

Two groups of experiments were carried out using the cascade impactor for characterizing particle size distribution of smokes. In the first group. The smoke box was used to generate smoke obscuration levels of 4%/ft from smoldering punk, 4%/ft from pyrolysis of PVC and ~ 10%/ft from pyrolysis of polyethylene. After the appropriate smoke obscuration levels were obtained the smoke source was removed and suction was applied to the cascade impactor to achieve a flow rate of 0.75 SCFM (45 SCFH) for 60 to 90 seconds depending on the expected grain loading* for the sample.

The following results have been obtained - 1.25 g of punk were pyrolyzed to give a grain loading of 1.65 mg/ft^3 at Ou = 4.0%/ft. This is in remarkable agreement with the grain loading of 1.67 mg/ft^3 obtained at Ou = 4.0%/ft

*mg solids collected/ft^3 of atmosphere sampled

after pyrolysis of 0.10 g of PVC linecord insulation. Finally 0.2 g of polyethylene insulation was pyrolyzed to give a smoke obscuration of 11.1%/ft and a grain loading of 6.61 mg/ft^3.

Table XXI summarizes the particle size distribution data obtained for these fuels and Ou levels.

The log probability plots (Figures 40-42) for the three smoke sources give mass median diameters, mmd, and geometric standard deviations, σ_g, as listed in Table XXII (entries marked with asterisk).

Figure 43 contains bar graphs of the three distributions in a manner which more graphically dramatizes the differences between distributions.

Our results would tend to indicate the following:

a) At the same level of smoke obscuration smoldering punk tends to produce twice as much aerosol less than 0.61 μm diameter as a smoldering plastic (0.44 mg < 0.61 μm for punk vs. 0.24 mg < 0.61 μm for PVC). This tends to confirm our previous hypothesis that smoldering punk generates a smoke particularly suited for detection via ionization detectors (which favor smaller particles).

b) At all levels of smoke obscuration smokes from smoldering plastics tend to generate larger particles than do smoldering punk (2.4 and 2.1 μm mmd's for pyrolysis of PVC and polyethylene vs. 0.95 μm mmd for smoldering punk).

Another group of cascade impactor characterizations of plastic and punk smokes was carried out. The data tabulated in Table XXII present the important particle parameters - grain loading, mass mean diameter, and standard deviation obtained at various smoke levels, Ou, rates of smoke generation, Δ Ou/Δ t, and ambient ralative humidities.

The polyurethane data conducted in triplicate (data discussed in order from top to bottom of table) show that while the conditions under which the various smokes were generated remain relatively unchanged (relative humidity and rate of obscuration) and the samples were taken at similar obscuration levels, there is considerable variability in the grain loading and particle statistics. Since plastic smokes are expected to produce large particles and are not readily detected by ionization detectors (whose sensitivity is known to decrease in the presence of large particles), the small particle size of polyurethane smokes at 4%/ft is somewhat surprising. Two separate runs under different conditions were therefore made for polyurethane at around 10%/ft. The first 10%/ft run seems to be in agreement with the runs at 4%/ft, by grain loading and particle statistics (similar). However, the second run, which took considerably longer for the achievement of the obscuration level has quite different statistics. We may note that the time for which the smoke remained in the smoke box before sampling were approximately 1.47, 1.78, 1.78, 1.37, and 9.64 minutes for the five runs, respectively. The latter polyurethane run for which the mmd increased to 1.66 μm and σ_g has decreased to 1.9 from the preceding values noted in Table XXII is indicative of smoke aging.

The next three runs for polyethylene illustrate the effects that R.H. can have on smoke properties. Note that the rate of obscuration was not recorded for the first measurement. However, it is comparable to the other two runs (same heater voltage). As can be seen, an increase in relative humidity results in an increase in median diameter. The 10.1% polyethylene run at a low $\Delta Ou/\Delta t$ of 0.5-1.0 (estimated value depending on the observer who interpreted the Ou vs. time curve) again shows that low rates of obscuration consistently give larger particles.

Now proceeding to the two punk runs, we note mmd's considerably lower than for the plastics tested (an exception being the first run for polyurethane that gave a mmd of 0.86 μm).

The last three tests for PVC linecord insulation are in agreement with the previous observations. That is, first, plastics produce larger particle sizes than punk and, second, low rates of smoke generation lead to increases in the mmd of the particles.

If we average the particle statistics for all smokes regardless of sampling conditions, the results shown in Table XXIII are obtained.

The performance data presented previously for ionization detectors - Fire Alert CPD 1212, Honeywell TC100A, PYR-A-LARM DI-2S, Becon MKII - show on an overall basis a decreasing sensitivity (as based on increased Ou levels) in order with punk - polyurethane - polyethylene - PVC. Or to generalize, the sensitivity of ionization detectors decreases with increasing particle size.

The important conclusions may be summarized as follows:

a) Ionization detector sensitivity to punk and plastic smokes show a decrease with increasing particle size.

b) Increased R.H.'s for similar smoke levels, i.e., Ou and $\Delta Ou/\Delta t$'s, lead to increased particle sizes.

c) Low smoke generation rates lead to increased particle sizes at fixed R.H.'s.

d) Rate of smoke generation and R.H. also affect ultimate grain loading and particle statistics.

e) Plastic degradation products produce larger sized particles than the standard calibration fuel - punk.

f) Sampling should be taken in at least triplicate.

g) There is need for additional efforts to obtain a better understanding of how aged smokes and other parameters such as $\Delta Ou/\Delta t$, R.H., etc., affect POC detector performance.

10.5 Multipoint Gas Sampling System Behavior

Transient response times for the pneumatic gas sampling system illustrated in Figure 6 were obtained for 3/8" I.D. tubing of lengths from 1000-5000 ft. The range of pressures investigated was from 685 mm to 505 mm Hg. Much lower pressures are attainable with the exhaust pump; however, the soft-walled PVC tubing started to collapse in the 505 mm Hg test condition. For a 450 mm Hg test the tubing was considerably deformed over its entire cross-sectional area (test data not presented herein). Comparisons between the measured response times and calculated response times are presented. The working forms of the equations upon which the calculated response times are based are given here. The details of the derivations and a few sample calculations are presented in Appendix A.

The internal flow dynamics in the sampling tubing is adequately described by solutions to the Bernoulli equation written in the following form:

$$v dv + \frac{dp}{\rho} + 1/2\ v^2\ de_v = 0 \qquad (3)$$

where $de_v = (4f/d)dL$, f is the friction factor and v = flow velocity, ρ = density. The friction factor is a function of Reynolds number and tube roughness (only for turbulent flow conditions) - Figure A-2, Appendix A. Solutions to the equation above are given for isothermal flows since the assumption of isothermal conditions is more realistic for long tubes than is an abiabatic process.

For isothermal conditions, Equation 3 may be integrated between plane 1 and 2 (Figure A-1, Appendix A) and rearranged to give*

$$G = v_1 \rho_1 = \left[\frac{p_1 \rho_1 \left[1 - \left(p_{2/p_1} \right)^2 \right]}{e_v - \ell n\ p_{2/p_1}} \right]^{1/2} \qquad (4)$$

for the mass flux G of the gas. The maximum possible mass flow, $m_{max} = G_{max} A$, where A is the cross-sectional area, is subject to the condition

$$\partial G / \partial p_2 = 0; \text{ thus:}$$

$$e_v - \ell n \left[p_{2/p_1} \right]^2 = \frac{1 - \left[p_{2/p_1} \right]^2}{\left[p_{2/p_1} \right]^2} \qquad (5)$$

*See nomenclature for definition of symbols.

Here P_2/p_1 is the critical pressure ratio. For inviscid flow ($e_v = 0$) of air (closely approximated in flow through nozzles and venturis), the maximum mass flow is obtained when P_2/p_1 ctit = 0.53 (from Eq. 4). Lowering p_2 below 0.53 p_1 dces not lead to an increase in the mass flow. If we assume inviscid flow, then p_2 = 7.79 psia (403 mm). In other words, we would obtain the maximum possible mass flow by simply providing a pump with the capability to reduce p_2 to 7.79 psia (403 mm). However, in order to overcome friction, p_2 must be reduced to some value below 7.79 psia (403 mm) depending on the frictional resistance.

Returning to Equation 3 we see that all parameters are known for a given L/d tube provided we assume a realistic value for f* from Figure A-2, Appendix A. Now the time required for a "slug" of gas to traverse a given length of tubing, L, is given by the residence time, t_r, which is

$$t_r = L/\bar{v}_1 \qquad (6)$$

Equation 6 assumes that the concentration field closely follows the velocity field, i.e., the mean mass concentration or the center of mass follows the mean flow velocity in the tubing.

Reference 129 presents an alternative approach for estimating the response time for pneumatic conveying of gas samples through long tubes based on Poiseuille's equation for laminar flow in tubes. From Poiseuille's equation the average velocity, i.e., velocity averaged over the cross-sectional area, is given by

$$\bar{v} = \frac{R^2 \Delta P}{8 \mu L} \qquad (7)$$

where: R = tube radius

ΔP = imposed pressure drop

μ = fluid viscosity.

Substituting $\bar{v}$ for $\bar{v}_1$ in Equation 6 allows one to calculate t_r.

One remaining semi-analytical approach was to measure the volumetric flow rate at the tube inlet with a flow meter and to use

$$Q = vA \qquad (8)$$

to obtain v, i.e., the mean flow velocity is simply the volumetric flow rate divided by the cross-sectional area. Once again substitute into Equation 6 to obtain t_r.

---

*As a first approximation determine the Reynolds number based on v_1 obtained for the assumptions of laminar flow (f = 0.1) and turbulent flow (f = 0.002). Repeat calculations for other values of f and construct charts of v_1 vs. P_2/p_1 for a given I.D. tube and fixed length. Use that value of f that gives a t_r that agrees most closely with the measured t_r. Use this value of f for various lengths and construct a t_r vs. L plot for P_2/p_1 as a variable parameter.

A comparison of measured response time with these three different analytical approaches is given in Figures 44-46. Figure 44 data show that when the pressure in the sampling system is not much lower than ambient, the closest agreement with the measured response time is based on the mean flow velocity at the tubing inlet. In the Bernoulli equation a friction factor of f = 0.025 was assumed while other properties were evaluated based on inlet conditions. In the Poiseuille equation the ΔP term is $\Delta P = 760 - 685 = 75$ mm Hg.

In Figures 45 and 46, it is noted that the best agreement with the measured response time is that based on the Bernoulli equation. The same approach was used to calculate the response times now with P = 630 and 505 mm Hg; however, a friction factor of f = 0.02 was used to account for a decrease in frictional resistance with increased flow velocity. The consistently poorest agreement with measured response times for all three graphs was obtained from Poiseuille's equation. Deviations greater than 100% are noted for certain measured response times.

Concentration of calibrated CO_2 in N_2 mixtures arriving at the NDIR analyzer was also investigated as a function of input CO_2 level. Here a single concentration input of 2.25% was injected into the multipoint system to see if a reduced concentration output arrived at the analyzer. Figure 47 data show that for a 1 ℓ 2.25% CO_2 "slug" of gas injected into the inlet of 4,000 feet of tubing, the maximum CO_2 output is only 0.9% (or 9,000 ppm). For a 14 ℓ input the maximum output was obtained, which is 1.79% (17,900 ppm).

Possible explanations for this reduced CO_2 level include at least the following:

1) Mixing of the CO_2 "slug" with air contained in the 4,000 ft. of tubing, i.e., a total volume of 87 ℓ of air which is 4 times greater than the highest volume input of 20 liters. Also mixing at the trailing edge of the "slug" with ambient air appears important.

2) Loss of CO_2 along the flow path to the NDIR analyzer - leaks at tubing connections or adsorption on the PVC tubing (a leak in the manifold section was corrected prior to obtaining the Figure 47 data for 2.25% CO_2). We believe that explanation No. 2 is unlikely since "bleeding in" the entire contents of the pressured mixing tank at a slight positive pressure through the same length of tubing led to a 2.25% CO_2 output on the NDIR analyzer. This result implies that mixing at the trailing edge of the CO_2 slug is controlling since the bleeding in of CO_2 was from a closed system, i.e., at no time was the tank volume depleted and the connecting valve open to atmosphere air. It does not, however, say that there are no leaks at tubing connections since they were at slightly positive pressures. Under slightly negative pressures air can be sucked in at any leaky connection(s) thereby diluting the CO_2 slug to cause a reduction in the CO_2 concentration at the NDIR analyzer.

This question of leaks in the pneumatic sampling system leading to gas dilution with air was examined directly. Following clamping of all tubing connections and further leak checking, 4,100 ft. of tubing was pressured positively to 3.5 psia over atmospheric. After 17 hours the system lost only 0.7 psia, i.e., was still 2.8 psia over atmospheric. Since our experiments require only around 10 to 20 minutes of test time it may be concluded, therefore, that our system is leak-free.

Data in Figure 47 for an input "slug" of 1,300 ppm of CO_2 show that after around 6.5 ℓ of gas are sampled the maximum CO_2 concentration output—1170 ppm CO_2—is reached. This 11% reduction in CO_2 is considerably less than the 17% reduction obtained for 22,500 ppm input of CO_2 shown in the same Figure. Thus, one might suspect that the unclamped system was not leak-free. However, prior to obtaining the plotted data another 1,300 ppm "slug" of CO_2 was sampled in the unclamped system. Since this run produced essentially the same curve as that shown, we are reasonably assured that the plotted data were obtained in a leak-free system.

XI. SUMMARY AND CONCLUSIONS FOR DETECTOR TEST PROGRAM

Laboratory screening of POC's, optical view-field, and contact type detectors under incipient and flaming combustion sources has led to the generation of a reliable data base for the performance characteristics of the various detectors under a range of mine environmental conditions. A small FM/GRI modified smoke box was used to assess detector performance under incipient conditions. Fuels examined included various plastics, moist and dry wood, and a standard calibration source—punk smoke. Detector performance was related to smoke concentration expressed in terms of percent obscuration per foot, Ou, derived from attenuation of a light beam of fixed path length, built into the test chamber. Detailed functional dependences of Ou or the percent obscuration per foot at alarm, Ou* (for those detectors that had pre-set alarm conditions), on flow velocity and rate of generation of smoke expressed by Δ Ou/Δ t were obtained. Particle size distributions were obtained for selected smokes and Ou levels using a pulsed UV laser photomicrography aerosol analysis system in conjunction with cascade impactor analyses.

Three different liquid fuels—methanol, ethanol, and isopropanol—were selected based on their different flame colors—blue, yellowish, and yellow—with much smoke, respectively, for screening of UV and IR optical view-field devices to flaming combustion sources. A number of solid materials—wood, polyurethane, and polystyrene—were also employed in screening of POC's and contact detectors. A test box employing stagnation flow of a radially expanding ceiling jet was constructed for these tests. Other parameters examined were size of the fire source, distance of fire source to detector, heat generation rate as measured by rate of ceiling temperature increase with thermocouples, and injection of water mists of 14 μm mean diameter. The same test box was also employed for screening of thermal or contact type detectors.

A pneumatic gas sampling system was developed for monitoring up to twelve mine locations at a single central location using various sensitive gas analysis instruments. Provisions for increasing the number of sampling points in multiples of twelve were incorporated into the system design. The response time for pneumatic conveying of a "slug" of gas was determined as a function of manifold pressure (expressed in terms of a ratio of manifold pressure to atmospheric pressure), and length of tubing. A comparison of the measured response time with calculated response times using three different fluid dynamic approaches was also made. Finally, efforts were also addressed toward determining the minimum volume of gas that has to be sampled for long tubing lengths in order to obtain a meaningful concentration measurement on the gas analyzers. In other words, the effects of dilution of an input "slug" of gas by the air volume contained in the tubing was examined.

A summary of the more important findings is as follows:

11.1 Products of Combustion Detectors (POC's)

1) Ionization Detectors

PYR-A-LARM DI-2S, Honeywell TC100A and Fire Alert CPD 1212 are unsuitable for detection of pyrolytic combustion products from plastics—PVC (three different types), polyethylene (from high amperage power cable), and flexible polyurethane foam. Smoke levels at alarm (apparent alarm for TC100A since its output was analogue in nature) ranged from about 10 to 40%/ft smoke obscuration, Ou*. This is 2.5 to 10 times the national standard for smoke detectors which requires alarm at 4%/ft or lower. Becon MKII initially responded to these plastic smokes at Ou equal to 2-6%/ft at an extremely sensitive trigger voltage setting. However, upon employing the factory's recommended setting procedure the Ou* levels were in the general range obtained for the three previous ionization detectors. A fairly strong velocity dependence was noted for PYR-A-LARM DI-2S, Honeywell TC100A and Becon MKII for various smokes. Fire Alert CPD 1212 which appeared to be the least sensitive to such changes showed an Ou* dependence on the rate of generation of smoke, Δ Ou/Δ t, and appeared to be sensitive to changes in relative humidity.

2) Photoelectric Detectors

Pyrotector SK700 (a near IR device) and ESL's No. 724 (a beacon lamp device), responded to pyrolytic combustion products from plastics at much lower Ou* levels than did the aforementioned ionization detectors. ESL's 724 exhibited an alarm dependence, requiring moderately higher Ou* levels for slowly moving smokes, i.e., the so-called "smoke entry" problem and an orientation dependence of the detector with regard to an oncoming smoke front. Pyrotector SK700 was completely independent of velocity and exhibited Ou* values that were less than 1%/ft for plastics, moist and dry wood, and around 2%/ft for punk smoke.

For flaming combustion of isopropanol, polystyrene, corrugated cardboard, polyurethane, and wood and mine ambient contaminants—water mists and rock dust—Pyrotector's SK700 performance was compared with ESL's 724L (an LED unit that emits in the visible region)*. An assessment based on the overall test results indicated superiority of the SK700 unit over the ESL 724L unit. ESL 724L did respond consistently at lower Ou* levels, however, for low rates of smoke generation, $\Delta Ou/\Delta t \lesssim 0.2\%/ft\text{-}min$ it alarmed well below its set point (thus indicating a false alarming tendency), and false alarmed to water and rock dusts. SK700 Ou* values ranged from 1.8 to 5.6%/ft, was completely insensitive to water mists, but did alarm to the rock dust cloud.

3) Semiconductor Detectors

"Taguchi" No. 109 exhibited an output voltage dependence on flow velocity in clean air for the circuitry employed in Figure 4B. The shape of the output voltage curves varied considerably with the heater voltages V_h = 0.8 V or V_h = 1.2 V; however, the magnitude of the voltage change was negligible in comparison with the output voltages obtained in the presence of smoke. At V_h = 0.8 V for polyurethane, PVC, and punk the percentage increase in TGS 109 voltage above baseline (0.2 V for Figure 4B circuitry) ranged from around 50% to 1,950% (Table VI) at smoke levels of Ou = 2%/ft or Ou = 4%/ft for the three fuels, respectively. The TGS 109 was highly sensitive to punk smoke while on an overall basis it was least responsive to PVC pyrolytic decomposition products. At V_h = 1.2 V for these three fuels, plus moist and dry wood, and polyethylene the voltage increases ranged from 95% to 1,440% (Table VII). In agreement with the manufacturer's literature on sensitivity to various hydrocarbons increased or comparable sensitivity at the higher heater voltage was obtained for all degradation products from the fuels tested. For polyurethane, however, the very large percentage increases in voltage output recorded for the other fuels (Table XVIII versus Table XVII data) was not obtained.

In the flaming combustion test series, TGS 109 showed a few, perhaps serious, shortcomings: no response to polyurethane foam, no initial (one minute or greater) response to polystyrene and corrugated cardboard, and essentially no initial response to wood; only after the flames went out with the cardboard and wood and smoldering with much glowing took place did TGS 109 respond adequately. Total insensitivity to water mist and rock dust cloud tests were very encouraging TGS results.

Under the most severe test conditions, i.e., subjecting the TGS 109 to repeated exposure to PVC degradation products, comprising essentially 50% by weight of HCl we have been unable to poison irreversibly this semiconductor (composed mainly of SnO_2) sensor. As the data in Figures 29 and 36 show it requires at most around several minutes to recover to 75% of its base line voltage level after exposure to PVC, polyurethane, and punk.

*This detector was new and strictly speaking test results would be biased toward the ESL 724L unit.

11.2 Optical View-Field (UV and IR Detectors) and Contact (Thermal) Type Detector Behavior

1) Pyrotector UV 30-2021 responded essentially instantaneously to the three test fuels—methanol, ethanol, and isopropanol. It was unaffected by the presence of fine water mists (mean particle size 14 microns), but became inoperative when the UV tube was coated with a thin layer of #9 diesel oil. Following this test, it required extensive cleaning with organic solvents to return the detector to its normal operation; thus, periodic cleaning of such devices on a regularly enforced basis would be required to maintain acceptable performance in a mine environment.

2) Pyrotector IR 30-2025 did not respond to the bluish methanol and yellowish ethanol flames. Its performance was affected significantly by the presence of both smoke and water mists. It was judged to be unsatisfactory for mine applications.

3) Rate compensated detectors Fenwal Detectafire (vertical #27121-1 and horizontal #27020-0 oriented types) and Thermotech No. 302AW135 (vertical orientation) supplied by Notifier Corporation were subjected to rather large temperature increases—18-47°F/min as based on air temperature, from pan burnings (different diameter pans) of isopropanol at selected heights from the detectors. The tests results indicated that Fenwal vertical was superior to Fenwal horizontal as the former was also to Thermotech vertical. However, close to a factor of three higher in cost for Fenwal vertical versus Thermotech vertical led us to conclude that three Thermotech units suitably positioned in a given enclosure would out-perform a single Fenwal unit. Since cost is an important factor in instrumenting a mine containing many miles of shaft entries and exits as well as selected tunnels, engineering cost effectiveness dictates selection of the Thermotech device.

11.3 Pneumatic Gas-Sampling System Behavior

Analytical calculations for the residence time to convey a "slug" of gas through 3/8" I.D. polyvinylchloride (PVC) tubing of lengths from 1,000 ft to 5,000 ft produced the following comparative results:

1) For pressures in the sampling manifold not much lower than ambient, i.e., 685 mm Hg the closest calculated agreement with the measured response time is based on the mean flow velocity at the tubing inlet. Response or residence time is given by $t_r = L/\bar{v}_1$ where L is the tubing length and $\bar{v}_1$ is the mean flow velocity at the inlet. Calculations based on an isothermal form of the Bernoulli equation and Poiseuille's equation for laminar flow in tubes gave corresponding poorer agreement with the measured t_r's.

2) At manifold pressures of 630 and 505 mm Hg the best agreement with the measured t_r was obtained from the Bernoulli equation.

3) Poiseuille's equation consistently gave the poorest prediction of t_r.

A strong dependence on the volume input of a "slug" of gas was evidenced for input concentrations of 0.13 and 2.25% CO_2. That is, for a 1 liter 2.25% CO_2 input through 4,000 ft of tubing, the maximum CO_2 output was only 0.9% (or 9,000 ppm). For a 14 liter input the maximum output was obtained which was 1.79% CO_2 (17,900 ppm). For 0.13% input CO_2, the comparable output figures are 0.07% (700 ppm) and 0.117% (1170 ppm), respectively. It appears that the most probable cause of this reduction is mixing of the CO_2 "slug" with the air contained in the 4,000 ft of tubing, i.e., a total of 87 liters of air which is four (4) times greater than the highest volume input tested—20 liters.

XII. COMMENTS ON METAL AND NON-METAL MINE FIRE DETECTION SYSTEM INSTALLATION

Based on the present fire detector performance tests and literature studies that cite mine shaft, mined out (from spontaneous combustion of sulfide ores) and fuel storage areas as important zones that would appear to benefit from fire/gas detection equipment, the following systems are proposed:

1) Shaft Areas - combinations of Pyrotector SK700's and TGS 109's. Becon MKII might also be employed along with these detectors because of its known behavior in the South African gold mines and the known strong response of ionization detectors to flaming combustion of cellulosic fuels. Because of the high cost of Becon MKII (approximately 5x as expensive as Pyrotector SK700) installation of such units in mines only appears justified to us on a cost basis if Pyrotector SK700 performs poorly in situ.

2) Fuel Storage Areas - an integrated system employing pairs of UV/IR/contact type detectors. Pyrotector UV 30-2021 illustrated good performance characteristics while being of modest cost (i.e., approximately one-fourth the price of other competitive units) and is, therefore, a logical choice for the UV device. A suitable IR device is presently lacking and, therefore, further laboratory screening on two recently available promising sensors is recommended. Either one or both contact types—Thermotech 302AW135 or Protectowire 155°F - PHSC—are also recommended.

3) Sealed-Off or Mined-Out Areas - Here gas sensing techniques appear applicable because of the probability of occurrence of spontaneous combustion. Because of the long times associated with spontaneous combustion, transient delay times for pneumatic gas conveying through tubes of long lengths are generally negligible.

John Wagner, Principal Investigator

Roger Welker

Abraham Fookson

Mary May

Allan Harper

dgc

XIII. REFERENCES

1. NFPA records.

2. Jarrett, S. M., et al., BuMines, "Health and Safety Report on the Major Mine Disaster," Sunshine Mine, May 2, 1972.

3. Harrington, D., "Lessons from the Granite Mountain Shaft Fire, Butte," BuMines, 1922.

4. Harrington, D., "Metal-Mine Fires and Ventilation," I.C. 6678, January 1933.

5. Williams, M. L., "Final Report on Mine Fire, Eureka Mine," May 3-19, 1949.

6. Crawford, F. S., "Final Report on Minor Mine Disaster, Copper Canyon Mine," BuMines, Battle Mountain, Lander County, Nevada, June 5, 1950.

7. Pynnenon, R. O. and Felegy, E. W., "Final Report on Mine Fire, Sunday Lake Mine," BuMines, Wakefield, Michigan, April 19, 1951.

8. Alpert, L. S., "Investigation of the Fire in the Cooper-Bessemer Air Compressor," Report SPE-55 Shell Chemical Corp., Pittsburgh, California, June 1954.

9. Whittaker, R. W. and Dovidas, C. M., "Report of Metal-Mine Explosives Fire, Federal No. 17 Shaft, St. Joseph Lead Company," Flat River, Missouri; Bureau of Mines, 201 Post Office Building, Vincennes, Indiana, May 25, 1956.

10. McCreary, H. J., "Report of Metal-Mine Fire Humboldt Mine," Nevada-Massachusetts Company, Tungsten, Nevada, Bureau of Mines, 49 Fourth Street, San Francisco, California, February 25, 1957.

11. Pynnonen, R. O. and Schell, H. L., "Final Report of Mine Fire - Montreal Mine," Oglebay Norton Company, Montreal, Wisconsin, BuMines, Duluth, Minn., March 31, 1958.

12. Zaverl, L. J. and Schell, H. L., "Final Report of Mine Fire - Newport Mine," The Mauthe Mining Company (Pickands Mather & Company, Operator), Ironwood, Michigan, BuMines, January 27, 1959.

13. Schell, H. L. and Pynnonen, R. O., "Final Report of Mine Fire - Buck Mine," Verona Mining Company (Pickands Mather & Company, Operator), Caspian, Michigan, BuMines, Duluth, Minn., July 21, 1959.

14. Anderson, L. G. and Beecroft, C. J., "Report of Mine Fire - Black Jack No. 1 Mine (Uranium)," Lance Corporation, Thoreau, New Mexico, BuMines, Phoenix, Arizona, May 21, 1960.

15. Plimpton, H. G., "Report of a Metal-Mine (Shaft) Fire - Burro Mines (Uranium)," Union Carbide Nuclear Company, Slick Rock, Colorado, BuMines, Salt Lake City, Utah, May 8-12, 1963.

16. Westfield, James, Knill, Lester D., and Moschetti, Anthony C., "Final Report of Major Mine-Explosion Disaster," Cane Creek Mine, Potash Division, Texas Gulf Sulphur Company, Grand County, Utah (Mine development under contract with Harrison International, Incorporated), BuMines, Lakewood, Colorado, August 27, 1963.

17. Murphy, E. M., Bercik, G. R., and Mutmansky, J. M., "Investigation of a Fire Involving Rigid Foam," White Pine Copper Company, White Pine Mine, White Pine, Michigan, BuMines, August 15, 1963.

18. Schell, H. L. and Schrader, A., "Final Report of Mine Fire," - White Pine Mine, White Pine Copper Company, White Pine, Michigan, BuMines, Duluth, Minn., May 12, 1964.

19. "Mine Fire and Explosion," Climax Mine, Climax Molybdenum Company, A Division of American Metal Climax, Inc., Climax, Lake County, Colorado, BuMines, July 8, 1964.

20. Poland, H. E. and Russell, K. U., "Report of Mine Fire, Cordero Mine," Cordero Mining Company, McDermitt, Nevada, BuMines, September 24, 1965.

21. Schell, H. L., "Final Report of Mine Fire, Homestake Mine," Homestake Mining Company, Lead, South Dakota, BuMines, Duluth, Minn., February 13, 1965.

22. Browne, H. F., "Report of Multiple-Fatal Natural Gas Condensate Fire," Texas Eastern Transmission Corporation, LaRose, Louisiana, BuMines, Dallas, Texas, January 10, 1966

23. O'Connor, J. A., Dovidas, C. M., and Capps, R., "Final Report on Major Mine-Fire Disaster - Belle Isle Salt Mine," Cargill, Incorporated, St. Mary Parish, Louisians, BuMines, Vincennes, Indiana, March 5, 1968.

24. Demkowicz, W. H., Pleasant Gap Diesel Powered Truck Fire, Pleasant Gap, Penn., BuMines, Johnstown, Penn., May 12, 1970.

25. Jarrett, S. M., Pynnonen, R. O., and Bernard, R. L., "Report on Major Hydrogen Sulfide Disaster, Barnett Complex Mine," Ozard-Mahoning Company, Rosiclare, Illinois, BuMines, April 12, 1971.

26. Hertzberg, M., et al., "The Spectral Growth of Expanding Flames - The Infrared Radiance of Methane - Air Ignitions and Coal Dust - Air Explosions," BuMines RI 7779 (1973).

27. BuMines - Verbal Disclosure

28. FMC Corporation - Phase 1 Report, "Improved Sensors and Fire Control Systems for Mining Equipment," USBM Contract HO 122053, December 1972.

29. FMC Corporation, "Improved Sensors and Fire Control Systems for Mining Equipment," USBM Contract HO 122053, May 1973.

30. Mitchell, D. W., Nagy, J., and Murphy, E. M., "Preventing Explosions from Gas Ignitions at the Face: A Progress Report," 13th International Conference, Gruvensicherheitlicher Versuchsanstalten, Paper No. 16, Dortmund, Germany, 1967.

31. "Automatic Fire Detection: False Alarms," F.P.A. Journal, No. 88, 146-148, October 1970.

32. Keenan, C. M., "Coal Mine Fires and Gas and/or Dust Ignitions Since Enactment of the 1952 Federal Coal Mine Safety Act," USBM Inf. Circ., 1967.

33. Scott, J. L., Marovelli, R. L., and Yancik, "Status Report on the Bureau's Fire and Explosion Program," Coal Age 77, pp. 92-99, 1972.

34. Private Communication, Safety in Mines Research Establishment, U. K.

35. Greuer, R. E., "Influence of Mine Fires on the Ventilation of Underground Mines," Michigan Technological Univ., USBM Contract SO122095, May 1973.

36. "Ventilation Studies and Escape Plans for Underground Hardrock Mines," BuMines SO230037, NTIS PB-232304, October 1973.

37. Riley, R. E., "Lessons We Can Learn from the Sunshine Mine Fire," American Mining Congress 1973 Convention, Denver, Colorado, September 10, 1973.

38. Wagner, J. P., "Survey of Toxic Species Evolved in the Pyrolysis and Combustion of Polymers," Fire Research Abstracts and Reviews, 14, 2, 1972.

39. Gaskill, J. R., "Smoke Hazards and Their Measurement - A Researcher's Viewpoint," Armstrong Symposium, Lancaster, Pa., March 8, 1973, UCRL-74573 (Reprint).

40. "Analysis of Noncoal Mine Atmospheres," MSA Research Corp., BuMines Contract No. SO231057, Monthly Reports 1-12, June 1973 to May 1974.

41. Hurn, R. W., "Diesel Emissions and Control," 63rd Annual Convention of Mine Inspectors, Institute of America, Checotah, Oklahoma, June 10-13, 1973.

42. Marshall, W. F., "NO_x from Diesel Engines - Control and Measurements Techniques," AIChE 75th National Meeting, Detroit, Michigan, June 3-6, 1973.

43. Wagner, J. P., Welker, R. W., and Harper, A., "Fire Alert Systems for Metal and Non-Metal Mines," Monthly Report #2, BuMines Contract SO144131, 1974.

44. Wagner, J. P., Fookson, A., Harper, A., and Welker, R.,"...Ibid...," Monthly Report #3, BuMines SO144131, 1974.

45. Wagner, J. P., "A Survey of the Principal Operational Characteristics of Fire Detector Mechanisms," Fire Research Abstracts and Reviews, Vol. 13, No. 1, 1971.

46. Wagner, J. P., "Overview of Fire Detector Principles," Polymer Conference Series, University of Utah, Salt Lake City, Utah, June 1973.

47. Delaney, C. L., "Fire Detection System Performance in USAF Aircraft," Technical Report AFAPL-TR-72-49, Air Force Aero Propulsion Laboratory, Air Force Systems Command, Wright-Patterson Air Force Base, Ohio, August 1972.

48. Fox, D. G., "Development of Feasibility Demonstration Hardware for an Integrated Fire and Overheat Detection System," AFAPL-TR-72, 105, May 1973.

49. Wagner, J. P., APL/JHU FPPA71, "Annual Summary Report - Fire Problems Program," Task V-A, pg. 45-46.

50. Pyrotronics Inc. - Private Communication, 1974.

51. MSA Catalogue - Section 10.

52. Green, H. L. and Lane, W. R., Particulate Clouds: Dusts, Smokes, and Mists, Van Nostrand Co. Inc., Princeton, N. J., (1957) also 1964 Edition.

53. Davies, C. N., Aerosol Science, Academic Press, London, 1966.

54. Fuchs, N. A., Mechanics of Aerosols, Pergamon Press, 1964.

55. Air Cleaning and Particle Technology Publications, Particle Technology Laboratory, Dept. of Mechanical Engineering, University of Minnesota, Minneapolis, Minn. 55455.

56. Friedlander, S. K., "The Characteristics of Aerosols Distributed with Respect to Size and Chemical Composition," Aerosol Science, Vol. 1 pp. 295-307, (1970).

57. Friedlander, S. K., "The Characteristics of Aerosols Distributed with Respect to Size and Chemical Composition - II," Aerosol Science, Vol. 2, pp. 331-340 (1971).

58. Wang, C. S. and Friedlander, S. K., "The Self-Preserving Particle Size Distribution for Coagulation by Brownian Motion," J. Colloid and Interface Science, Vol. 24, No. 2, pp. 170-179, June 1967.

59. Kennedy, R. H., "The Assessment of Ambient Conditions to which Fire Detectors are Exposed," Symposium on Automatic Fire Detection, Connaught Rooms, London, March 1972.

60. Green, H. L. and Lane, W. R., Reference 52 Preceding, p. 168, 130, 9 (1957).

61. Gross, D., et al., "Smoke and Gases Produced by Burning Aircraft Interior Materials," NBS Building Series 11, 1969.

62. Ives, J. M., Hughes, E. E., and Taylor, J. K., "Toxic Atmospheres Associated with Real Fire Situations," NBS Report No. 10807, 1972.

63. Boettner, E. A., et al., "Pyrolytic Products of Plastics: Analysis and Toxicity," Final Report PHS Grant No. OH-00148, U. of Michigan, July 1970.

64. Sarofin, A. A., Wagner, J. P., and Tewarson, A., "Gas Evolution During the Pyrolysis and Combustion of Acrylonitrite/Styrene Polymers," Symposium on Environmental Impact of Nitrite Barriers Containers, Rensselaer Polytechnic Institute, Hartford, Conn., July 1973.

65. Martin, B. L., and Hoenig, S. A., "A Review of Carbon Monoxide Monitoring Techniques," Prepared for NIOSH Cincinnati, Contract IRO 1 EC-00467-01.

66. Verdin, A., "Gas Analysis Instrumentation," John Wiley and Sons, N. Y., 1973.

67. Chaffee, D. L., "A Study of Fire Alarms and Fire Alarm Systems," Naval Civil Engineering Laboratory, TN-980, Port Hueneme, Calif., August 1968.

68. Custer, R. and Bright, R., "Fire Detection: The State-of-The-Art," NBS TN 839, 1974.

69. Fire Protection Handbook, National Fire Protection Association, 13th Edition, 1969.

70. Operation School Burning No. 2, Los Angeles Fire Department, NFPA, 1961.

71. Bukowski, R. W., "Suggested Performance Specifications for Single-Station Smoke Detectors," NBS Technical Memorandum, April 18, 1974.

72. Farzane, N. G. and Ilyasov, V., "Automatic Gas Detectors," JPRS 61505, March 18, 1974.

73. Chebotarev, O. V., et al., "Atmospheric Studies at Chemical Enterprises," JPRS-52566, March 9, 1971.

74. Pavlenko, "Gas Analyzers," AD 666090, June 1967.

75. Nakauchi, S. and Tsutsui, Y., "A Study on the Pneumatic Tube Type Fire Detector," Report of Fire Research Institute of Japan, Vol. 7, No. 1-2, December 1956.

76. "Discussion of a New Principle in Fire Detection," A.I.A. File No. 31-i-31, Fenwal, Inc., Ashland, Massachusetts, 1951.

77. Notifier of Western Pennsylvania, Pittsburgh Penna. Sales brochure, "Thermotech Rate Anticipation Heat Detector."

78. Fenwal Brochure MC-212B.

79. Walter Kidde, Belleville, N. J., "Continuous Fire Detection System Brochure."

80. Protectowire Sales Brochure, Pembroke, Mass.

81. Lawson, D. I., "A Possible Method of Protecting Automatic Warehouses from Fire," Reprint from the Fire Protection Review, January 1971.

82. Elphick, M., "Semiconductors Photodetectors," EEE Magazine, pp. 28-37, February 1971.

83. Waters, G. L. C., "Advances in Infra-Red Fire Detection," Fire International, 27, pp. 67-70, January 1970.

84. Pyrotector, Hingham, Mass. Sales Brochure 30-2021.

85. Deboo, G. J. and Burrous, C. N., Integrated Circuits and Semi-conductor Devices, McGraw Hill, New York, 1971.

86. "Instrumentation in Analytical Chemistry," ACS Reprint Collection, pp. 42-48, ACS, Washington, D. C., 1973.

87. Hertzberg, M., Fourth Quarter Report, BuMines, Pittsburgh, Penn., June 30, 1972.

88. Cohen, J., Edelman, S., and Vezzetti, C. F., "Pyroelectric Effect in Polyvinylfluoride," Nature Physical Science, Vol. 233, September 6, 1971.

89. Astheimer, R. W. and Schwarz, F., "Thermal Imaging Using Pyroelectric Detectors," Applied Optics, Vol. 7, No. 9, September 1968.

90. Victory Engineering Corp. (VECO), Springfield, N. J., "Pyroelectric IR Detectors Sales Brochure."

91. Detector Electronics Corp., Minneapolis, Minn., "UV Sales Brochure."

92. Fenwal Inc., Ashland, Mass., "UV Sales Brochure."

93. McGraw-Edison Corp., East Orange, N. J., "UV Sales Brochure."

94. Grabowski, G. J., "The Future of Automatic Fire Protection," Colloquia on Fire Problems, Applied Physics Laboratory, Johns Hopkins University, May 6, 1971.

95. Putnam, T. M. and Parker, J. E., "Tests of Combustion Product Detectors in a Radiation Environment," Fire Technology, 5, 4, pp. 273-283, November 1969.

96. Fire Alert Co. - Bulletin No. 890.

97. Dal Nogare, S. and Juvet, R. S., Jr., Gas-Liquid Chromatography, pp. 217-227, Interscience, New York, 1962.

98. Goodmann, P. and Donaghue, T., "Kryptonate-Based Instrumentation Development for Automobile Exhaust Pollutants - Phase I Report: Feasibility," Panametrics Inc., Waltham, Mass., NTIS NYO-4069-1, March 1970.

99. Lawson, D. I., "A Laser Beam Fire Detection System," Reprint from Institution of Fire Engineers Quarterly; and "Recent Development in Fire Research in the United Kingdom," Colloquia on Fire Problems, Applied Physics Laboratory, Johns Hopkins University, March 18, 1971.

100. Electro-Signal Lab., Rockland, Mass., Tech. Report, "Incandescent Lamp Life in Smoke Detectors, Rockland, Mass., March 23, 1972.

101. Firth, J. G., Jones, A., and Jones, T. A., Ann. Occup. Hyg. Vol. 15, pp. 321-326, Pergamon Press, 1972.

102. Byrd, N. G., "Space Cabin Atmosphere Contaminant Detection Techniques," NASA, CR-86047, July 1968.

103. Senturia, S. D., "Fabrication and Evaluation of Polymeric Early-Warning Fire-Alarm Devices," NASA CR-134764, 1975.

104. Bean, R. C., "Formation and Utilization of Stable Lipid Membranes with Multiple Resistance States," AD-725783, April 1971.

105. Leibecki, H. F., "Electrically Conductive Polyfluorinated Ethylene," NTIS, N72-20131, January 1970.

106. Ferber, B. I. and Weiser, A. H., "Instruments for Detecting Gas in Underground Mines and Tunnels," BuMines IC 8548 or PB 210-991 (1972).

107. Carroll, Jr., H. B. and Armstrong, F. E., "Accuracy and Precision of Several Portable Gas Detectors," BuMines, NTIS PB-227-218, December 1973.

108. Snyder, D., et al., "Instrumentation for the Determination of Nitrogen Oxides Content of Stationary Source Emissions," NTIS PB 209190, January 1972.

109. MSA Portable Instruments Brochure Section 3, p. 5, Mine Safety Appliances Co., Pittsburgh, Penn.

110. Blurton, K. F. and Bay, H. W., "Controlled-Potential Electrochemical Analysis of Carbon Monoxide," American Laboratory, pp. 50-55, July 1974.

111. Bergman, I. and Windle, D. A., "Instruments Based on Polarographic Sensors for the Detection, Recording and Warning of Atmospheric Oxygen Deficiency and the Presence of Pollutants such as Carbon Monoxide," Ann. Occup. Hyg. Vol. 15, pp. 329-337, Pergamon Press 1972.

112. Liebhafsky, H. A. and Cairns, E. J., Fuel Cells and Fuel Batteries, John Wiley and Sons, N. Y., 1968, pp. 447-453.

113. "Portable, Compact, Low Cost NO_2, CO, and CH_4 Gas Analyzer for In-Mine Monitoring," February-March 1974, BuMines Contract HO230050, Andros, Inc., Berkeley, California.

114. Thunder Scientific Corp., Albuquerque, N. M., Sales Brochures.

115. Bennewitz, P. F., "The Brady Array - A New Bulk-Effect Humidity Sensor," Society of Automotive Engineers, No. 730571, Detroit, Mich., May 14-18, 1973.

116. Leitz, F. B., "Electrochemical Carbon Dioxide Sensor," AD 655936, May 1967.

117. Reyes, R. J., Martin, C. F., and Neville, J. R., "An Improved Electrochemical Carbon Dioxide Sensor," AD 660557, July 1967.

118. Villarroel, F., et al., "Army CO_2/O_2 Concentration Monitor (Model I)," AD 737003, December 1971.

119. Villarroel, F. and Woods, R. L., "Analog Flueric Gas Concentration Sensor," AD 774280, June 1973.

120. Sidor, R. Peterson, N. H., and Burgess, W. A., "A Carbon Monoxide-Oxygen Sampler for Evaluation of Fire Fighter Exposures," Am. Industrial Hygiene, pp. 264-274, June 1973.

121. Lucero, D. P., "Design of Membrane-Covered Polarographic Gas Detectors."

122. Farber, E. A., et al., "Hydrogen and Oxygen Sensor Development," NASA-CR-133891, October 1972.

123. "The Continuous Monitoring of Mine Air by the Tube Bundle Technique," A Note on Installation and Maintenance, National Coal Board, Scientific Control, Harrow, U. K., October 1972.

124. Fink, Z. J. and Adler, D. T., "A Continuous Monitoring System for Mine Gas Concentrations," BuMines, Advance Copy, Pittsburgh, Penn., 1974.

125. Wagner, J. P. and Tewarson, A., Internal Report, Factory Mutual Research Corp. (FMRC) Norwood, Mass., January 2, 1973.

126. Heskestad, G., "Escape Potentials from Apartments Protected by Fire Detectors in High-Rise Buildings," FMRC Serial No. 21017, June 1974.

127. Bright, R. G., National Bureau of Standards - Private Communication.

128. Alpert, R. L., "Calculation of Response Time of Ceiling-Mounted Fire Detectors, NFPA 76th National Meeting, May 18, 1972, also Fire Technology, pp. 181-195, 1973.

129. "Private Communication," BuMines, Pittsburgh, Penn.

130. Wagner, J. P., Welker, R. W., and Fookson, A., "Fire Alert Systems for Metal and Non-Metal Mines," Phase Report No. 1, Gillette Research Institute, October 1, 1974.

131. Rodgers, S. J., "Analysis of Non-Coal Mine Atmospheres," Contractors Meeting Seminar, PMSRC, Bruceton, Penn., December 1974.

132. Stevens, R. and Blake, E. R., "Mine Shaft Fire and Smoke Protection System," Phase Report No. 2, FMC Corporation, San Jose, California.

133. Greuer, R. E., "Influence of Mine Fires on the Ventilation of Underground Mines," Michigan Technological University, USBM Contract SO122095, May 1973.

134. Petajan, J. H., et al., "Extreme Toxicity from Combustion Products of a Fire-Retarded Polyurethane Foam," Science, 187: 742-744, February 28, 1975.

135. Winkler, P., "Relative Humidity and the Adhesion of Atmospheric Particles to the Plates of Impactors," Journal of Aerosol Science, 5:235-240, 1974.

136. Anglo American Electronics Laboratory note on Becon MKII Detector, Booysens Reserve Rd., Theta Township, Johannesburg, S. A.

137. Overman, R. T. and Clark, H. M., Radioisotope Techniques, p. 140, McGraw Hill, Inc., N. Y., 1960.

138. Monthly Progress Reports Nos. 2 and 4, "Fire Alert Systems for Metal and Non-Metal Mines," Contract No. SO144131, Gillette Research Institute, Rockville, Maryland.

139. Bird, R. B., et al., Transport Phenomena, p. 186, John Wiley & Sons, New York, 1960.

TABLES

TABLE I

HIGHLIGHTS OF METAL-MINE FIRES UP TO YEAR 1933

		Time Period	Quoted Breakdown	# Fatalities
A.		up to 1933	-	600
		1916-1922 inclusive	-	240
		1922-1933	-	20
B.	(1)	prior to 1917	Open Flames - at least 66% of fires (50% candles and oil, 2% carbide lights, 10% heating or other fires, 4% electricity 4% smoking, 30% unknown or miscellaneous, such as lightning, explosives, spontaneous combustion, etc.)	
	(2)	prior to 1922	35% ignition of timber by candles, 10% heat to warm oil or for a similar purpose, 10% from burning surface structures sent underground, 12% spontaneous combustion, 7% electricity, 3% explosives, 3% carbide lights, 20% unknown or miscellaneous causes	
	(3)	1933 period	30%-40% electricity	

TABLE II

ILLUSTRATIVE FIRE DATA AND PROBABLE FIRE ORIGIN OR CAUSE FOR METAL AND NON-METAL MINES (1949-1972)

Mine	Date (year)	Probable Fire Origin or Cause	Fatalities
Eureka, Ramsey Michigan (soft hematite ore body)	1949	electrical wiring & equipment	-
Copper Canyon Mine, Copper Canyon Mining Co., Battle Mountain, Nevada	1950	oxy-acetylene torch - hot rivet fell into shaft & ignited timber guide	-
Sunday Lake Mine, Sunday Lake Iron Co. Pickands Mather & Co., Wakefield, Mich.	1951	cigarette ignited wood blocking	-
Shell Chemical Corporation Pittsburg, California	1954	air compressor - high temperature of metal surface ignited lubricating oil and/or carbonaceous products	-
St. Joseph Lead Company Flat River, Missouri	1956	explosives fire - heat generated by friction of car wheels against bed ignited paper cartons and then explosives contained therein	-
Humboldt Mine, Nevada-Massachusetts Co., Tungsten, Nevada	1957	electrical - most probably some fault in pump power circuit	0
Montreal Mine, Oglebay Norton Co. Montreal, Wisconsin	1958	electrical fire in converter	0
Newport Mine, The Mauthe Mining Co., Pickands Mather & Co., Ironwood, Mich.	1959	believed electrical failure	0
Buck Mine, Verona Mining Co., Pickands Mather & Co., Caspian, Michigan	1959	electrical failure on shaft station	0
Black Jack No. 1 Mine (Uranium) Thoreau, New Mexico	1960	heat generated by oversized light bulb in cabinet or cigarette in lagging or station roof	0
Burro Mines (Uranium) Union Carbide Nuclear Company Slick Rock, Colorado	1963	short circuit in one or more power cables ignited dry timber around shaft; or cigarette or burning match dropped on combustible	0
Cane Creek Mine, Potash Div. Texas Gulf Sulphur Company, Utah	1963	combustible gases in shop area (total hydrocarbons analyses 1.31-6.7% after explosion) ignited by electrical arc, sparks, etc.	18
White Pine Mine White Pine Copper Co., White Pine, Mich.	1963	self ignition of rigid urethane foam	0
White Pine Mine White Pine Copper Co., White Pine, Mich.	1964	friction or electrical failure near a conveyor belt	0
Climax Climax Molybdenum Co. Climax, Colorado	1964	fire & explosion in main intake air raise - intake air raise & fan station were sealed to control fire, thus probable cause not determined	1 1 injured
Cordero Mine Cordero Mining Co., McDermitt, Nevada	1965	spontaneous combustion of sulfide ore or ground support timber or both; or from blasting	0
Homestake Mine Homestake Mining Co., Lead, South Dakota	1965	spontaneous combustion of sulfide materials in sand backfill	0
Texas Eastern Transmission Corporation Larose, Louisiana	1966	ignition of large volume of volatile hydrocarbons and natural gas by static electricity or smoking materials	7
Belle Isle Salt Mine Cargill, Incorporated St. Mary Parish, Louisiana	1968	electrical fault, oxy-acetylene torch or frictional ignition of belt conveyor; however, evidence does not favor any one of three possibilities	20 - CO poisoning 1 - skull fracture
Pleasant Gap Limestone Pleasant Gap, Pennsylvania	1970	hot hydraulic fluid under pressure ignited by electrical arc from bare battery cable and reinforcing wires	0
Barnett Complex Mine Ozark-Mahoning Co., Rosiclare, Illinois	1971	not fire related - H_2S poisoning	7
Sunshine Mine Kellogg, Idaho	1972	spontaneous combustion in worked out and abandoned area of mine	91

TABLE III

HIGHLIGHTS OF SELECTED COMBUSTION CHARACTERISTICS FOR A FEW MINE COMBUSTIBLES (35)

Combustible	Fire Type	Burning Rate or Related Characteristic	Other Characteristics
Timber	Oxygen or fuel rich depending on fuel loading, ventilation, etc. Most accidental fires are oxygen rich.	M_v = 2.29-8.5 lb/ft^2-hr M_b = 66-330 ft/hr (estimated) M_b > 20 ft/hr (against air flow)	O_2 rich: 0.1-0.5% CO, 3-5% CO_2, 16-18% O_2 Fuel rich: 5-8% CO, 18-20% CO_2, 2-5% H_2, 0-1% O_2 (Above - Av. Values)
Mineral Oil	Fuel rich for $A/\dot{M}_a$ > 0.153	Burning rate of 40 lb/min for 10 minutes in ventilation current 22,000 ft^3/min is minimum to start fuel rich timber fire (in tunnel 45 ft^2 cross section).	Expected Products for fuel rich: CO, CO_2, high molecular weight hydrocarbons.
Polyurethane Foam	Fuel rich when applied to 75% of roadway perimeter	M_v = 7.38-20 lb/ft^2-hr	Fuel rich - HCN, organic cyanides, acetonitrile, benzene, ethylbenzene, and acrylonitrile (38)

A = oil surface area; $\dot{M}_a$ = volumetric air flow rate
M_v = mass rate of fuel evolution per unit surface area
M_b = linear burning rate

TABLE IV

MEASURED GAS AND PARTICULATE CONCENTRATIONS DURING NORMAL MINE OPERATIONS [40]

Mine Operation	CO-CO_2 Concentrations	Condensation Nuclei (CN)	NO_x-SO_2 Concentrations
Shot Firing[+] or Blasting	Peak CO concentrations ranged from 20 to 100 ppm. CO_2 peaks were up to 400 ppm above background. Increase and decay of CO, CO_2 depends on mine ventilation and location of sampling site.	$\gg 1 \times 10^5$ particles/cm^3	Peak NO_x ranged generally from 20ppm to 100 ppm or sometimes even higher. Peak SO_2 often greater than 10 ppm.
Diesel Operations[++] (return air sampling site Anaconda mine)	Peak ~ 20 ppm CO (10 ppm CO background) Peak ~ 1200 ppm CO_2 (800 ppm background)	$> 1 \times 10^7$ particles/cm^3	-

[+] CO/CO_2 ratios ranged from 1/5.6 to 1/9.5

[++] CO/CO_2 ratios ranged from 1/41.5 to 1/64.6

TABLE V

SUMMARY OF CALLS RECEIVED

Type of System	Number of fire calls by system installed	Number of false calls	Ratio of false calls: fire calls
All Types	489	5441	11.1:1
Heat	193	2146	11.1:1
Smoke	101	1429	14.1:1
Heat and smoke	18	410	22.8:1
Sprinkler	101	1048	10.4:1
Manual	55	243	4.4:1
Mixed	18	137	7.6:1
Unspecified	3	27	9.0:1

Note: the total number of false calls includes one false call from gas detector equipment.

TABLE VI

REASONS FOR FALSE CALLS

Reason for false calls	Totals (all types of equipment)	
	Number	Per cent
Total (all reasons)	5441	100
Ambient conditions	1410	26
Mechanical and electrical	2507	46
Communication	901	17
Unspecified and unknown	623	11

TABLE VII

OVERALL EXPECTED CHARACTERISTICS OF CONVENTIONAL FIRE DETECTORS* (49)

Detector Type**	Actuated by	Relative Response Time		Overall Expected Frequency of False Alarms
		Flash Fire	Smoldering Fire	
Ionization	Products of	2***	1-2	High
Laser beam	Combustion	1-2	1	High
	"			
Photoelectric beam	Visible	4	1	Moderate-High
Light transmission or absorption	Smoke			
Light scattering		4	1-2	Moderate
Light refraction		5	3	Moderate
Light reflection		4	1-2	
Ultraviolet Infrared	Light	1	5	High
Fixed temperature Bimetallic elements, ampule devices, eutectic solders and metals that fuse or melt, thermocouples, and thermistors	Heat	3	5	Low
Rate of Rise Orifice and Pneumatic tube devices		3	4	Low to moderate
Fixed temperature combined with rate of rise		3	4	Low

*Based on opinion of author derived from published test programs, discussions with other personnel in the field and current trends in the field.

**Under the present classification scheme, direct contact includes fixed temperature, rate of rise, fixed temperature combined with rate of rise, optical view-field-ultraviolet and infrared, product of combustion-ionization, laser beam, photoelectric, and more recently "Taguchi" type solid state sensors.

***Note numbers 1 to 5 indicate fastest to slowest response conditions, respectively.

TABLE VIII

SIZES OF AIR-BORNE CONTAMINANTS (51)

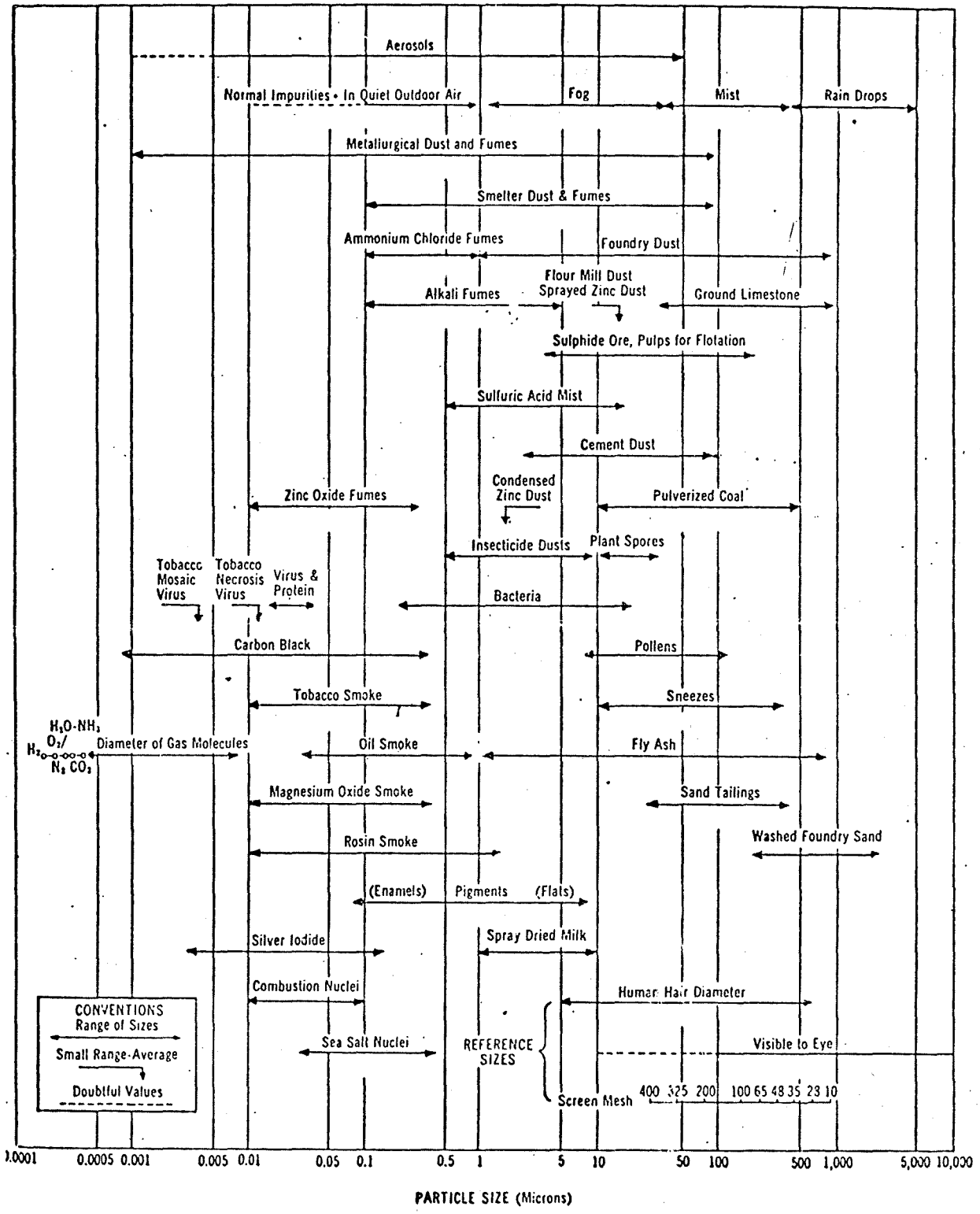

TABLE IX

CHARACTERISTICS OF DIFFERENT PHOTODETECTOR DEVICES (82)

Photoemissive - are vacuum tubes in which light impinges on a metal cathode, releasing one electron per photon of light. Photomultiplier plates are often contained in the same tube envelope. Standard for sensitivity comparison. Has poor long-term stability and high quiescent power consumption, needs high voltage power supplies, and has poor shock and vibration resistance characteristics.

Photovoltaic - absorbs light and produces an output voltage; does not need an external power supply. Most common materials are Si and Se. Se exhibits good response in the UV and is inexpensive, however, it exhibits hysteresis to light. Si photodetectors show promise in replacing Se as cost declines. Does not exhibit serious hysteresis and has microsecond response times.

The Si solar cell optimized for resistance to nuclear radiation (N junction on top), exhibits poor response in the UV, a broad band response in the visible, and a peak in the near infrared. Si photocells with enhanced blue response are now available.

Photoconductive junction type (sometimes called photosensitive) - Conducitivity changes as the device absorbs light. Reverse biasing of photovoltaic junction photocells leads to operation in the photoconductive mode. Si is again the most popular material for junction photocondutive cells. For reverse biasing PIN processing is preferred to the conventional PN junction. PIN photodiodes operated with reverse bias can have response times as fast as one nanosecond. Light history effects are absent in PIN cells in either the photovoltaic or photoconductive modes.

Bulk-effect photoconductive cells - behave like resistors whose resistance decreases nonlinearly with an increase in light intensity. The usual materials are CdS and CdSe. Usually have sharp-peaked spectral responses unless they are specially compensated. Require a low voltage power supply. Major disadvantages are slow response and light hysteresis.

TABLE X

CHEMICALS THAT CAN REACT WITH AMMONIA TO PRODUCE AIRBORNE PARTICULATES SUFFICIENT TO ALARM IONIZATION SMOKE DETECTORS (96)

CHEMICAL	FORMULA	COMMON USES
Chlorine	Cl_2	Solvents; cleaning agents; pesticides and herbicides; plastics and fibers; water and sewage treatment.
Hydrogen Chloride (hydrocholoric acid)	HCl	Food processing; pickling and cleaning metals; industrial acidizing; general cleaning.
Hydrogen Fluoride, (hydrofluoric acid)	HF	Polishing and etching of glass; metal pickling; stone and brick cleaners; laundry products.
Phosgene	$COCl_2$	Bleaching agent; chlorinating agent; dyes; plastics.
Trichloroethylene	C_2HCl_3	Metal degreasers; dry cleaning; refrigerant and heat exchange liquid; fumigants; general cleaning agent.
		NOTE: These chemicals are frequently employed in household and industrial cleaning preparations.

TABLE XI

SENSITIVITY AND APPLICABILITY OF VARIOUS GAS SENSING TECHNIQUES

Methods Used in Gas Signals		Sensitivity, mg/liter	Region of Application
1. Mechanical	volumetric	10^{-1}	Signals are simple and reliable. In connection with low sensitivity, the significance of the methods of this group has dropped sharply with the exception of the volumetric. The chromatographic method is widespread, but not a continuous method of analysis.
	densometric	10^{-1}	
	sonic and ultrasonic	10^{-1}	
	diffusion	10^{-1}	
	chromatographic	10^{-1}	
2. Thermal	thermochemical	10^{-1}-10^{-2}	Applicable either for analysis of two component mixtures differing sharply with respect to thermal conductivity or for fuel gases. Widely used to analyze hydrocarbons.
	thermoconductometric	10^{-1}-10^{-2}	
3. Electrical	electrochemical	10^{-3}-10^{-4}	Applicable for analyzing a large number of compounds.
	ionization	10^{-4}-10^{-5}	
4. Optical	ultraviolet-spectrophotometric	$\sim 10^{-5}$	The same
	infrared spectrophotometric	$\sim 10^{-5}$	
	photometric	$\sim 10^{-5}$	
	luminescent	$\sim 10^{-5}$	
5. Magnetic	magneto-mechanical	10^{-1}	Signals are simple and reliable, but application is limited to analysis of gases having paramagnetic properties (oxygen, nitrogen oxides).
	thermomagnetic	10^{-1}	
6. Spectrometric	mass-spectrometric	10^{-2}-10^{-3}	Complex with respect to structure but efficient for certain multicomponent mixtures. The region of application is limited to substances of relatively simple structure.
	radio-spectrometric	10^{-2}-10^{-3}	

TABLE XII

GAS CONCENTRATION RATIOS FOR VARIOUS MINE OPERATIONS (131)

	CO/CO_2	CO/NO_x	CO_2/NO_x
Blasting	0.1 - 0.7	3-14	4-24
Diesel	0.05-- 0.1	7-10	85-95
Leaky Bulkhead	0.05	10	3,000
Fire (Return Air)	0.04	300	70,000
Fire (Sealed Bulkhead)	0.02	1,650	80,000

TABLE XIII

PARTICLE SIZE CUT-OFFS FOR SPHERICAL PARTICLES

@ 0.75 SCFM, 25°C, 760 mm Hg:

Stage No.	$D_{p,50}$ Sp. Gr. = 1.0
0	16
1	8.6
2	3.9
3	2.4
4	1.2
5	0.61
Back-up Filter	0

TABLE XIV

FIRE DETECTOR SELECTION AND TEST STATUS

	Type	Supplier	Model No./Part No.	Current Status***
A.	Contact Type			
	Fixed Temperature (Frindex)	Walter Kidde	S135-F/600898	n.t.
	Continuous Wire:			
	Thermistor	Walter Kidde	(Specify Temperature & Length)	n.p.
	Eutectic Salt Type	Walter Kidde	>250°F (Specify Temperature & Length)	n.t.
		Fenwal	>255°F Brochure 4.11.2 (MC-212B)	n.p.
	Twisted Cable/Fusible Plastic	Protectowire Co.	155°F - PHSC	n.t.
	Rate of Rise	Omit	Omit	-
	Pneumatic Tube System	Walter Kidde-Atmo Unit	500-1/600245	n.p.
	Fixed Temp. w/Rate of Rise or Rate Compensated	Thermotech	302-AW135	t
		Fenwal	27020-0 (Flat-Flush Mounting)	t
			27121-1 (Cylindrical)	t
B.	Optical View Field			
	Ultraviolet	Pyrotector	30-2021	t
		Fenwal	P/N 10-190017-102	n.p.
	Infrared	Pyrotector	30-2025	t
C.	Products of Combustion (POC)			
	Ionization - α Ray	Pyrotronics	DI-2S	t
		Honeywell	TC-100A	t
		Fire Alert (Walter Kidde)	CPD-1212	t
	- β Ray	Anglo American Electronics of SA	Beacon MKII*	t
	Photoelectric	Electro Signal Lab (ESL)	724	t
		Pyrotector	SK 700 (Near IR LED device)	
	Taguchi	Figaro Engineering	No. 109**	t

*Following Bureau of Mine's recommendations - provided by FMC.
**Following Bureau of Mine's recommendations - provided by Collins Radio.
***n.t. = not tested; n.p. = not purchased; t = tested.

TABLE XV

FUEL SELECTION FOR FIRE DETECTOR SCREENING AND TESTING

Fuel	Use or Location	Test Conditions	Test Chamber*
Punk Smoke	Standard Solid Fuel	Glowing	S
Polystyrene pellets	Molded parts	Flaming	L
Polyvinylchloride (PVC)	Electrical Insulation and Piping	Pyrolytic Degradation	
a) Line Cord			S
b) Rigid Pipe			S
c) Tubing (Soft-Walled)			S
Polyethylene	Electrical Insulation for Power Cable	Pyrolytic Degradation	S
Polyurethane (Flexible Reticulated Foam)	Bulkheading and Other Uses	Pyrolytic Degradation Flaming	L,S L
Wood (Pine) - Moist and Dry Conditions	Various Supports	Pyrolytic Degradation Flaming	S L
Corrugated Cardboard	Packing Material	Flaming	L
Methanol - MeOH	Standard Liquid Fuel	Flaming - Blue Color	L
Ethanol - EtOH	Standard Liquid Fuel	Flaming - Yellowish Color	L
Isopropanol	Standard Liquid Fuel	Flaming - Yellow (much smoke)	L

*L = large box (Figure 5). All tests in this box were flaming, including some smoldering combustion for wood and cardboard.
S = small box (Figure 3).

TABLE XVI

EFFECT OF TRIGGER LEVEL ADJUSTMENTS ON BECON MKII FOR SELECTED FUELS AND FLOW VELOCITIES

Alarm Setting	Fuel	Flow Velocity (ft/min)	Ou* (%/ft)
2-3%/ft Punk at 100 ft/min	Polyurethane	100	5.2
Mfgrs. Instructions	Punk	35	10.0
		100	1.6
		170	0.8
		225	0.6
	Moist Wood	100	4.3
	Polyurethane	100	9.0
		225	7.2
	PVC - Tubing	100	19.2
		225	10.0
	Polyethylene	100	18.1

TABLE XVII

PERFORMANCE HIGHLIGHTS FOR TGS 109 FOR SELECTED SMOKES

(V_h = 0.8 Volts)

Source of Smoke	Time for Ou to Reach 4%/ft or (2%/ft) Level (min)	$\frac{\Delta Ou}{\Delta t}$ (%/ft-min)	Flow Velocity (ft/min)	% Increase in TGS Voltage above Base-line at Ou = 4, or (2) (%/ft)
Punk	● 7.4	0.4	225	1935
	◆ 5.3	0.7	225	1425
	□ (2)	1.2	100	(180)
	△ 6.7	0.6	170	870
	▲ (2.7)	1.0	35	(375)
PVC	● 1.1	6	35	60
	o 2	6	100	130
	▲ 2.4	3	170	85
Polyurethane	▲ (3.6)	1	225	(53)
	◆ 3.4	2	170	79
	3	2	170	74
	o 10	0.5	100	220
	● 6	1	35	100
	4.6	1.3	35	100

TABLE XVIII

PERFORMANCE HIGHLIGHTS FOR TGS 109 FOR SELECTED SMOKES

(V_h = 1.2 Volts)

Source of Smoke	Time for Ou to Reach 4%/ft or (2%/ft) Level (min)	$\frac{\Delta Ou}{\Delta t}$ (%/ft-min)	Flow Velocity (ft/min)	% Increase in TGS Voltage above Base-line at Ou = 4, or (2) (%/ft)
Punk	■ 4.2	1	100	1438
Dry Wood	▲ 4.3	1	35	630
Moist Wood	o 5	0.85	35	517
PVC (Flexible Tubing)	● 2.5	2.7	170	455
Polyethylene	● 2.5	1.6	170	680
Polyurethane	□ 9.5	0.4	35	94

TABLE XIX

COMPARATIVE PERFORMANCE OF RATE COMPENSATED DETECTORS FOR FLAMING COMBUSTION

		Fenwal (Vertical)				Thermotech (Vertical)			
Fuel	Distance	Time to Alarm	Detector Temp. at Alarm[b]	Rate of Temp. Rise[a] Max.	At Alarm	Time to Alarm	Detector Temp. at Alarm[b]	Rate of Temp. Rise[a] Max.	At Alarm
	(feet)	(min:sec)	(°F)	(°F/min)		(min:sec)	(°F)	(°F/min)	
MeOH[c]	7	3:53	120	18	35	-	N.A.	-	-
EtOH	7	1:37	122	20	18	3:15	127	18	7
Isopropanol	7	1:31	124	23	18	3:06	137	23	7
MeOH[d]	7	1:42	115	20	13	12:06	144	20	2
MeOH	5	1:36	118	25	16	6:37	140	25	4
EtOH	5	1:00	127	29	29	1:42	138	25	11
Isopropanol	5	0:43	129	27	27	1:12	142	25	14
MeOH	3	0:50	124	27	25	1:15	140	32	14
EtOH	3	0:39	122	36	36	0:48	140	41	36
Isopropanol	3	0:36	122	40	40	0:43	140	47	47

[a] As obtained by fixing a thermocouple to the detector.

[b] Based on air temperature.

[c] First run of the day.

[d] Repeat of c. Box was already warm when d was run.

TABLE XX

DETECTOR PERFORMANCE HIGHLIGHTS FOR VARIOUS FUELS AND AMBIENT CONTAMINANTS

Fuel	Ignition Mode	Pyrotector SK 700 Ou* - %/ft (Time to Alarm)	ESL 724L Ou* - %/ft (Time to Alarm)	TGS 109 Voltage Increase-Volts[a], Time of Increase	Thermotech 302AW135 (Time to Alarm)
Isopropanol (140 cc) (run stopped before fuel consumed)	Glowing Filament	3.2 (1.1 min)	1.2 (0.6 min)	0.74 V for Alcohol vapor, 1.4 V Plateau at 10.4 Ou (V_h = 0.8)	(4.6 min) Ou* = 13.6%/ft T = 131°F Rate = 4.7°F/min
Isopropanol (140 cc) "	Glowing Filament	5.6 (1.5 min)	3.3 (0.9 min)	0.36 V in 1 min, 0.5 in 5.5 min (V_h = 1.2 V)	(4.6 min) Ou* = 14.8%/ft T = 125°F Rate = 7.0°F/min
Polystyrene Pellets (50 gms, 0.5 gms of fuel consumed in test)	Glowing Filament (matches imbedded in fuel)	3 (34 sec)	2.8 (12 sec)	ΔV = 0 for 1.3 min after ignition ΔV_{max} = 1.3 V at 3 min (V_h = 0.8 V)	N.A.
Corrugated Cardboard (11.6 gms)	" "	3.2 (3.6 min)	1.2 (2 min)	ΔV = 0 for 1 min ΔV_{max} = 6.1 at 4.5 min (V_h = 0.8 V)	N.A.
Polyurethane Foam (9.4 gms)	" "	1.8 (45 sec)	1.3 (34 sec)	ΔV = 0 for Entire Run (V_h = 0.8 V)	N.A.
Wood Slivers (5.35 gms)	" "	N.A.[b]	0.35 (20 sec)	ΔV = 0.12 V for 1.1 min ΔV_{max} = 1.24 V at 4.4 min (V_h = 0.8 V)	N.A.
Ambient Contaminants					
Water Mist	Tri-Jet Fogger	N.A. 10 min test	2.3 (4.3 min)	ΔV_{max} = 0.02 Volts therefore N.R. (V_h = 0.8 V)	N.A.
Rock Dust	Air Blast				
46 gms	5 sec	(several seconds)	(several seconds)[c]	N.R. (V_h = 0.8 V)	N.A.
30 gms	5 sec	(10 sec)	(12)[d]	N.R. (V_h = 0.8 V)	N.A.

a. Voltage Above Baseline - Baseline approximately 0.2 volts at start of test series.

b. SK 700's alarm setting was Ou* = 1%/ft. Ou_{max} was 0.67%/ft, thus alarm was not anticipated.

c. Dust approximately 2 ft from ceiling.

d. Dust approximately 7 ft from ceiling.

N.A. - no alarm.

N.R. - no response.

TABLE XXI

PARTICLE SIZE DISTRIBUTIONS FOR SELECTED FUELS AND Ou LEVELS

	4%/ft punk		4%/ft PVC		11%/ft Polyethylene	
$D_{p,50,\mu m}$	mass mg.	cum.% < $D_{p,50}$	mass mg.	cum.% < $D_{p,50}$	mass mg.	cum.% < $D_{p,50}$
0.61	0.44	35.5	0.24	12.8	0.87	17.5
1.2	0.29	58.9	0.29	28.2	0.22	21.9
2.4	0.17	72.6	0.42	50.5	1.28	47.7
3.9	0.05	76.6	0.28	65.4	1.48	77.5
8.6	0.13	87.1	0.21	76.0	0.62	90.0
16.0	0.16	100.0	0.16	84.5	0.26	99.8

TABLE XXII

PARTICLE PARAMETERS FOR VARIOUS FUELS UNDER DIFFERENT SMOKE CONDITIONS AND RELATIVE HUMIDITIES

Smoke	Ou (%/ft)	(%/ft-min)	Grain Load (mg/ft^3)	mmd (μm)	Standard Deviation, σ_g	% R.H.
Polyurethane	3.68	2.5	1.41	0.86	3.7	40
	3.74	2.1	1.68	1.24	3.2	40
	3.75	2.1	1.42	1.34	3.2	40
	9.48	6.9	2.48	1.00	3.2	~41
	9.64	1.0	1.66	1.66	1.9	37
Polyethylene	3.83	---	2.68	1.6	5.0	40
	3.89	5.4	5.81	2.9	6.2	56
	3.98	4.5	1.82	2.1	2.6	44
	10.1*	0.5-1.0	6.61	2.1	3.4	40
Punk	3.73*	0.5-1.0	1.65	0.95	5.8	40
	3.82	2.1	0.49	0.81	2.6	39
PVC	3.63*	~0.5	1.67	2.4	6.7	40
(linecord)	3.72	0.5	3.22	4.7	3.6	38

*First group of experiments

TABLE XXIII

AVERAGE PARTICLE PARAMETERS FOR
VARIOUS SMOKES (DATA FROM TABLE XXII)

Smoke Source	mmd, (μm)	σ_g
Punk	0.88	4.5
Polyurethane	1.22	3.1
Polyethylene	2.2	4.5
PVC	2.8	4.7

FIGURES

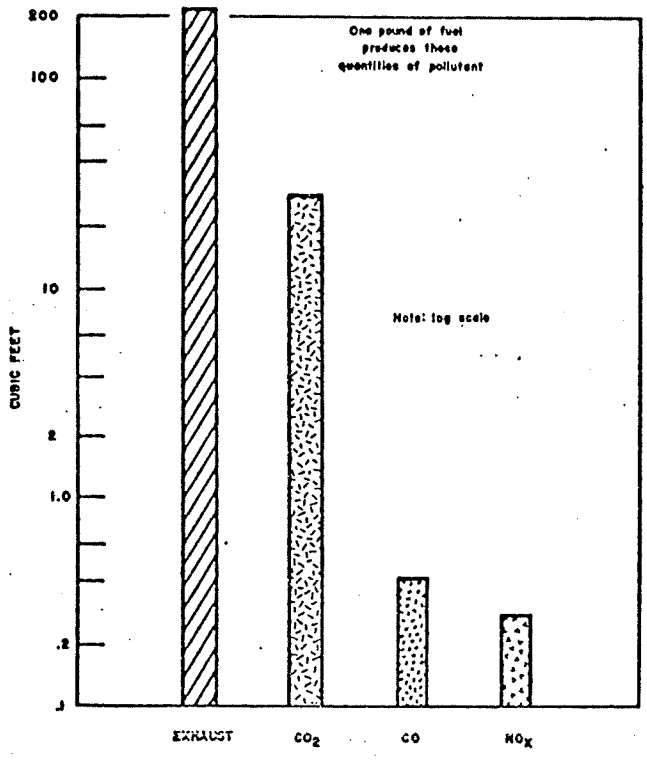

FIGURE 1.–Products of Diesel Combustion.

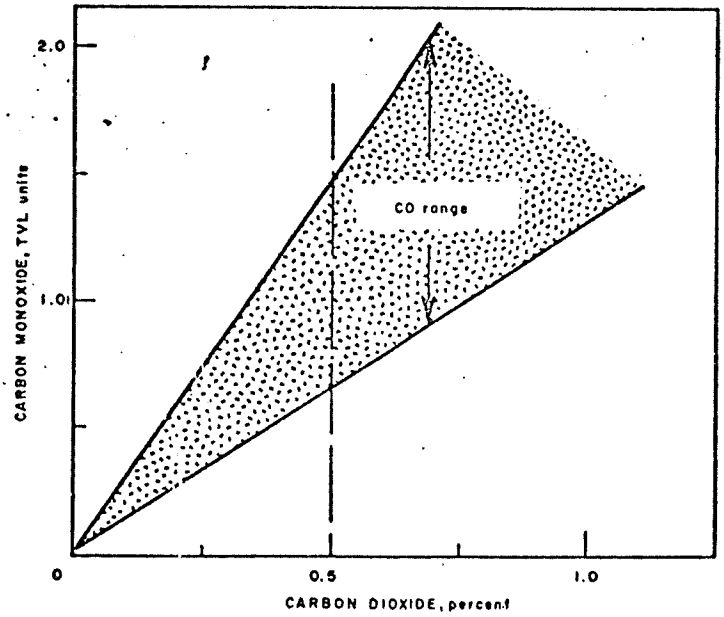

FIGURE 2.–Correspondence of Carbon Monoxide to Carbon Dioxide Concentration in Exhaust Gas Residue (Note: 1 TLV Unit Equals 50 ppm Carbon Monoxide

Figure 3. Sketch of Smoke Box (See text for basic dimensions).

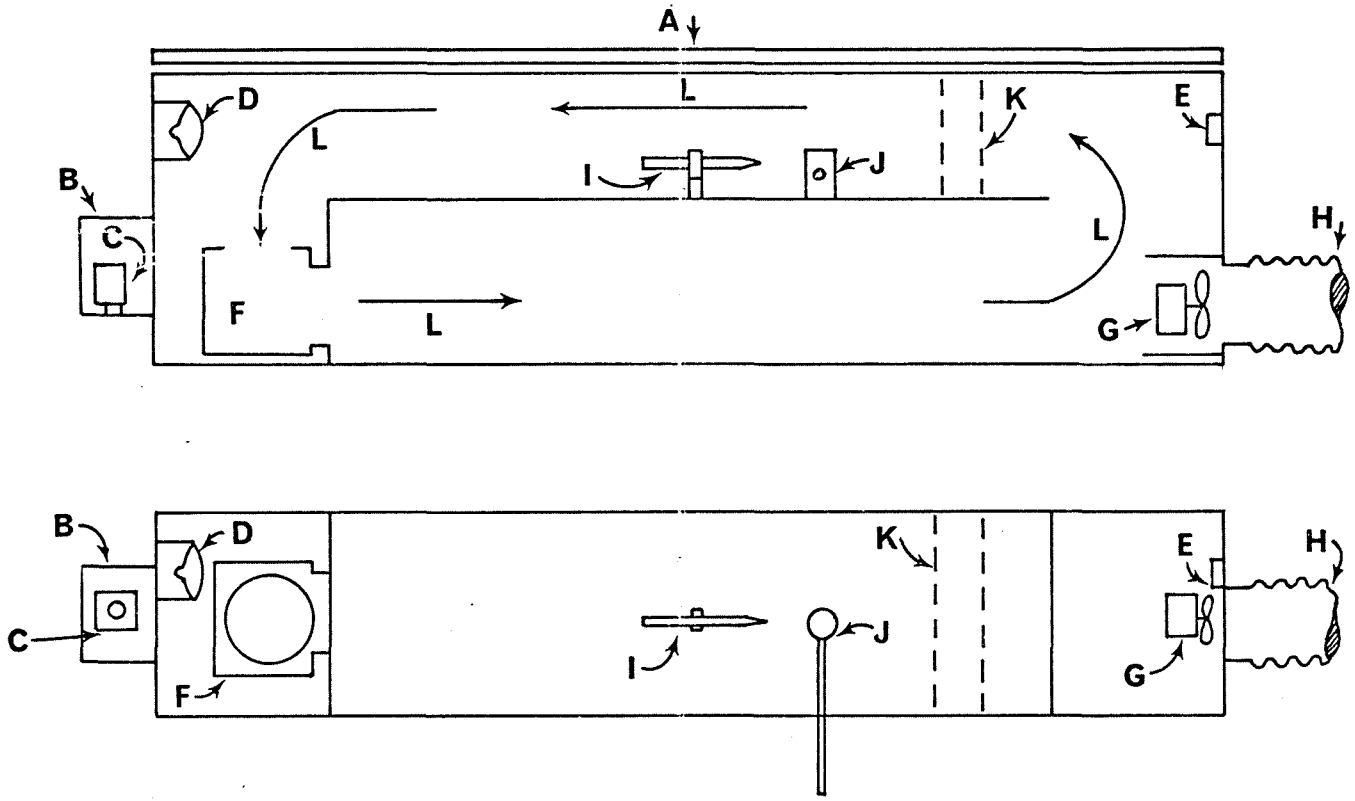

A. Hinged, gasketed, latched lid
B. Smoke generating chamber
C. Pyrolyzer for wood and plastic
D. Sealed beam light bulb, no. 4515
E. Photocell
F. Circulating fan
G. Exhaust fan (opening is baffled when fan is off)
H. Exhaust duct, to fume hood
I. Hot wire anemometer
J. Cascade impactor
K. ¼' square screen air flow straightener
L. Direction of circulating air flow

Figure 4A. Circuit for Measuring the Degree of Smoke Obscuration in the Smoke Box.

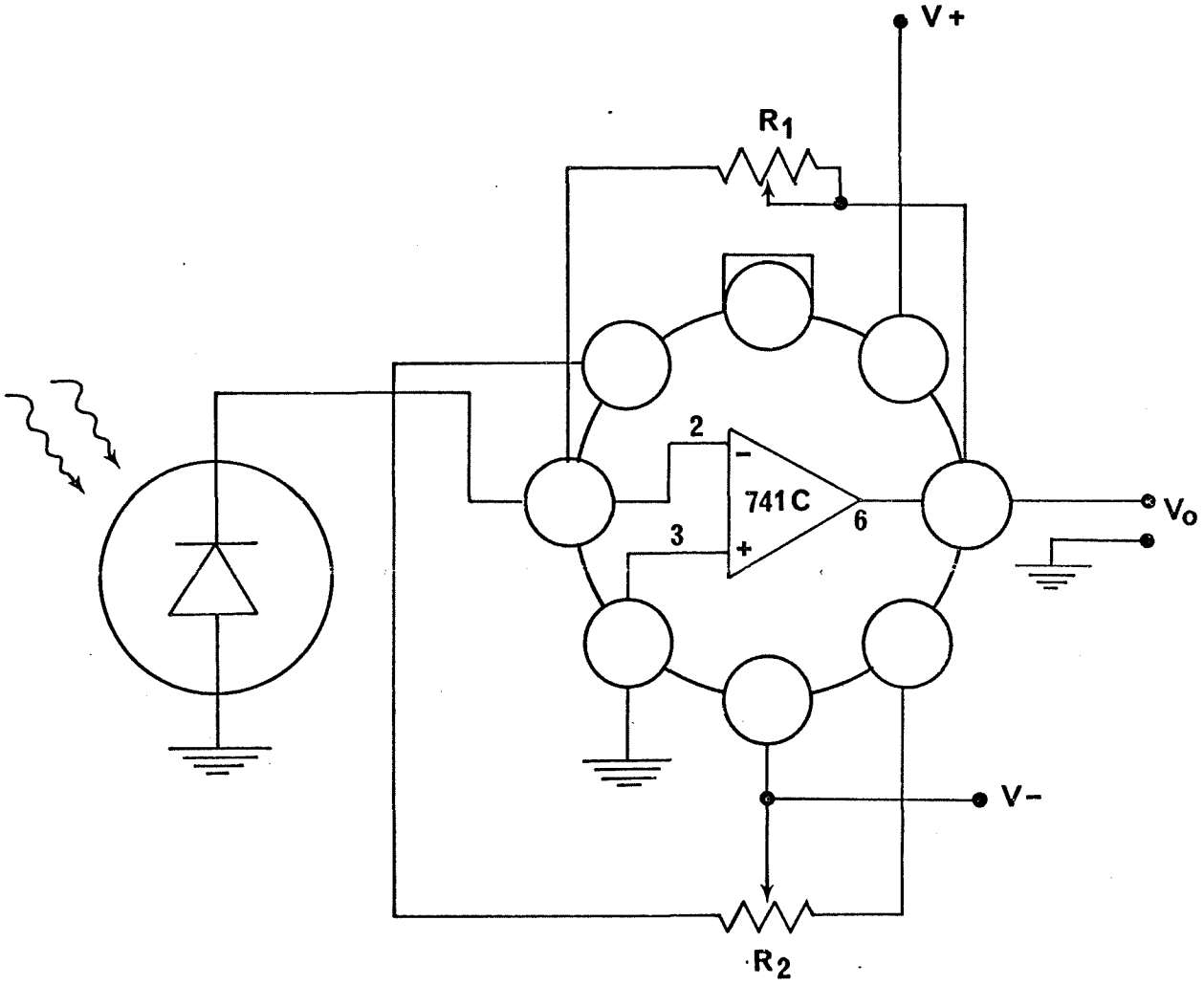

R_1 Feedback resister. 50 K potentiameter

R_2 Offset null. 10 K potentiameter

V+ +15 VDC

V- -15 VDC

V_o Output voltage. This is proportional to the intensity of illumination of the photocell.

Figure 4B. Circuit for Measuring the Resistance of the Taguchi 109.

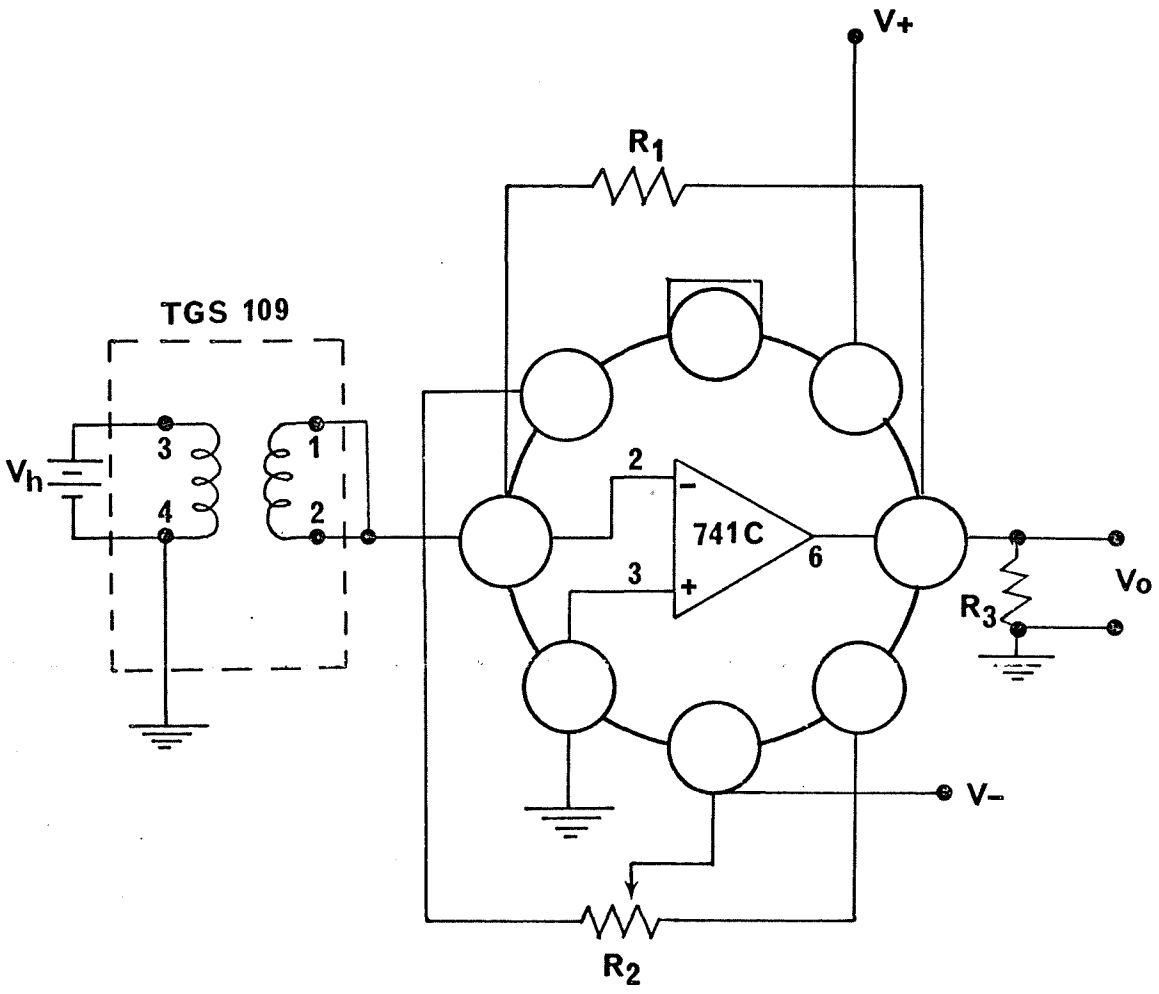

TGS 109	Taguchi gas sensor no. 109
R_1	10.53 K (see text)
R_2	10 K potentiameter
R_3	10 K
V+	+15 VDC
V-	-15 VDC
V_h	Heater voltage. In these tests, 0.8 or 1.2 VDC

Figure 5. Schematic of Test Set-Up for Flaming Combustion Sources.

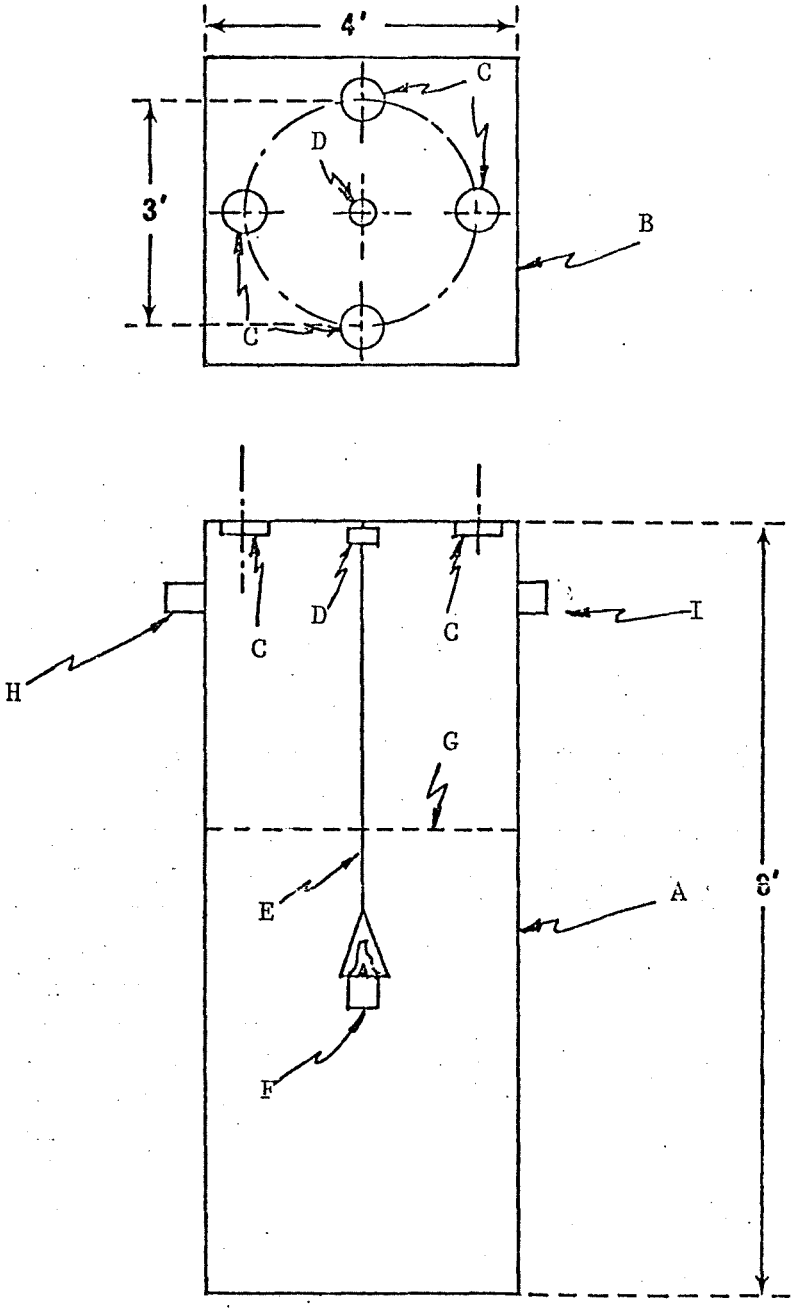

A. Test chamber. Skeleton: Unistrut; sides: Transite
B. Roof of test chamber, showing mounted fire detectors.
C. Fire detector.
D. Load cell, for measuring burning rate.
E. Suspension wire, whose length may be varied.
F. Cup for burning combustibles.
G. Mesh screen, whose height is adjustable.
H. Light source.
I. Sensor for light source, for measuring absorbance due to smoke.

Figure 7. Transient Time Response/Pump Horsepower Requirements for Various Tube Diameters and Pressure Ratios of 0.88, 0.26.

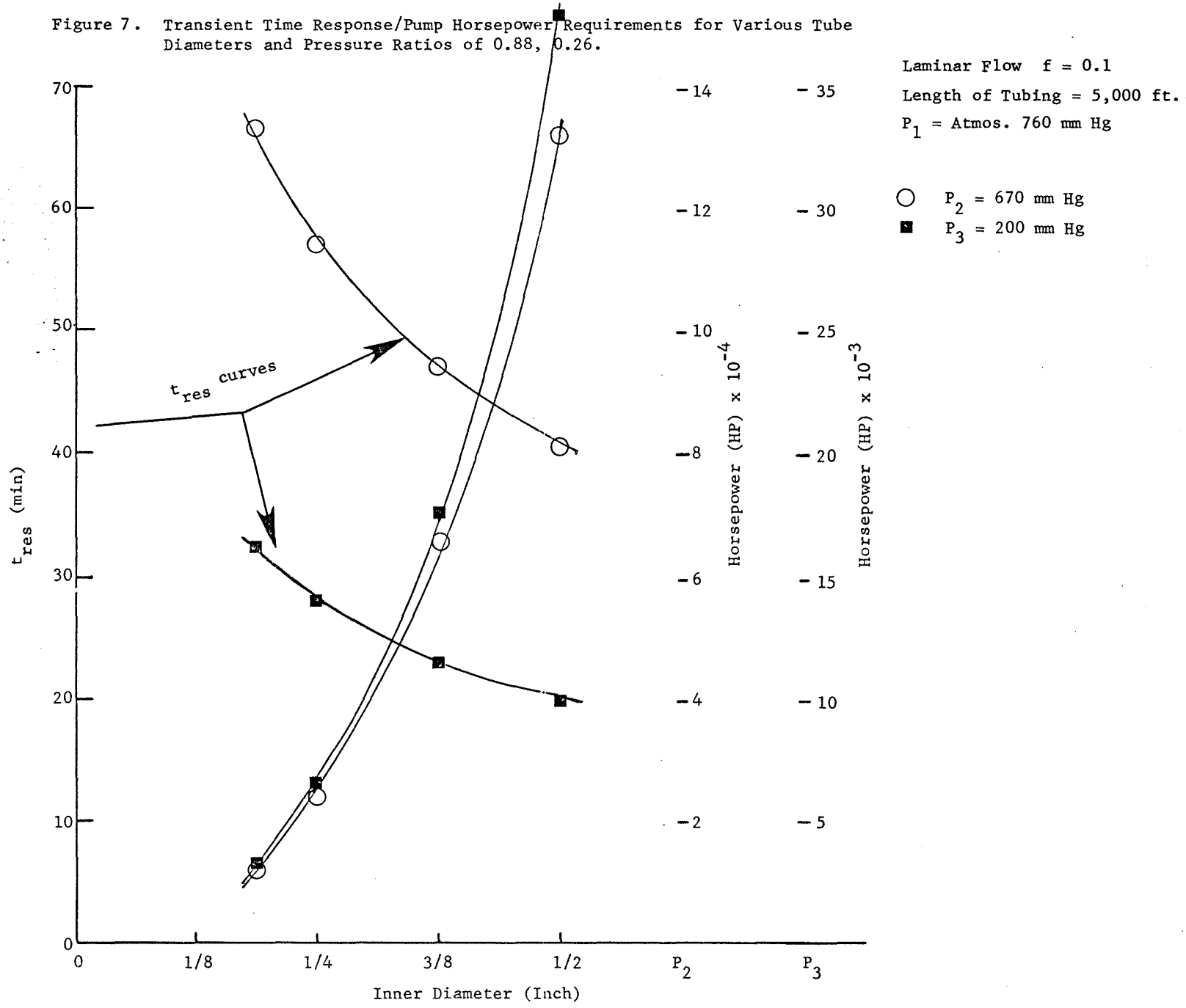

Figure 8. Diagram of Pulsing Laser Photomicrography Analysis System.

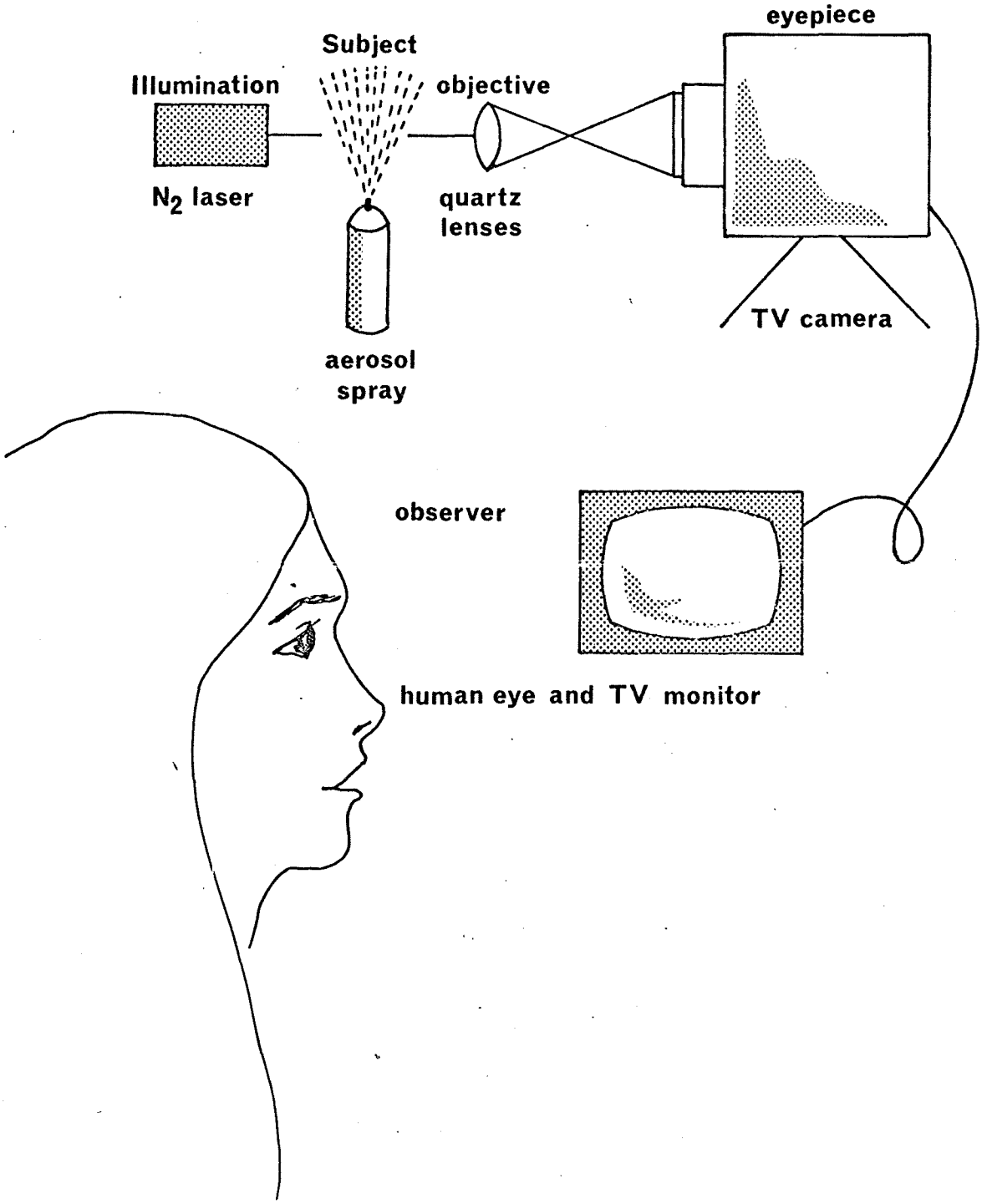

Figure 9. Plot of Ou* vs. Δ Ou/Δ t at 23 ft/min Flow Velocity for ESL PSD No. 724.

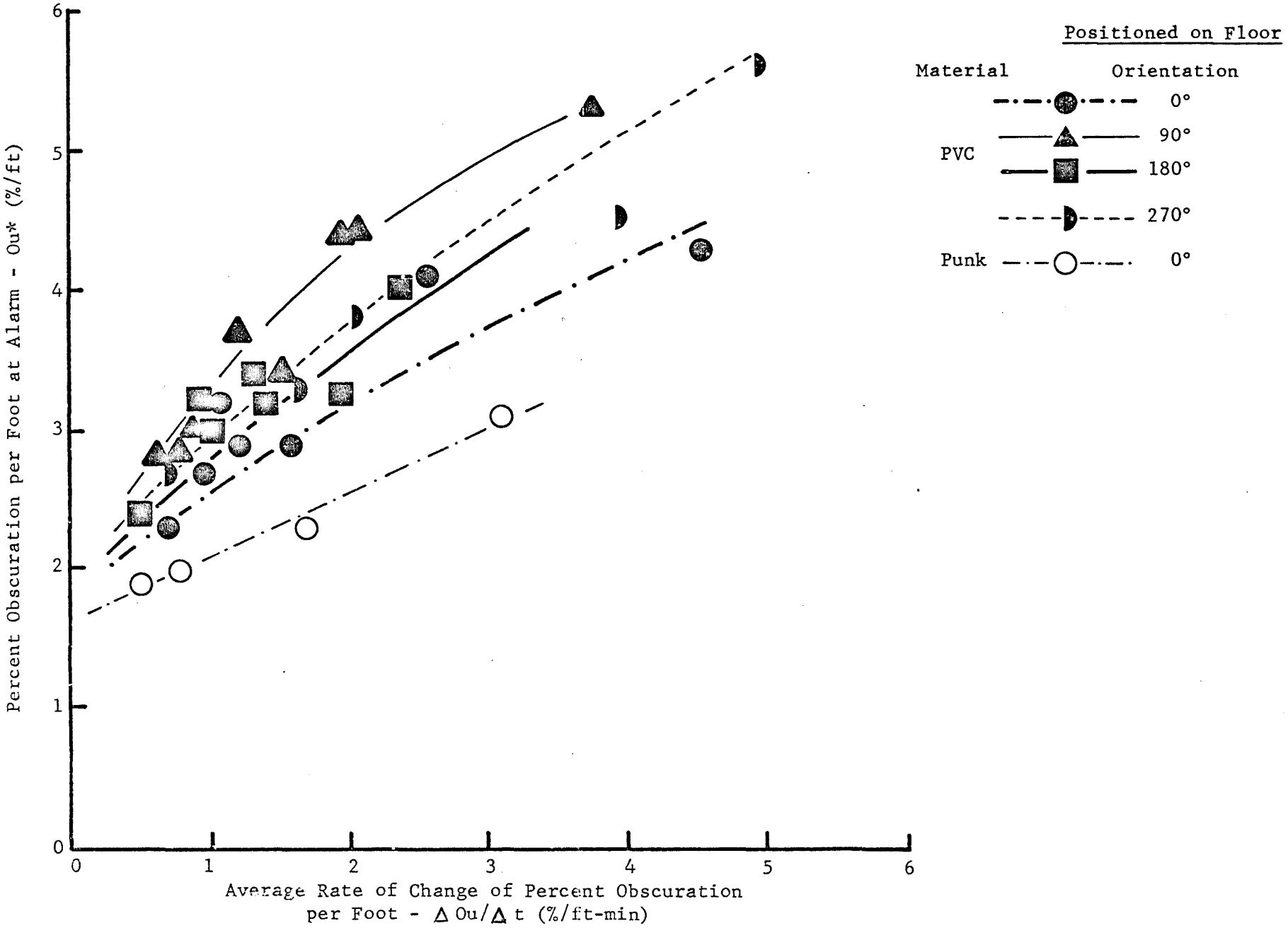

Figure 11. Plot of Ou* vs. $\bar{v}$ for ESL PSD No. 724 (Δ Ou/Δ t-1.0-1.5%/ft-min).

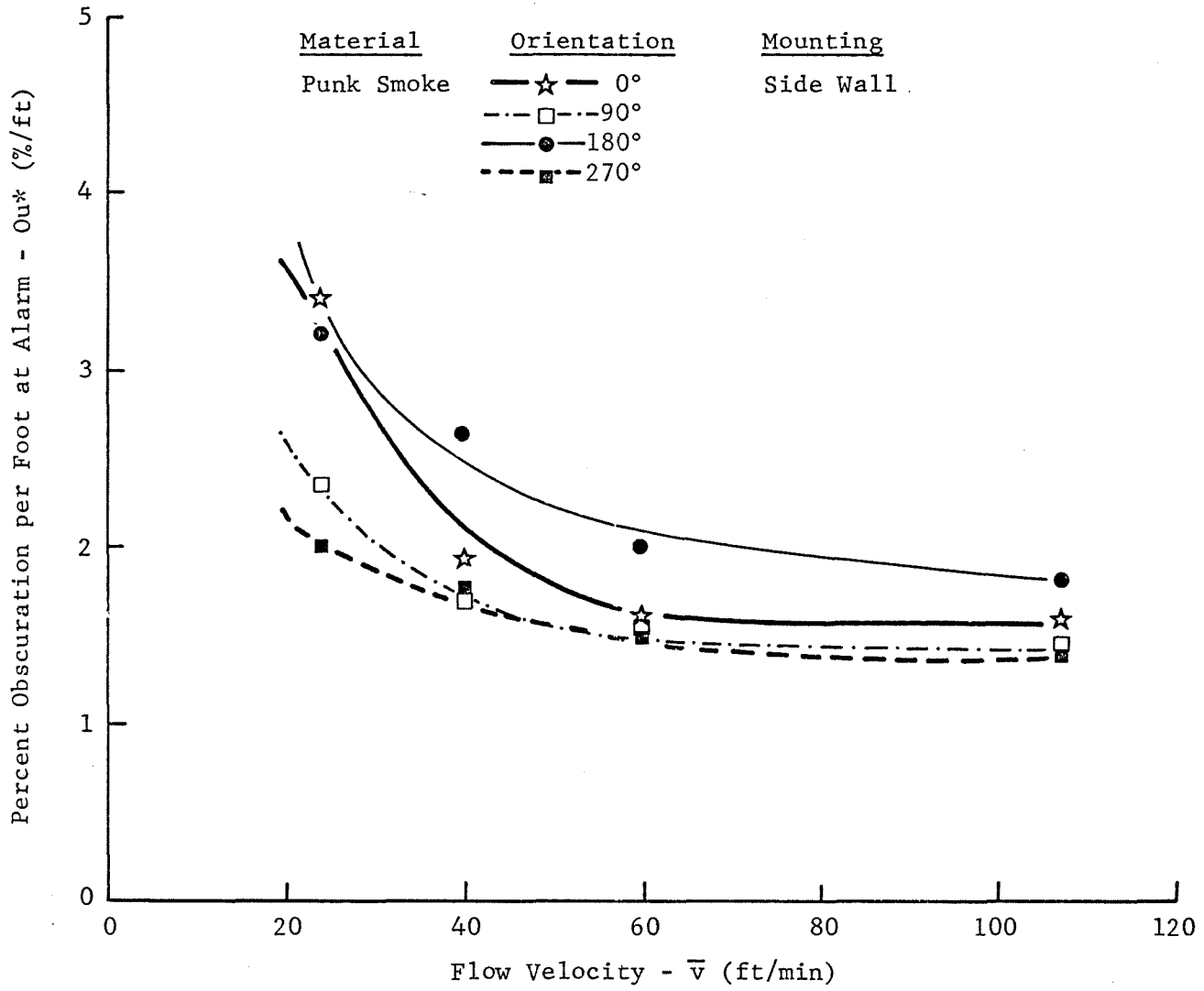

Figure 12. Plot of Ou* vs. $\bar{v}$ for ESL PSD No. 724 (Δ Ou/Δ t - 1.0-1.5%/ft-min) - Ceiling Mounting.

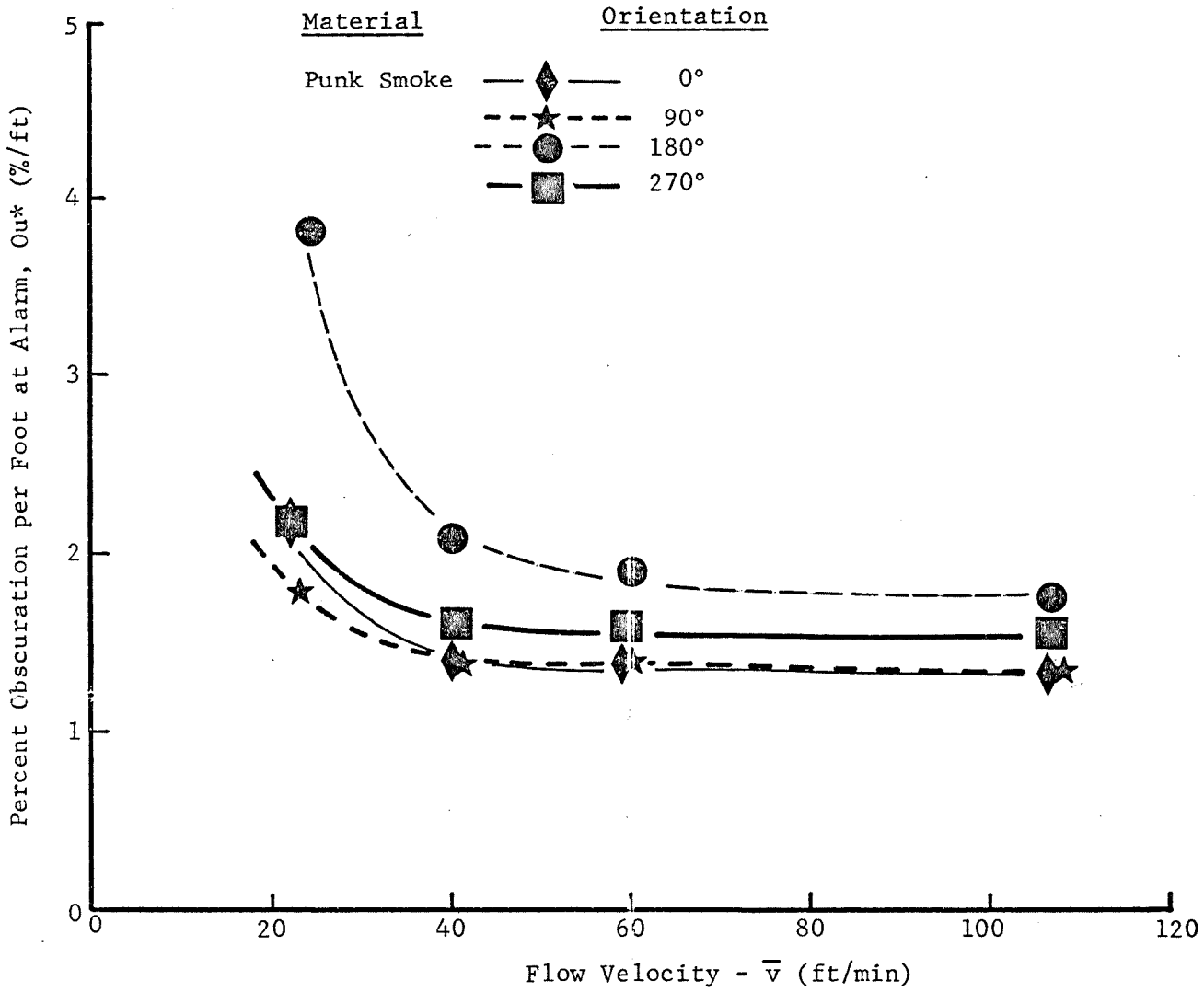

Figure 13. Plot of Ou* vs. $\bar{v}$ for Pyrotector SK 700 LED Smoke Detector.

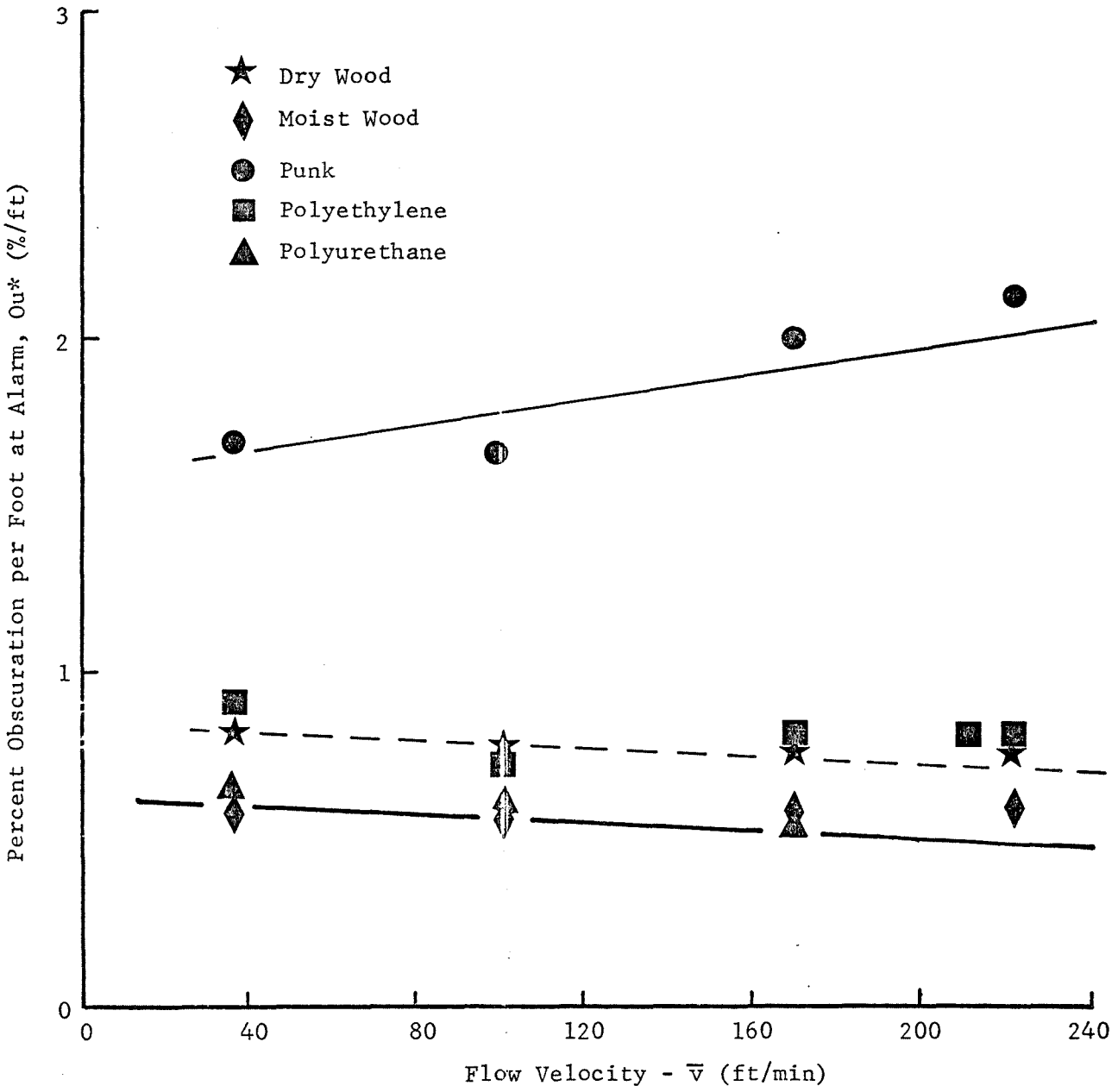

Figure 14. Plot of Ou* vs. $\bar{v}$ for Fire Alert CPD 1212 Ionization Detector for Punk Smoke (Δ Ou/Δ t - 1.0-1.5 %/ft-min).

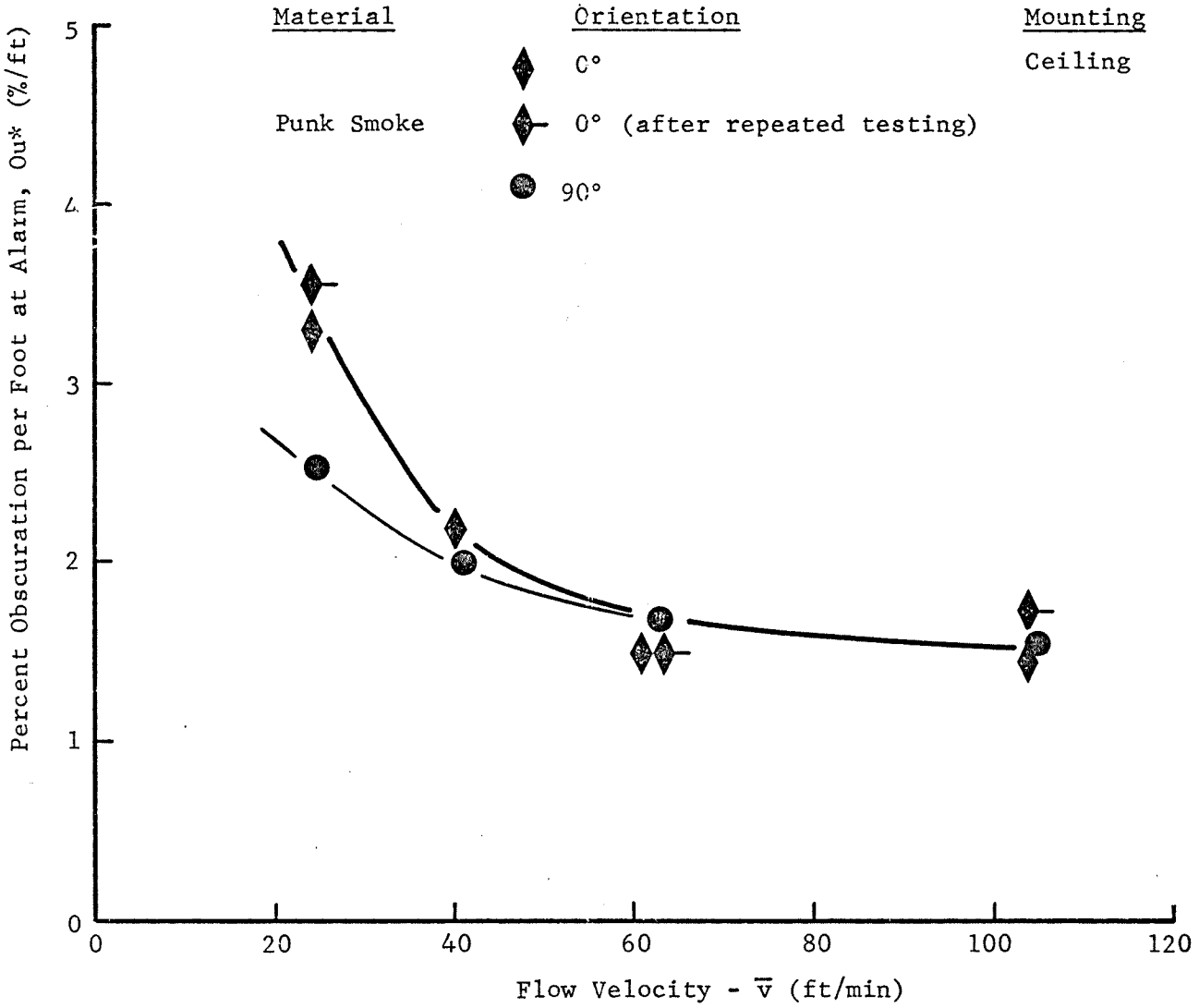

Figure 15. Plot of Ou* vs. $\bar{v}$ for Fire Alert CPD 1212 Ionization Detector for PVC Smokes.

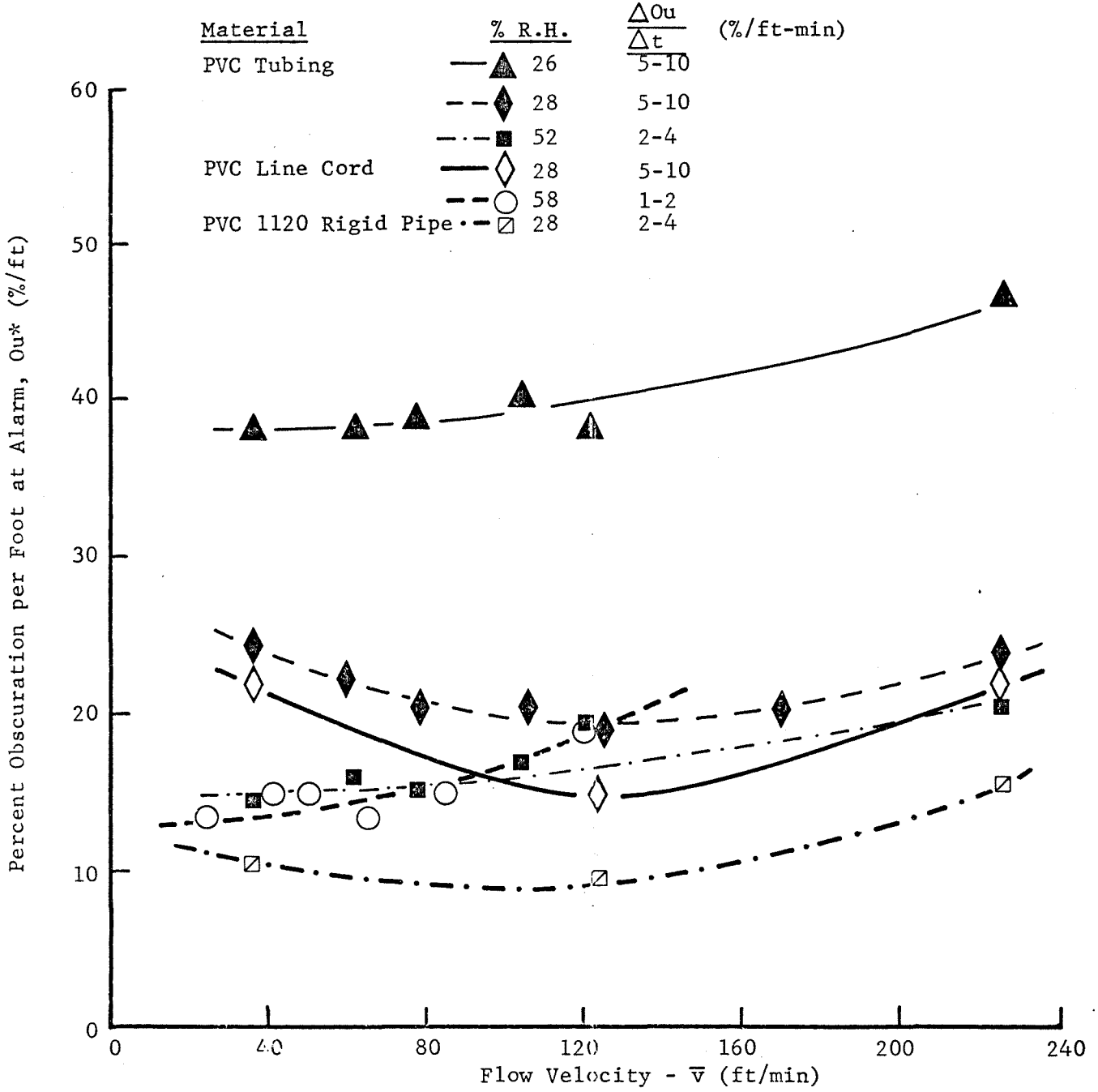

Figure 16. Plot of Ou* vs. $\bar{v}$ for Fire Alert CPD 1212 Ionization Detector.

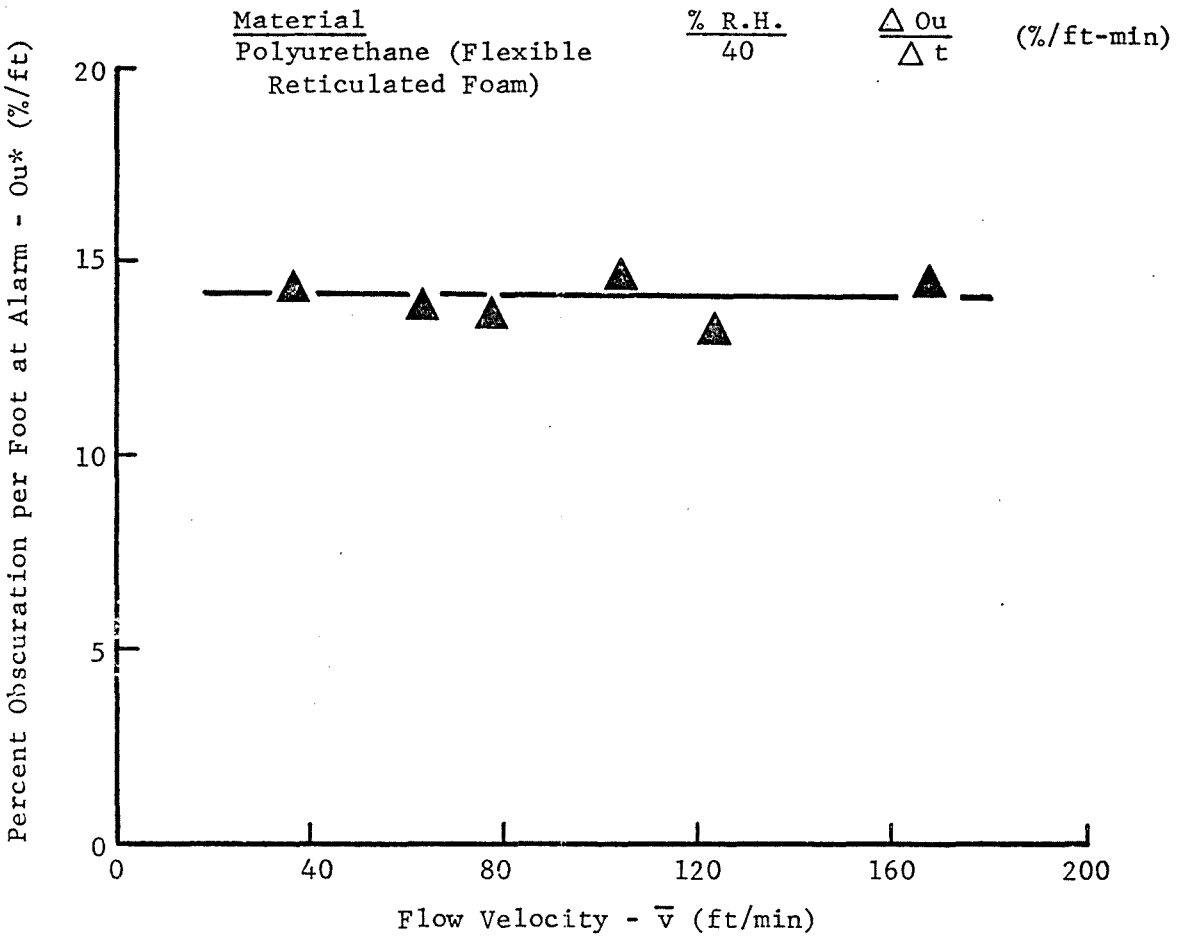

Figure 17. Plot of Ou* vs. Δ Ou/Δ t for Fire Alert CPD 1212 Ionization Detector (Ceiling Mounted).

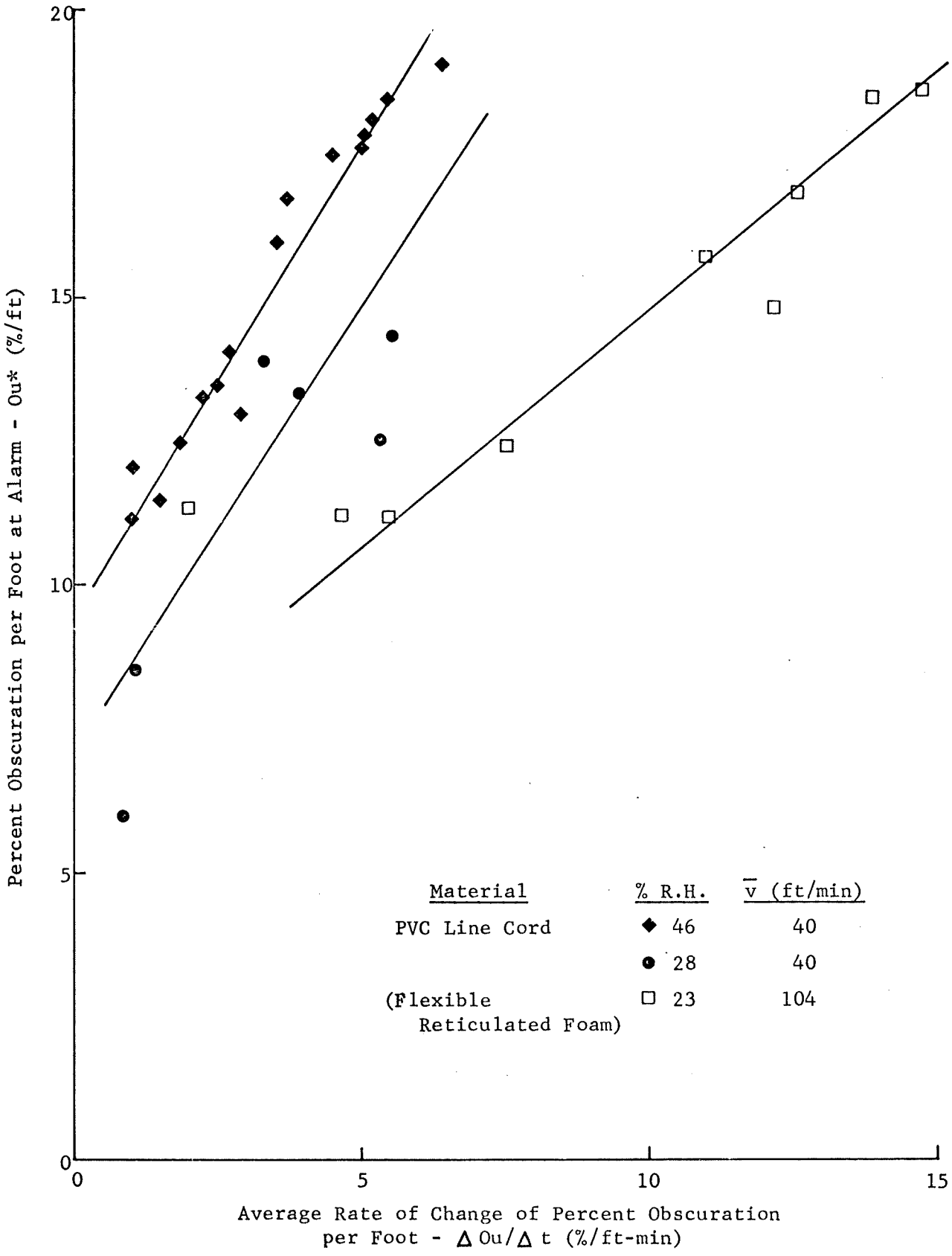

Figure 18. Comparative Performance of Honeywell Ionization Detector TC 100A for Punk and Plastic Smokes (% R.H. = 39).

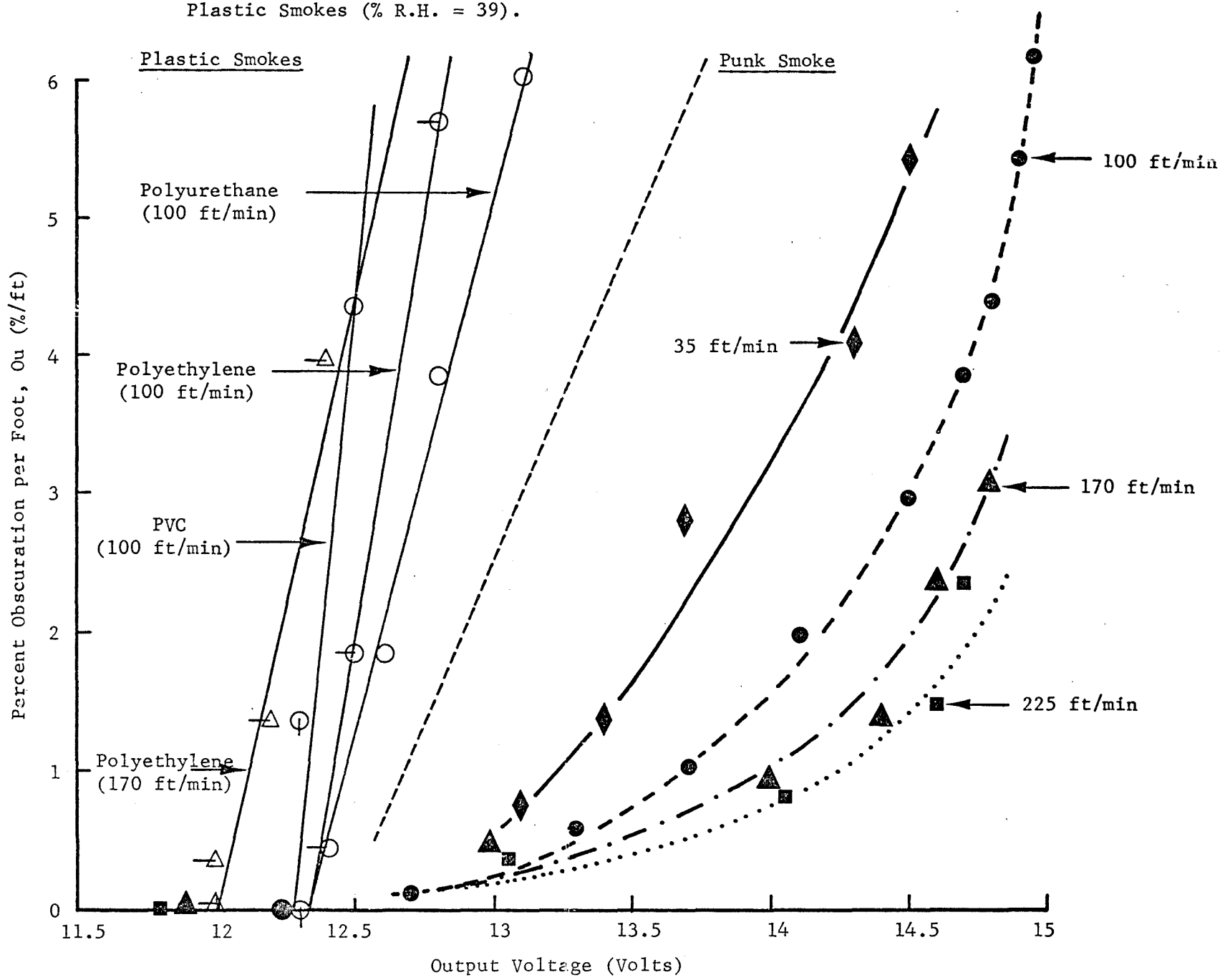

Figure 19. Honeywell TC100A Performance for Plastic Smokes (% R.H. = 39).

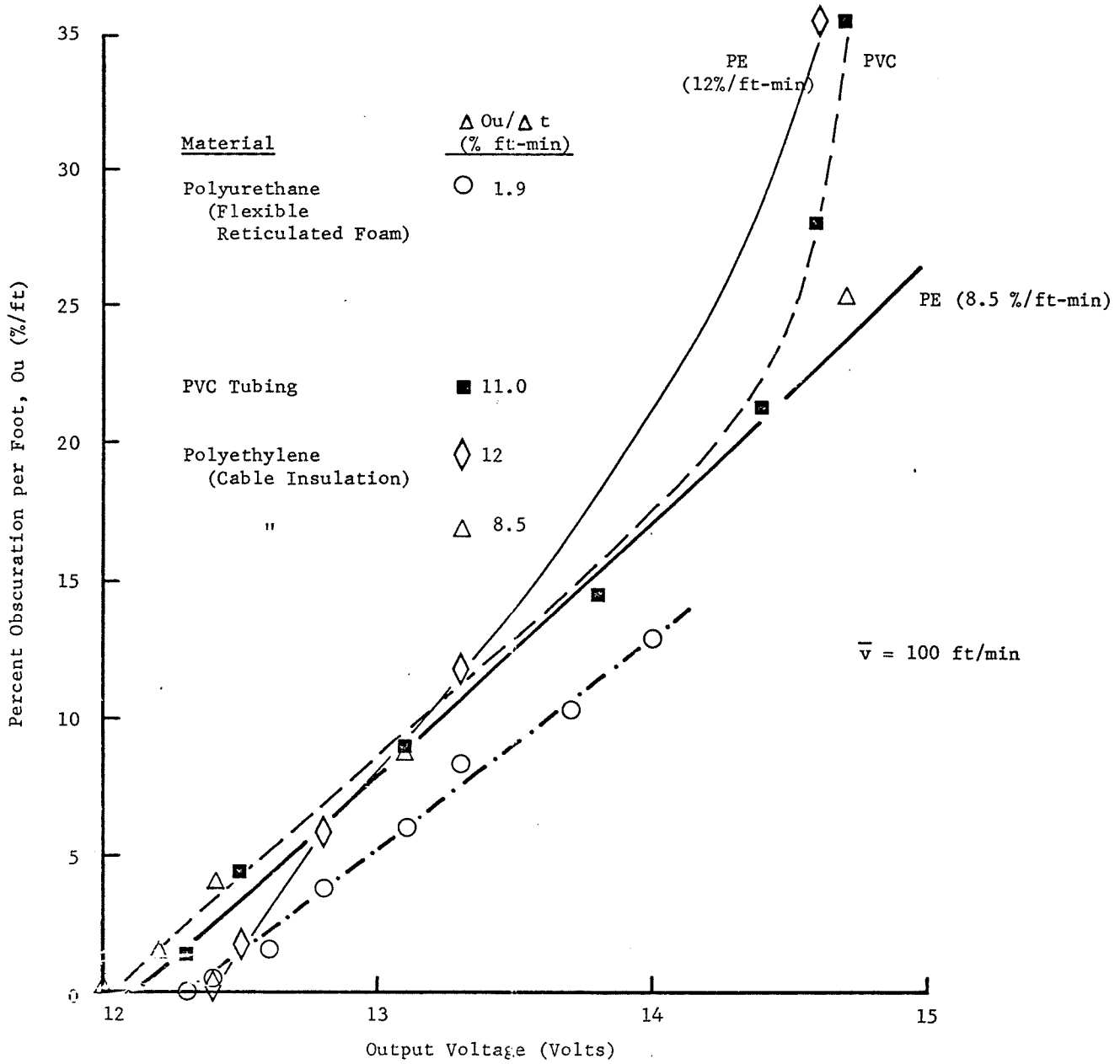

Figure 20. Honeywell TC100A Performance for Moist Wood Smokes.

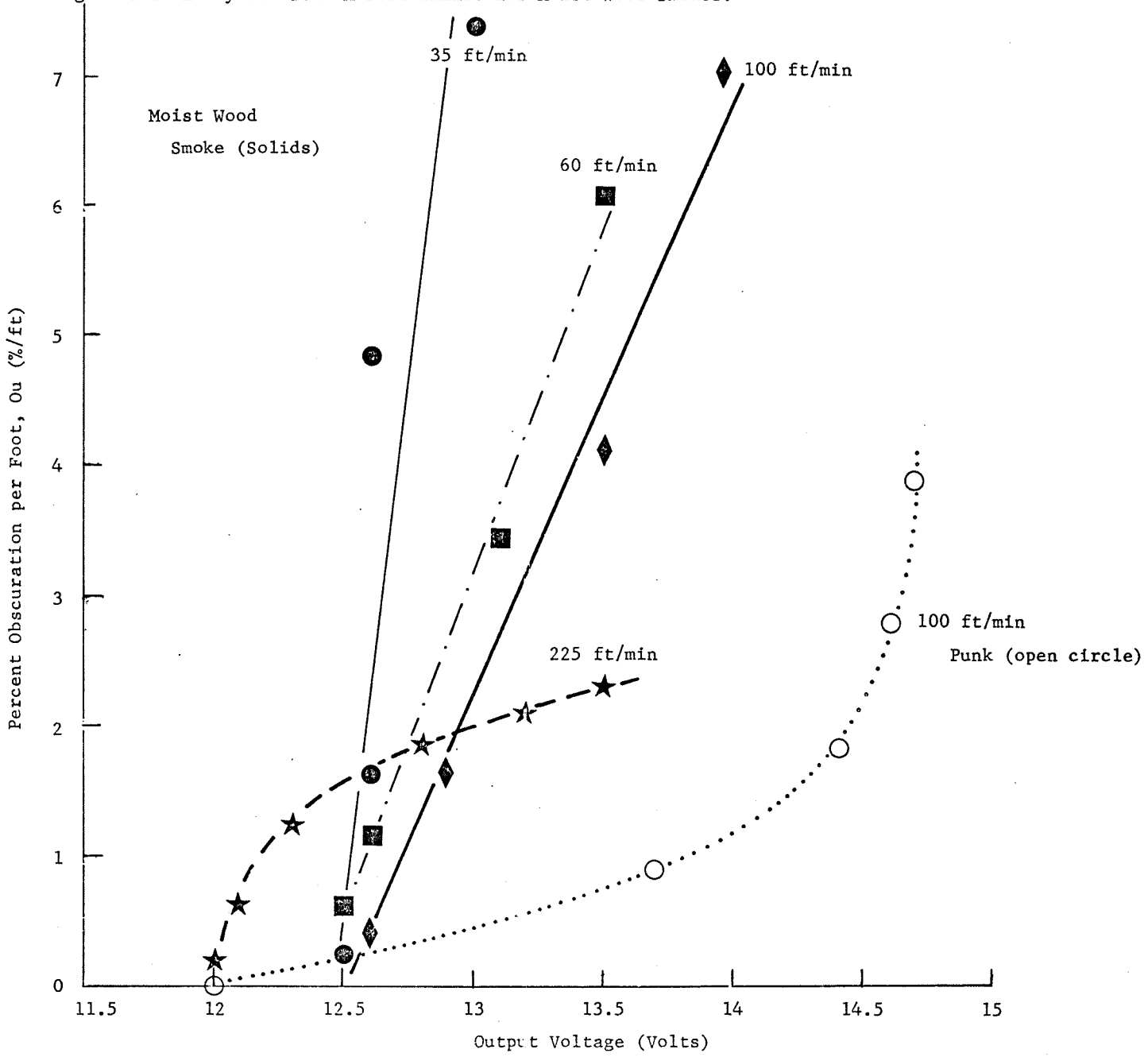

Figure 21. Honeywell TC100A Performance for Dry Wood Smokes.

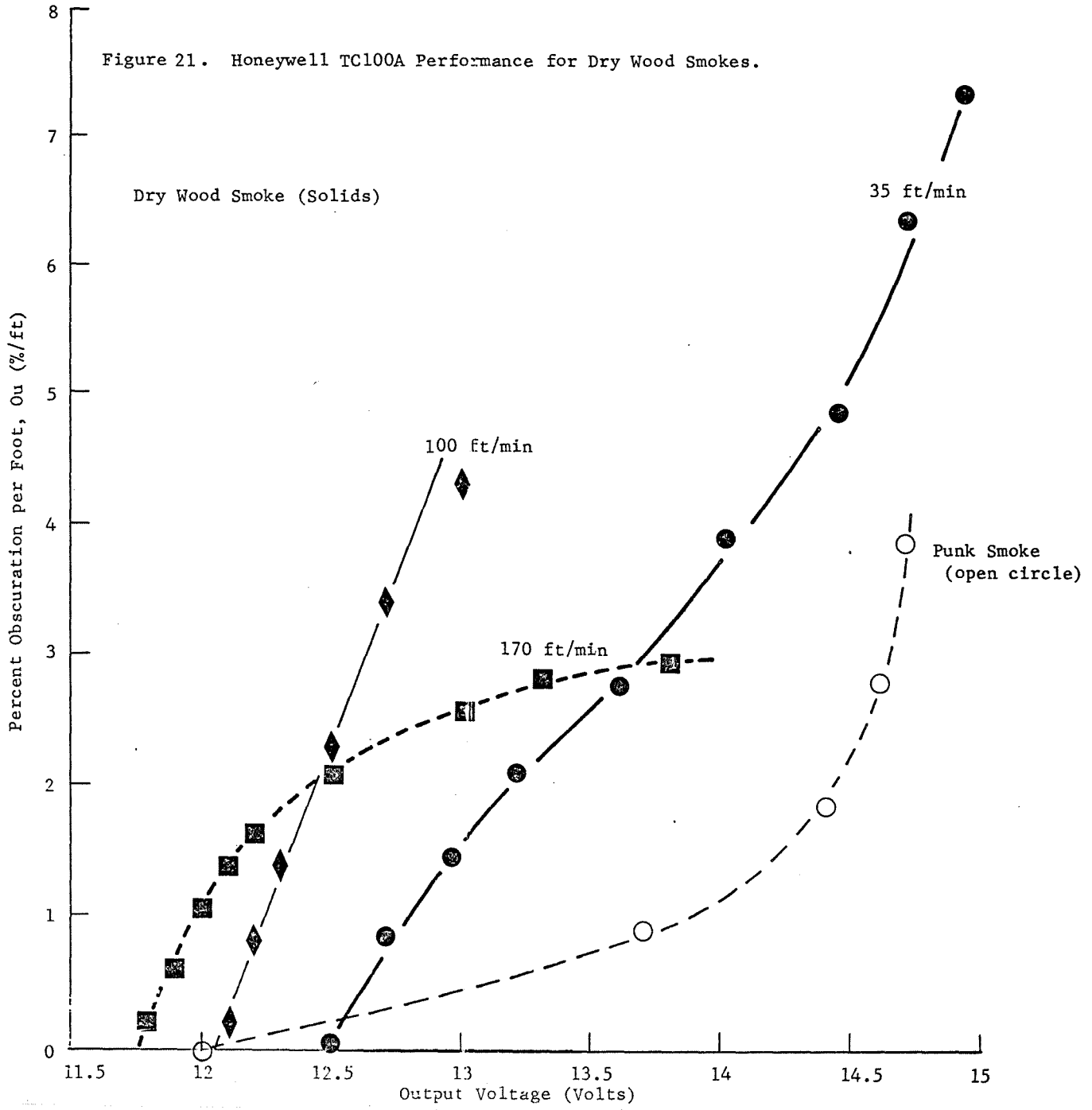

Figure 22. Plot of Ou* vs. $\bar{v}$ for Pyr-A-Larm DI-2S Ionization Detector.

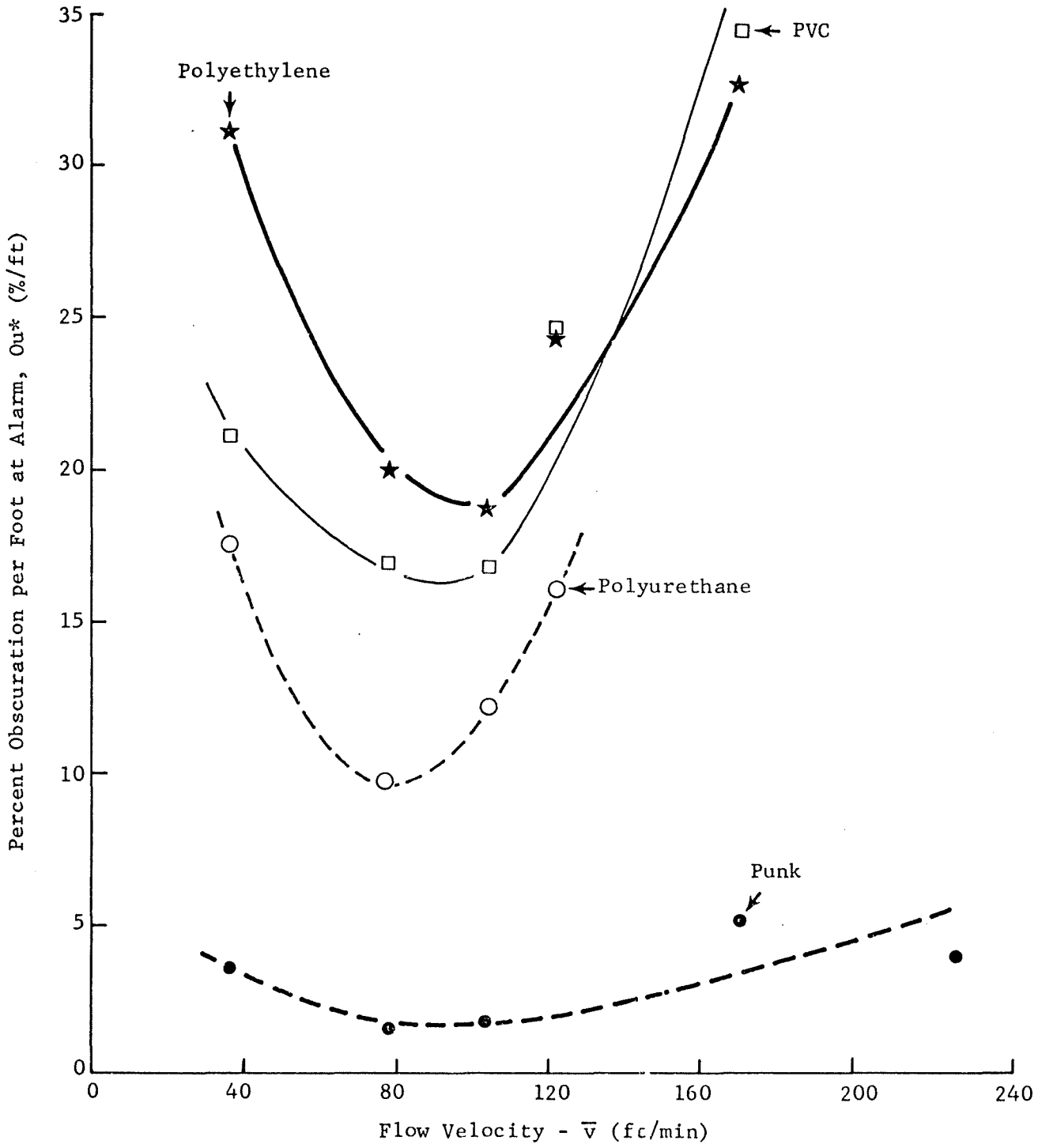

Figure 23. Plot of Ou* vs. $\bar{v}$ for Becon MKII Ionization Detector.

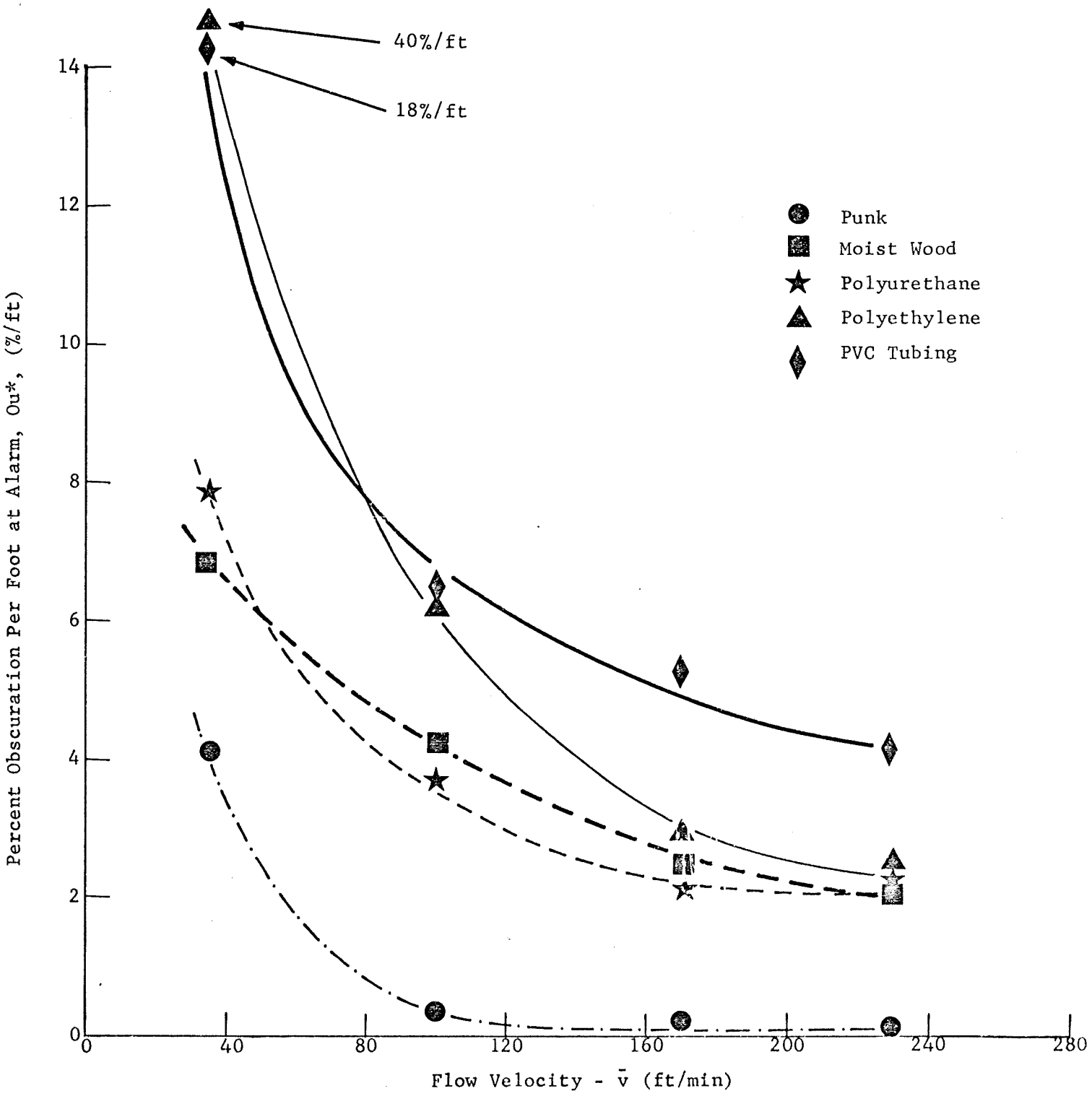

Figure 24. Taguchi 109 Output vs. Time for Various Flow Velocities - Clean Air (V_h = 0.8 Volts).

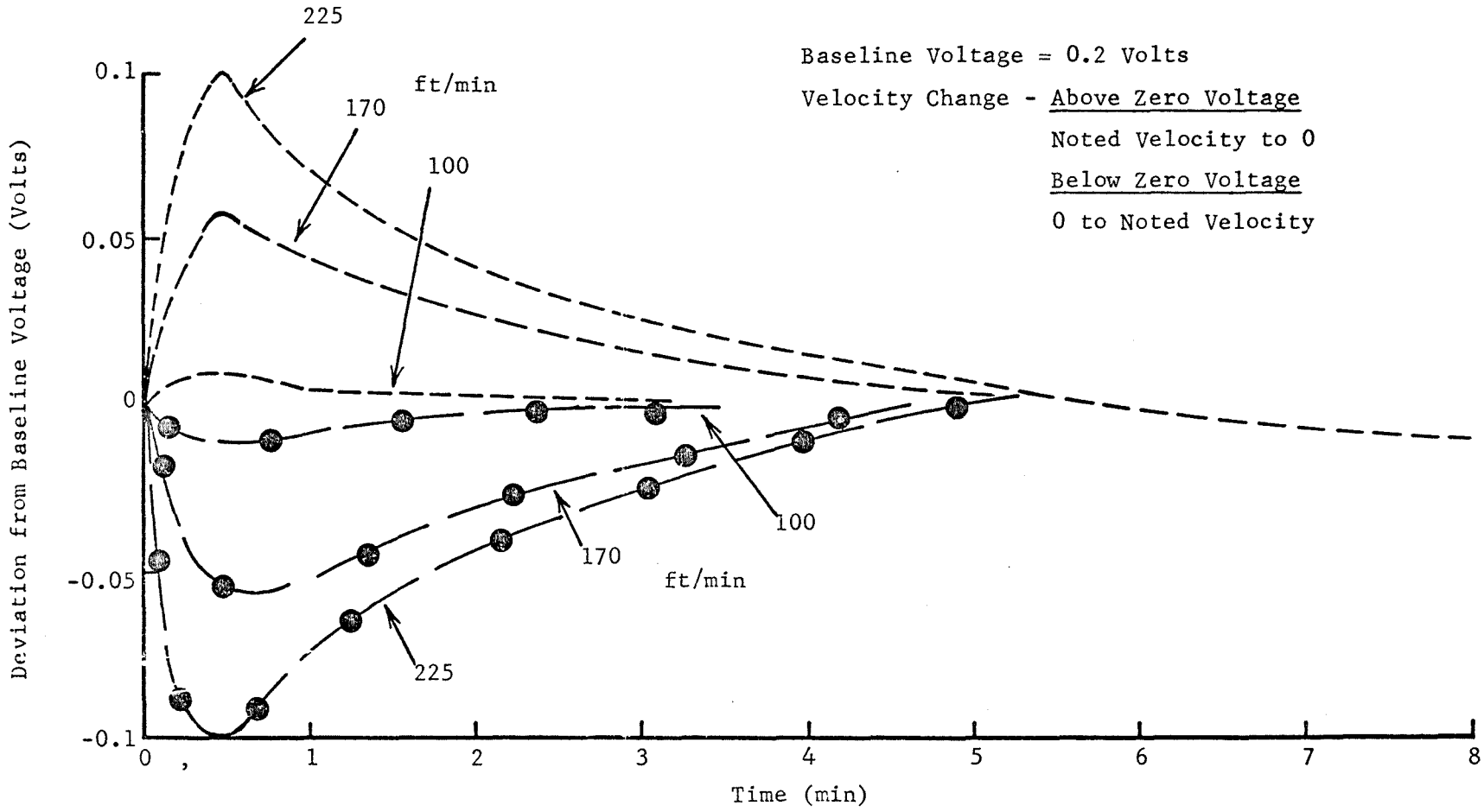

Figure 25. Taguchi 109 Behavior for Punk Smoke (% R.H. = 30) - V_h = 0.8 Volts.

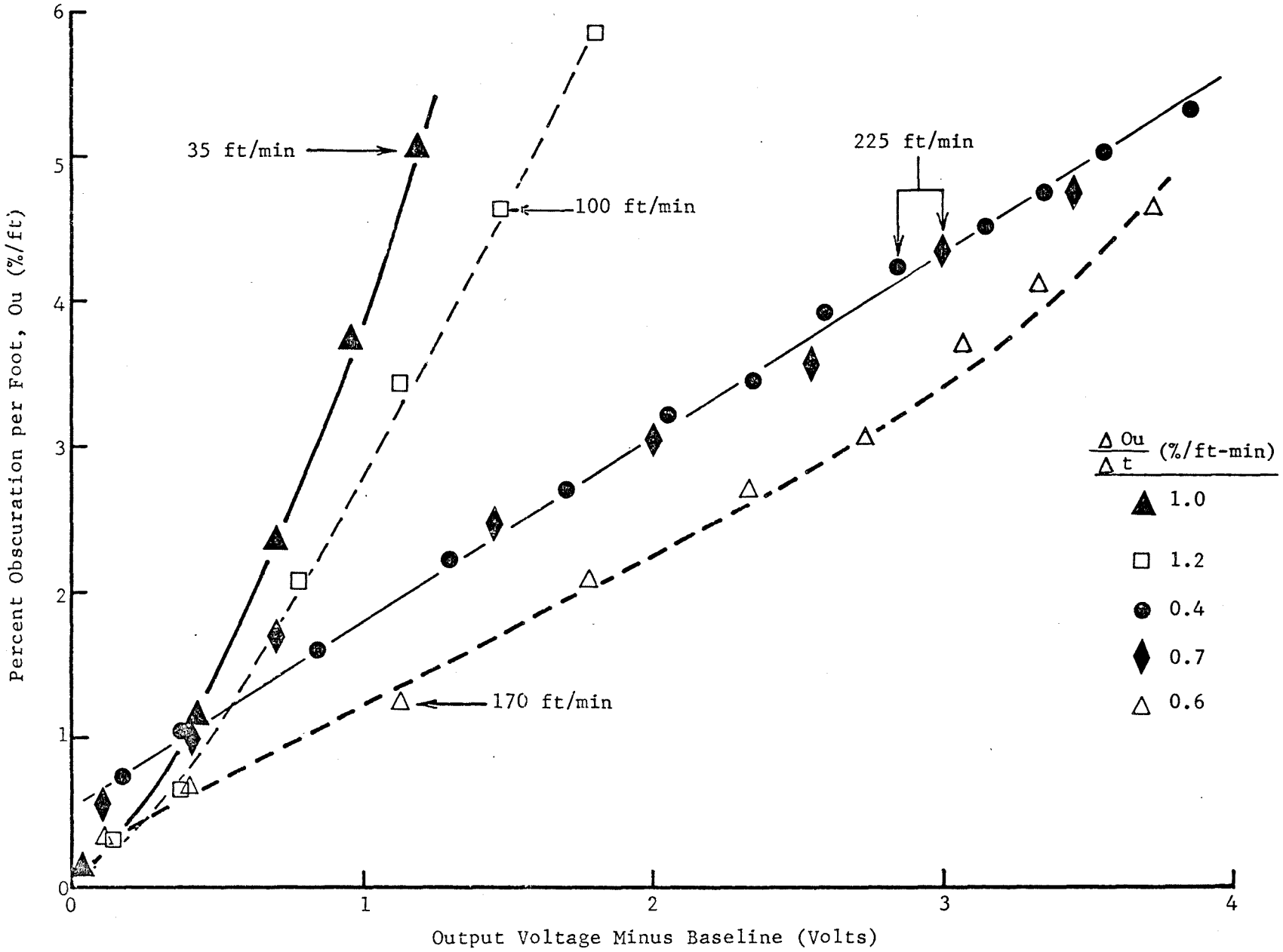

Figure 26. Taguchi 109 Behavior for PVC Smoke (% R.H. = 31) - V_h = 0.8 Volts.

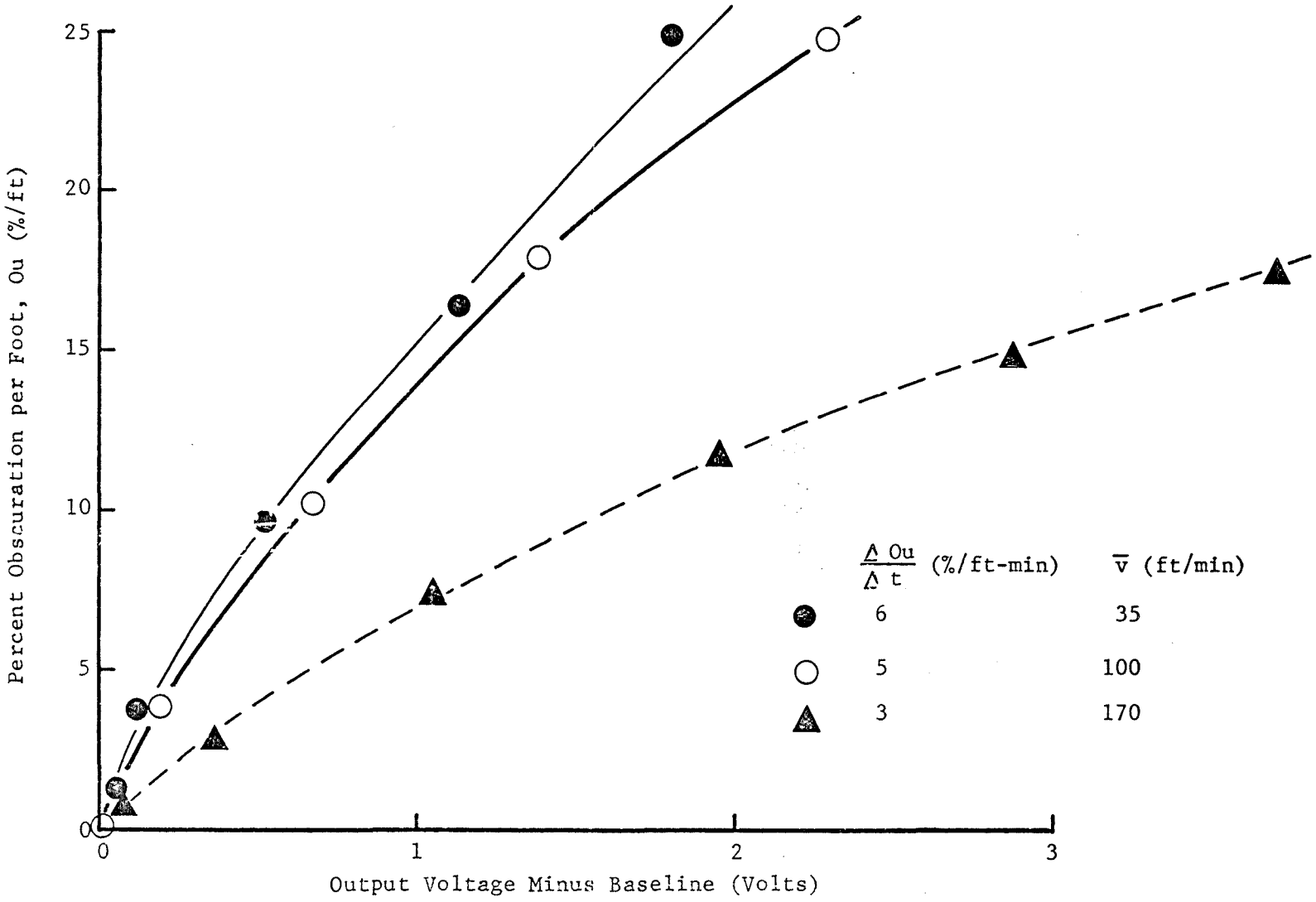

Figure 27. TGS 109 Behavior for Polyurethane Smoke and Flaming Combustion.

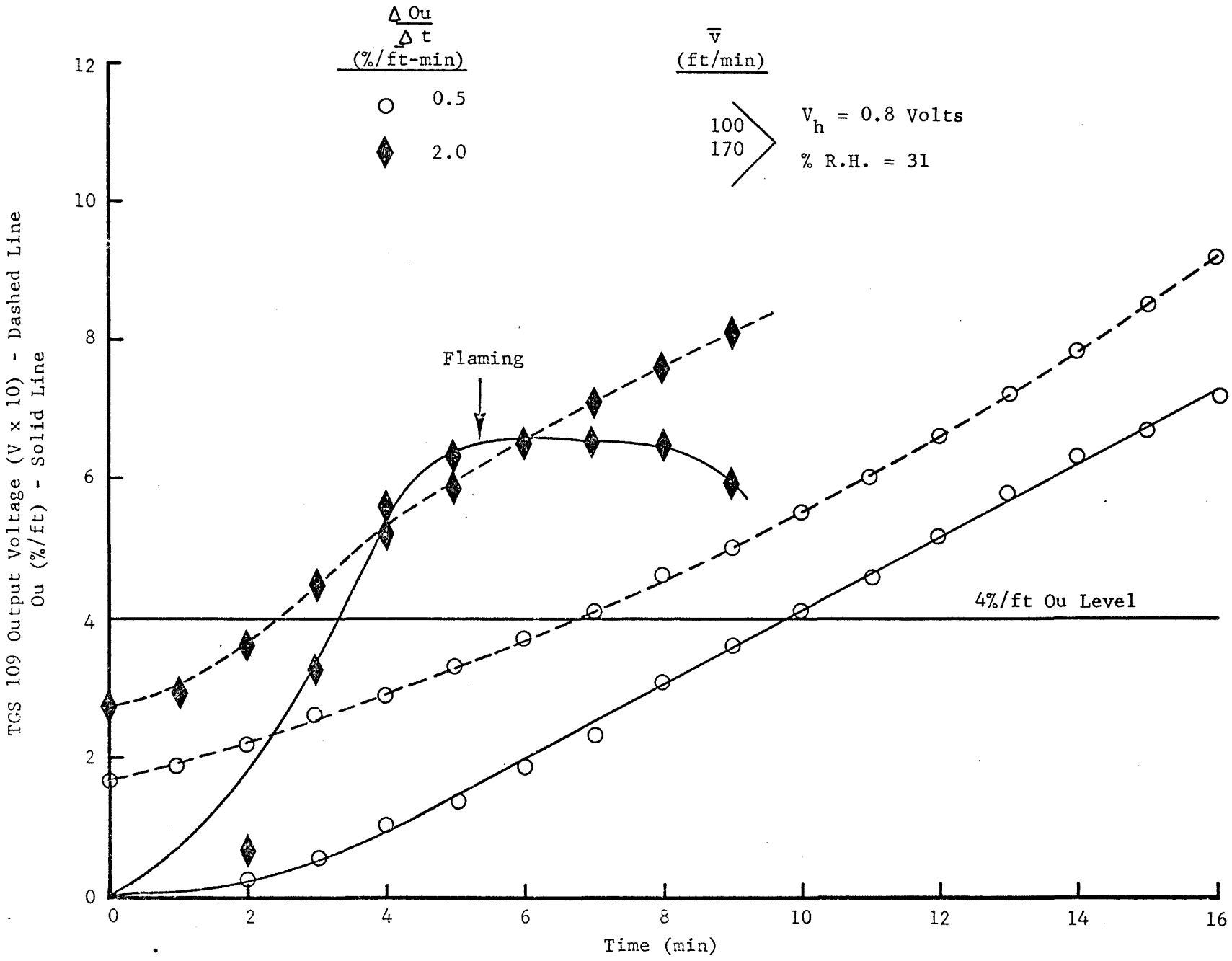

Figure 28. TGS 109 Behavior for Polyurethane Smoke and Flaming Combustion.

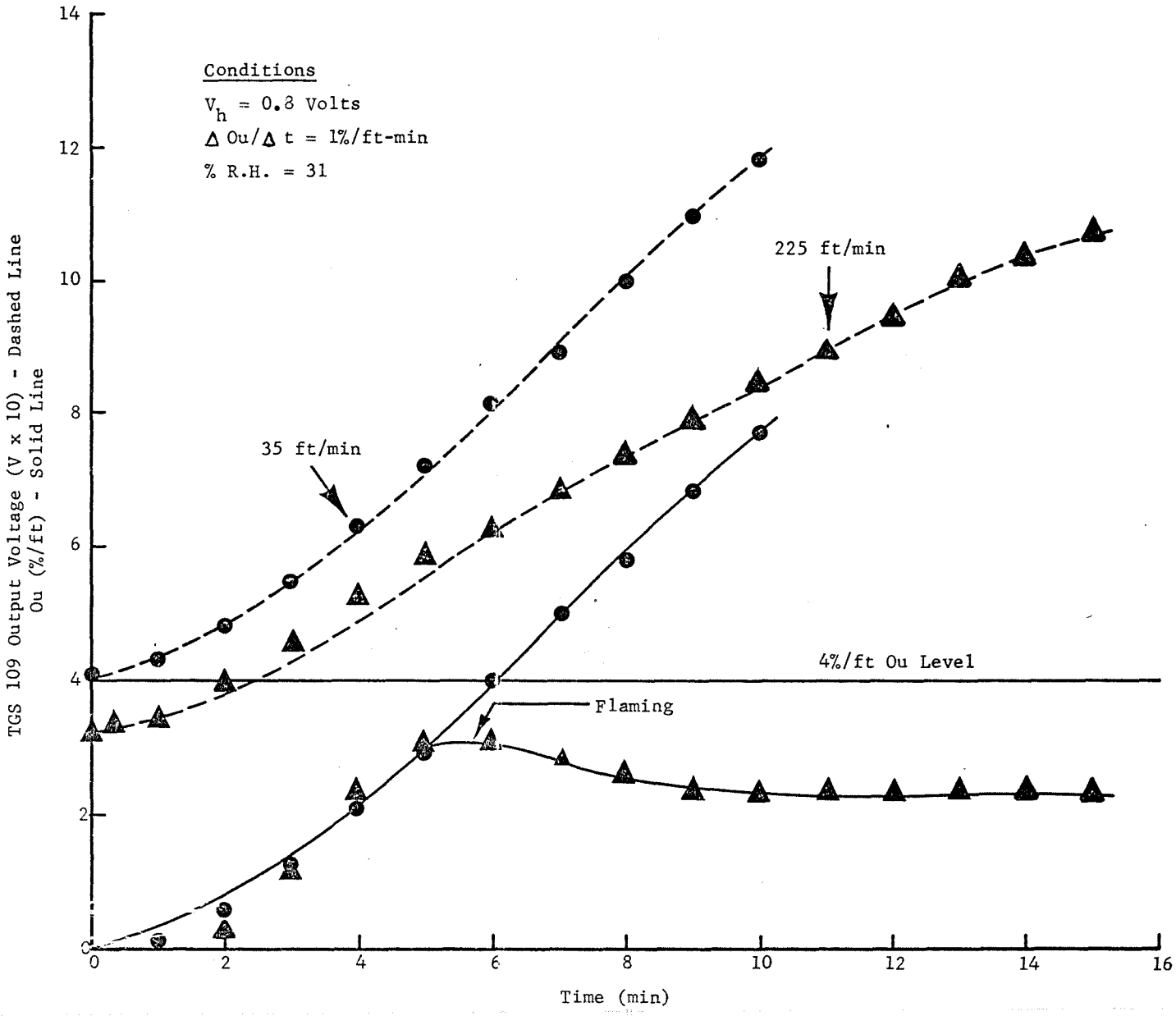

Figure 29. TGS 109 Selected Decay Plots for Three Different Fuels (V_h = 0.8 V).

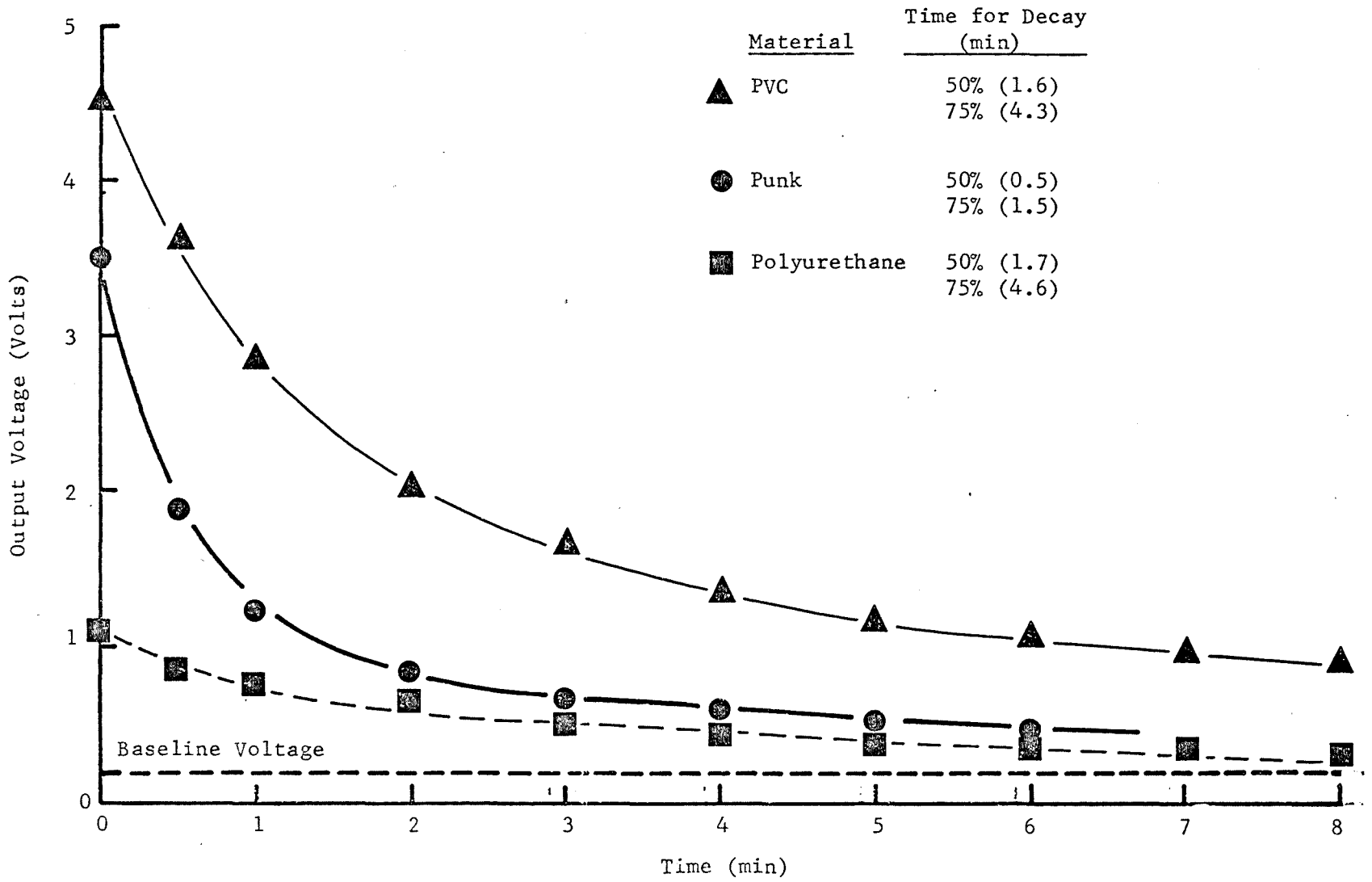

Figure 30. Taguchi 109 Output vs. Time for Various Flow Velocities - Clean Air - V_h = 1.2 Volts.

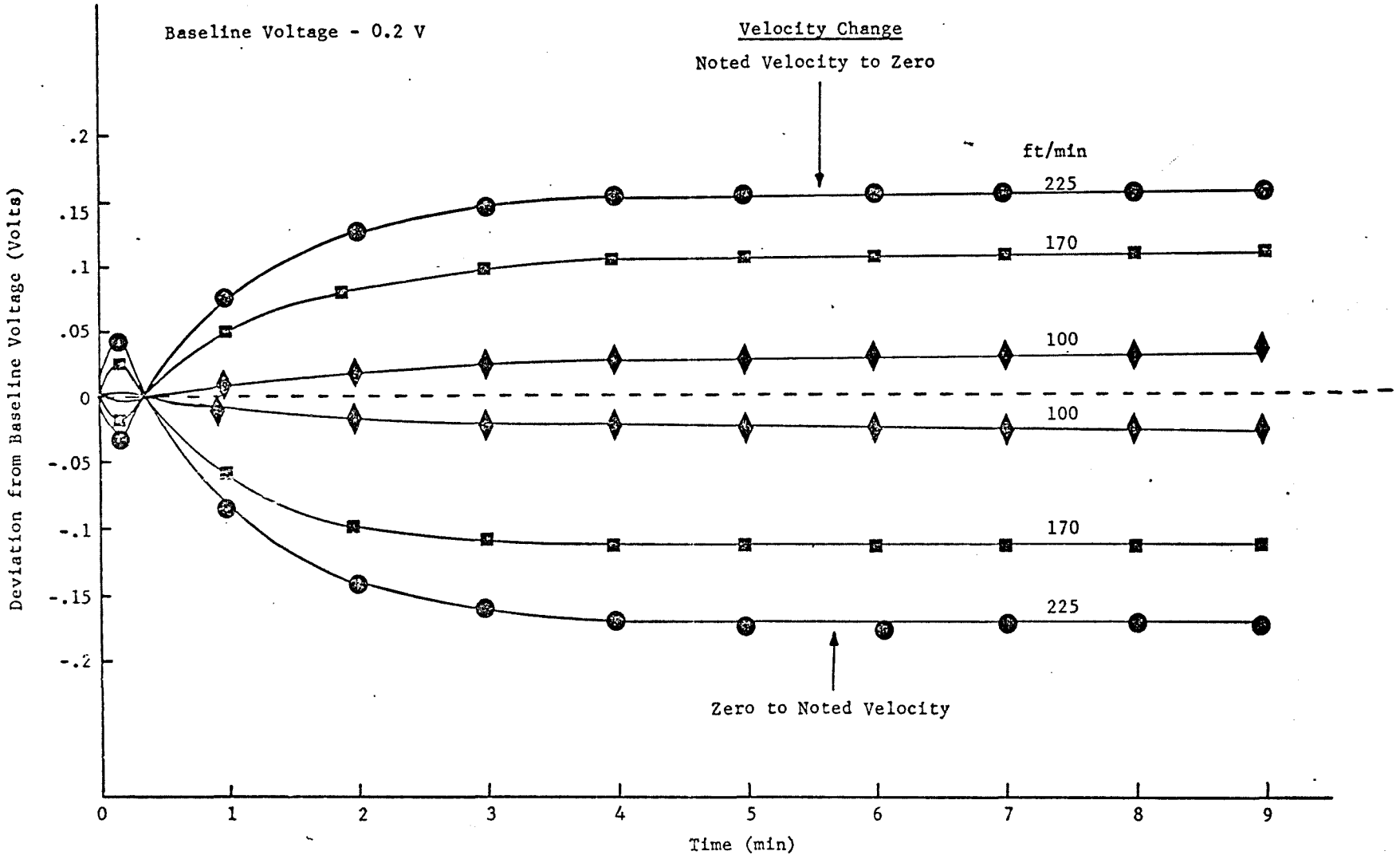

Figure 31. Taguchi 109 Behavior for Punk Smoke - V_h = 1.2 Volts.

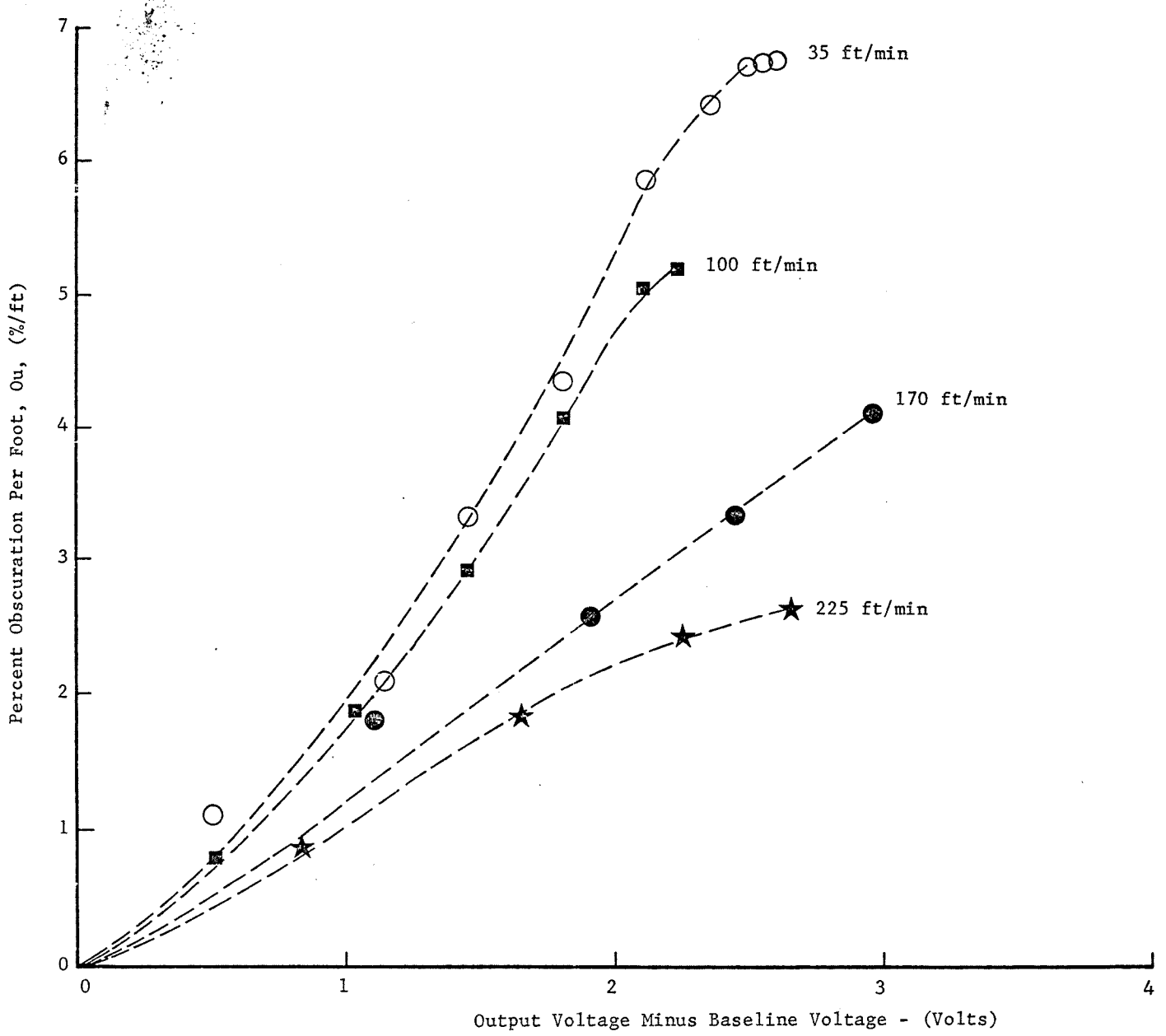

Figure 32. Taguchi 109 Behavior for PVC Flexible Tubing - V_h = 1.2 Volts.

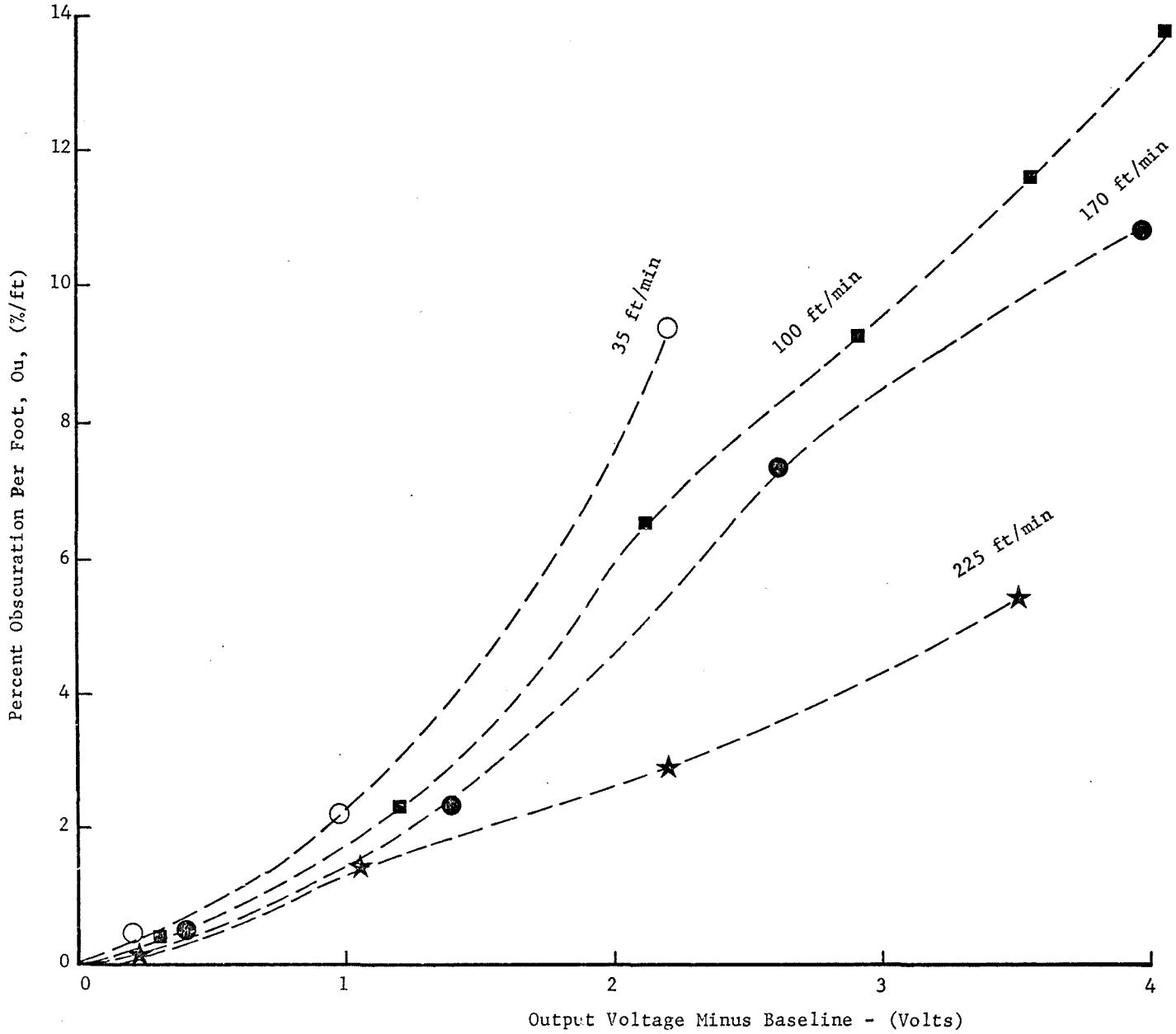

Figure 33. TGS 109 Behavior for Polyurethane and Polyethylene - V_h = 1.2 Volts.

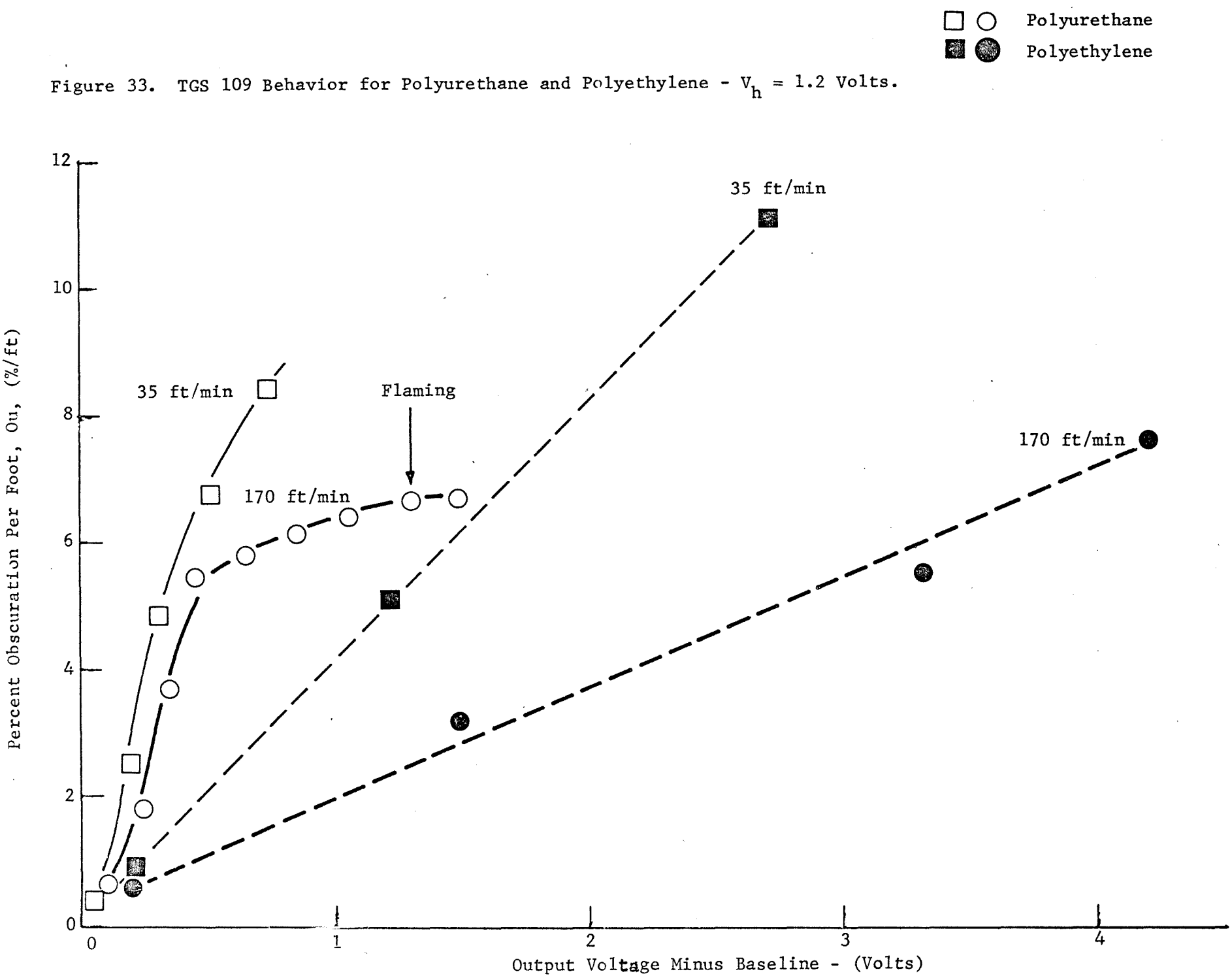

Figure 34. Taguchi 109 Behavior for Dry Wood - V_h = 1.2 Volts.

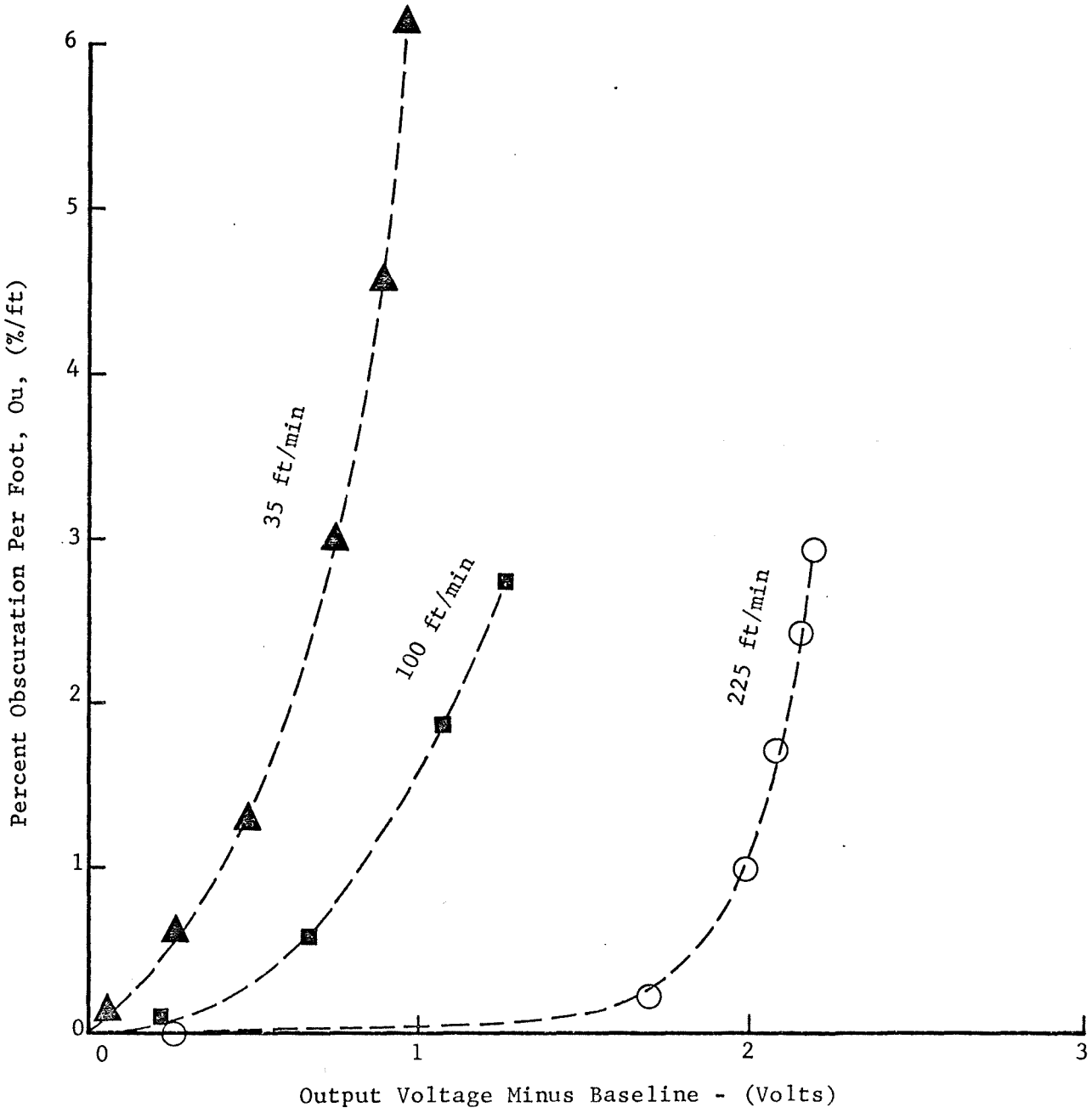

Figure 35. Taguchi 109 Behavior for Moist Wood - V_h = 1.2 Volts.

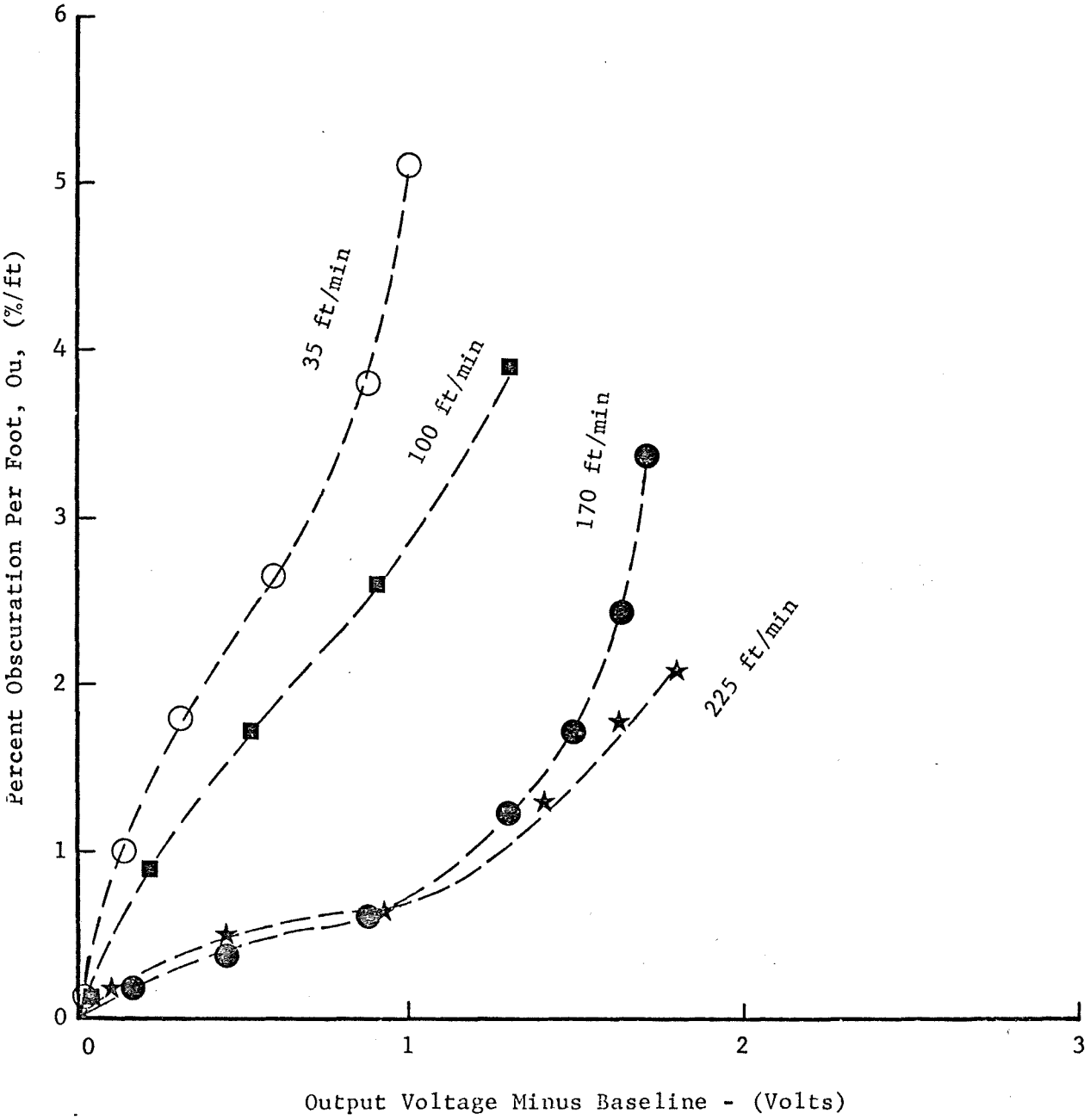

Figure 36. TGS 109 Selected Decay Plots for Three Different Fuels - V_h = 1.2 Volts.

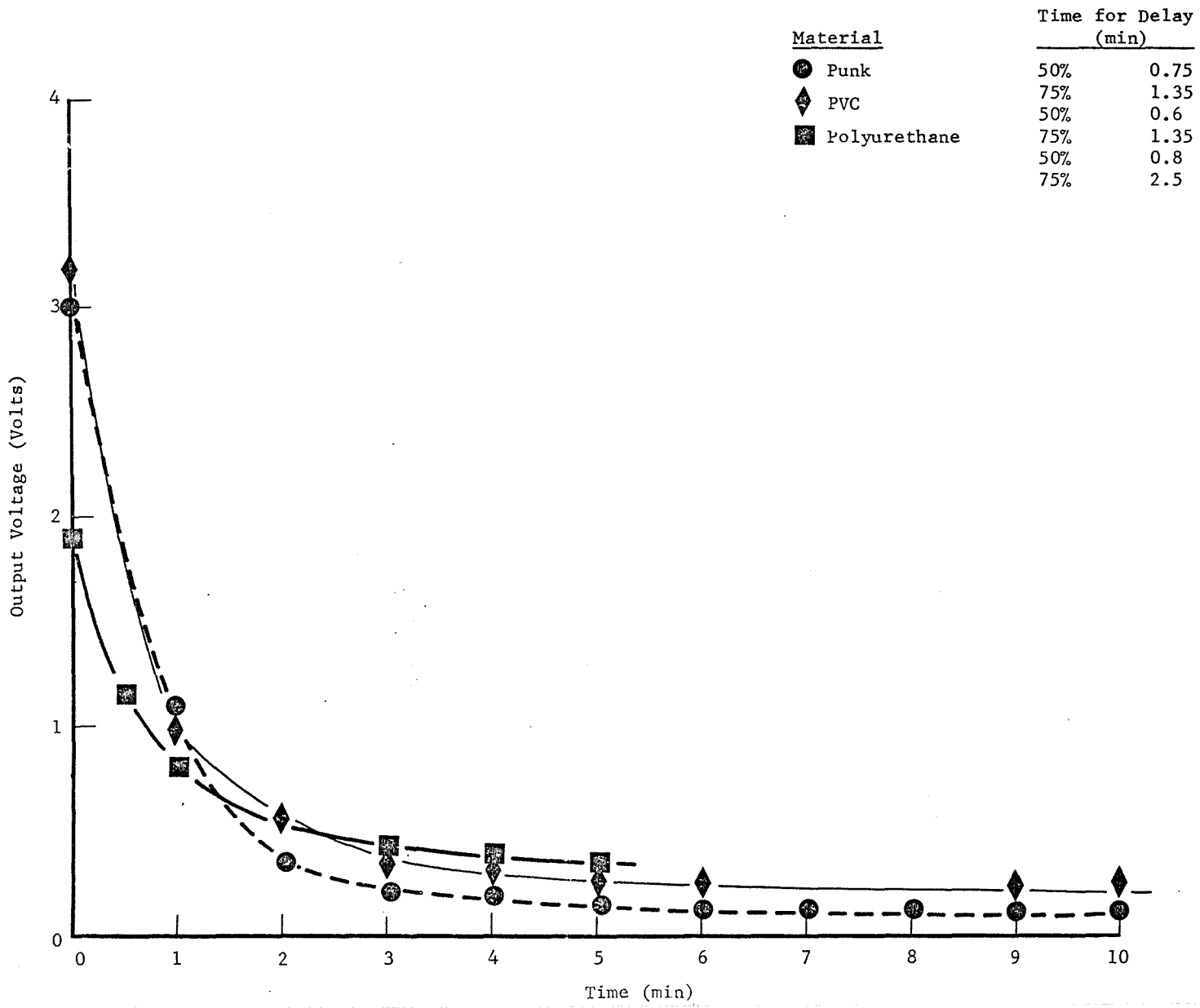

Figure 37. Circuit Schematic and Position of Detectors in Ceiling of Box (looking down).

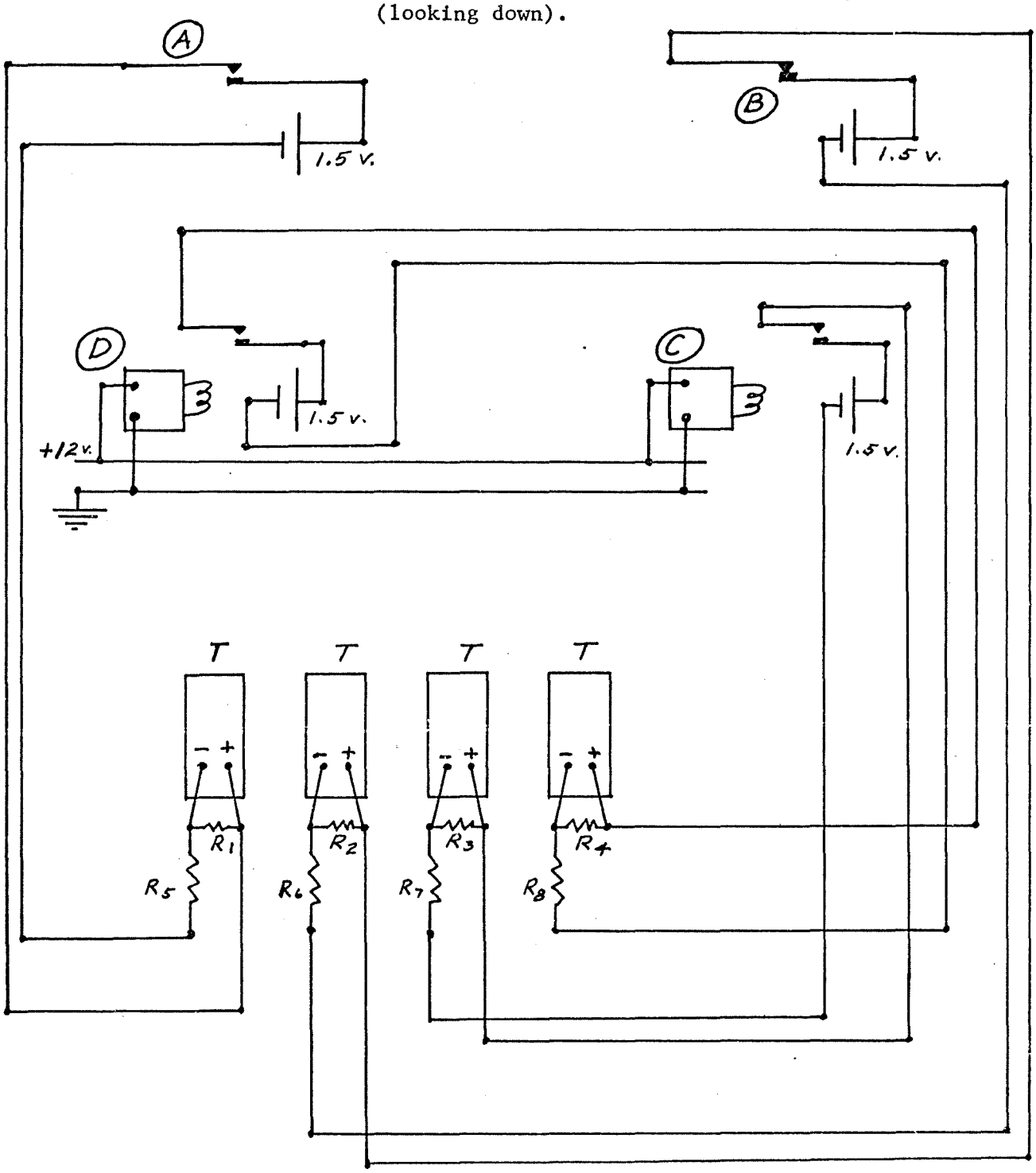

$R_1 = R_2 = R_3 = R_4 = 1$ K ; $R_5 = R_6 = R_7 = R_8 = 68$ K

T Transducer couplers for Brush 4-channel recorder. (This is not in ceiling)

A Fenwal Detectafire, vertical orientation, NO contacts.

B Fenwal Detectafire, horizontal orientation, NC contacts.

C Pyrotector 30-2021, UV detector, NO contacts.

D Pyrotector 30-2025, IR detector, NO contacts.

Figure 38. Response Time Behavior of Fenwal Rate Compensated Thermal Detectors - Vertical vs. Horizontal Orientation.

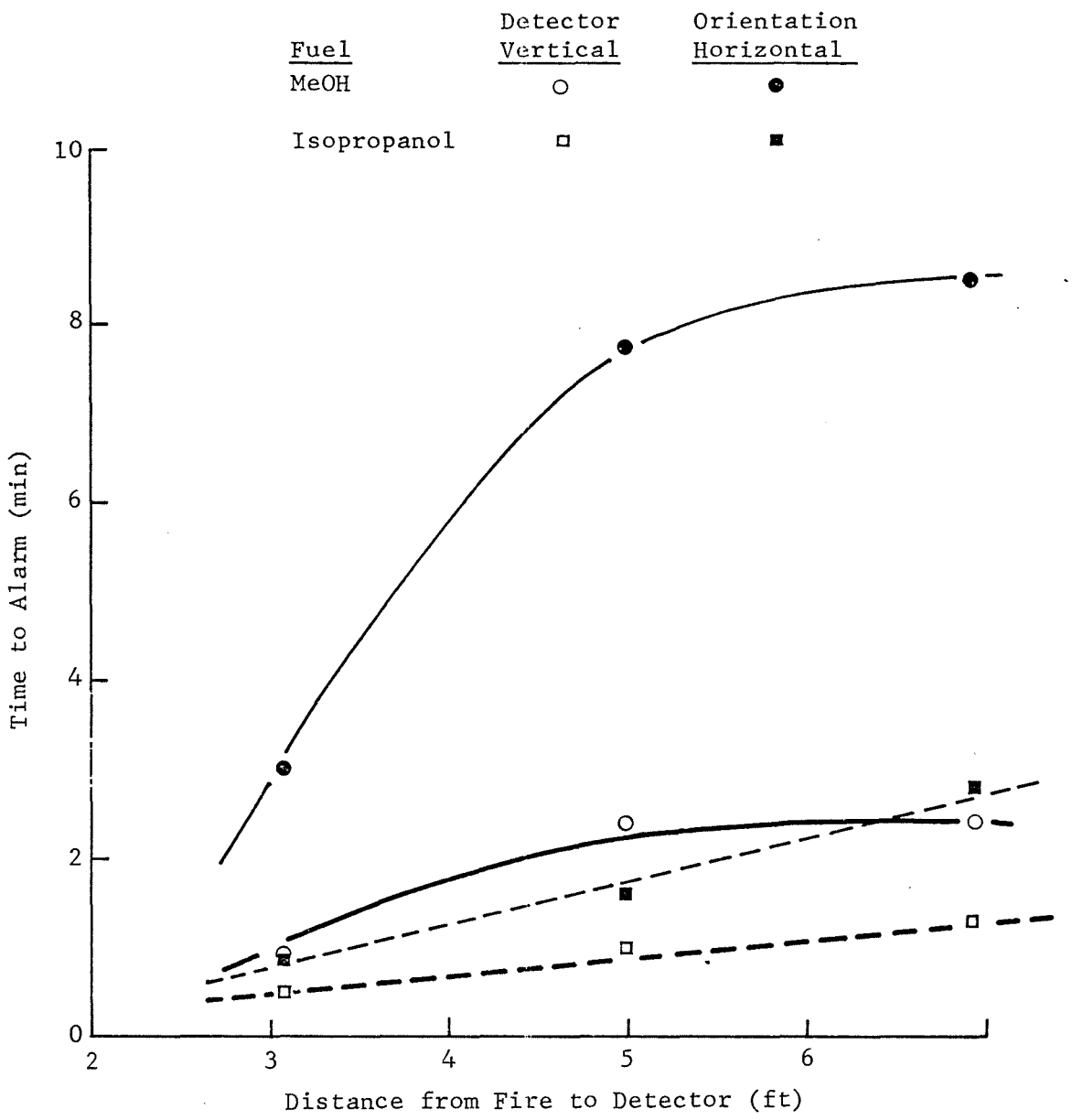

Figure 39. Air Temperature at Alarm for Fenwal Rate Compensated Thermal Detectors - Vertical vs. Horizontal Orientation.

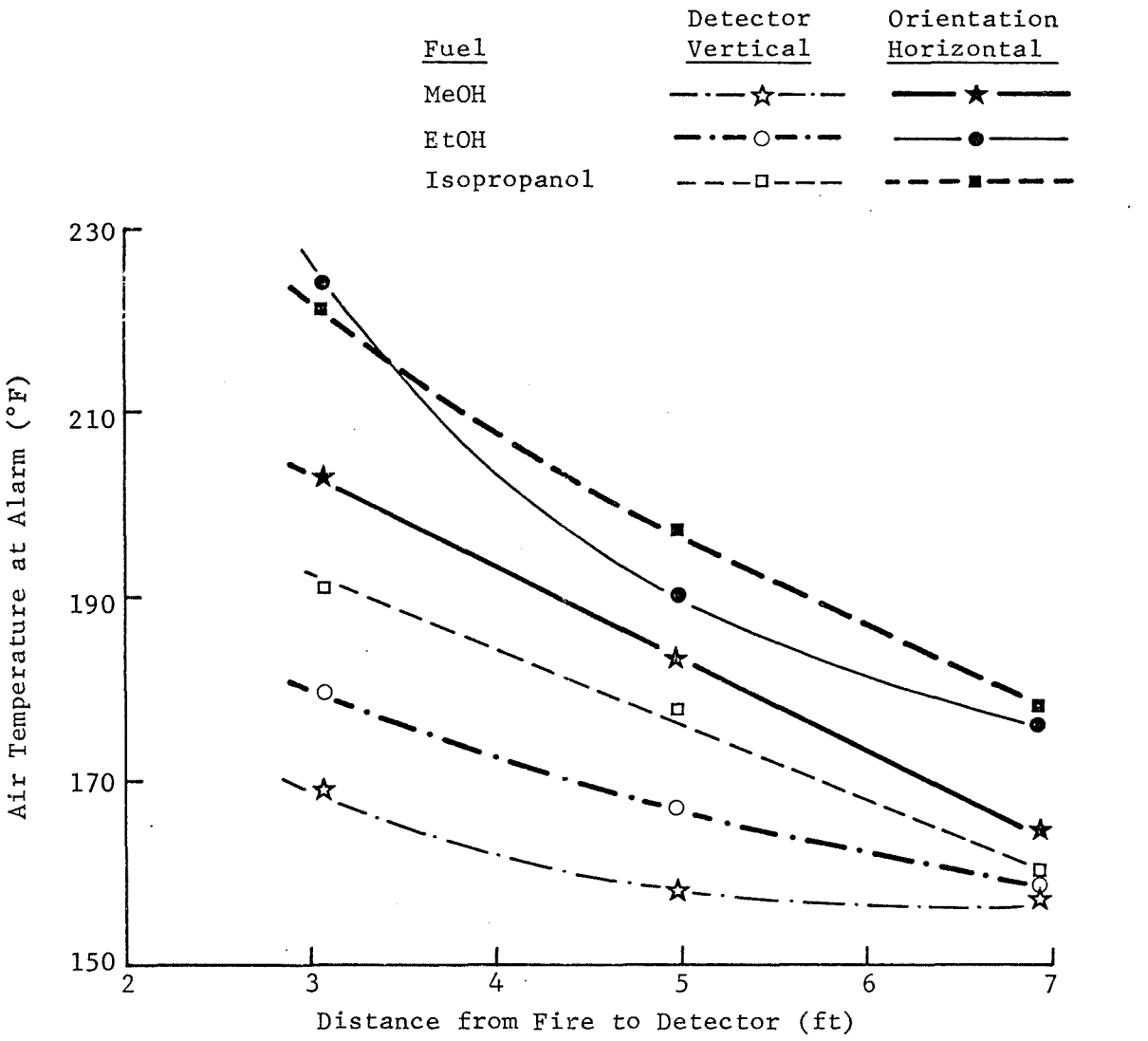

Figure 40. Probability Plot for 4.0%/ft. Punk Smoke.

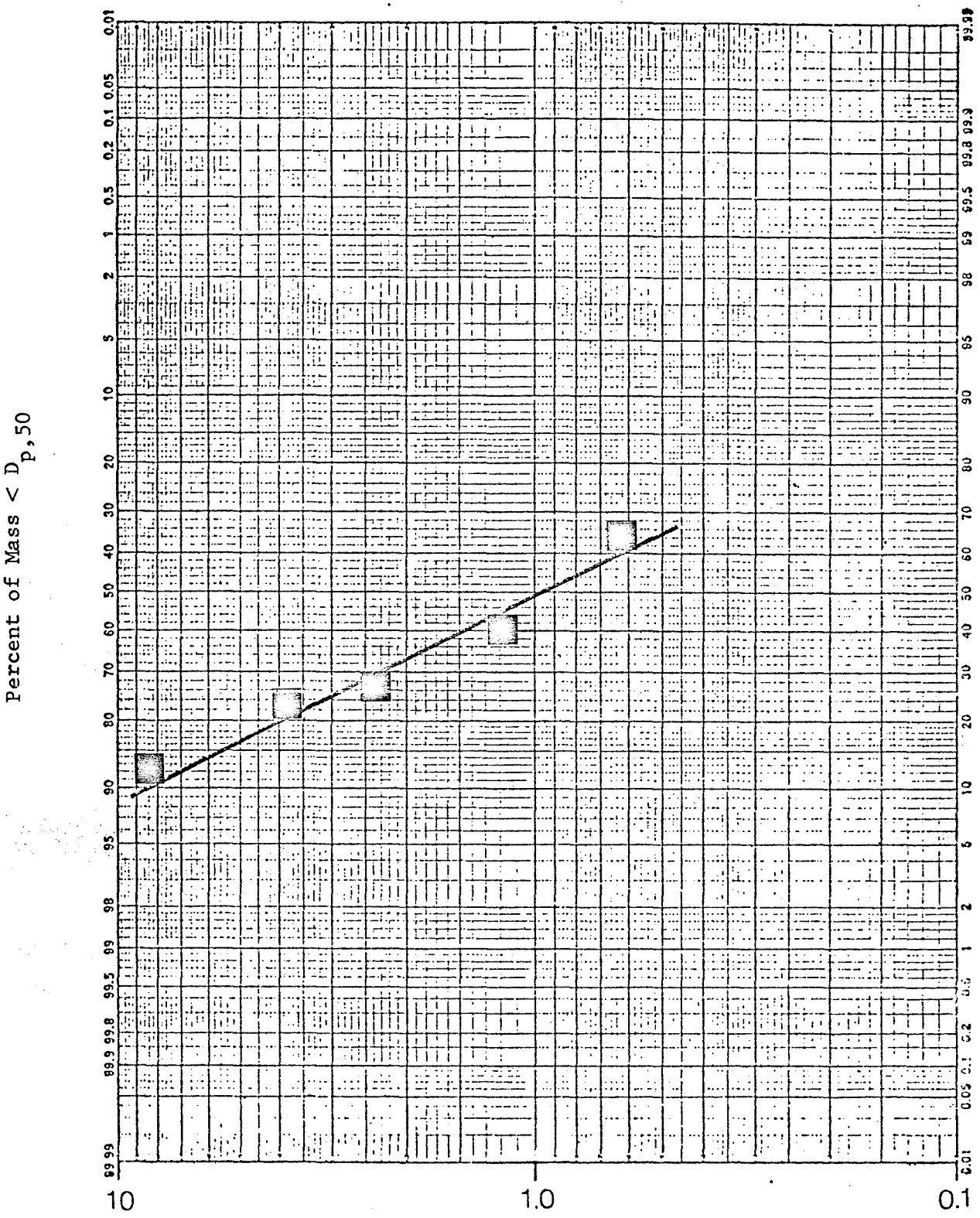

Figure 41. Probability Plot for 4.0%/ft. PVC Linecord Insulation Smoke.

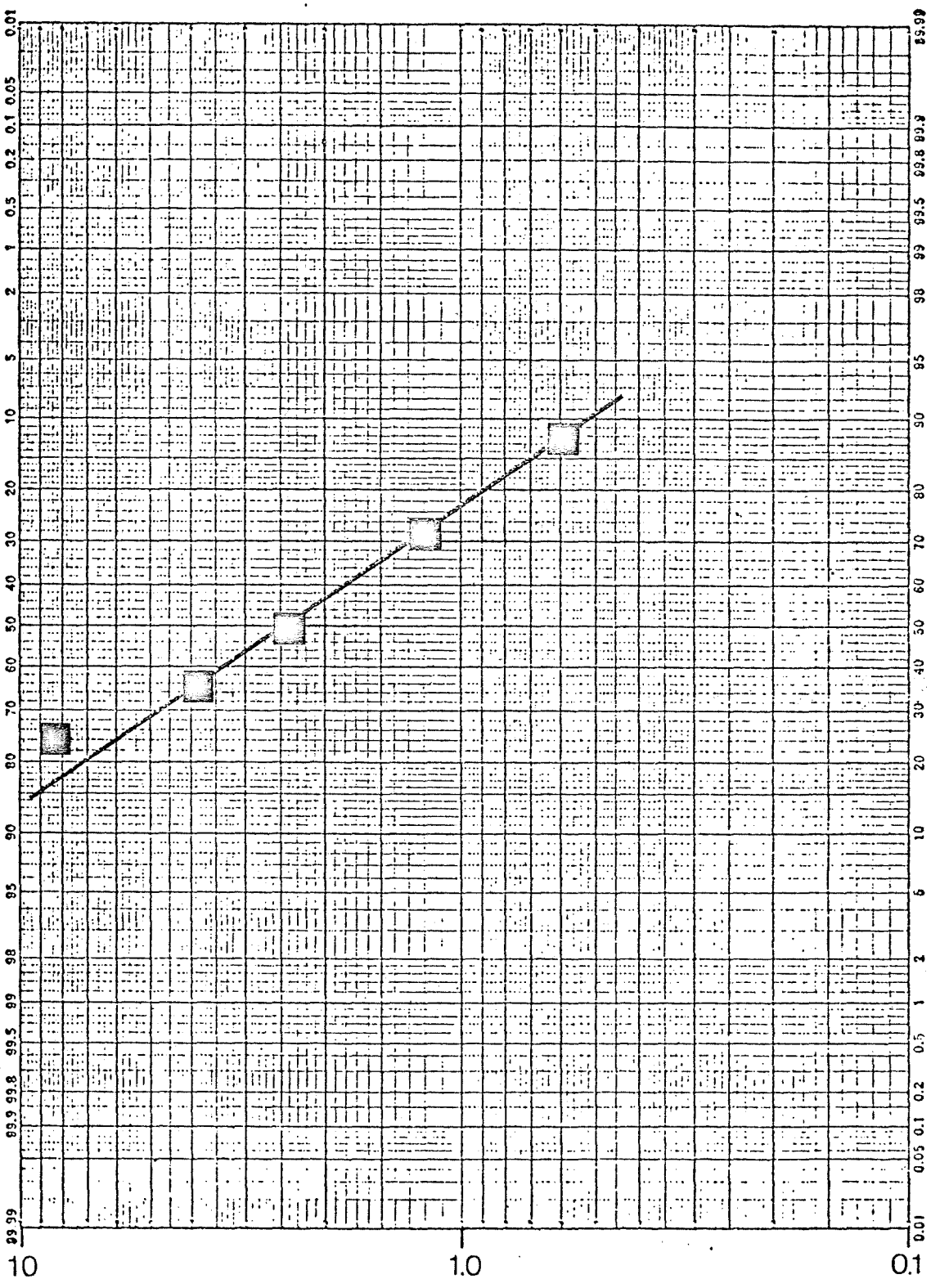

Figure 42. Probability Plot for 11.1%/ft. Polyethylene Insulation Smoke.

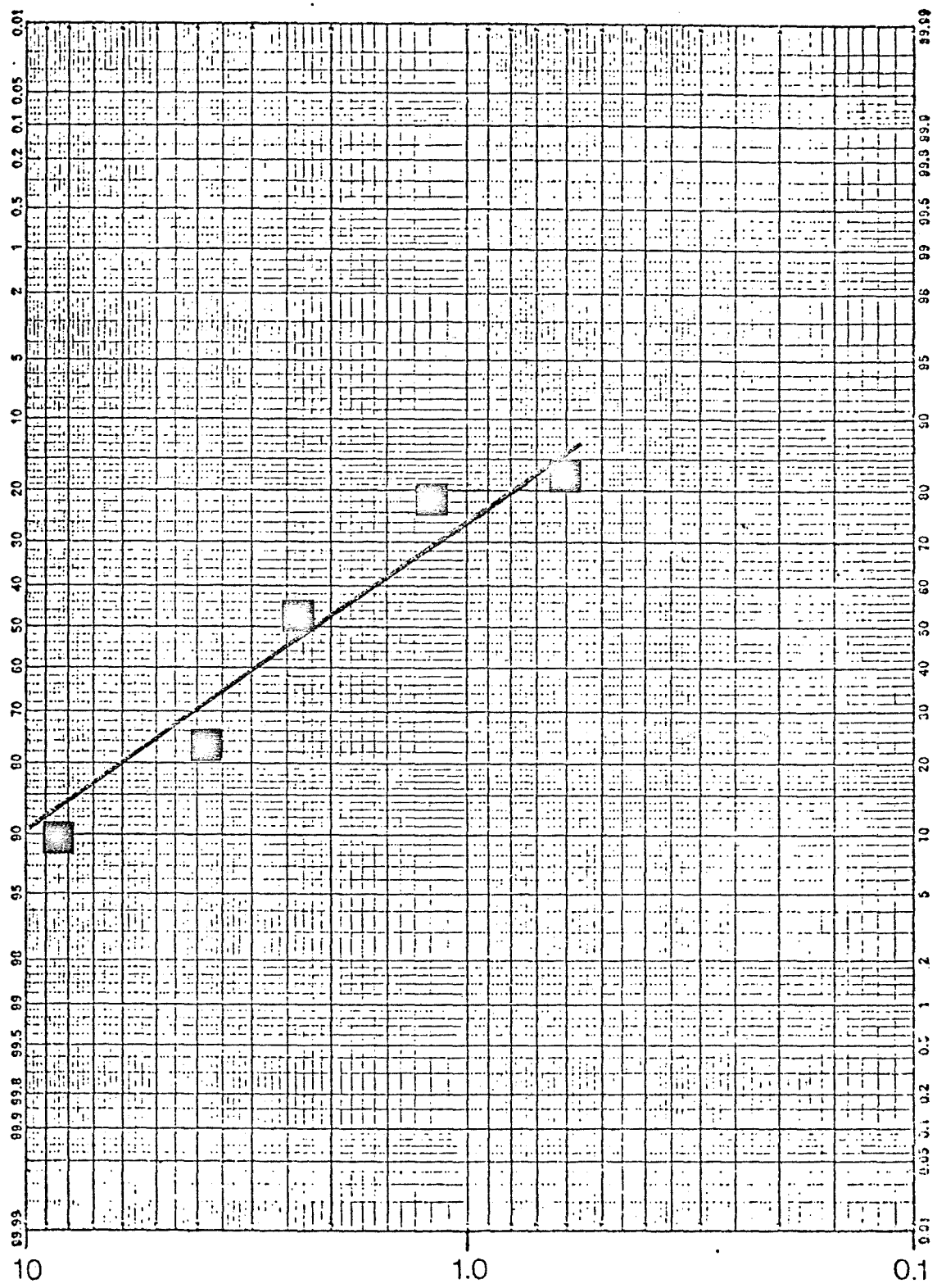

Figure 43. Comparative Mass Distributions for Selected Smokes.

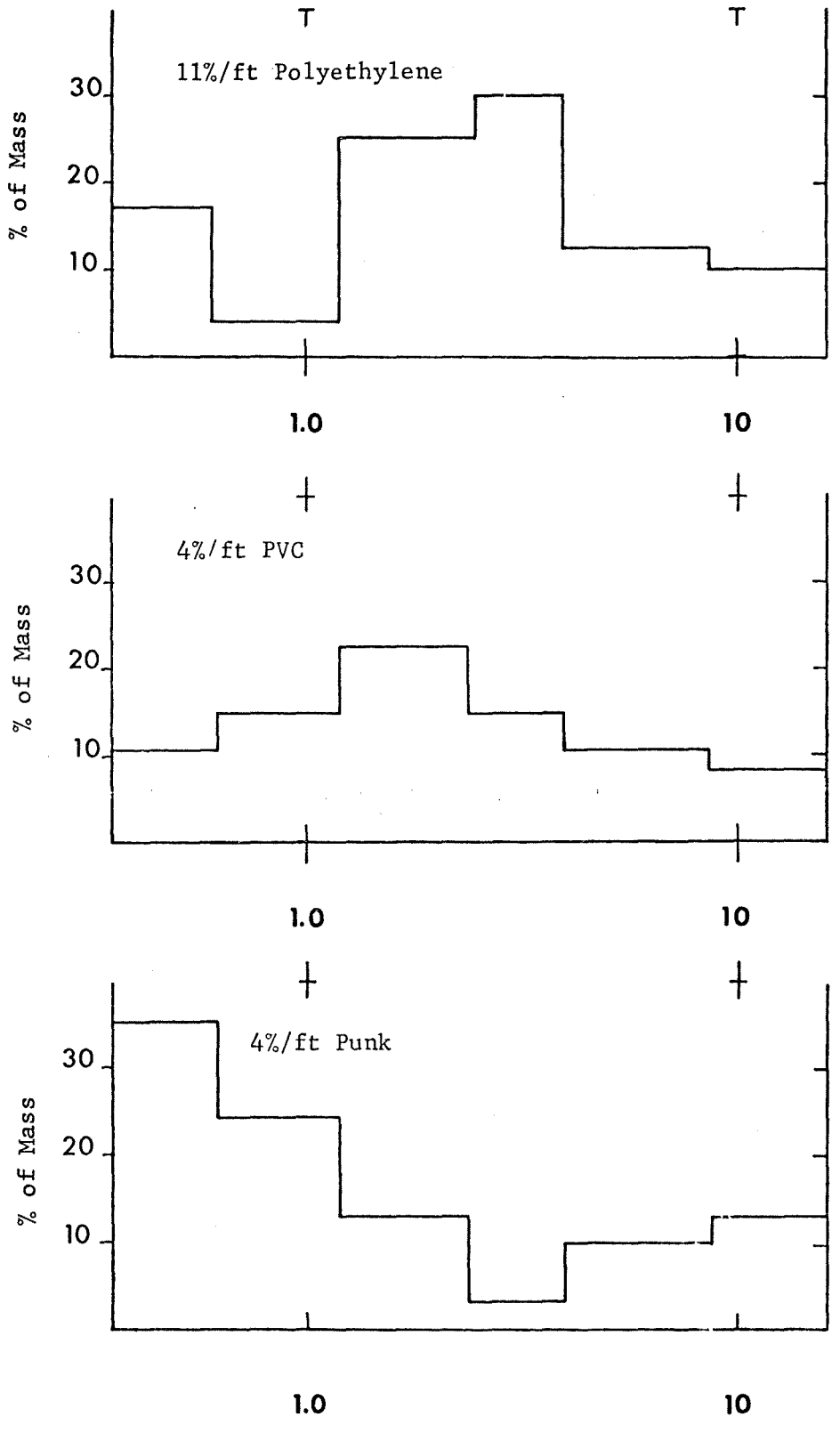

Figure 44. Comparative Response Time Behavior for Pneumatic Sampling in Long Tubes (I.D. - 3/8", P_2 = 685 mm Hg).

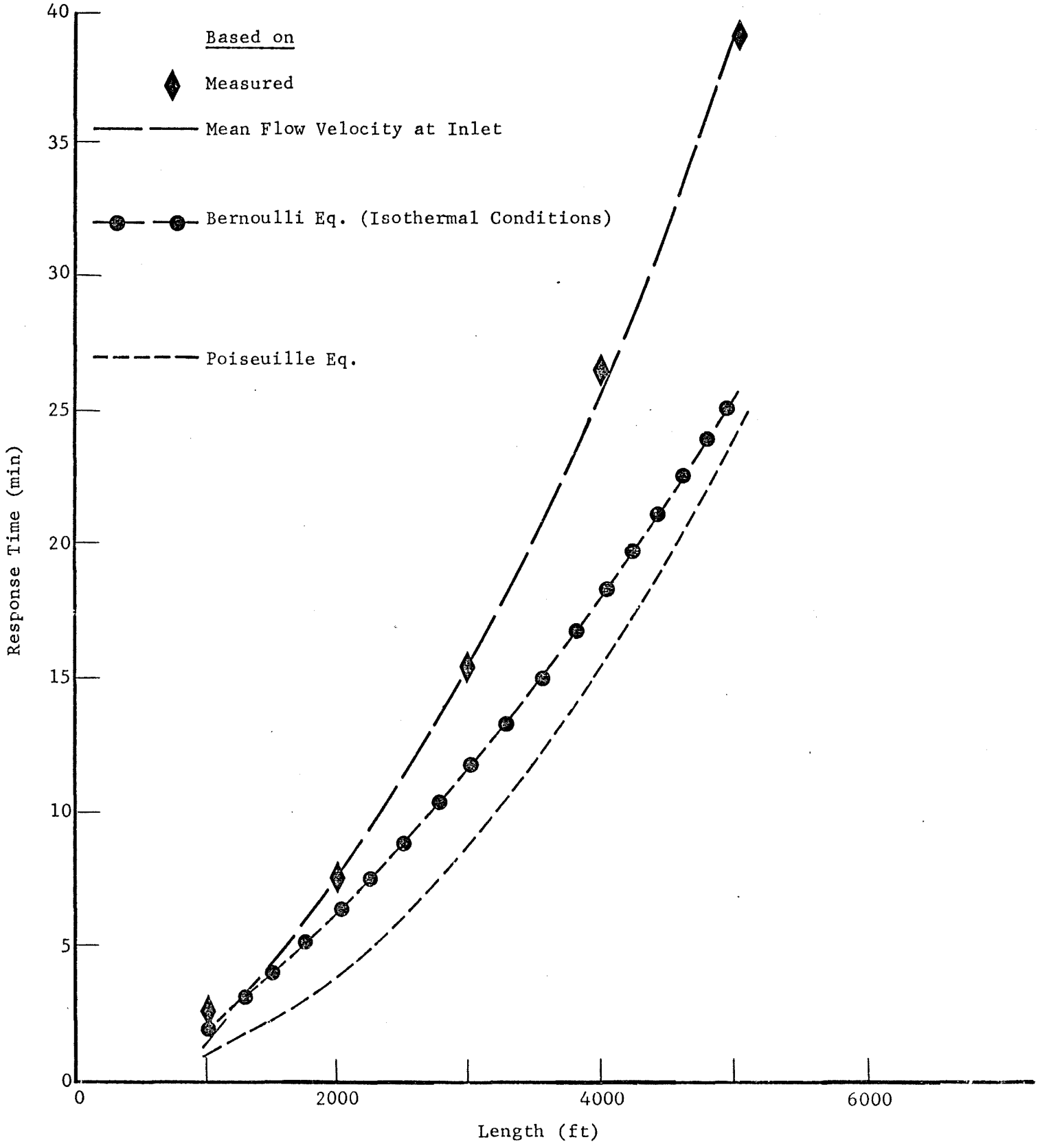

Figure 45. Comparative Response Time Behavior for Pneumatic Sampling in Tubes (I.D. 3/8", P_2 = 630 mm Hg).

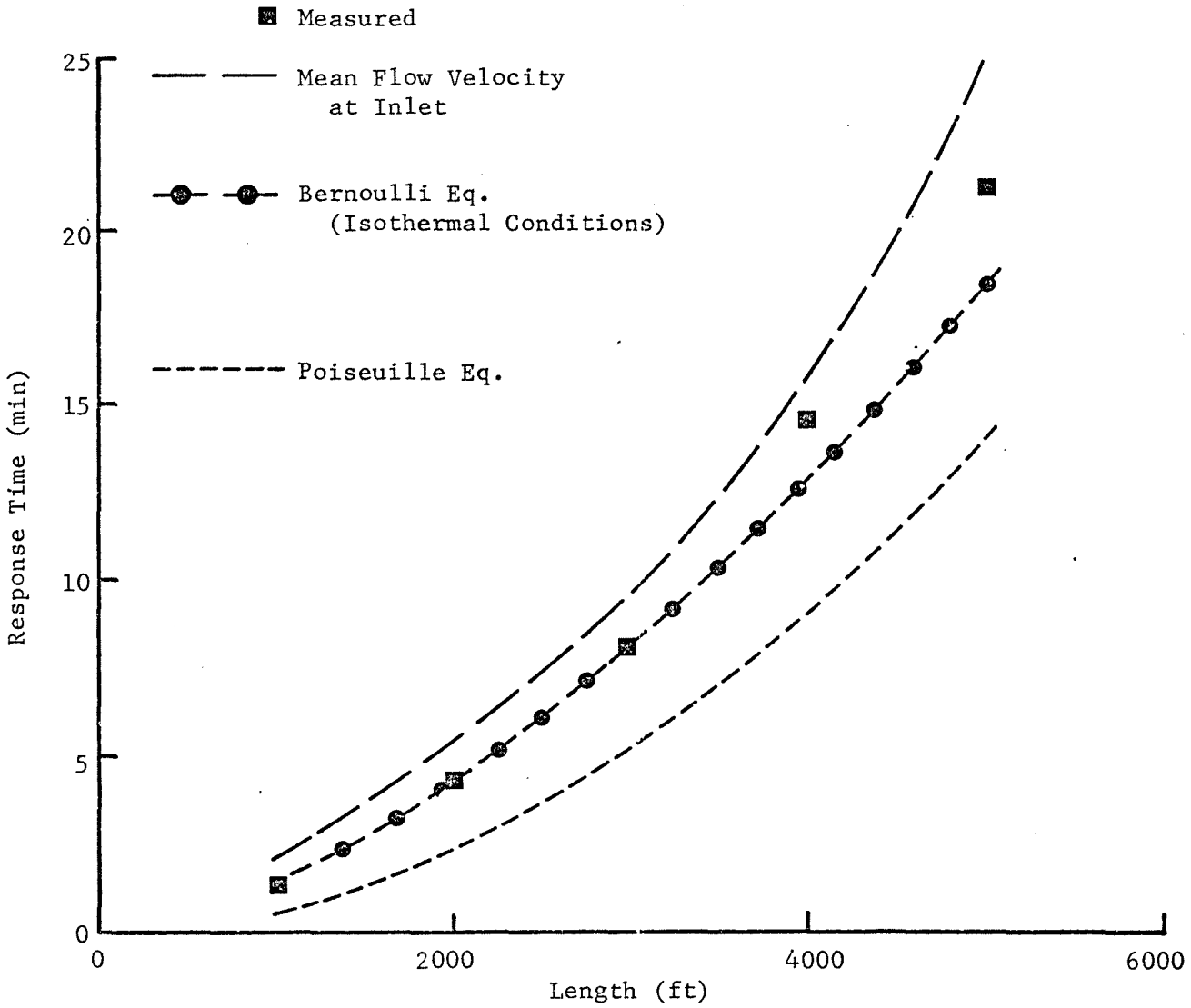

Figure 46. Comparative Response Time Behavior for Pneumatic Sampling in Long Tubes (I.D. = 3/8", P = 505 mm Hg).

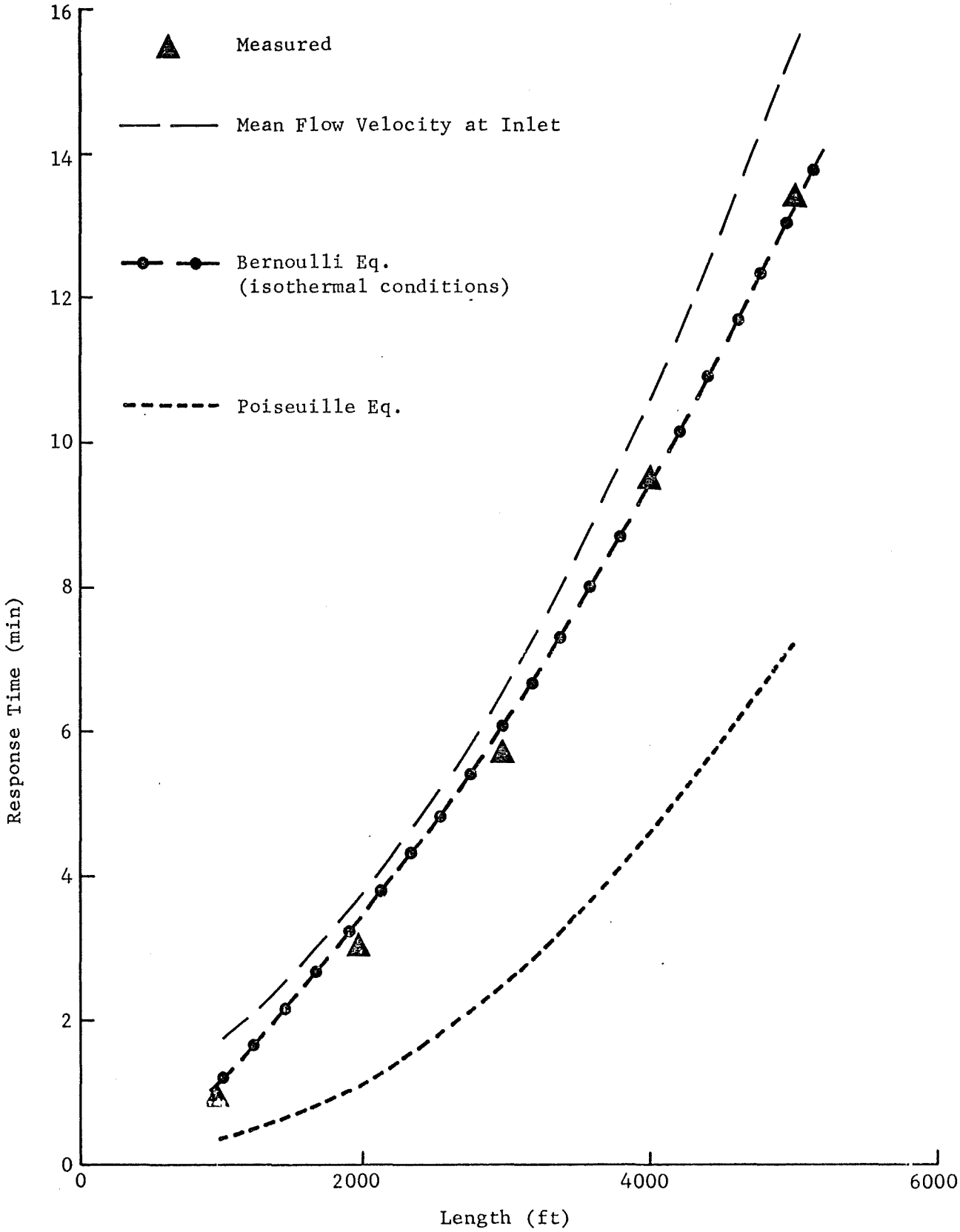

Figure 47. Measured CO_2 Concentration vs. Volume of CO_2 for 4,000 ft of 3/8" I.D. Tubing.

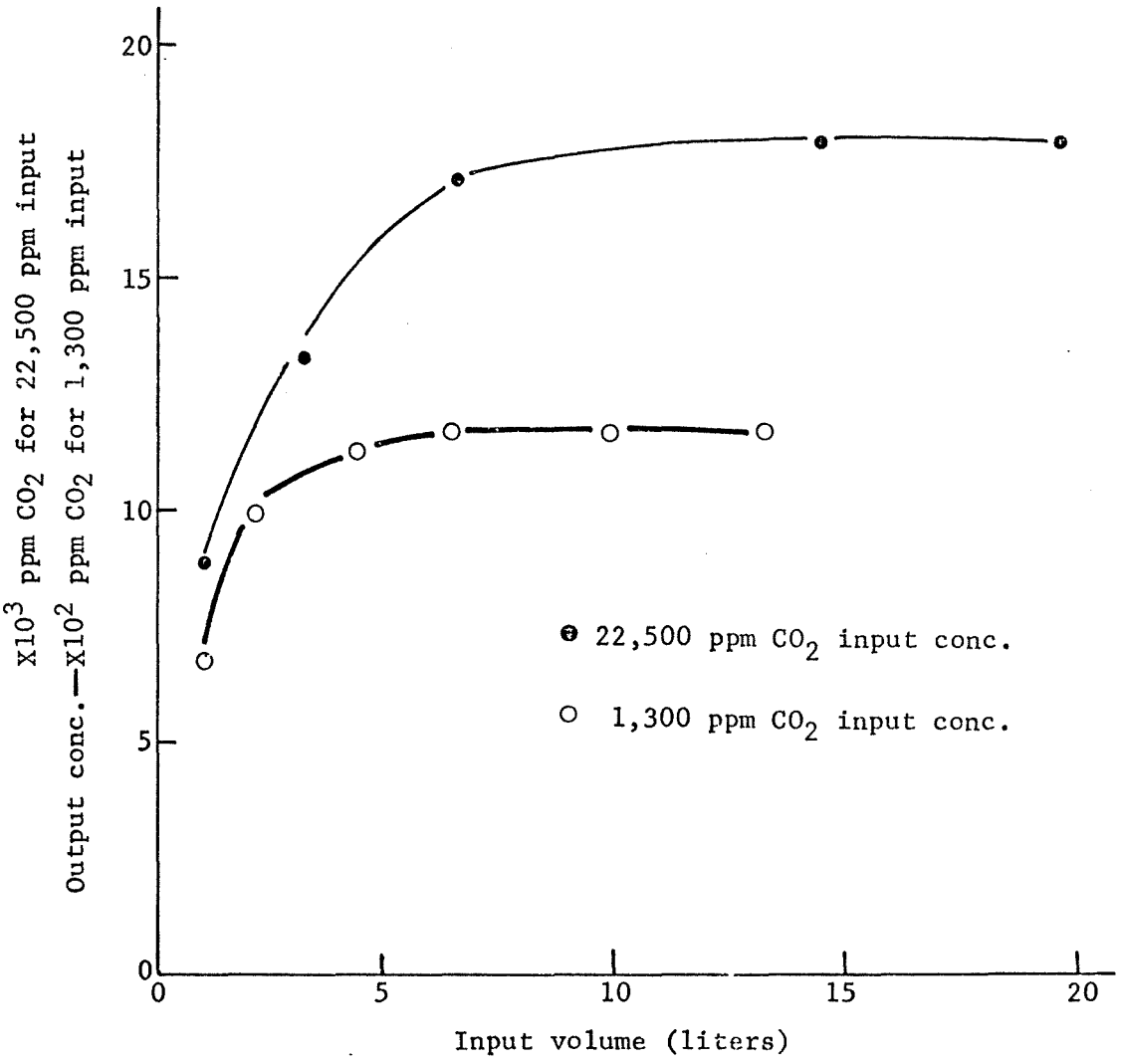

APPENDIX A

APPENDIX A

DERIVATION OF EQUATIONS AND CALCULATIONS

1) Isothermal Flow

For horizontal one dimensional flow in a duct of constant cross section, the Bernoulli equation may be written as

$$v dv + d(p\hat{V}) - p\hat{V}\frac{d\hat{V}}{\hat{V}} + \frac{1}{2}v^2 de_v = 0 \qquad (A\text{-}1)$$

For isothermal flow of an ideal gas

$$p\hat{V} = RT \quad \therefore \; d(p\hat{V}) = 0$$

$$\hat{V}_2/\hat{V}_1 = p_1/p_2$$

$$\frac{dv}{v} = \frac{d\hat{V}}{\hat{V}}$$

Now substituting in A-1 gives

$$2\frac{dv}{v} - 2RT\frac{dv}{v^3} + de_v = 0$$

which integrates to

$$e_v = -RT\left\{\frac{1}{v_2^2} - \frac{1}{v_1^2}\right\} - 2\ell n\frac{\hat{V}_2}{\hat{V}_1} \qquad (A\text{-}2)$$

Using continuity

$$v_2^2 = \left(\frac{v_1}{\hat{V}_1}\right)^2 \hat{V}_2^2 = v_1^2\left(p_1/p_2\right)$$

in A-2 and solving for v_1^2 we obtain

$$v_1^2 = \frac{RT\left\{\frac{(p_1/p_2)^2 - 1}{(p_1/p_2)^2}\right\}}{e_v + \ell n\ (p_1/p_2)^2} = \frac{p_1\hat{V}_1\{1-(p_2/p_1)^2\}}{e_v - \ell n\ (p_2/p_1)^2} \qquad \text{(A-3)}$$

Solving for v_1 and dividing by $\hat{V}_1$ we obtain

$$G \equiv v_1/\hat{V}_1 = \left\{\frac{p_1/\hat{V}_1\ (1-(p_2/p_1)^2)}{e_v - \ell n\ (p_2/p_1)^2}\right\} \qquad \text{(A-4)}$$

for the mass velocity. Multiplying G by the cross-sectional area, A, gives the mass flow rate $GA = \dot{m}$ lbm/sec.

The maximum value of G is obtained from $\frac{\partial G}{\partial p_2} = 0$; we obtain

$$e_v - \ell n\ (p_2/p_1)^2 = \frac{1 - (p_2/p_1)^2}{(p_2/p_1)^2} \qquad \text{(A-5)}$$

2) Adiabatic Flow

For flow of an ideal gas in ducts of constant cross section, the macroscopic mechanical energy balance

$$\Delta(\hat{U} + p\hat{V} + 1/2v^2) = \hat{Q} = \hat{W} \qquad \text{(A-6)}$$

where

$$\hat{H} = \hat{U} + p\hat{V}$$

is the enthalpy/mass may be used to show that

$$p\hat{V} + 1/2\left(\frac{\gamma-1}{\gamma^2}\right) v^2 = \text{Const.}$$

when no work is done on the system. This follows readily from

$$\Delta H = \int_{T_1}^{T_2} C_p dT = \frac{\gamma}{\gamma-1} R\Delta T$$

and substitution of the equation of state

$$p\hat{V} = RT$$

into (A-6).

Now substituting

$$p\hat{V} + 1/2 \left(\frac{\gamma-1}{\gamma}\right) v^2 = p_1\hat{V}_1 + 1/2 \left(\frac{\gamma-1}{\gamma}\right) v_1^2$$

and

$$d(p\hat{V}) = - \frac{\gamma-1}{\gamma} vdv$$

$$\frac{d\hat{V}}{\hat{V}} = \frac{dv}{v}$$

into the Bernoulli equation

$$vdv + d(p\hat{V}) - p\hat{V} \frac{d\hat{V}}{\hat{V}} = - 1/2 \, v^2 de_v$$

and rearranging gives

$$\frac{\gamma+1}{\gamma} \frac{dv}{v} - 2p_1\hat{V}_1 + \frac{\gamma-1}{\gamma} v_1^2 \frac{dv}{v^3} = - de_v \qquad \text{(A-7)}$$

Integrating (A-7) between planes 1 and 2 and using

$$\frac{1}{v_2^2} - \frac{1}{v_1^2} = \frac{1}{v_1^2}\left(\frac{\hat{V}_1^2}{\hat{V}_2^2} - 1\right)$$

gives

$$\left\{p_1\hat{V}_1 + \frac{\gamma-1}{2\gamma} v_1^2\right\} = \frac{e_v - \frac{\gamma+1}{2\gamma} \ell n \left(\frac{\hat{V}_1}{\hat{V}_2}\right)^2}{\frac{1}{v_1^2}\left\{1 - \left(\frac{V_1}{V_2}\right)^2\right\}}.$$

Solving for v_1 gives

$$v_1 = \left\{\frac{p_1\hat{V}_1}{\dfrac{e_v - \frac{\gamma+1}{2\gamma} \ell n \left(\frac{\hat{V}_1}{\hat{V}_2}\right)}{1 - (\hat{V}_1/\hat{V}_2)^2} - \frac{\gamma-1}{2\gamma}}\right\}^{1/2}$$

The mass velocity is given by

$$G \equiv \frac{v_1}{\hat{V}_1} = \left\{\frac{p_1/\hat{V}_1}{\dfrac{e_v - \frac{\gamma+1}{2\gamma} \ell n \left(\frac{\hat{V}_1}{\hat{V}_2}\right)^2}{(\hat{V}_1/\hat{V}_2)^2} - \frac{\gamma-1}{2\gamma}}\right\}^{1/2} \qquad \text{(A-8)}$$

The maximum possible value of G is obtained when $\frac{\partial G}{\partial p_2} = 0$. Under this condition, it can be shown that

$$(p_2/p_1)^{2/\gamma} = \frac{1}{1 + \frac{2e_v\gamma}{\gamma+1} - \ell n\ (p_2/p_1)^{2/\gamma}} \qquad \text{(A-9)}$$

and/or

$$\left(\frac{\hat{V}_1}{\hat{V}_2}\right)^2 = \frac{1}{1 + \frac{2e_v\gamma}{\gamma+1} - 2\ell n \frac{\hat{V}_1}{\hat{V}_2}} \qquad \text{(A-10)}$$

3) Estimates of Pump Horsepower and Time for Terminal Volume Filling

A single probe of the 12 point gas sampling system in Figure 6 may be simplified to that in Figure A-1 to a close approximation where V_T represents the sum of the internal volume of the traps, manifold, filter system, a given valve, tubing connections, and internal volume of the small pump.

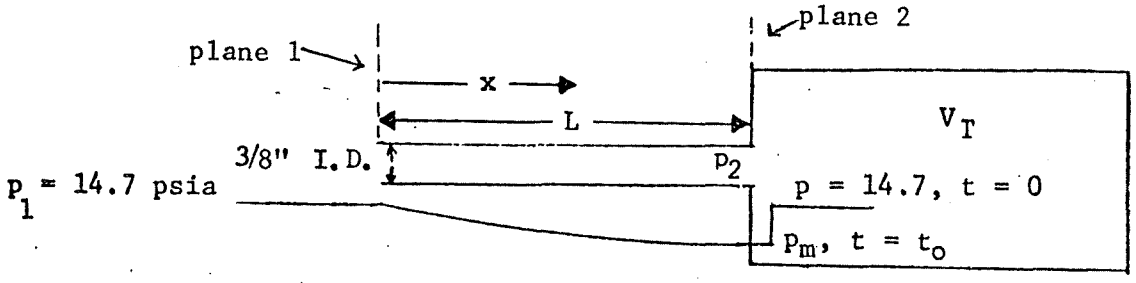

Figure A-1. Schematic of Simplified Test Set-Up for Multipoint Sampling System.

An estimate of the pumping requirements may be obtained by integrating the steady state macroscopic mechanical energy balance:

$$1/2\ \Delta\ v^2 + \int_1^2 dp/\rho + \hat{W} + \hat{E}_v = 0 \qquad \text{(A-11)}$$

where

$\hat{W}$ = work done per unit mass of fluid

$\hat{E}_v$ = total rate of viscous dissipation of mechanical energy per given mass between planes 1 and 2. If we neglect the rate of viscous dissipation of mechanical energy and, furthermore, assume the conditions at the pump can be returned to those of plane 1 by adiabatic pumping and cooling, then Equation A-11 integrates to:

$$-\hat{W} = 1/2\ gv_1^2 \left[1 - \left(p_1/p_2\right)^2\right] + \frac{RT\gamma}{\gamma-1}\left[\left(p_1/p_2\right)^{\frac{\gamma-1}{\gamma}} - 1\right] \qquad \text{(A-12)}$$

Solutions to Equation A-12 will provide an estimate of the power needed to produce a given flow velocity for both isothermal and adiabatic conditions.

The time required for filling V_t may be obtained from a mass balance which equates the mass rate of flow into the terminal volume set equal to the rate of mass increase within the volume:

$$\dot{m} = \rho_2 v_2 A = \rho_1 v_1 A = V_T \frac{d\rho}{dt} \qquad \text{(A-13)}$$

Assuming the filling process occurs adiabatically and reversibly:

$$d\rho/\rho = 1/\gamma \, dp/p$$

and using $$p\gamma = c^2\rho g$$

we obtain:

$$\frac{V_T g}{c^2} \frac{dp}{dt} = \dot{m} = \rho_2 v_2 A = \rho_1 v_1 A \qquad \text{(A-14)}$$

Integrating A-14 we obtain

$$t_v \cong \frac{V_T g \Delta p}{c^2 \dot{m}} \cong \frac{V_T g p_m}{c^2 \dot{m}} \qquad \text{(A-15)}$$

4) Sample Calculations

The main problem in using the Bernoulli equation results in selection of a suitable value for the friction factor. Figure A-2 shows that the friction factor varies between the limits imposed by laminar and turbulent flow in "hydraulically smooth" tubes. The <v> in the Reynolds number is the cross-sectionally averaged velocity; it is independent of tube length, i.e., the graph is strictly applicable for non-accelerating flows.

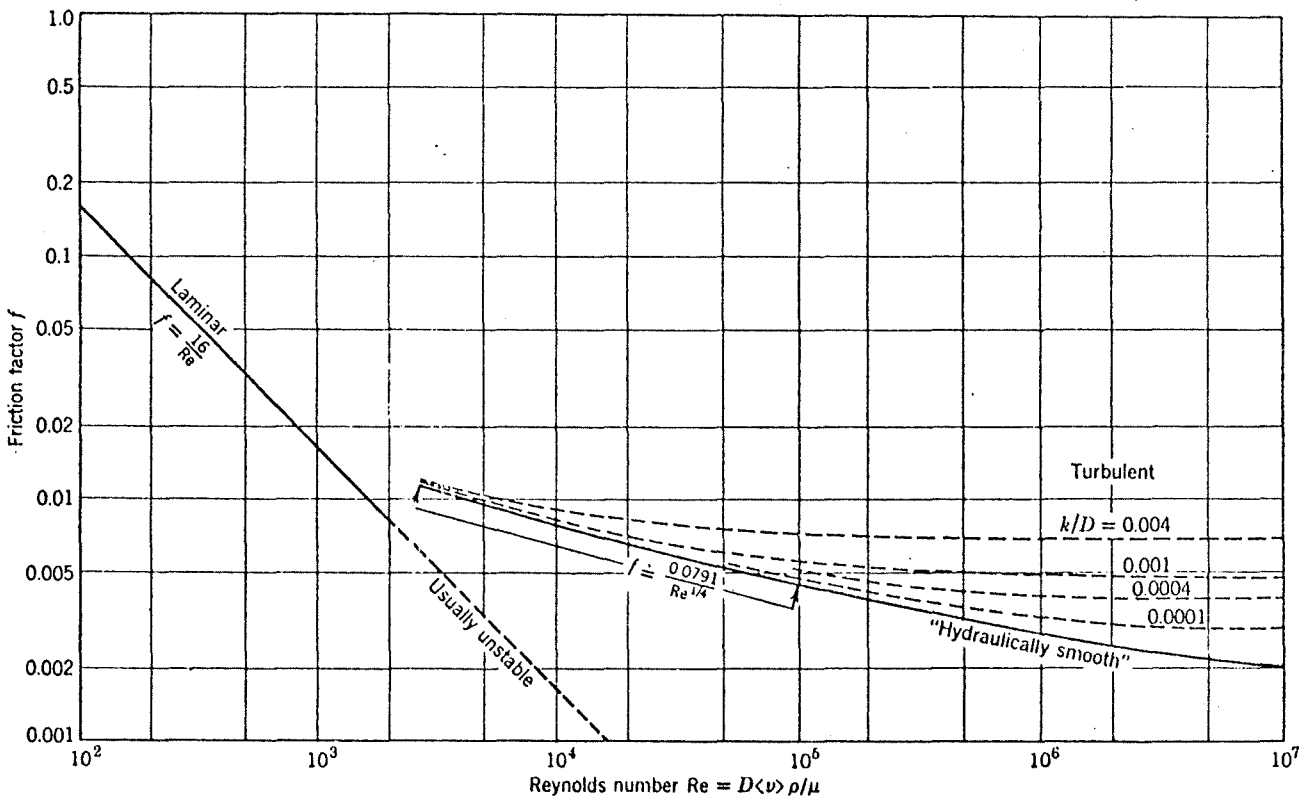

Figure A-2. Friction Factors for Tube Flow (139)

The measured pressure profiles shown in Figure A-3 for tube lengths up to 4,000 ft. show a linear behavior. Selection of a suitable friction factor could be done for incremental lengths and Equation A-4 used to calculate v for that length, using this v to calculate t_r for that incremental length, etc. and summing up all the incremental t_r's to obtain the overall residence time. This approach is clearly not applicable here. Instead by trial and error we found a friction factor that upon substitution into A-4 or Eq. 4 and then into Equation 6 (text) for t_r gave a value for t_r that agreed with its measured value at 1,000 ft. This value of f was then used to generate t_r values for tubing lengths up to 5,000 ft. Selected sample calculations illustrating our approach follow.

Sample Calculations - Transient Response Time for 3/8" I.D. Tubing, Horsepower, and Terminal Volume Filling Time

In the Bernoulli equation a friction factor of f = 0.025 was assumed while other properties were evaluated based on inlet conditions. Now

$$G_{max} = \left\{ \frac{p_1 \rho_1 \left[1 - \left(p_2/p_1 \right)^2 \right]}{e_v - \ell n \; p_2/p_1} \right\}^{1/2}$$

for the mass flux of the gas. The maximum possible mass flow, $\dot{m}_{max} = G_{max} \times A$, where A is the cross-sectional area of the tubing. Substituting into $e_v = 4 fL/d$ when L = 4,000 ft., the frictional resistance f = 0.025 gives $e_v = 12{,}800$. Now for the run for which P_2 = 505 mm we obtain

$$G_{max} = \left[\frac{\frac{32.2 \times 14.7 \times 144}{13.35} \left(1 - \left(\frac{505}{760} \right)^2 \right)}{12{,}800 \quad - \quad (-2.18)} \right]^{1/2}$$

$$G_{max} = .472 \text{ lb m/ft}^2 \text{ sec}$$

Now $v_1 = G_{max} \times V_1 = (.472)(13.35) = 6.30$ ft/sec and thus the minimum residence time is

$$t_{res} = 4{,}000 \text{ ft} / 6.30 \frac{\text{ft}}{\text{sec}} = 634 \text{ sec or } 10.6 \text{ min.}$$

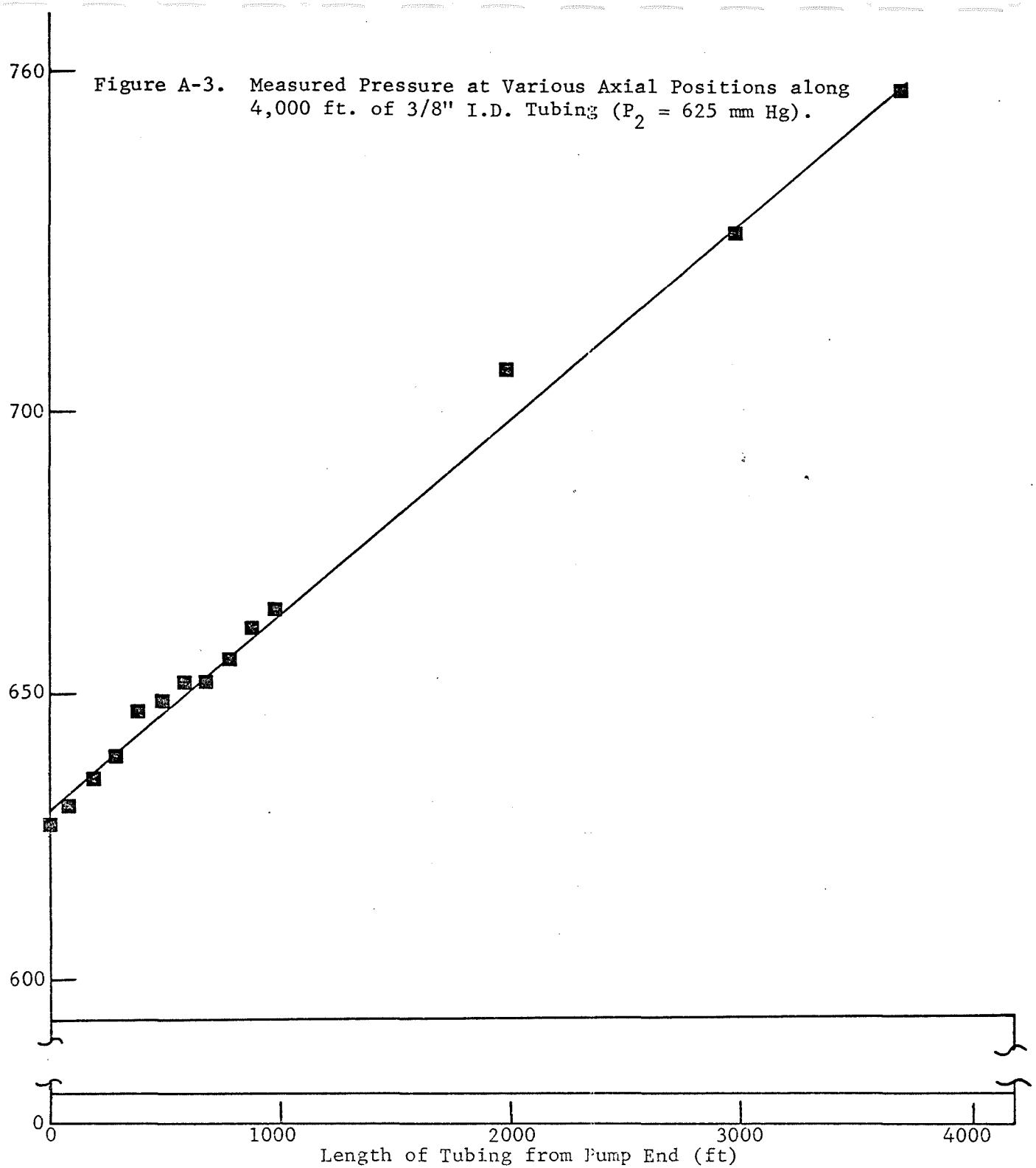

Figure A-3. Measured Pressure at Various Axial Positions along 4,000 ft. of 3/8" I.D. Tubing (P_2 = 625 mm Hg).

The mass flow rate is:

$$\dot{m} = G_{max} A = .472 \left[\pi/4 \times (.375)^2 \times 1/144\right]$$

$$\dot{m} = 3.62 \times 10^{-4} \text{ lb m/sec}$$

Therefore, the volumetric flow rate is

$$V_o = \frac{3.62 \times 10^{-4}}{7.5 \times 10^{-2}} \quad \frac{\text{lb}_{m/sec}}{\text{lb}_{m/ft^3}} = 4.82 \times 10^{-3} \text{ ft}^3/\text{sec}$$

or 136 cc/sec

The Reynolds number is given by

$$Re = \frac{4}{\pi} \dot{m}/d\mu = \frac{4}{\pi} \times \frac{3.62 \times 10^{-4}}{(.375 \times 1/12)(1.2 \times 10^{-5})}$$

$$Re = 1229$$

Since Re is less than 2,000 we have laminar flow.

Now find the horsepower required to produce this flow velocity:

$$-\hat{W} = 1/2\ gv_1^2 \left(1 - \left(P_1/P_2\right)^2\right) + \frac{RT\gamma}{\gamma-1} \left(\left(P_1/P_2\right)^{\frac{\gamma-1}{\gamma}} - 1\right)$$

$$= 1/2\ (32.2)\ (6.30)^2 \left(1 - \left(\frac{760}{505}\right)^2\right) + \left(\frac{1545.3}{29}\right) \frac{(530)\ 1.4}{0.4} \left(\left(\frac{760}{505}\right)^{\frac{.4}{1.4}} - 1\right)$$

$$= (16.1)\quad 39.69 \quad -1.26 \quad + \quad 53.3 \times 1855 \times .124$$

$$= \qquad -805 \quad + \quad 12,248$$

$$\hat{W} = -11,442 \text{ ft}_{f/lb_m}$$

$$P = \dot{m}\left|\hat{W}\right| = \left(3.62 \times 10^{-4} \frac{\text{lb}_m}{\text{sec}}\right) \left(1.14 \times 10^{+4} \text{ ft } \frac{\text{lbf}}{\text{lb}_m}\right) \left(5.05 \times 10^{-7} \frac{\text{hp hr}}{\text{ft lbf}}\right) \left(\frac{3600 \text{ sec}}{\text{hr}}\right)$$

$$P = .0075 \text{ hp}$$

The removal of gas from the terminal volume, V_T, assuming V_T = 1 liter for principally the manifold, traps, and connecting hoses we arrive at

$$t_v = \frac{V_t\ gp_m}{c^2\ \dot{m}} = \frac{\left(\frac{1}{28.3}\right) (32.2) \left(14.7 \times \frac{505}{760}\right)}{(1.11)^2 \times 10^6 \times 3.62 \times 10^{-4}}$$

$$= 3.6 \text{ sec}$$

This is negligible with respect to the transient response time t_r of 10.6 min.

If we repeat the calculations for t_r using f = 0.020, we will obtain the curve as indicated by the Bernoulli equation in Figure 46.

NOMENCLATURE

A	cross section area, ft^2
a	tube radius, in.
c	sound speed, $\sqrt{\gamma gRT}$
d	tube diameter, in.
e_v	friction loss factor associated with viscous dissipation, dimensionless
$\hat{E}_V$	total rate of viscous dissipation of mechanical energy per given mass, ft lbs/lbm
f	friction factor, a measure of the resistance to flow, dimensionless
g	acceleration of gravity, 32.2 ft/sec^2
G	mass flow velocity, lbm/ft^2-sec
H	enthalpy, Btu
$\hat{H}$	enthalpy per mass, Btu/lbm
L	tube length, ft
$\dot{m}$	mass flow rate - lbm/sec
p	pressure, lb_f/ft^2
P	power consumed, horsepower
R	gas constant, ft $lbf/lb_{mole}{}^oR$
Re	Reynolds number, dimensionless
T	Temperature, ^oR
$\hat{U}$	internal energy per unit mass, Btu/lbm
v	flow velocity, ft/sec
V	potential, volts
V_T	volume, ft^3
$\hat{V}$	specific volume, $1/\rho$, ft^3/lbm
x	distance coordinate (distance from tube entrance)
$\hat{W}$	work done per unit mass of fluid, ft lbf/lbm
ρ	density, lbm/ft
μ	viscosity, lbm/ft sec
σ_g	geometric standard deviation

γ ratio of specific heats, C_p/C_V, dimensionless

Subscripts

1, 2 conditions at planes 1, 2, respectively

Overlines

$\hat{}$ per unit mass

ACKNOWLEDGMENTS

The authors wish to acknowledge the typing of Mrs. Diane Clarke and illustrations of Mr. Donald Mason and Mrs. Pat Schooley.

The constructive technical comments of Dr. Martin Hertzberg, Technical Project Officer of USBM, are also gratefully acknowledged.